Genehmigt vom Fachbereich Biologie
der Fakultät für Mathematik, Informatik und Naturwissenschaften
an der Universität Hamburg
auf Antrag von Priv.-Doz. Dr. T. KAISER
Weiterer Gutachter der Dissertation:
Prof. Dr. T. MARTIN
Tag der Disputation: 14. Oktober 2011

Hamburg, den 30. September 2011

Professor Dr. J. Fromm
Vorsitzender des Fach-
Promotionsausschusses Biologie

Tribology of dental enamel facets of Ungulates and Primates (Mammalia): Tracing tooth-food interaction through 3D enamel microtexture analyses

Dissertation

Zur Erlangung der Würde des Doktors der Naturwissenschaften
des Fachbereichs Biologie, der Fakultät für Mathematik, Informatik und
Naturwissenschaften der Universität Hamburg

vorgelegt von
Ivan Calandra
aus Lyon

Hamburg, 2011

Table of contents

Acknowledgements ---------- 8

Abstract ---------- 10

1. Introduction ---------- 13
- 1.1 Mammal teeth and food ---------- 14
- 1.2 Terminology ---------- 16
- 1.3 Review of previous dental microwear research ---------- 17
- 1.4 Grit and dust *versus* phytoliths ---------- 20
- 1.5 Fracture and deformation theory, and microwear formation ---------- 23
- 1.6 Hypotheses ---------- 27
  - 1.6.1 Robustness of DASTA texture parameters across filtering thresholds (hypothesis 1) ---------- 28
  - 1.6.2 Testing for characteristics of food and masticatory biomechanics through the DASTA (hypothesis 2) ---------- 29
  - 1.6.3 Primate diets assessed by the SSFA (hypothesis 3) ---------- 29
  - 1.6.4 DASTA, food biomechanics and tooth function of primates (hypothesis 4) ---------- 30
  - 1.6.5 Microtexture analyses with small sample sizes (hypothesis 5) ---------- 31

2. Methods ---------- 33
- 2.1 Specimen selection ---------- 34
- 2.2 Material ---------- 35
- 2.3 Molding procedure ---------- 36
- 2.4 Data acquisition with the µsurf custom ---------- 40
- 2.5 Pre-processing of the 3D surface data ---------- 42
- 2.6 Dental Areal Surface Texture Analysis ---------- 43
- 2.7 Scale-Sensitive Fractal Analysis ---------- 46
- 2.8 Statistics ---------- 48
  - 2.8.1 Robust statistics ---------- 48
  - 2.8.2 Trimming ---------- 50
  - 2.8.3 Statistical tests ---------- 51
  - 2.8.4 Regressions and correlations ---------- 52
  - 2.8.5 Software ---------- 53
- 2.9 Summary ---------- 53

3. Results ---------- 55
3.1 The effect of trimming ---------- 56
3.2 Ungulates ---------- 57
3.2.1 Robustness of DASTA texture parameters across filtering thresholds (hypothesis 1) ---------- 57
3.2.2 Testing for characteristics of food and masticatory biomechanics through the DASTA (hypothesis 2) ---------- 57
3.3 Primates ---------- 64
3.3.1 Primate diets assessed by the SSFA (hypothesis 3) ---------- 64
3.3.2 DASTA, food biomechanics and tooth function of primates (hypothesis 4) ---------- 68

4. Discussion ---------- 71
4.1 Tracing chewing mechanisms in ungulates: 3D tribology of enamel microtexture ---------- 72
4.1.1 Robustness of DASTA texture parameters across filtering thresholds (hypothesis 1) ---------- 72
4.1.2 Testing for characteristics of food and masticatory biomechanics through the DASTA (hypothesis 2) ---------- 73
4.2 Teasing apart the contributions of hard dietary items on 3D dental microtextures in primates ---------- 75
4.2.1 Primate diets assessed by the SSFA (hypothesis 3) ---------- 75
4.2.2 DASTA, food biomechanics and tooth function of primates (hypothesis 4) ---------- 80
4.3 Microtexture analyses with small sample sizes (hypothesis 5) ---------- 82
4.4 General discussion ---------- 82
4.4.1 SSFA *versus* DASTA ---------- 82
4.4.2 Taxon-independent characteristics of the microtexture relating to tooth function ---------- 84
4.4.3 3D high-resolution scanning and microtextures ---------- 87

5. Conclusions and further perspectives ---------- 91

6. References ---------- 97

7. Appendices ---------- 115

Acknowledgements

I first thank my advisor, Thomas Kaiser, who designed this exciting project, exciting enough for me to work on it for three whole years! He also improved substantially the quality of this thesis. Ellen Schulz (University of Hamburg) was really involved in that project. We conceived most of the work together. She was and still is a keystone in the organization and administration of the working group.

I would also like to thank Gilles Escarguel (University of Lyon) who first showed me what paleontology really is and how exciting it is. He is the one who introduced me to Gildas Merceron (University of Lyon) when I was still one of his students.

Gildas is definitely the person who helped me and guided me the most on my way leading to this Ph.D. thesis and further. I started in the microwear research with him during my Master 1 practical work in Hamburg. Even though I worked with him for just three months, this opened up a world of opportunity to me. Thanks to him, I was in contact with Thomas Kaiser and his team, and this is how I found the present Ph.D. project. But Gildas keeps helping me: he helped me with my projects through numerous discussions, he commented an earlier version of this thesis, he invited me to excavate in Greece with him, he led me to my first post-doc project in Dijon and so on. For all this, he deserves more than just a short paragraph at the beginning of my work but that's all I can do here!

This work would have taken much longer if it weren't with the help of Hamburger students (Mirella Skiba, Anna Roeder and Britta Kerstin) who scanned many samples for me and of our technical assistant, Nelson Mascarenhas, who was always ready to help, and always with a smile.

The technical personal of the museums where I collected specimens kindly guided me into their collections.

The section 4 partially stems from the Bachelor theses of two students, Mona Pinnow and Susanne Krohn, which are heartily thanked.

I am very grateful to Rand R. Wilcox (University of Southern California) who answered all my questions regarding the application of his R functions to my datasets. The whole R community is also acknowledged for developing and maintaining such helpful packages and for the great support it provides through the R-help mailing list.

Martin V. Angel was kind enough to correct the English of this thesis in the twinkling of an eye. He did improve the quality of the English a lot, even though he hates split infinitives (a nasty American habits)! His help is very very greatly appreciated.

Cécile, Fleur, Henri, Laurent, Lul, Sacha, Simone and Vincent lent me a hand to check the final version.

Mrs. Sült-Wüpping and Mr. Brändel gave me a valuable hand with the wheels of bureaucracy. I probably wouldn't have gone through without them.

Finally thanks to all those who helped me love the life in Hamburg and in Germany (just to cite a few, sorry for the ones I forgot): Alexander, Caro, Claudia, Fredde, Helga, Jan, Juan Pablo, Julia, Lisa, Maren, Michi, Mona, Patrick, Sarah, Simone, Sven, Svenja, Sylwi, Tina, Tobi, Volker…

… And all those who did not forget about me while I was away (just a few as well): Alexandra, Alexandre, Ben, Binome, Coco, Dom, Élo, Élow, Fleur, Flo, Henri, Karine, Lul, Marion, Nathalie, Reno, Tibo, Vincent.

This research was supported by the "Deutsche Forschungsgemeinschaft" (DFG, German Research Foundation, KA 1525/8-1) and is part of the DFG Research Unit 771 "Function and performance enhancement in the mammalian dentition - phylogenetic and ontogenetic impact on the masticatory apparatus".

Abstract

The present Ph.D. thesis concerns the development of a new method of dental microtexture analysis and its application to the understanding of dental function in extant large herbivorous terrestrial mammals.

High energy uptake is required in mammals to maintain the high metabolic rate that makes the group unique. Teeth represent one of the major structural prerequisites that govern the efficiency of energy uptake. Hence teeth have played a crucial role in mammalian evolution. Moreover because they are frequently well preserved in the fossil record, methods have been developed so that the link between the dental characteristics to the foods consumed in extant species can be used as a tool to reconstruct the diets of extinct ones.

The dental microwear analysis is now a well-established tool for assessing the diets of both extant and extinct species using the patterns of scratching and pitting of the enamel surfaces of teeth. This method has been applied in two dimensions (2D) for some time, but the recent development of 3D techniques has allowed more sophisticated quantification of surface texture patterns.

For my Ph.D. project, a technique of 3D automated enamel microtexture analysis, termed dental areal surface texture analysis (DASTA), has been developed. This method is based on standardized industrial surface texture parameters. In industrial applications these parameters are also used functionally to characterize surfaces subject to wear. Parameters that robustly underscore inter-specific signals in terms of diet and chewing mechanics on enamel facets have been identified.

This methodology has been applied on two groups of herbivorous mammals. The first group is composed of four ungulates: *Connochaetes taurinus*, *Equus grevyi*, *Giraffa camelopardalis*, and *Diceros bicornis*. They represent two contrasted dietary traits (browsers and grazers) and two contrasting digestive strategies (ruminant and non-ruminant). Eleven wear-related parameters characterizing textural features such as the height, the volume, the furrows, the density of peaks, and the isotropy of the microtexture allow robust discrimination between grazers and browsers across digestive strategies. The tooth wear in the grazers (*C. taurinus* and *E. grevyi*) results in greater textural relief because of the higher abrasion resulting from chewing grass, whereas the browsers (*G. camelopardalis* and *D. bicornis*) have flatter tooth relief because the processing of tree leaves results in peak removal through either attrition or hydrodynamic pressures.

The second dataset is composed of eight primate species with known diets: *Alouatta seniculus*, *Gorilla gorilla*, *Lophocebus albigena*, *Macaca fascicularis*, *Pan troglodytes*, *Papio cynocephalus*, *Pongo abelii*, and *Theropithecus gelada*. Primates are mostly frugivores but supplement their diets with a diversity of alternative food resources (seeds, grass, tree leaves, bark, roots, tubers, and animals). It was first tested whether the scale-sensitive fractal analysis (SSFA; Scott *et al.* 2005; Scott *et al.* 2006) can assess key properties of their diets. The complexity and heterogeneity of textures correlate with the proportion of fruits consumed. A large textural fill volume indicates that a species's diet includes hard items, such as fruits or bark. Finally the anisotropy signal is found to relate to the ingestion of grass components.

Furthermore, these food items in primate diets have different biomechanical properties than in the diets of the selected ungulates. The DASTA indicates that primates feeding on large hard items (seeds, nuts, bark) have larger textural reliefs than primates whose diets include small hard items (grit and phytoliths). Based on the fracture and deformation theory proposed by Lucas *et al.* (2008) these results are interpreted as to show that large hard items fracture the enamel, whereas small hard items plastically deform it. The transition from brittle fracture to plastic deformation, therefore, depends on the size of the particle indenting (food particle). The results are in accordance with, and empirically support, the fracture and deformation theory on primates.

It was found that, besides discriminating dietary traits, industrial parameters reflect the end result of the dynamic interactions between food particles and enamel functional facets. Even though still speculative, a model is proposed to meld the results on both groups and to lay the basis for a general theory of dental wear. The DASTA points to a gradient in texture relief from leaf browsers with the flattest relief, to grazers with intermediate reliefs, to frugivores with the highest relief. The relief will be flattened in leaf browsers because of peak removal. Local fracturing will cause deep features in the textural signal of large hard object feeders (frugivores). Grazers will have intermediate reliefs because abrasives in/on grass would plastically indent the enamel surface. In ungulates with shearing action, the scars will be scratches; whereas in primates with crushing action prevailing, shallow pits will be the result. This gradient relates to interactions between food particles and enamel surfaces and to their fracture and deformation behaviors when they contact each other. This is the first step towards a universal theory of tooth wear.

Equus grevyi, upper tooth row, scale = 20 mm
From Schulz *et al.* (submitted, fig. 1)

1. Introduction

1. Introduction

The present Ph.D. thesis summarizes the work I have done for the last three years on 3D dental enamel microtexture analysis and dental function at the Biocenter Grindel and Zoological Museum of the University of Hamburg.

1.1 Mammal teeth and food

Mammals have evolved teeth that are capable of effectively and efficiently reducing a large variety of structurally diverse food components into small pieces (Hillson 2005), and, at the same time, that are able to resist fracture and abrasion (Popowics *et al.* 2001; Lucas 2004; Ungar 2008). Because most mammals have only one set of permanent dentition (Hillson 2005), their teeth have to retain their functionality for the entire life span. It is, therefore, to be expected that teeth show a high level of diet- and function-specific adaptation at all observational scales, from the whole tooth row at the milli- to centimeter scales (e.g. Fortelius 1985; Pérez-Barbería & Gordon 2001; Archer & Sanson 2002; Evans *et al.* 2007; Heywood 2010; Kaiser *et al.* 2010), to the enamel microstructure at the nano- to micrometer scales (e.g. Rensberger & von Koenigswald 1980; Young *et al.* 1987; Lucas *et al.* 2008; Kalthoff 2011).

Food is one of the main bonds between an organism and its environment. In the case of mammals, all the energy required to maintain their high metabolism is extracted from their food. There is, therefore, a need to extract nutrients as efficiently as possible from the ingested food (Rensberger 1995; Prinz & Lucas 1997). In all mammals but some primates (a few use tools to prepare the food before ingestion), the whole mechanical processing of the food takes place in the mouth. During mastication, teeth and muscles act together to reduce the ingested food into as small pieces as possible. This is both to maximize the surface areas of the fragments for enzymes to act on, and to allow the enzymes to access to nutrients previously enclosed in indigestible components (such as seed shells or lignin; Fortelius 1985; Prinz & Lucas 1997; Lucas 2004). Only if this step is efficiently carried out, can the guts extract the most out of the food ingested.

The role of saliva is four-fold:

(1) it lubricates the food particles so reduces the potential tooth wear from abrasives by washing them off (Prinz 2004);

(2) it serves to glue the food particles together to form a bolus that can be swallowed safely (Prinz & Lucas 1997);

(3) it acts to neutralize some harmful chemicals in the food (Owen-Smith *et al.* 1993; Shimada 2006; Mau *et al.* 2009);

(4) it contains enzymes, notably an α-Amylase that hydrolyzes starch into maltose in the mouth (Chauncey *et al.* 1963; Jacobsen *et al.* 1972; Mau *et al.* 2010).

During my Ph.D. I have focused on teeth and mechanical processing, and so the role of saliva will not be discussed further.

During mastication not only is the food broken up but also the teeth suffer damage. Even though teeth rarely break completely (Thenius 1989, and personal observations from collections; one exception being the canines of carnivores, van Valkenburgh 1996), food particles do fracture and abrade teeth at fine scales, resulting in the so-called dental microwear. *Microwear* refers to all the microscopic marks or scars on the tooth surfaces resulting from the wear by food particles. These marks are classified into two major categories, namely pits and scratches, depending on their length-to-breadth ratio (Gordon 1982; Grine 1986).

In those organisms that possess enamel, microwear is usually analyzed on the enamel instead of dentine for two reasons. Firstly, enamel is functionally more important than dentine because most of the processing occurs on the enamel surfaces. Indeed enamel either covers the whole tooth occlusal surface throughout early to moderate wear stages (or even later stages, especially in some carnivores and primates; Hillson 2005) or it stands above the softer dentine basins (especially in rodents and ungulates; Rensberger *et al.* 1984; Kaiser 2002; Hillson 2005). Second, enamel is mechanically (Xu *et al.* 1998; Lucas 2004) and chemically (Quade *et al.* 1992; Wang & Cerling 1994) more stable than dentine, rendering it more suitable for studies on fossils (morphology and/or isotope chemistry). In those mammals that, like Xenarthrans, lack enamel altogether (Ferigolo 1985; Hillson 2005), microwear studies have been conducted on the dentine and have yielded valuable results (Green 2009; see also Williams *et al.* 2009 on dinosaurs). However, the limitations of dentine studies as mentioned above limits a widespread use of dentine for analyses on fossils.

1.2 Terminology

Some of the terms used commonly in the dental research are poorly defined. Others have different meanings depending on the field of research where they are employed. I thus define some of the most important terms that I will use further herein. I stress that these definitions might not be generally accepted; they are both meaningful and pragmatic and are used consistently throughout this study.

Wear is defined as "the loss of volume of an object" (Lucas 2004, p. 181). Wear results from both mechanical and chemical processes. Mechanical processes play a larger role in tooth wear (Lucas 2004) and specimens with artifacts or chemical alterations can be easily identified and left aside (Teaford 1988; King *et al.* 1999).

Attrition refers to the "loss of tooth volume [wear] resulting from tooth-tooth contacts" (Dahlberg & Kinzey 1962, p. 242, translated from French), whereas *Abrasion* is defined as the "loss of tooth volume [wear] resulting from contacts between the tooth surface and foreign elements [such as food particles]" (Dahlberg & Kinzey 1962, p. 242, translated from French). Even though these terms can be confusing (Lucas 2004), their use is widespread in the dental research and I will therefore use them according to these definitions.

A *Facet* "is a wear surface, the orientation of which is dictated by interactive wear against one or several other facets" (Fortelius 1985, p. 7).

Hardness is the measure of "the resistance to deforming under indentation" (Lucas 2004, p. 269) and *Toughness* is "a measure of the resistance to crack growth in a material" (Lucas 2004, p. 266).

Plastic deformation refers to an irreversible change in shape of a material in response to applied forces, while *Brittle* materials fracture, break rather than deform (Lucas 2004).

"*Shear* is the action […] resulting from applied stresses which cause parts of the teeth to slide relative to each other in a direction nearly parallel to their planes of contact; *Crush* is the action resulting from stresses applied between two hard bodies in a direction nearly perpendicular to the approaching or actual plane of contact between them" (Kay & Hiiemae 1974, p. 228). *Shearing* and *Crushing* therefore only refer to

the relative motions of the surfaces; the food particles between the surfaces undergo compressive and tensile loads in both actions (Lucas 2004).

1.3 Review of previous dental microwear research

In this section, I review the main developments and results of the dental microwear research over the last 35 years. Microwear is a very vast topic, and so this review is selective rather than exhaustive.

P. L. Walker (1976) published one of the first microwear studies, on the incisors of primates. However, the first influential molar microwear analyses on mammals were conducted independently on rodents (Rensberger 1978) and on hyraxes (A. Walker *et al.* 1978). Notably Walker *et al.* (1978) examined the microwear patterns on the upper molars of *Procavia johnstoni* and *Heterohyrax brucei* with a scanning electron microscope (SEM). They found that the surfaces of the browsing *H. brucei* resemble those of *P. johnstoni* during the wet season when it, too, browses. The surfaces of the molars of both species show numerous pits. In contrast, during the dry season when individuals of *P. johnstoni* are grazers, the molar enamel surfaces show more scratches and fewer pits. Thus Walker *et al.* (1978) showed for the first time that dental microwear analysis has the potential to discriminate between different diets among mammals, and to even detect seasonality in feeding habits.

Following up on these works, numerous studies have applied dental microwear analyses, albeit with a wide variations in methodologies, to almost all mammalian families (see reviews in Grine *et al.* 2002; Ungar *et al.* 2003; Scott *et al.* 2009). Semi-automated methods have been developed to quantify the microwear patterns (e.g. with Microware, Ungar *et al.* 1991; Ungar 1995). All these studies have confirmed the results of Walker *et al.* (1978) that dietary categories can be distinguished by the differing proportions of pits and scratches on the enamel facets.

All these studies have relied on the analysis of high magnification SEM photographs (100 to 500×), which is time consuming and requires expensive equipment (Solounias & Semprebon 2002), making the analysis of large samples problematic. To solve these problems, Solounias & Semprebon (2002) proposed new methodology employing low-magnification (35×) stereomicroscopy. They recorded different types of pits and

scratches on a standard area (0.16 mm^2) on each surface. This method is much faster and cheaper, making it possible to analyze large samples. Although the scale of these observations differs from SEM studies (section 4.4.3), Solounias & Semprebon (2002) were able to differentiate statistically the feeding categories of the different ungulates (grazer, leaf-browser, fruit-browser, seasonal-regional mixed-feeder and meal by meal mixed-feeder). Subsequent work confirmed their results (e.g. Semprebon *et al.* 2004a; Semprebon *et al.* 2004b; Green *et al.* 2005; Nelson *et al.* 2005; Palombo *et al.* 2005; Rivals *et al.* 2007; Green 2009; Rivals *et al.* 2009b, a; Solounias *et al.* 2010).

Merceron *et al.* (2004; 2005a) further refined the low-magnification stereo-microscopy method by using 30× magnification which they increased to 120× on computer screen, and analyzed a standard 0.09 mm^2 area. They were able to successfully define precise size-based categories for these features, which allowed better quantification of the microwear patterns. This quantification was further eased by the use of imaging software like Optimas (Media Cybernetics®) and was subsequently applied in numerous studies (e.g. Merceron *et al.* 2005b; Merceron *et al.* 2006a; Merceron *et al.* 2006b; Merceron *et al.* 2007; Calandra *et al.* 2008; Goillot *et al.* 2009; Gomes Rodrigues *et al.* 2009; Peigné *et al.* 2009; Calandra *et al.* 2010; Merceron *et al.* 2010b; Ramdarshan *et al.* 2010).

The results of all these 2D microwear studies are consistent: the consumption of abrasive grass scratches the enamel facets, while browse and hard food more likely produce pits. This association between diets and microwear patterns enables reference databases to be assembled. The microwear patterns observed in fossil teeth can, therefore, be compared with entries in such databases. The diets of extinct species can then be inferred and their paleoenvironments can be reconstructed (see references above).

Most of the recent studies have aimed at reconstructing the diets of extinct organisms. Extensive work has also been conducted on reconstructing jaw movements from scratch orientation (e.g. Mills 1955; Teaford & Walker 1983; Gordon 1984; Young & Robson 1987; Teaford & Byrd 1989; Goswami *et al.* 2005; Charles *et al.* 2007), but there have been few studies on the microwear pattern in non-mammalian taxa though (Purnell 1995; Williams *et al.* 2009; Darras *et al.* 2010).

The effectiveness of 2D microwear methods is unavoidably limited by the large intra- and inter-observer errors that result from the great influence the orientation of the surface has on its appearance (both under the SEM and stereomicroscope) and because counting single features is hardly reproducible (it is even truer for heavily pitted or heavily scratched surfaces) (Grine *et al.* 2002).

The recent development of three-dimensional (3D) techniques addresses these limitations. Ungar *et al.* (2003) acquired 3D representation of the enamel facets with tandem scanning confocal microscopy, thus solving almost completely the problems caused by the orientation of the surface, since the surface is no longer projected onto a two-dimensional (2D) plane (but see section 2.4 and Fig. 2.4). The analysis of these 3D surfaces is further automated through "scale-sensitive fractal analysis" (SSFA), which renders the analysis both faster and more reproducible. SSFA extracts 3D attributes of the *microtexture* of the whole surface; so single features, such as pits and scratches, are no longer considered. Scott, Ungar and coworkers termed this method "dental microwear texture analysis" (Scott *et al.* 2005; see section 2.7).

This method led to the publications of several papers on a variety of mammalian families, which all pointed out that the consumption of hard food items can be discriminated from tough foods based on the complexity, anisotropy and textural fill volume parameters of the surfaces of primates (Scott *et al.* 2005; Scott *et al.* 2006; Krueger *et al.* 2008; Ungar *et al.* 2008; Merceron *et al.* 2009; Scott *et al.* 2009). Complexity and anisotropy of the surfaces can also identify differing bone consumption rates among carnivores (Schubert *et al.* 2010; Ungar *et al.* 2010). This method was also applied to ungulates and it was shown that grazers have more anisotropic and less complex surfaces than browsers (Ungar *et al.* 2007). Moreover this 3D approach has the potential to identify seasonal and sexual differences in diet (Merceron *et al.* 2010a). Finally, it has been applied to the incisors of bioarcheological groups (Krueger & Ungar 2010).

The last development in microwear techniques is the topic of my Ph.D. project, which is based on the 3D methodology of Ungar, Scott and coworkers. But following Kaiser & Brinkmann (2006), numerous standardized parameters developed for the quantification of industrial surfaces were used (Schulz *et al.* 2009, 2010a, b, submitted). This has led to the development of "dental areal surface texture analysis" (DASTA), which quantifies 3D roughness parameters from the surface (Schulz *et al.* 2010a; Calandra *et al.* submitted; Schulz *et al.* submitted). These parameters are standardized

and can, therefore, be readily compared between studies. Furthermore, they can now be quantified by every 3D acquisition and processing software package. This method and its applications are the subject of my Ph.D. Details, results and implications will be discussed in sections 2-4.

Throughout this work, *microwear* analyses will refer to 2D semi-quantitative scoring methods that count microwear features (e.g. Walker *et al.* 1978; Solounias & Semprebon 2002; Merceron *et al.* 2005a; Rivals *et al.* 2007). *Microtexture* analyses will refer to methods that quantify the surface texture. Both the SSFA and the DASTA are microtexture analyses.

1.4 Grit and dust *versus* phytoliths

The debate over which food items are responsible for microwear has received a lot of attention recently. Unfortunately no consensus has emerged on this, because no conclusive data are available yet to settle the question. I now briefly review this debate.

This debate centers in particular around which agent(s) is responsible for the intensive scratching observed on the enamel facets of grazing ungulates. Two possible agents have been proposed: (1) *endogenous phytoliths* or (2) *exogenous grit and dust*.

Phytoliths are amorphous siliceous bodies that are deposited either intracellularly or extracellularly in the vegetation (Piperno 2006). Poaceae (grass) deposit more phytoliths in their tissues than other angiosperms (like foliage) do (Epstein 1999; Hodson *et al.* 2005; Piperno 2006).

Damuth & Janis (2011) recently reviewed the role of these phytoliths in the plant physiology and their influence on the feeding behaviors of herbivores. High phytolith concentrations both increase the abrasiveness and decrease the nutritional quality of grass, and influence the growth rates of juveniles and mature females in voles (Massey & Hartley 2006; Massey *et al.* 2007). Small mammals seem sensible to this factor and select grasses with fewer phytoliths (Massey & Hartley 2006; Cotterill *et al.* 2007; Massey *et al.* 2007). The same influence has been observed on leaf-eating insect (e.g. Massey *et al.* 2006). The phytolith concentration does not have an important influence on the feeding preferences of larger mammals. Massey *et al.* (2009) showed that although grazing sheep select the most palatable grass species, phytolith concentrations are only

partially responsible for determining palatability. The effect that phytoliths have on the feeding behaviors of herbivores varies between insects, and small and large mammals. Higher phytolith concentrations in any case play a role in feeding preferences (see also references in Damuth & Janis 2011).

Baker *et al.* (1959) measured the hardness of the silica phytoliths in oats and found that they are harder than sheep's enamel. This was the first experiment to support the hypothesis that phytoliths are the physical agents responsible for the microwear scratches. Walker *et al.* (1978) found that the amount of rock particles (*i.e.* grit) in fecal pellets of hyraxes is similar in the browsing species *Heterohyrax brucei* as the grazing species *Procavia johnstoni*. The quantities of phytoliths are much higher in the grazer's diet as phytoliths are almost absent from the browser's diet. Walker *et al.* (1978) concluded that the silica phytoliths, and not the rock particles, are responsible for the intense scratching of the enamel surface of the grazer. This study, however, concerned only two species.

In a more recent indentation study Sanson *et al.* (2007) found that the tooth enamel is harder than silica phytoliths, and so concluded that silica phytoliths cannot scratch the enamel. Grass is shorter, so the grazers feed closer to the ground, where dust deposited on the plants and soil particles (grit) ingested with the plant material (geophagy) are probably responsible for the intense scratching seen on the enamel of the grazers, which is associated with grass consumption. Unlike Walker *et al.* (1978), Mainland (2003) found similar amounts of phytoliths in the dung of browsing and grazing sheep, but different amounts of grit, concluding that grit ingested with the plant material may account for the intense scratching. This last study only addressed the problems in two populations of a single species.

Merceron *et al.* (2005a) presented results on the microwear pattern of the lowland gorilla (*Gorilla gorilla gorilla*). The gorilla lives in humid forests where it feeds on tall grasses. These authors concluded that the intense scratching of the gorilla's enamel facets can result neither from deposited dust because of the humid environment, nor from the ingestion of soil because the grasses they eat are tall. Hence they favored the phytolith hypothesis. Results from Solounias & Semprebon (2002, p. 24) "do not support the hypothesis that grit and dust may cause an increased number of scratches on tooth enamel". Instead, from the microwear pattern of species inhabiting dry and open habitats (camels, vicugna and pronghorn antelope) or consume soil together with

plant roots (African bush pig), they concluded that grit and dust rather produce pits, gouges and coarse scratches. Merceron *et al.* (2004) also explained the more intense pitting in *Rangifer tarandus* (Reindeer) by the ingestion of grit together with ground lichens. Mainland (2000) studied the microwear pattern of seaweed-eating sheep and found that it is the ingestion of grit together with seaweed (which does not contain silica phytoliths) that produce their rather pitted enamel facets. She, however, emphasized that the vertical jaw movements of the sheep when feeding on this structurally specific diet have a large influence on the types of features produced (pits *vs.* scratches).

Damuth & Janis (2011) recently reviewed the data on hypsodonty and its causes. They concluded that, even though the phytoliths probably play a role, it is the consumption of grit and dust that is the main driver of the evolution of hypsodonty. Hypsodonty therefore relates more to feeding in open and dry habitats than to feeding on grasses (Mendoza & Palmqvist 2008). There is, however, no need for the same abrasives to be responsible for the scratching of the enamel at the microwear level and for the evolution of hypsodonty since scratching does not necessarily lead to higher wear rates.

A last point concerns the hardness of phytoliths and grit relative to tooth enamel. Gügel *et al.* (2001) performed chewing experiments and found that phytoliths alone can produce microwear features. While these experiments do not demonstrate that phytoliths do wear enamel *in vivo*, they show that they have the potential to do so. They unfortunately focused only on pits, leaving the question open for scratches.

It is known that softer materials can wear harder ones (Boyde 1984). Moreover, the hardness of enamel is probably inhomogeneous, and varies with the internal structure and orientation of enamel prisms. Finally, the hardness of phytoliths may also vary from one plant species to another, and even within a single plant species (Damuth & Janis 2011). Indentation experiments such as Sanson *et al.* (2007) might not therefore help to settle the question.

In summary, there seems to be more evidence supporting the phytolith hypothesis. This does not mean that grit and dust have no influence on the microwear of enamel; they certainly play an important role as well. The issue is still unresolved but this does not jeopardize the results of microwear/microtexture analyses. Indeed, whatever the main scratching agent is, both phytoliths and grit are almost always associated with

and more abundant in/on grasses than in/on the foliage of trees (Merceron *et al.* 2007). Answering this question will nevertheless allow for more precise dietary and environmental assessments based on tooth microwear/microtexture.

1.5 Fracture and deformation theory, and microwear formation

It might seem logical to think that tooth wear reduces the functionality of the teeth. While this is true in the very early stages of wear or with excessive wear as in senile animals (Pérez-Barbería & Gordon 1998b; Lucas 2004), some wear is needed before teeth become fully functional. Tooth wear is therefore a functionally necessary mechanism (Osborn & Lumsden 1978; Pérez-Barbería & Gordon 1998b; Lucas 2004; Hillson 2005).

Tooth wear can be separated into two categories: attrition and abrasion (see section 1.2). It is stressed that wear is never purely attritional or purely abrasional; when considering chewing systems both processes are occurring simultaneously across every single wear facet during a complete masticatory cycle. Only the relative proportion of attrition to abrasion varies from one type of facet to another: some facets are attrition-dominated, while others are abrasion-dominated, depending on the chewing movements (Butler 1952, 1972; Kay & Hiiemae 1974). The relative proportion of attrition *vs.* abrasion also depends on the type of food consumed (section 4.1.2). Finally, the relative proportion of attrition increases with the processing of food: as the food gets reduced into small pieces, the teeth come closer to each other (Kay & Hiiemae 1974).

Attrition is defined as tooth-tooth contacts (section 1.2). This meaning was however defined at the macroscopic scale. Attrition does not necessarily involve actual contact between antagonistic teeth at the microscopic scale; the surfaces may come very close together without making physical contact. Also the zones where contact does occur may not be continuous and contacts may be at points rather than across areas. Attrition therefore only implies that the tooth surfaces come very close to each other, and a threshold defining how close is “very close” needs to be fixed. Again, this discussion is beyond the main focus of this thesis, so the definition of attrition as stated in section 1.2 will be used below.

On a macroscopic scale, attrition can sharpen the teeth and has been proposed as an

important mechanism maintaining tooth functionality throughout the whole lifetime of a mammal, either through normal masticatory action (Osborn & Lumsden 1978) or through "thegosis" (Every 1960, 1970, 1975; see Murray & Sanson 1998 for a critical review). This process is known to occur even before birth in some mammals (Teaford & Walker 1983). At microscopic scales though, these contacts are more likely to flatten surfaces by breaking off the peaks (section 4.1.2).

Attrition contacts provide information on the chewing movements across the wear facets. On the other hand, abrasion-dominated facets are more informative for the reconstruction of diets because they result directly from the wear generated by food contacts. Gordon (1982) noted that the dichotomy between attrition and abrasion facets is evident only at very low magnification, and becomes blurred at higher magnifications. The distinction between facet types is, therefore, largely irrelevant to microwear/microtexture analysis as presented in this work (Gordon 1982).

The analysis of dental microwear looks for associations between known diets and the observed microwear patterns. A basic assumption of microwear analysis is that the microwear pattern is dependent only on the biomechanical properties of the food items being processed. This means that it is largely independent of the underlying morphology or of the phylogenetic structure of the studied organisms (Semprebon *et al.* 2004a). The enamel microstructure, which is used in taxonomy (e.g. Escala & Gállego 1977; von Koenigswald 2004a, b; Martin 2007), probably has an influence on the microwear formation (Gordon 1988). This effect, however, seems to be relatively minor (Gordon 1982) since numerous studies have found that there is a strong association between microwear patterns and diets of extant species with known diets, across Orders (e.g. Solounias & Semprebon 2002; Semprebon *et al.* 2004a). No single proxy can predict with 100% accuracy, and microwear analysis is no exception. The some deviation from the expectations can result from the phylogenic and morphological influences on the microwear, but, as already stated, this influence seems minor. Hence dental microwear analysis can be assumed to be a reliable proxy for dietary reconstructions.

The observed microwear pattern is a short-term signal, typically reflecting the diet during the last few days of an animal's life ("Last Supper Syndrome"; Teaford & Oyen 1989a; Teaford & Robinson 1989; Solounias *et al.* 1994; Merceron *et al.* 2010a; Schulz *et al.* 2011). This implies that the method can sample both local and/or seasonal signals, which can be either a strength or a weakness of the method, depending on the goals of the study.

Beside the associations between microwear patterns and diet, some studies have focused on the mechanical causes of these associations. Wear processes and interactions between food particles and tooth surfaces were extensively studied by Lucas and coworkers (Lucas 2004).

As discussed in the previous section, hard food items are more likely to produce pits on the surface, whereas the consumption of more abrasive foods results in scratches.

Both pits and scratches, however, result from the same indentation processes: scratches are produced by shearing motions, whereas pits are caused mainly by the crushing component (Gordon 1982; Lucas 2004). Pits can also be generated by fracturing the surface, when a fragment of the surface is chipped off (Lucas 2004; Lucas *et al.* 2008). Lucas *et al.* (2008) concluded that the transition from plastic to brittle deformation is dependent on the size of the indenting particle (section 4.2.2).

Lucas (2004) stated that mechanical damage to food items can be avoided by two mechanisms (1) stress-limited and (2) displacement-limited defenses. Stress-limited mechanisms refer to objects being structurally organized so as to prevent the formation of cracks. These objects are called "hard" (Lucas 2004). Examples of hard food items are seeds, bark and silica (as exogenous grit and dust, or endogenous phytoliths, see section 1.4). The displacement-limited mechanisms prevent any cracks that are initiated from propagating through the structure. This is achieved through high toughness and such objects are therefore called "tough". Tree leaves and grass blades are considered to be tough foods (Lucas 2004).

In order to initiate fracture into hard food, high compressive loads must be applied between the antagonistic teeth (Fig. 1.1a). A pit on the enamel facet may result, either from indentation or from brittle fracture (Lucas 2004; Lucas *et al.* 2008). Conversely, shearing is required to efficiently propagate a crack through tough food items (Lucas 2004; Fig. 1.1b); a mechanism that can only be efficient, if increased tooth-tooth contact occurs along surfaces functioning as shearing blades, *i.e.* attrition (see section 1.2). This shearing will more likely produce scratches on the enamel facets.

These processes are easily understood. When you want to eat a nut, you first have to break the shell with a nutcracker. You therefore press onto the nutcracker with some force (sometimes as hard as possible!) and, at some point, the shell breaks. It is difficult to initiate fracture, but once it is done, the whole structure tends to break into pieces (brittle fracture; Lucas 2004). On the other hand, you pressing a tree leaf will not break

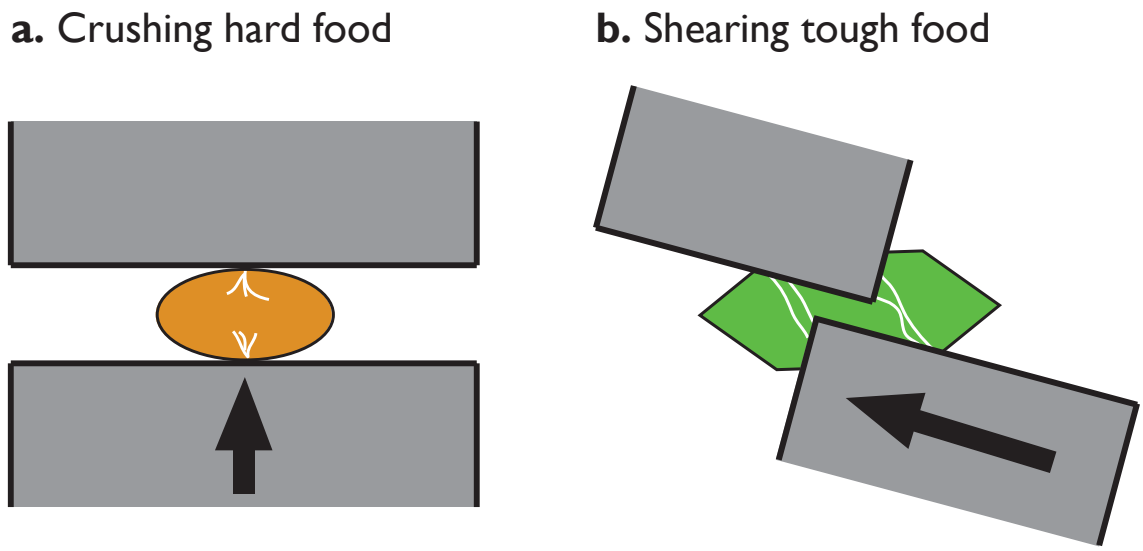

Figure 1.1. Schematic representation of the crushing and shearing processes. (**a**) When processing hard foods (like a seed, *orange ellipse*), the two opposing surfaces (*gray blocks*) move perpendicularly to each other (*black arrow*) and induce fractures (*white wavy lines*) into the hard object through crushing. (**b**) On the contrary, the cracks (*white*) need to be propagated through tough foods (like a tree leaf, *green polygon*). This is achieved through movements of the opposing surfaces parallel to each other (*arrow*), a process known as shearing. Elements not to scale.

it into small pieces. A leaf has to be torn so that the fissure extends from one side to the other, and then you need to repeat the process to comminute the leaf into smaller and smaller pieces (Lucas 2004).

Teeth are also structured so as to avoid mechanical damage, in the same way food particles are. Enamel is a very hard material (Lucas 2004), and species specializing on hard diets usually have thick enamel to prevent fracture (e.g. Kay 1981; Popowics *et al.* 2001; Ungar *et al.* 2008). However, protection based solely on hardness can be hazardous, since a single crack can be disastrous. So in addition to a covering of hard enamel, other dental structures block crack propagation, rendering the teeth tougher. Hunter-Schreger bands (HSB) are "light and dark bands of enamel seen under light microscopy. These bands are a phenomenon of the variation in the reflective property of sets of prisms, depending upon the direction of the prisms with respect to the source of light" (Rensberger & von Koenigswald 1980, p. 481). Cracks occur preferentially between the enamel prisms rather than across them, so the presence of HSB effectively blocks crack propagation (Rensberger & von Koenigswald 1980; Fortelius 1985; Xu *et al.* 1998; Martin *et al.* 2003; Lucas *et al.* 2008). Dentine is tougher than enamel, so it can

better resist cracking (Xu *et al.* 1998). Any cracks that do occur rarely, if ever, extend beyond the enamel-dentine junction (Xu *et al.* 1998; Lucas *et al.* 2008).

These processes are diet-specific: the consumption of hard objects results in the formation of pits, while chewing tough materials generates scratches on the enamel facets. These processes are function-specific as well: pits results from the compressive loads needed to initiate the fracturing of hard objects, whereas scratches are produced by the shearing forces required to comminute tough items.

It is clear that microwear is not completely independent on the underlying morphology, since facet orientation and chewing movements, for example, are related to tooth morphology. Even though the biomechanical properties of food are the same for all herbivores, the dynamics of chewing differ between mammalian orders and families (e.g. Hiiemae 1978). Diet- and function-specific processes can however be used to further define chewing biomechanics within a group (see section 4).

It implies that comparisons across mammalian orders are difficult. This is why the results on different orders cannot be readily interpreted within a common mechanistic framework. The same general wear processes, however, apply to all mammals, posing the following questions:

(1) How can food with specific biomechanical properties be broken down?

(2) What are the requirements of tooth biomechanics and chewing dynamics to process such foods?

(3) How do the tooth micro- and macrostructures relate to these requirements?

Based on the results of this thesis, I will suggest some partial answers to these questions (section 4.4.2).

1.6 Hypotheses

My Ph.D. thesis is organized along five hypotheses related to filtering options (hypothesis 1), diet and tooth function (hypotheses 2-4), and sample size (hypothesis 5). The five hypotheses are presented here, and will then be discussed separately (sections 4.1-4.3).

1.6.1 Robustness of DASTA texture parameters across filtering thresholds (hypothesis 1)

3D standardized texture parameters are still quite new and until now, we know little about the influence of the necessary pre-processing filtering on biological surface data. In particular the stability of surface texture parameters after applying texture filter algorithms is still a matter of uncertainty (Schulz *et al.* submitted). In 2D surface profiles topometric information is split into three classes of geometric information: (1) form, (2) waviness and (3) roughness (Thomas 1991). Here, form describes the broad scale geometry, which is of limited use in evaluating tooth wear (Kaiser & Brinkmann 2006). Waviness includes longer wavelength (more widely spaced) surface alterations from its nominal shape, while roughness includes the finest (shortest wavelength) alterations. There is, however, no consensus about the wavelength threshold, which separates 2D roughness from 2D waviness (Thomas 1991). This holds true with 3D data.

Dental enamel forms a complex 3D network of crystallites, which, when exposed by wear on the occlusal surface, is responsible for highly structured, low amplitude alterations reflecting the local resistance towards abrasion. The frequency of these alterations is lower than the frequency of scars. On the ectoloph of the Black Rhino (*Diceros bicornis*) the regular pattern of groves can be seen with the naked eye (Rensberger & von Koenigswald 1980). On the other hand, the wear-related pattern of scars corresponds to the microwear/microtexture (sections 1.1-1.3). Similar to technical surfaces, wear features bear a functional signal (Schulz *et al.* 2010a). Hence it is necessary to separate wear-related surface features from structure-related ones. Therefore, the hypothesis that wavelength thresholds in ISO/FDIS 25178-2 (International Organization for Standardization 2010; section 2.6) filtering options should reflect chewing mechanics and anatomy is tested. It is expected that after separating structural features what remains is the wear-induced pattern of scars, which is morphology-free but instead reflects feeding and environmental traits (hypothesis 1; Schulz *et al.* submitted).

This hypothesis is specifically tested on a dataset of ungulates (Schulz *et al.* submitted) because they represent different enamel structure types and because ungulates are widely used as paleoenvironmental indicators (section 1.3).

1.6.2 Testing for characteristics of food and masticatory biomechanics through the DASTA (hypothesis 2)

In herbivores, endogenous (phytoliths) and exogenous (grit and dust) abrasives are responsible for most of the tooth wear (Damuth & Janis 2011; section 1.4). Within a spectrum of adaptations relating herbivores with their diets, grazers from open habitats would be at the most abrasion-dominated (Baker *et al.* 1959; Healy & Ludwig 1965; Sanson *et al.* 2007), while browsers from closed habitats would generally have the smallest amounts of abrasive wear (Janis & Fortelius 1988). This hypothesis focuses on cheek dentitions of grazers and browsers only, because they represent the most extreme traits within a continuum of feeding traits (Schulz *et al.* submitted). These traits are represented by four model species which partially coexist in the sub-Sahara African savannah ecosystems (section 2.2). They also correspond to two post-oral digestive strategies: the Grevy's zebra and the Black Rhinoceros are hindgut fermenters while the Blue Wildebeest and the Giraffe are ruminating foregut fermenters.

Once the influence of the pre-processing has been assessed (hypothesis 1), it is tested whether functional parameters as specified in ISO/FDIS 25178-2 (International Organization for Standardization 2010), ISO 12781-2 (International Organization for Standardization 2011) and in industrial surface analysis (motif, furrow, direction, isotropy, and flatness analysis) can be employed to robustly distinguish dietary traits across systematic affinities and digestive strategies (Schulz *et al.* submitted). Testing this hypothesis represents a new innovative approach in dietary reconstruction because the standardized 3D surface analysis has been developed to functionally characterize technical surfaces but the potential to assess biological life history traits is still unknown. The power of 46 industrial 3D parameters as a toolsets to approach dental functional traits in relation to food and masticatory biomechanics is investigated (hypothesis 2; Schulz *et al.* submitted).

1.6.3 Primate diets assessed by the SSFA (hypothesis 3)

Primates consume highly diverse diets that include resources that most ungulates rarely consume, including fruits, seeds, grass, tree leaves, bark, roots, tubers, and animal resources. Fruits are the main component in the diets of many primates. Fruits are considered to be hard items, because they contain seeds that can fracture (*sensu* Lucas *et al.* 2008) the enamel and produce significant scars on occlusal surfaces. Other items are hard, such as seeds, bark, and insect cuticles and these can fracture the enamel as

fruits do (Lucas 2004). Substantial consumption of fruit and of other hard items results in many large and deep pit-like surface features; a pattern which is characteristic of the consumption of hard objects (Scott *et al.* 2006; Scott *et al.* 2009). Until now it has never been tested as to whether the fruit proportion can be used as a continuous variable and whether this proportion can be correlated with microtexture patterns.

Seeds in particular are of great interest because they are consumed in large proportion together with fruits. They represent the hard parts of fruits while the flesh itself is soft. Primates can process the seeds in four different mechanisms (Corlett & Lucas 1990; Lucas & Corlett 1998; Lucas 2004): destroy, spit, swallow or clean them. Most frugivore primates use several or all of these mechanisms in combination as they exploit and disperse the same fruits, with different frequencies (Lambert & Garber 1998). However, the microtexture pattern on the facets of post-canine teeth cannot detect and/or discriminate between seed spitting, swallowing and cleaning because these three mechanisms do not involve contacts between the seeds and the molars. Whereas seed destroying, involving the seeds being crushed by the premolars and molars in order to extract their content, will impact molar enamel facets and therefore produce patterns accessible to microtexture analysis. Even if the consumption of seeds and of hard items in general is occasional or incidental, it can significantly impact the enamel facets ("fallback foods"; Solounias & Semprebon 2002; Ungar *et al.* 2008; Scott *et al.* 2009; Merceron *et al.* 2010a) and should therefore be taken into account when reconstructing diets.

Theropithecus gelada consumes large amounts of grass leaves (Gippoliti & Hunter 2008; Gron 2008). When the grass is sheared, both the hard silica phytoliths that it contains or the grit and dust deposited on it (section 1.4) can scratch the enamel surface. The resulting scars run roughly parallel to the direction of mastication (Mills 1955), producing a strictly oriented microtexture pattern (Scott *et al.* 2006).

With this primate dataset, the following hypothesis was tested (Calandra *et al.* submitted): The scale-sensitive fractal analysis can be used to infer key aspects of the diets of primates, in particular the proportion of fruits and the consumption of other hard items and grass (hypothesis 3).

1.6.4 DASTA, food biomechanics and tooth function of primates (hypothesis 4)

As explained in section 1.5 and as it will be tested in hypothesis 3, a large part of microwear research focuses on the relationship between diet and microwear patterns.

Further on, it is expected that microtextures are also largely influenced by the set of biomechanical forces, which make the occlusal surface an integral functional interface between the individual and its environment. This means that textures need to be considered as the result of a dynamic feedback mechanism between food biomechanics, neuromuscular system of the chewing apparatus and the environmental stimuli. Lucas *et al.* (2008) developed a theory of deformation and fracture mechanics of the enamel of hard object feeder primates. They proposed that the wear behavior of enamel is dependent on the size of the indenter: large particles (seeds, nuts) fracture the enamel whereas small particles (grit, but more likely dust, and phytoliths) indent it. The DASTA is used to empirically test this theory by quantifying interactions that reflect biomechanical properties of food as well as function of a specific tooth area (hypothesis 4). Specific ISO texture parameters originally designed to functionally classify technical surfaces were selected and applied to enamel surfaces of primates (Calandra *et al.* submitted).

1.6.5 Microtexture analyses with small sample sizes (hypothesis 5)

Enamel surface microtexture databases for extant species with known diets (concerning mainly ungulates and primates) are being created using the two microtextural methods presented in section 1.3 (see also sections 2.6-2.7) (Ungar *et al.* 2007; Krueger *et al.* 2008; Ungar *et al.* 2008; Scott *et al.* 2009; Merceron *et al.* 2010a; Schubert *et al.* 2010; Schulz *et al.* 2010a; Ungar *et al.* 2010; Calandra *et al.* submitted; Schulz *et al.* submitted). The microtexture pattern can be highly variable in time as a result of overprinting (Teaford & Oyen 1989a; Solounias & Semprebon 2002), so these databases include a large number of specimens per species in order to establish a robust estimate of the microtexture pattern for a given food resource. However, most studies on extinct species, especially on primates, have to rely on the small number of fossils available (e.g. Ungar *et al.* 2004; Ungar 2005; Merceron *et al.* 2006a; Scott *et al.* 2006; Merceron *et al.* 2009). This raises the question of whether databases with large samples do indeed provide a good reference for comparison with small samples of fossils. Small samples require specific statistical methods that are different from the widely used methods based on large samples.

Therefore, it is tested whether microtexture analyses of small samples ($5 \leq n \leq 10$) are as effective as large samples ($n > 15$) in inferring diets, and in reconstructing the diets of extant species (hypothesis 5). The testing of this hypothesis is based on the results from the previous hypotheses (2 to 4). It is therefore tested last.

µsurf custom

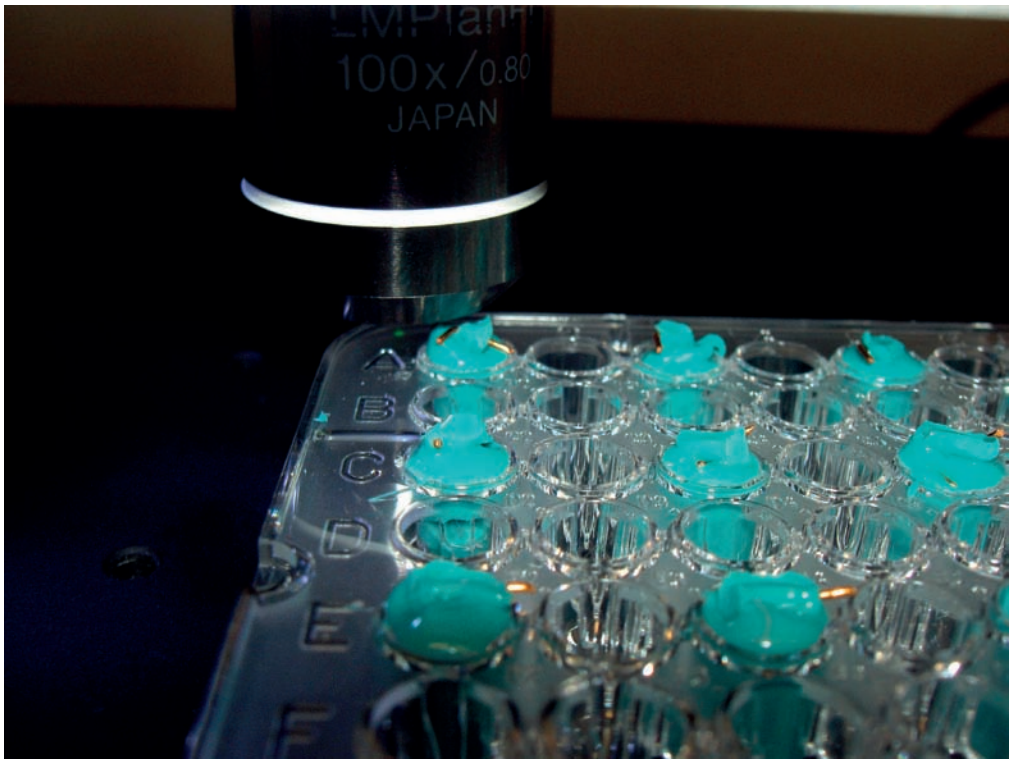

2. Material and Methods

2. Material and Methods

This section describes the methodology applied to quantify the microtexture patterns of biological surfaces (Schulz *et al.* 2009, 2010a, 2010b submitted). This procedure has been used on all the datasets presented in this study.

2.1 Specimen selection

Care has been taken to use only adult specimens showing an intermediate wear stage that corresponds to a fully functional dentition. For this, only individuals where the third upper molar (M^3) is already in occlusion (*i.e.* worn) have been subsequently analyzed. This corresponds to Individual Dental Age Stage 3 (Anders *et al.* 2011). Animals with signs of malocclusion, other dental disease or malformation, *postmortem* alteration, or enamel facets covered with glue have not been considered.

Even some specimens that seem to show a clear diet-related microwear pattern to the naked eye or to low magnification fail to reveal, at high magnification, any food-related microtexture (e.g. flat surfaces or chemical alterations). The very high resolution used (section 2.4) probably enhances this problem because every single detail of the microtexture can be clearly seen. Very clean specimens are therefore needed, which are difficult to find.

Specimens also need to be very clean because the developed 3D method is automated. 2D scoring microwear methods quantify only the selected features (pits, scratches, gouges…; section 1.3). The inter-microwear space ("background") of the microwear photograph is not taken into account. On the other hand, 3D methods quantify the whole texture. There are no features or background textures that are eliminated based on the decision of the observer; both have the same importance. While it is possible manually to erase defects or dust particles from a 3D surface model (section 2.5), such manipulation is both time consuming and subjective, and introduces intra- and inter-observer errors (section 1.3). The automation of 3D methods has the advantages of making the analysis much faster and reduces errors generated by intra- and inter-observation (Ungar *et al.* 2003).

In summary, a large proportion of the specimens has been excluded and only the data from specimens that display a clear food-related microtexture has been retained.

2.2 Material

Two groups of mammals were included in this work. First, a total of thirty upper cheek dentitions of four African ungulates (Linnaeus, 1766) were evaluated (Schulz *et al.* submitted):

- the Blue Wildebeest, *Connochaetes taurinus* (Burchell, 1824), Bovidae, Cetartiodactyla, ruminating foregut fermenter, n = 7;
- the Grevy's zebra, *Equus grevyi* Oustalet, 1882, Equidae, Perissodactyla, hindgut fermenter, n = 7;
- the giraffe, *Giraffa camelopardalis* (Linnaeus, 1758), Giraffidae, Cetartiodactyla, ruminating foregut fermenter, n = 7;
- the Black Rhinoceros, *Diceros bicornis* (Linnaeus, 1758), Rhinocerotidae, Perissodactyla, hindgut fermenter, n = 9.

The specimens included in this dataset are all adult wild-caught individuals housed at the Zoologisches Museum Hamburg and Museum für Naturkunde Berlin (Appendix 2.1). Only originals were used (Schulz *et al.* submitted).

E. grevyi inhabits semi-arid grass/shrub land mainly in Kenya (Klingel 1974; Rubenstein 1986; Rowen & Ginsberg 1992; Williams 2002), where up to 70% of its diet results from grazing long and dry grasses, the remaining 30% are acquired by browsing notably either during droughts or in areas of overgrazing (Klingel 1974; Williams 2002). *C. taurinus* occupies similar environments to *E. grevyi* and it feeds on fresh short grasses (88%), and up to 12% browse depending on season (Owaga 1975; Skinner & Smithers 1990; Gagnon & Chew 2000; Ego *et al.* 2003). Traditionally both are considered as grazers (Fortelius & Solounias 2000; Solounias & Semprebon 2002). *D. bicornis* inhabits savannah and succulent bushveld areas (Joubert & Eloff 1971) where more than 50% of what it consumes is acquired by browsing mainly acacia leaves and twigs, herbs and succulents (Joubert & Eloff 1971; Mukinya 1977; Oloo *et al.* 1994). The browsing *G. camelopardalis* occurs in arid and dry-savannahs dominated by *Acacia* wood- and scrublands of sub-Saharan Africa (East 1984; Fennessy & Brown 2010). Its diet consists of nearly 80% acacia browse, seeds, pods, fruits and shouts, and 10-20% of herbaceous perennials (Leuthold & Leuthold 1972; Pellew 1984).

The second dataset (Calandra *et al.* submitted) includes eight species of Primates Linnaeus, 1758: *Alouatta seniculus* (Linnaeus, 1766); *Gorilla gorilla* (Savage, 1847); *Lophocebus albigena* (Gray, 1850); *Macaca fascicularis* (Raffles, 1821); *Pan troglodytes*

(Blumenbach, 1775); *Papio cynocephalus* (Linnaeus, 1766); *Pongo abelii* Lesson, 1827; and *Theropithecus gelada* (Rüppel, 1835). Their diets are diverse and vary seasonally, so the mean annual proportions of each food component given in the literature has been assumed (Table 2.1).

Wild caught specimens of *T. gelada* are difficult to find in collections because of its limited geographic range; despite comprising only two specimens, this species was included in the dataset, because it is the only real grazer available (Gippoliti & Hunter 2008; Gron 2008). *Alouatta seniculus* is the second species with a very limited number of specimens (n = 3) and retained, because it is the only primate species available that predominantly consumes large amounts of tree leaves (Palacios & Rodriguez 2001; Gron 2007; Boubli *et al.* 2008).

The specimens are housed at four different institutions in Germany: Anatomische Sammlung des Institutes für Anatomie und Zellbiologie der Universität Greifswald, Senckenberg Forschungsinstitut und Museum in Frankfurt am Main, Museum für Naturkunde Berlin, and Zoologisches Museum Hamburg (ZMH). All ZMH specimens were molded from originals; the others from high-resolution epoxy casts of the whole tooth rows from the dental cast collection of the ZMH (Appendix 2.2).

2.3 Molding procedure

Some components of the following sections (2.3-2.6) have already been published (Schulz *et al.* 2010a). Here I present an extended and adjusted version of the protocols used in the molding procedure, data acquisition and pre-processing. The microtexture analysis was not termed yet for this first publication. The "dental areal surface texture analysis" (DASTA) has only recently been defined (Calandra *et al.* submitted; Schulz *et al.* submitted). Section 2.6 details the basic DASTA (but it is still possible to adapt some steps in the analysis depending on the data set).

A facet on the upper first (M^1) or second (M^2) molar (Fig. 2.1a-b) was selected and cleaned with ethanol or acetone. Each facet was individually molded because neither entire tooth rows nor skulls can be scanned easily: whole teeth are difficult to orientate and complete skulls cannot be fitted below the objective of the microscope. The facets were molded using the high resolution silicone-A dental impression material Provil novo Light C.D. fast set EN ISO 4823, type 3, light (Heraeus Kulzer GmbH, Dormagen,

Table 2.1. Primate dietary and habitat information.

Species	Diet [a]	Seed treatment [b]	Habitat	References
Alouatta seniculus	Fruits (52%) Leaves (35%) Other vegetation (13%)	Swallower	Brazil, South America Rain forest Arboreal	Palacios & Rodriguez (2001) Gron (2007) Boubli *et al.* (2008)
Gorilla gorilla	Grass (55%) Fruits (45%)	Swallower	Central Africa Lowland and swamp forests Terrestrial	Remis *et al.* (2001) Cawthon Lang (2005a) Merceron *et al.* (2005a) Walsh *et al.* (2008)
Lophocebus albigena	Fruits (43%) Insects (36%) Leaves (10%) Bark (9%)	Destroyer	Central Africa Primary, secondary forests Upper canopy	Lambert *et al.* (2004) Oates *et al.* (2008a)
Macaca fascicularis	Fruits (82%) Leaves Flowers Insects	Spitter (>70%), destroyer, swallower, cleaner	Sumatra, Indonesia Tropical rain forests Lower canopy, terrestrial	Corlett & Lucas (1990) Lucas & Corlett (1998) Wich *et al.* (2002) Cawthon Lang (2006c) Ong & Richardson (2008)
Pan troglodytes	Fruits (<90%) Leaves (16%) Others	Swallower, cleaner	Cameroon, Africa Variety of woodlands Terrestrial and arboreal	Lucas 2004 Tweheyo *et al.* (2004) Cawthon Lang (2006b) Moscovice *et al.* (2007) Oates *et al.* (2008b)
Papio cynocephalus	Fruits (35%) Grass (30%) Other vegetation	Spitter	Kenya, Africa Savanna, open woodland, and gallery forests Terrestrial	Norton *et al.* (1987) Lucas (2004) Cawthon Lang (2006a) Kingdon *et al.* (2008)
Pongo abelii	Fruits (mainly figs; 68%) Other vegetation (17%) Insects (9%)	Spitter, swallower, destroyer	Sumatra, Indonesia Primary rain forest Arboreal	Cawthon Lang (2005b) Taylor (2006) Wich *et al.* (2006) Singleton *et al.* (2008)
Theropithecus gelada	Grass blades (90%) Grass seeds	Destroyer	Ethiopia, Africa Grasslands along gorges of open, and high plateaus Terrestrial	Lucas (2004) Gippoliti & Hunter (2008) Gron (2008)

[a] Percentages (when available) do not necessarily add up to 100 because of rounding and other unlisted minor resources. [b] Definitions after Lucas (2004).

Germany). To enable precise orientation of the molds, a rectangular, bent copper wire (about 2 × 5 mm) was inserted in the mold to indicate the mesial and buccal directions of the facet in relation to the saggital plane of the skull (Fig. 2.1d). Microtiter plates with 96 wells (Carl Roth GmbH1Co KG, Karlsruhe, Germany) were used as specimen holders of facet molds, although only 24 wells were filled to leave enough space between the samples (Fig. 2.1c). The molds were orientated as horizontally as possible to ease the scanning (see section 2.4 and Fig. 2.4). Surface measurements were then taken directly from the mold, and the data were subsequently reversed (see section 2.4). This procedure was adopted to avoid having to undertake yet another step of casting and reversing the mold with epoxy resin (Schulz *et al.* 2010a).

For the ungulates, the mesial enamel facet of the metacone on the original upper first (M^1) or second (M^2) molar was measured (Fig. 2.2, Appendix 2.1; Schulz *et al.* 2010a, submitted). For the primates, the standard primate microwear phase II facet #9 (Kay & Hiiemae 1974) on the M^2 was molded (Calandra *et al.* submitted).

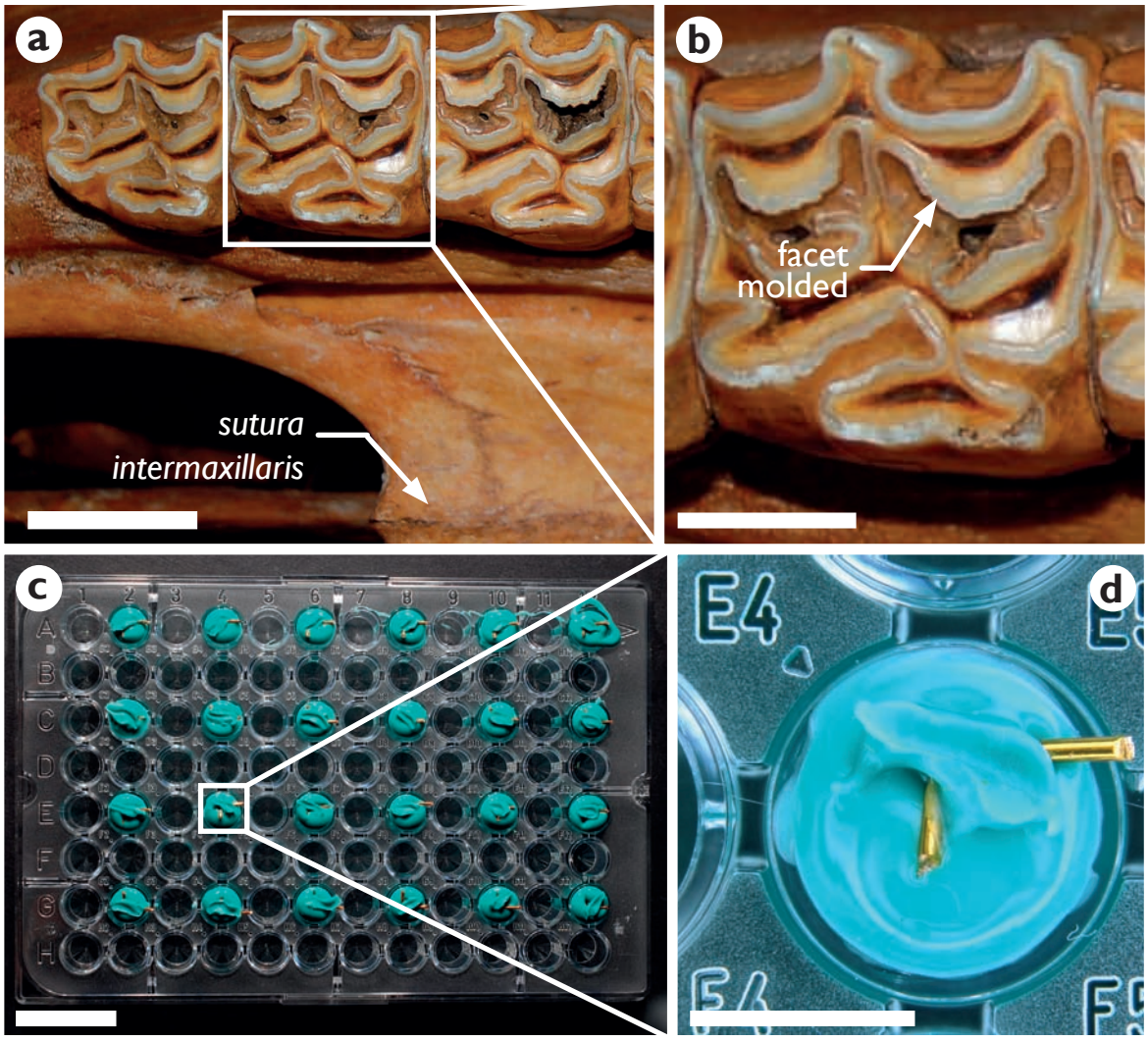

Figure 2.1. Molding and measuring facets. The high-resolution impression-molding material is applied on the tooth facet of the right second upper molar of *Equus grevyi* [ZMH-9386] (**a-b**). A microtiter plate is used to arrange twenty-four tooth facet molds for measurement (**c**). The mold is turned upside down and mounted into a well (**d**). A copper wire is added on the molding material, the long side orientated parallel to the *sutura intermaxillaris*, thereby indicating the mesial and buccal directions of the tooth row (**d**). Mesial is to the right. Scale bars: **a**, **c** = 20 mm; **b** = 10 mm; **d** = 5 mm. Modified from Schulz *et al.* (2010a, fig. 2).

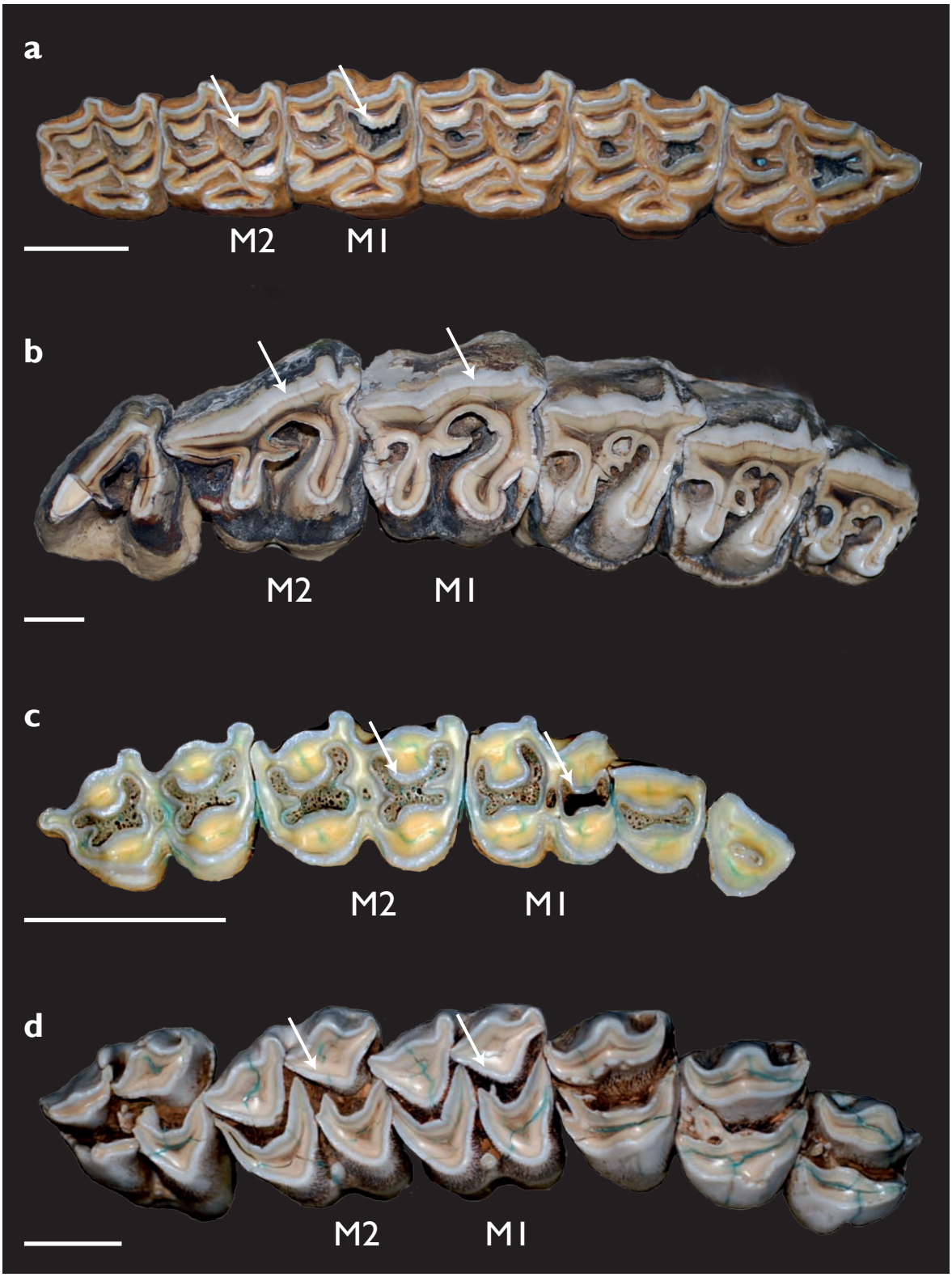

Figure 2.2. Upper right dentitions of the specimens for each ungulate species. (**a**) *Equus grevyi* [ZMH-9386], (**b**) *Diceros bicornis* [ZMH-1865], (**c**) *Connochaetes taurinus* [ZMH-6775], and (**d**) *Giraffa camelopardalis* [ZMH-9426]. Occlusal view, mesial toward the right. Scale bars = 20 mm. Arrows indicate sampled facets on the first and second molars. From Schulz *et al.* (submitted, fig. 1).

2.4 Data acquisition with the µsurf custom

A variety of measurement methods is available to analyse topographic 3D data of surfaces at a microscopic scale. Considering only non-contact methods available for surfaces having a lateral structural size lower than 100 µm and a structural depth between 1 mm and 1 nm, three optical methods of data acquisition are available: interferometry, confocal disc-scanning and confocal laser scanning microscopy.

The confocal disc-scanning system was chosen for this approach because it has three advantages over the other devices (Schulz *et al.* 2010a, submitted):

(1) there are no disturbances by incoherent white light as with interferometers,

(2) the lateral resolution is enhanced by the confocal effect (Diaspro 2002),

(3) it has a higher lateral resolution than the confocal laser scanning microscopes (Born & Wolf 1999).

During the development and adjustments required to apply this method to enamel facets, we were confronted to several technical issues. These stem mainly from the fact that 3D scanning devices and software packages were initially developed for industrial applications. Biological objects are much more complex in every aspect. In the context of dental microtexture, the textures of enamel facets are much more difficult to scan and analyze than industrial surfaces (which are relatively flat, reflect light very well, and do not have such complex wear features).

The high resolution disc-scanning confocal 3D surface measurement system µsurf custom (Fig. 2.3a, c; NanoFocus AG, Oberhausen, Germany) was used to acquire 3D surface data (Fig. 2.3b; Schulz *et al.* 2010a). It has a blue LED light source which has been used with a 100× long distance objective (long distance = 3.4 mm!). The actual resolution in x and y is 0.16 µm, and 0.06 µm in z. The field of view is 160 × 160 µm. Up to four non-overlapping measurements per facet were taken, depending on the size, tilt and cleanness of the facets, to increase the sampling area. Scans with less than 95% of recorded points or with defects such as dust particles have not been included in the subsequent analysis. In the case of primates only, eight out of 97 measurements have between 90 and 95% recorded points; the rest have more than 95% recorded points.

The height of most measurements of the enamel facet (typically between 20 and 40 µm in z) largely exceeds the height of industrial surfaces analyzed ($\delta z < 10\mu m$). The

number of scanning steps is limited, as is the vertical resolution. This is not an issue for most facets because they can be orientated very close to the horizontal, but some present a very steep and irregular profile that can exceed 60 µm (the technical limit of the µsurf custom for a vertical resolution of 0.06 µm), which prohibits the analysis of complete tooth rows, or even single tooth.

Although the 3D surface scanning is not completely independent of the orientation of the scanned surface, it is a definite improvement over 2D methods. But the sample and the light source are immobile during scanning, so some areas cannot be reached by the light beam and do not reflect light back toward the camera (Born & Wolf 1999; Diaspro 2002). The position and extent of these areas depend on the orientation of the surface, as well as on the size (depth-to-area ratio) of the features (Fig. 2.4). Hence, the mold has always been orientated as horizontally as possible, in order to limit these shadow zones. The extent of these shadow zones is also reduced using the brighter blue LED, compared with using the former green LED.

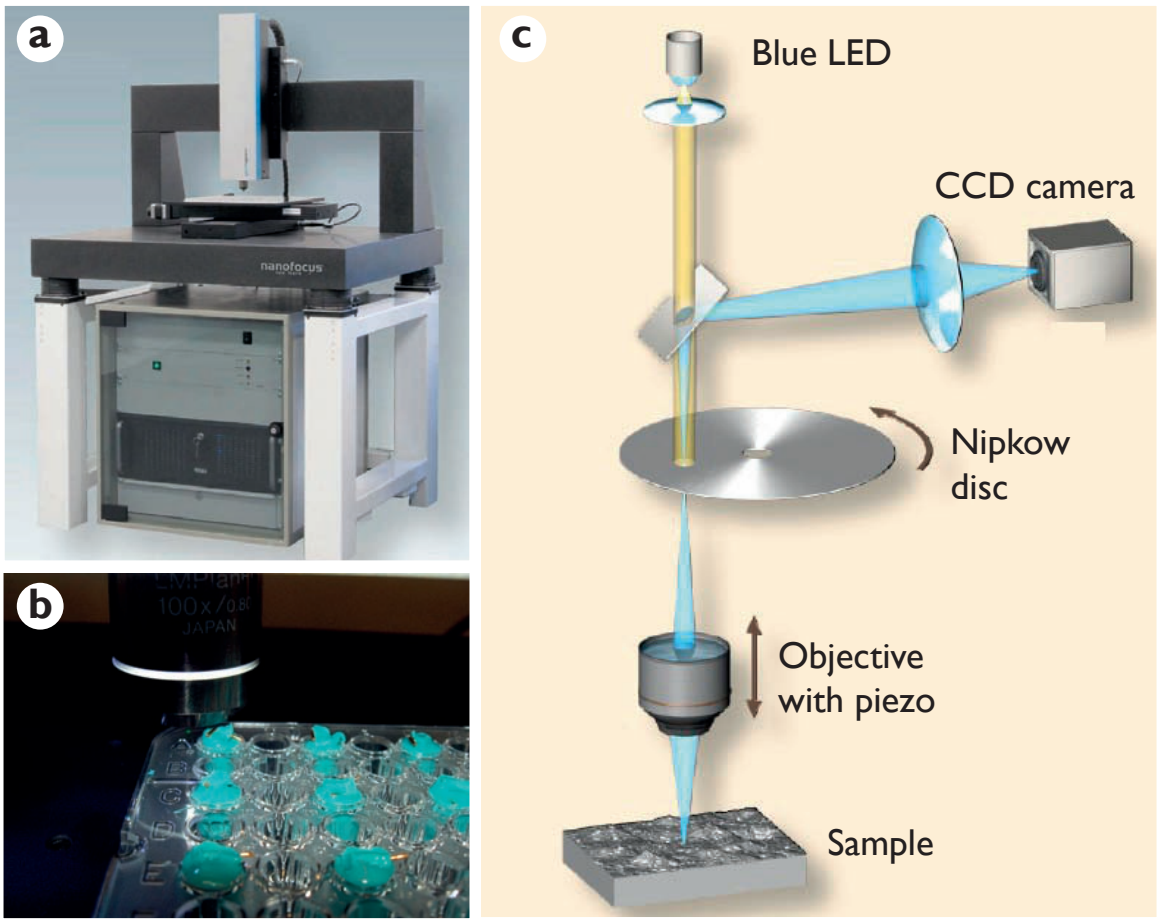

Figure 2.3. Data acquisition with the µsurf custom (**a**) with a 100× objective (**b**). The functioning of the optics is schematized in **c**. **a** and **c** from NanoFocus AG.

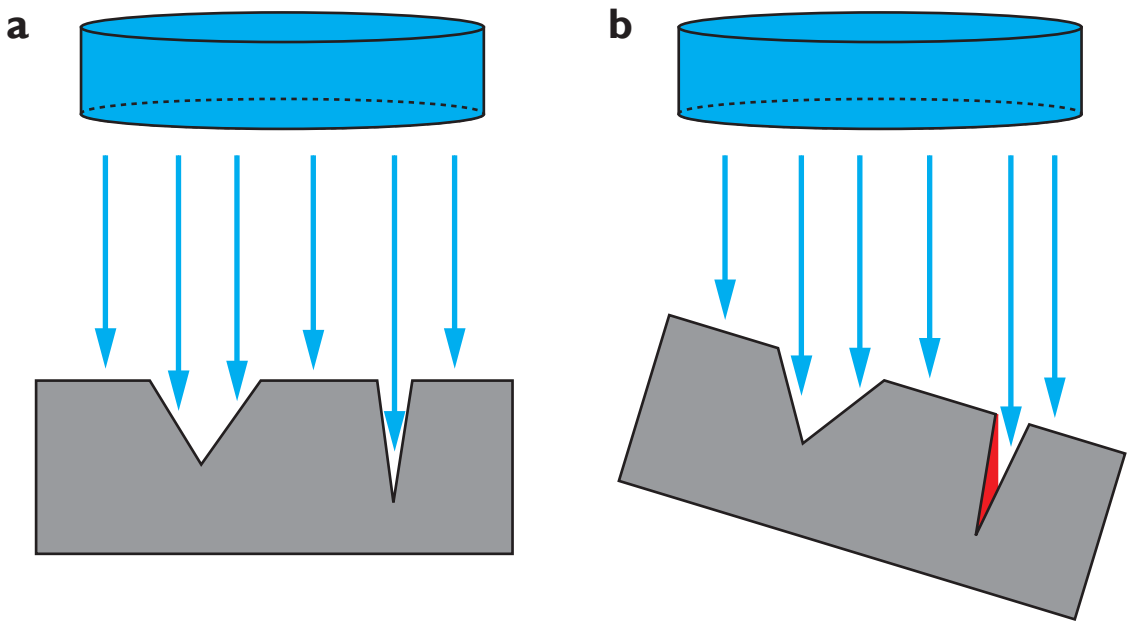

Figure 2.4. Scheme representing the influence of the orientation of the surface relative to the light source on the scanning and on the presence of shadow zones. (**a**) The surface (*gray block*) is perfectly horizontal and the light beam (*blue arrows*) from the blue LED light source (*blue cylinder*) can reach and be reflected from every point on the surface. (**b**) The surface is tilted and a shadow zone appears where the light beam cannot reach and be reflected (*red triangle*). This shadow zone results in non-recorded points.

2.5 Pre-processing of the 3D surface data

Biological surfaces are highly complex, so there is no one optimal pre-processing method for the preparation of the surfaces (see section 4.1.1). This is more a problem of standardization between the different research groups. I expect that the 3D devices and software packages will continue to develop, so their capacities will overlap, making it possible to run the microtexture analyses compatible with other research groups, while still maintaining the opportunities to explore other ways.

The 3D surface measurements were pre-processed according to the following procedure (Schulz *et al.* 2010a, submitted). Primary measurements were prepared in batch using a template in µsoft Analysis Premium v. 5.1 (NanoFocus AG; a derivative of MountainsMap® Analysis software by Digital Surf, Besançon, France).

This pre-processing template has:

(1) mirrored all the surfaces in z (to compensate for the molding procedure) and the surfaces from right molars in x (to have the same orientation for all teeth),

(2) leveled them (least square plane by subtraction),

(3) filled the <5% of unrecorded points (a selection dependent value = mean).

Unlike Scott *et al.* (2006), the unrecorded points have been filled and defects from the surfaces have not been manually removed. This procedure is completely automated, making it less susceptible to intra- and inter-variations between observers, as well as making the analysis more reproducible and faster to run.

2.6 Dental Areal Surface Texture Analysis

First, the Dental Areal Surface Texture Analysis (DASTA hereafter; Schulz *et al.* 2009, 2010a, 2010b, submitted; Calandra *et al.* submitted) has been applied using the same software as for the pre-processing, namely µsoft Analysis Premium. The DASTA extracts mainly 3D ISO/FDIS 25178-2 (ISO hereafter) texture parameters (International Organization for Standardization 2010), but the software can extract parameters from other norms as well.

On the pre-processed surfaces, a spatial filter (de-noising median 5 x 5 filter size and Gaussian 3 x 3 filter size, default cut-offs are used) has been applied, for the DASTA only.

But before 3D surface texture parameters can be applied to the surface data, filtering operators should be employed after ISO/FDIS 25178 (International Organization for Standardization 2010; Schulz *et al.* submitted). The default operator is the set of so-called S-Filters. As default the areal Gaussian filter (one of the S-Filters) is applied, which excludes the smallest scale elements from the surface resulting in the so-called primary surface. In order to suppress form alterations (e.g. the curvature of a cylinder) the F operator is applied, which results in the S-F surface (International Organization for Standardization 2010). Subsequently the L-Filter removes the low frequency alterations. The final product is called S-L surface (International Organization for Standardization 2010).

To test for the influence of the wavelength filtering options on the textures

parameters (hypothesis 1), three variations of form removal have been applied on the ungulate dataset (Schulz *et al.* submitted):

(A) the primary surface (Fig. 2.5) was calculated with the S filter only;

(B) the S-F surface was calculated by removing the form with a second order polynomial, which should be sufficient to remove the coarse morphology of the surface since dental enamel ridges are mainly curved along the bucco-lingual axis like a cylinder;

(C) the S-L surface was calculated by applying the highest power 12 of the polynomial to remove the whole impact of form and waviness.

For the inter-specific differences among both ungulates and primates, the S-F surfaces have been used because they are more indicative (hypotheses 2-4).

Subsequently a set of 46 surface textures parameters were quantified on the three surface types using (1) the ISO/FDIS 25178-2, (2) motif, (3) furrow, (4) direction, (5)

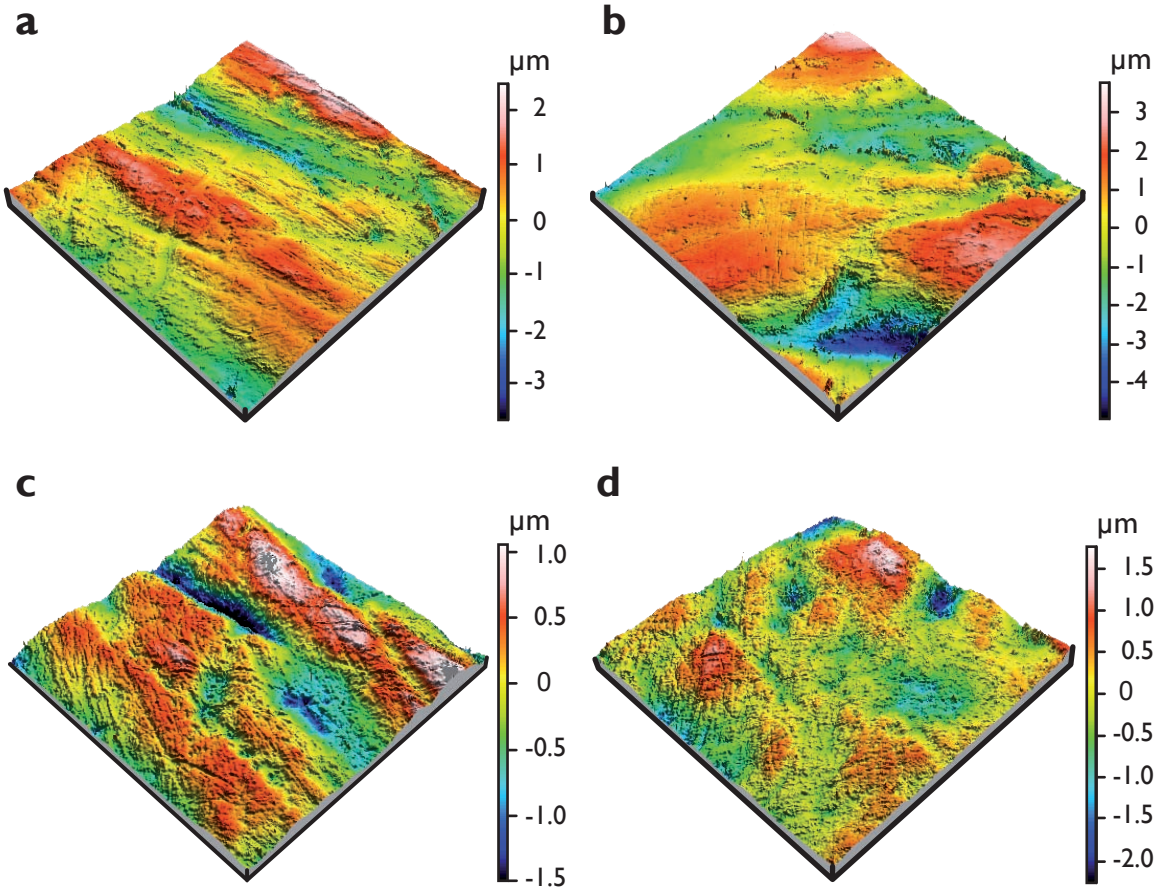

Figure 2.5. Meshed axiomatic 3D models (160 × 160 µm) of tooth enamel surfaces on the second upper molar of ungulates. (**a**) *Equus grevyi* [ZMH-9386], (**b**) *Diceros bicornis* [ZMH-1865], (**c**) *Connochaetes taurinus* [ZMH-6775], and (**d**) *Giraffa camelopardalis*. From Schulz *et al.* (submitted, fig. 2)

Table 2.2. Description, standard, and units of the applied parameters according to ISO/FDIS 25178-2, motif, furrow, texture direction, texture isotropy, and flatness analysis.

	Description (condition)	Standard	Unit
S10z	ten-point height of the surface	ISO 25178	µm
S5p	five-point peak height	ISO 25178	µm
S5v	**five-point valley height**	**ISO 25178**	**µm**
Sa	arithmetical mean height or mean surface roughness	ISO 25178	µm
Sal	auto-correlation length (s = 0.2)	ISO 25178	µm
Sda	**mean dale area**	**ISO 25178**	**µm²**
Sdq	root mean square gradient of the scale limited surface	ISO 25178	no unit
Sdr	developed interfacial area ratio of the scale limited surface	ISO 25178	%
Sdv	closed dales volume	ISO 25178	µm³
Sha	**mean hill area**	**ISO 25178**	**µm²**
Shv	closed hills volume	ISO 25178	µm³
Sku	kurtosis of the scale limited surface	ISO 25178	no unit
Smc	areal material ratio function of the scale limited surface (p = 10%)	ISO 25178	µm
Smr	areal material ratio function of the scale limited surface (c = 1 µm under the highest peak)	ISO 25178	%
Sp	maximum peak height	ISO 25178	µm
Spc	arithmetic mean peak curvature	ISO 25178	1/µm
Spd	**density of peaks**	**ISO 25178**	**1/µm²**
Sq	**standard deviation of the height distribution, or RMS surface roughness**	**ISO 25178**	**µm**
Ssk	skewness of the scale limited surface	ISO 25178	no unit
Std	direction	ISO 25178	°
Str	aspect ratio (s = 0.2)	ISO 25178	no unit
Sv	maximum pit height	ISO 25178	µm
Sxp	peak extreme height difference in height between p% and q% (p = 50%, q =97.5%)	ISO 25178	µm
Sz	maximum height of the scale limited surface	ISO 25178	µm
Vm	**material volume at a given height (p = 10%)**	**ISO 25178**	**µm³/µm²**
Vmc	material volume of the core (p = 10%, q =80%)	ISO 25178	µm³/µm²
Vmp	material volume of peaks (p = 10%)	ISO 25178	µm³/µm²
Vv	void volume at a given height (p = 10%)	ISO 25178	µm³/µm²
Vvc	void volume of the core (p = 10%, q =80%)	ISO 25178	µm³/µm²
Vvv	void volume of the valley (p = 80%)	ISO 25178	µm³/µm²
nmoti	number of motifs	motif	no unit
meh	mean Height	motif	µm
mea	mean Area	motif	µm²
mev	mean Volume	motif	µm³
madf	maximum depth of furrows according the = vectorisiation of the micro-valley network	furrow	µm
metf	mean depth of furrows	furrow	µm
medf	mean density of furrows	furrow	cm/cm²
Tr	direction isotropy	direction	%
Tr1R	first Direction	direction	°
Tr2R	second Direction	direction	°
Tr3R	third Direction	direction	°

Table 2.2. (continued)

	Description (condition)	Standard	Unit
IsT	isotropy	isotropy	%
FLTt	peak to valley flatness deviation of the surface (Gaussian Filter, 0.025mm)	ISO 12781-1	µm
FLTp	peak to reference flatness deviation (Gaussian Filter, 0.025mm)	ISO 12781-1	µm
FLTv	reference to valley flatness deviation (Gaussian Filter, 0.025mm)	ISO 12781-1	µm
FLTq	root mean square flatness deviation (Gaussian Filter, 0.025mm)	ISO 12781-1	µm

Parameters in bold are the ones applied on the primate dataset. From Schulz *et al.* (submitted, table 2).

isotropy, and (6) flatness (Schulz *et al.* submitted). Parameter descriptions are given in Table 2.2. Six ISO parameters from these were selected on the primate dataset because of their significance.

2.7 Scale-Sensitive Fractal Analysis

The Scale-Sensitive Fractal Analysis (SSFA hereafter) was adapted for the dental research by Ungar, Scott and coworkers (Ungar *et al.* 2003; Scott *et al.* 2005; Scott *et al.* 2006; see section 1.3). The SSFA "is based on the principle that the texture of a surface changes with the scale at which it is observed. The apparent profile length of a surface, the apparent area of that surface, and the apparent volume of features on it change with the scale of observation" (Scott *et al.* 2009, p. 408). This means that length, area, and volume of features are larger at fine scales than at coarser ones (Scott *et al.* 2006, figs. 2-4).

The SSFA extracts six texture parameters from a pre-processed (section 2.5) 3D surface:

(1) Area-scale fractal complexity, *Asfc*

(2) Heterogeneity of area-scale fractal complexity, *HAsfc*

(3) Exact proportion length-scale anisotropy, *epLsar*

(4-5) Textural fill volume on a coarse (*Tfv*) and fine (*Ftfv*) scale

(6) Scale of maximum complexity, *Smc*.

Because *Ftfv* and *Smc* have almost never been biologically discussed in other studies (Scott *et al.* 2005; Scott *et al.* 2006; Ungar *et al.* 2007; Scott *et al.* 2009; Merceron *et al.* 2010a; Ungar *et al.* 2010), these two parameters are not further discussed here. The

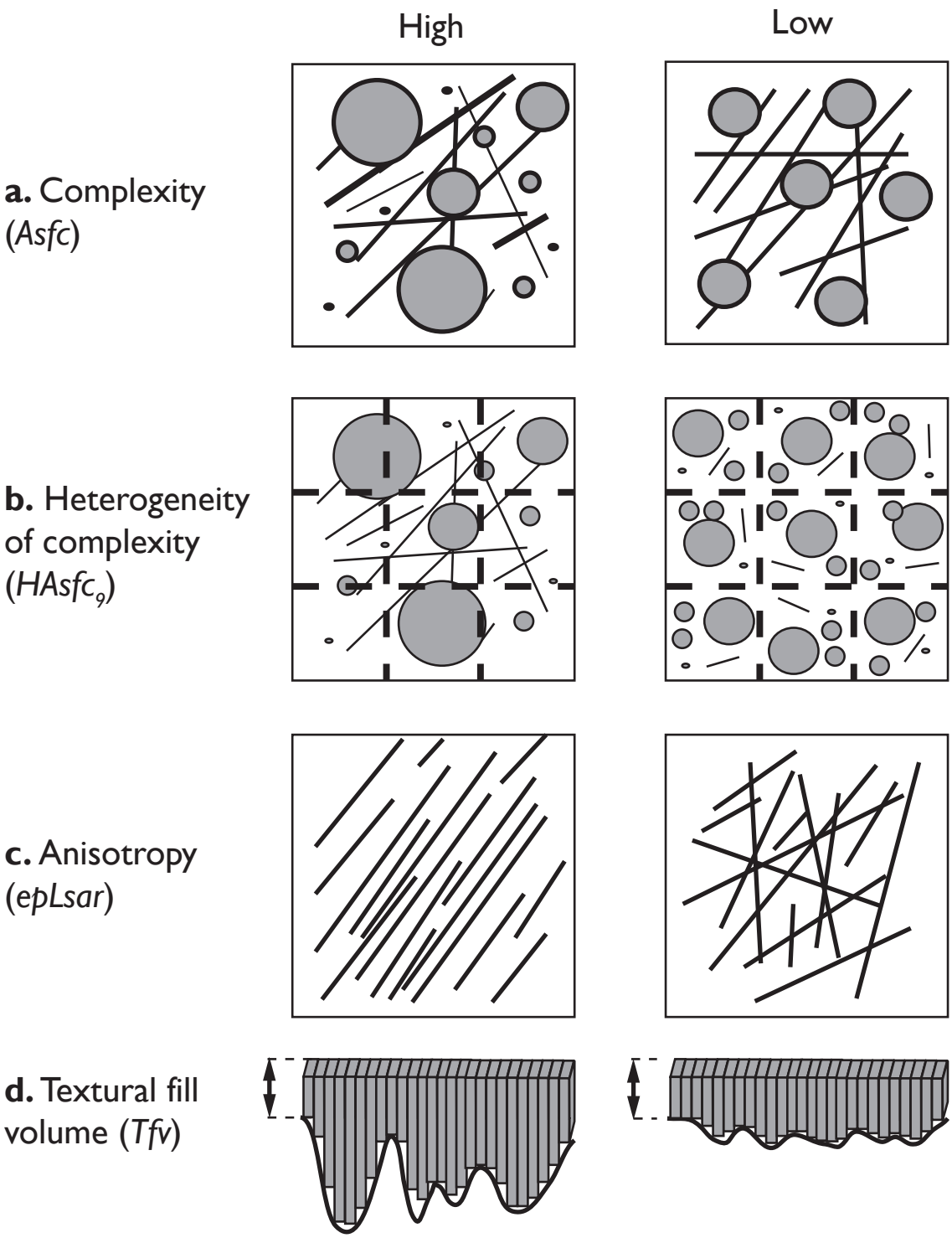

Figure 2.6. Schematic hypothetical microwear surfaces with either high (**left**) or low (**right**) values for the SSFA parameters complexity (*Asfc*, **a**), heterogeneity of complexity (*HAsfc*, in this case $HAsfc_9$, **b**), anisotropy (*epLsar*, **c**), and textural fill volume (*Tfv*, **d**). After Scott *et al.* (2006, fig. 1).

Table 2.3. Description and meaning of the SSFA parameters (modified from Scott *et al.* 2009).

Name	Parameter	Description	Example
Area-scale fractal complexity	*Afsc*	Change of the surface roughness with scale.	A surface with pits and scratches of different sizes will have a high *Asfc*.
Heterogeneity of area-scale fractal complexity	$HAsfc_n$	Calculated by splitting a surface into smaller sections with equal numbers of rows and columns. *Asfc* for each section and its median (*HAsfc*) for each surface are then calculated.	A surface with variations of features across the area will have a high *HAsfc*. $HAsfc_9$ and $HAsfc_{81}$ are the heterogeneities associated with a 3x3 and 9x9 splitting of the surface, respectively.
Textural fill volume	*Tfv*	Computed by filling a surface with square cuboids of a given scale. The surface waviness is removed so that only the roughness is examined.	A surface showing lots of and/or large and/or deep wear features at the computational scale is expected to have a high *Tfv*.
Exact proportion length-scale anisotropy	*epLsar*	A measure of the orientation of the surface wear features.	A surface characterized by the scratches running in the same direction is expected to have high *epLsar* values.

other four SSFA parameters can be readily interpreted in biological terms and linked to characteristics of the diet, as can be seen from the descriptions in Fig. 2.6 and Table 2.3.

The SSFA was run using the Toothfrax and Sfrax software packages (www.surfract.com) following Scott *et al.* (2006). This method was applied only on primates (sections 3.3.1 and 4.2.1).

2.8 Statistics

I have chosen to stray away from the standard statistics applied commonly in our field (such as *F*-test ANOVA) and developed procedures to apply the robust statistics from Wilcox (2003, 2005). A mathematics-free account of the rationale behind the statistic tests is presented in this section (Calandra *et al.* submitted).

2.8.1 Robust statistics

The median of the parameters derived from the several (up to four) measurements of a single facet was calculated (Scott *et al.* 2006; Appendix 2.3.1). This median value per specimen was subsequently used for further analysis. Inter-specific differences

have been tested for using one-way analyses of variance (ANOVA; Appendix 2.3.4) and regression analyses have been applied on some parameters if possible and meaningful (Appendix 2.3.3).

The relevance of the *F*-test usually applied in ANOVA design is dependent on three assumptions:

(1) random sampling, that seems reasonable but needs to be assumed with such biological data;
(2) the normality of the distribution of each species for each response variable;
(3) the homogeneity of the variances of the species for a given response variable, the so-called homoscedasticity (Keselman *et al.* 1998; Wilcox 2003, 2005).

The violation of these assumptions can result in significantly increased type-I (probability to detect a false difference) and type-II (probability of not detecting a genuine difference, related to the power of the test) errors. The central limit theorem states that by increasing the number of individuals, the *F*-test becomes more robust to violations of these assumptions (Wilcox 2003).

The present data are clearly neither normal nor homoscedastic (e.g. Figs. 3.1-3.2 and 3.4-3.5), and the numbers of individuals are small ($2 \leq n \leq 10$; Appendices 2.1-2.2). Hence, the standard *F*-test is inappropriate. So robust tests have been applied according to Wilcox (2003, 2005). Robust means that there is simultaneously a good control over type-I error and a large power. Robustness is crucial when applying statistics on small samples and when dealing with non-normal and/or heteroscedastic data.

Tests that are not influenced by heteroscedasticity are called heteroscedastic tests. Additionally two approaches can be applied to cope with non-normal data. The first is based on the trimmed mean, while the second ranks the data. There is no consensus about which type of test best describes data, because each characterizes data in a different way (Wilcox 2003). This is why both have been applied and compared: the Welch-Yuen heteroscedastic omnibus test ("Welch-Yuen test" hereafter; Welch 1938; Yuen 1974) coupled with a heteroscedastic pair-wise test analogous to Dunnett's (1980) T3 ("Dunnett test" hereafter) applied on trimmed means, and a heteroscedastic rank-based test that performs Cliff's (1996) method for all pairs ("Cliff test" hereafter).

Significance has been defined when $p \leq 0.05$. This cut-off value has been used consistently throughout this work.

Least square regression and Pearson's correlation coefficient are also inappropriate when dealing with non-normal and heteroscedastic data (Wilcox 2003, 2005). Here too, robust tests following Wilcox (2003, 2005) were chosen.

Regressions were estimated with two methods because no single one is best in all situations (Wilcox 2003). The methods TSTS and MGV (Wilcox 2003) both remove outliers and then apply the heteroscedastic Theil-Sen (Theil 1950; Sen 1968) estimator on the remaining data. The correlation coefficients were estimated by the percentage bend correlation coefficient coupled with a percentile bootstrap to estimate its confidence interval (Wilcox 1994).

Details on these procedures are given in the next three sub-sections, 2.8.2-2.8.4. More details on the calculations, meanings and limitations of the tests are given in Wilcox (2003, 2005).

2.8.2 Trimming

Trimming is the first main approach to compensate for non-normality. It excludes the highest and lowest parts of a distribution. The amount of trimming required on a given dataset cannot be known *a priori*, but simulations indicate that a symmetrical 20% trimming (*i.e.* 20% on each side of the distribution, so a total of 40% data excluded) generally gives good results (Wilcox 2003). The smaller the sample size, the larger the amount of trimming should be (R. R. Wilcox, pers. comm. 2010).

Zero, 5, 10, 15, and 20 percent symmetrical trimming were compared. Only an even number of values can be removed from the distribution. Exactly half of the trimmed values from the upper part and half from the lower part of the distribution are excluded. Depending on the number of specimens (n), a given percentage of trimming (tr) might not trim at all.

The computation of the number of excluded data points (n_{ex}) is straightforward.

First compute: $y = n \times tr \times 2$ [The factor 2 is because trimming is symmetrical]

n_{ex} is the closest smaller even integer from y. If $y < 2$ then $n_{ex} = 0$. If $2 \leq y < 4$ then $n_{ex} = 2$. If $4 \leq y < 6$ then $n_{ex} = 4$. And so on.

For example, with $n = 7$, trimming occurs between 14% and 15%, meaning that 14% trimming will not remove any data ($7 \times 0.14 \times 2 < 2$) while 15% will remove the highest value and the lowest one ($2 \leq 7 \times 0.15 \times 2 < 4$), leaving $n = 5$ for the analyses.

The trimmed mean is hence computed as the mean of the trimmed distribution, *i.e.* only values that are not trimmed are included in the computation of the trimmed mean.

The samples generally include five to 10 specimens per species (Appendices 2.1-2.2). This means that 5% and 10% trimming do not remove any data (Table 2.4); they are therefore irrelevant to use with the sample sizes. Trimming with 20% seems to be extreme for the sample sizes: even the smallest samples (*n = 5*) are trimmed (leaving only three individuals). 15% trimming seems to be a fine amount to test since only species with at least seven specimens are trimmed; the others keep all of their individuals (Table 2.4). The effects of the amount of trimming on the significance of the microtexture parameters are discussed on the primate dataset (section 3.1). On this dataset, 15% of symmetrical trimming gives consistent results. This amount of trimming has, therefore, been generally used on other datasets.

2.8.3 Statistical tests

Prior tests for normality and homoscedasticity have not been run for two reasons. First, the available tests such as Shapiro-Wilk (Shapiro & Wilk 1965) or Anderson-Darling (Anderson & Darling 1952, 1954) and Levene (1960) or Brown-Forsythe (Brown & Forsythe 1974) tests do not have enough power to detect small departures from normality and homoscedasticity, respectively, which can still render the *F*-test invalid (Markowski & Markowski 1990; Wilcox 2003). Second, the heteroscedastic tests with trimming or ranking perform way better than the *F*-test in case of heteroscedasticity and/or non-normality and nearly as well in case of simultaneous homoscedasticity and normality (Wilcox *et al.* 1986; Moser *et al.* 1989; Wilcox 2003). There is therefore no reason not to employ heteroscedastic tests coupled with trimming or ranking. It is even truer with the present data.

The Welch-Yuen heteroscedastic omnibus test with 0% and 15% symmetrical trimming was first applied on each parameter. Similarly to the *F*-test, it tests whether at least one of the species has a different (trimmed) mean than the other species. Whenever a significant difference was found, a Dunnett test with the same amount of

	Trimming			
n	5%	10%	15%	20%
5				x
6				x
7			x	x
8			x	x
9			x	x
10		x	x	x

Table 2.4. Amount of trimming required to remove data depending on the number of specimens per group (*n*). *Crosses* are in the cells where trimming occur for a given n and amount of trimming.

trimming was subsequently employed to reveal the source of the difference. This test is however liberal since the *p* values are not controlled for the so-called family-wise error (FWE).

The second approach often used to cope with departures from normality is based on the ranking of the data. The *F*- or Welch-Yuen tests test for the equality of the (trimmed) means. On the other hand, ranking methods test for the equality of the distributions. Because of this, applying an *F*-test on ranked data renders the interpretations difficult in biological terms. Most rank-based tests such as the Wilcoxon-Mann-Whitney (Wilcoxon 1945; Mann & Whitney 1947) or the Kruskal-Wallis (Kruskal & Wallis 1952), though independent of the underlying distribution, are still subjected to the homoscedasticity assumption (Wilcox 2003). Therefore, a heteroscedastic rank-based test, Cliff test, has been applied. The FWE is controlled via Hochberg's (1988) method. Cliff test computes, for all pairs of species, the probability that an observation from the species I is smaller than from species J. The estimated probability is called $\hat{P}$ (pronounce "p hat"):

$$\hat{P} = P(I<J) + \tfrac{1}{2} P(I=J)$$

Since the Dunnett test is liberal, detailed attention was paid especially to the pairs of species where significant differences are detected with both Dunnett and Cliff tests.

The Welch-Yuen, Dunnett, and Cliff tests all need at least 3 specimens per species to be run. While the tests can be run with 3 individuals, the results can only be indicative.

2.8.4 Regressions and correlations

Since none of the available regression method is best in all situations, and since it cannot be known *a priori* which one is the most appropriate, Wilcox (2003) advises applying several methods that can be of interest, and then comparing them graphically. The MGV and TSTS methods (Wilcox 2003) have been chosen because they both are robust and seemed to fit the data quite well (Fig. 3.3). The MGV detects and removes outliers with a "boxplot rule", which is based on the interquartile range. It then applies the Theil-Sen estimator to the remaining values. This estimator is computed by calculating the median of the slopes and intercepts for all pairs of points having distinct X values. The second regression method, the method TSTS, is based on the same principle as MGV. Both methods differ concerning the outlier detection rule: method TSTS detects *regression* outliers (*i.e.* points with large residuals) with an S-type modification of the Theil-Sen estimator (Wilcox 2003).

Correlations were estimated with a percentage bend correlation coefficient (r_{pb}), which removes outliers before computing the estimates (Wilcox 1994). The outlier detection is based on the median and its absolute deviation (MAD). This estimator is however influenced by heteroscedasticity. One approach is to combine it with a percentile bootstrap method, which computes a 95% confidence interval (CI) for r_{pb}: if the 95% CI includes 0, then X and Y are independent; if it does not include 0, then X and Y are positively correlated if $r_{pb} > 0$, and negatively otherwise (Wilcox 2003).

2.8.5 Software

The whole statistical procedure was carried out with the open-source software R 2.12.1 (R Development Core Team 2010). The following R packages were used for data mining and processing: doBy (Højsgaard *et al.* 2010, v. 4.2.3), R.utils (Bengtsson 2010, v. 1.6.2), RSvgDevice (Luciani 2009, v. 0.6.4.1), and xlsReadWrite (Suter 2010, v. 1.5.4). All statistical tests were carried out using functions written by Wilcox (2005) which are included in the package WRS (Wilcox & Schönbrodt 2010, v. 0.12.1).

I have written scripts in order to run the exact same procedures on all my data sets, and to do so faster. Some of these scripts are supplied as appendices (Appendices 2.3). An explanation of the programming is however beyond the scope of this work.

2.9 Summary

The protocol developed for the dental microtexture analyses is as follows.

(1) A mold of the considered facet on the M^1 or M^2 of carefully selected individuals was made and each facet was scanned with the µsurf custom and all measurements were pre-processed in batch in µsoft Analysis Premium (Schulz *et al.* 2010a).

(2) Two analyses were run on these pre-processed measurements in order to quantify their microtextures: the scale-sensitive fractal analysis (Scott *et al.* 2005; Scott *et al.* 2006) and the dental areal surface texture analysis (Calandra *et al.* submitted; Schulz *et al.* submitted); both of which are completely automated.

(3) Robust statistics were applied in ANOVA designs and regression analyses following Wilcox (2003, 2005) (Calandra *et al.* submitted). All data mining and statistical procedures were run from scripts in the open-source software R.

Connochaetes taurinus [photo: Ellen Schulz]

3. Results

3. Results

This section describes the results on the effect of trimming on the significance and the results of the microtexture analyses on both datasets (ungulates and primates).

3.1 The effect of trimming

The effect of trimming is considered only on primates because it is the most heterogeneous dataset in terms of sample sizes (Calandra *et al.* submitted). The results are then extrapolated to other datasets.

Except for four pairs out of 21, results from Dunnett tests are not different from 0% to 15% trimming of the SSFA parameters *Asfc*, *epLsar*, and *Tfv* (Table 2.3, Appendix 3.3). More significant differences are found with 15% trimming, probably because of extreme values, some of which can be considered as outliers, are removed prior to analysis, reducing the range of each species and therefore accentuating the gaps between them. However, the Welch-Yuen test with 15% trimming does not find significant difference for $HAsfc_9$ or $HAsfc_{81}$, while it does with 0% trimming (Table 3.6). This means that the heterogeneity of complexity is greatly influenced by extreme values. In fact, the boxplots show outliers (unfilled dots in Fig. 3.4c-d), which are removed by the trimming process, in *Pongo abelii* and *Lophocebus albigena*, where most of the significant differences are in $HAsfc_9$ and $HAsfc_{81}$. Cliff tests detect significant differences only between *Macaca fascicularis* and *Papio cynocephalus* (Appendix 3.4). This result is consistent with the fact that there is basically no significant difference between the species for both *HAsfc* parameters. ISO parameters are found to behave the same way as SSFA parameters in respect of the effect of trimming on significance (Table 3.6, Appendix 3.3-3.4).

Although discarding 30% of the data seems problematic considering small samples, simulations by Wilcox (2003) have found that trimming is a powerful method for dealing with non-normal data and that the increased robustness of estimations achieved through trimming greatly exceeds the negative effects of reduced sample sizes. Fifteen percent symmetrical trimming gives more robust results because more significant differences are found for some parameters, while the tests do not detect differences for other parameters. It thus seems that control over type-I error and power

are well balanced. I therefore chose to generally apply 15% symmetrical trimming to my data. Work on other data sets (ungulates and others not shown) also supports this conclusion. 15% trimming has therefore been applied on ungulates.

3.2 Ungulates

3.2.1 Robustness of DASTA texture parameters across filtering thresholds (hypothesis 1; Schulz *et al.* submitted)

Three out of the 46 tested surface parameters (Table 2.2) are found to indicate the dietary traits with both Dunnett and Cliff tests, independently of the surface type (Tables 3.2-3.3, Appendix 3.1). The surface parameters *Sa* (arithmetical mean height, ISO/FDIS 25178), *medf* (mean density of the furrows, furrow analysis), and *IsT* (texture isotropy) provide qualitatively stable patterns for the primary surface (A), the S-F surface (B) and the S-L surface (C) (Fig. 3.1). As expected the ISO/FDIS 25178 height parameter *Sa* decreases when form (B) and waviness (C) are removed for each species. But the inter-specific patterns remain qualitatively stable. The primary surfaces (A) are characterized by a high degree of dispersion of *Sa* values mostly, as indicated by the large upper and lower quartiles (Fig. 3.1, Table 3.1). The furrow parameter *medf* and the texture isotropy *IsT* stay in most cases stable for the three surface types. I observe a consistent increase of *IsT*. The only exception is for *Connochaetes taurinus* in which the S-F surface seems to have lower isotropy than the primary and the S-L surfaces.

Fourteen parameters individually allow distinction of the four species (primary surface, Table 3.3). The S-F surface (B) is characterized by small standard deviations (Table 3.1). Nineteen parameters on the S-F surface significantly underline inter-specific differences (Figs. 3.1-3.2, Tables 3.2-3.3, Appendices 3.1-3.2). When using the algorithm with maximum form and waviness removal leading to the S-L surface (C), only ten parameters allow inter-specific distinctions (Figs. 3.1-3.2, Table 3.3).

3.2.2 Testing for characteristics of food and masticatory biomechanics through the DASTA (hypothesis 2; Schulz *et al.* submitted)

The two grazing species *Connochaetes taurinus* and *Equus grevyi* are characterized by high values of height (*Sa*, *Sq*, *Sxp*), volume (*Smc*, *Vmc*, *Vv*, *Vvc*, *Vvv*), feature (*Spd*), motif (*mev*), furrow (*metf*), flatness (*FLTt*, *FLTp*, *FLTq*) parameters, and a low values

Table 3.1. Descriptive statistics on ungulates: values of the parameters for the primary (A), S-F (B), and the S-L (C) surfaces.

		Primary surface (A)				S-F surface (B)				S-L surface (C)			
	Stat	cotau	dibic	eqgre	gicam	cotau	dibic	eqgre	gicam	cotau	dibic	eqgre	gicam
Sa	Mean	1.581	0.515	1.249	0.658	0.814	0.457	0.694	0.325	0.378	0.243	0.404	0.197
	SD	0.349	0.614	0.192	0.547	0.133	0.268	0.098	0.196	0.097	0.121	0.101	0.121
Sdv	Mean	2.4E-11	2.2E-11	2.6E-11	1.6E-09	8.8E-09	9.810	8.6E-09	47.930	4.4E-09	1.4E-08	38.678	38.726
	SD	8.3E-09	1.9E-07	1.0E-08	6.9E-09	1.0E-08	20.024	5.3E-09	26.007	3.4E-09	1.7E-08	18.613	34.528
Shv	Mean	1.2E-10	9.4E-11	1.1E-10	2.7E-09	8.6E-09	0.828	8.7E-09	9.309	3.6E-09	5.5E-09	5.811	8.376
	SD	8.3E-09	1.9E-08	9.3E-09	8.5E-09	6.5E-09	1.786	6.6E-09	5.719	1.9E-09	3.2E-09	2.690	7.849
Smc	Mean	2.248	0.989	1.847	3.907	1.141	0.648	1.066	0.488	0.432	0.319	0.512	0.268
	SD	5.476	6.365	2.261	5.554	0.192	0.407	0.177	0.291	0.094	0.148	0.157	0.176
Spd	Mean	0.313	0.288	0.275	11132.800	0.094	0.034	0.059	0.035	0.090	0.034	0.055	0.033
	SD	13132.668	2291.561	6791.448	26596.168	0.046	0.014	0.019	0.029	0.041	0.014	0.020	0.027
Sq	Mean	2.110	0.827	1.734	0.865	1.186	0.698	1.014	0.503	0.747	0.495	0.749	0.382
	SD	0.462	0.717	0.220	0.700	0.193	0.359	0.205	0.304	0.247	0.262	0.251	0.221
Sxp	Mean	4.839	1.560	4.190	1.971	2.101	1.285	1.764	0.947	1.205	0.708	1.154	0.585
	SD	1.329	1.157	0.674	1.607	0.402	0.686	0.234	0.572	0.423	0.351	0.267	0.328
Vmc	Mean	1.803	0.537	1.428	0.782	0.865	0.498	0.736	0.321	0.307	0.218	0.365	0.182
	SD	0.438	0.668	0.254	0.641	0.190	0.317	0.119	0.196	0.075	0.101	0.102	0.130
Vv	Mean	2.306	0.850	1.885	1.065	1.227	0.687	1.126	0.517	0.500	0.357	0.579	0.294
	SD	0.531	1.005	0.353	0.876	0.196	0.427	0.178	0.310	0.120	0.171	0.163	0.188
Vvc	Mean	2.126	0.752	1.689	0.933	1.107	0.609	1.012	0.449	0.421	0.307	0.499	0.250
	SD	0.474	0.960	0.296	0.781	0.177	0.392	0.162	0.272	0.097	0.146	0.148	0.169
Vvv	Mean	0.294	0.089	0.267	0.133	0.124	0.079	0.107	0.064	0.087	0.050	0.078	0.044
	SD	0.097	0.063	0.046	0.102	0.023	0.039	0.011	0.036	0.029	0.025	0.019	0.023
mev	Mean	22.497	10.182	14.287	9.832	26.347	12.164	16.049	19.876	13.425	7.444	17.997	9.208
	SD	19.035	16.335	7.088	19.948	12.737	8.480	7.313	19.336	2.464	4.049	11.734	6.194
medf	Mean	4804.960	4910.968	4616.770	5018.405	4965.711	4971.109	4647.466	4919.237	4935.453	4915.724	4561.106	4883.213
	SD	179.122	215.434	144.440	233.674	219.986	187.539	145.001	230.094	221.612	200.103	193.765	236.204

Table 3.1. (continued)

		Primary surface (A)				S-F surface (B)				S-L surface (C)			
	Stat	cotau	dibic	eqgre	gicam	cotau	dibic	eqgre	gicam	cotau	dibic	eqgre	gicam
	SD	0.220	0.302	0.141	0.266	0.245	0.234	0.122	0.227	0.235	0.234	0.162	0.238
Tr1R	Mean	4.578	63.506	13.380	63.469	28.551	67.558	37.879	67.564	28.552	67.558	37.880	67.563
	SD	24.645	41.527	54.022	57.628	30.663	30.755	51.763	41.382	30.662	30.755	51.763	41.382
IsT	Mean	37.013	52.806	31.749	31.749	34.882	58.523	33.680	54.714	39.114	61.115	37.981	57.488
	SD	13.684	13.451	10.887	10.887	13.577	15.306	10.892	15.892	13.916	11.109	9.321	17.277
FLTp	Mean	3.716	2.262	3.308	1.501	1.711	0.976	1.564	0.716	0.540	0.401	0.735	0.305
	SD	0.617	2.549	0.540	1.486	0.357	0.614	0.222	0.451	0.121	0.194	0.324	0.213
FLTq	Mean	1.960	0.612	1.545	0.772	0.714	0.418	0.644	0.277	0.173	0.125	0.228	0.097
	SD	0.414	0.722	0.240	0.675	0.177	0.277	0.110	0.172	0.026	0.059	0.101	0.077
FLTt	Mean	10.723	5.098	8.413	4.775	3.710	2.168	3.479	1.602	1.141	0.832	1.476	0.640
	SD	2.069	4.244	1.312	3.555	0.833	1.211	0.525	1.052	0.270	0.401	0.615	0.475

cotau = *Connochaetes taurinus*, dibic = *Diceros bicornis*, eqgre = *Equus grevyi*, gicam = *Giraffa camelopardalis*, SD = standard deviation. Parameters: see Table 2.2. From Schulz *et al.* (submitted, appendix 1).

for isotropy (*IsT*) on their S-F surfaces (Fig. 3.2, Tables 3.2-3.3). The reverse pattern is evident in the browsing *Diceros bicornis* and *Giraffa camelopardalis*. Eleven (*Sa*, *Smc*, *Sxp*, *Vmc*, *Vv*, *Vvc*, *Vvv*, *IsT*, *FLTt*, *FLTp*, *FLTq*) out of the nineteen parameters allow distinction to be made between the grazers and the browsers (Fig. 3.2, Table 3.3). The ruminants within the sample (*C. taurinus* and *G. camelopardalis*) have significantly higher *medf* values (mean density of the furrows) than their non-ruminating counterpart species (*E. grevyi* and *D. bicornis*, respectively). In fifteen tested parameters *G. camelopardalis* shows higher variation as compared to the other species (Fig. 3.2, Table 3.1). In the feature parameters *Sdv* (closed dales volume) and *Shv* (closed hill volume), *Vv* (void volume), *Vvv* (void volume of the valleys), *Vvc* (void volume of the core), and *mev* (mean volume), the spread exceeds the ones of the remaining species by more than a factor two (Table 3.1). The feature parameters *Sdv* (closed dales volume) and *Shv* (closed hill volume) in particular indicate pronounced valley and hill structures in *G. camelopardalis*.

Table 3.2. Analytical statistics on ungulates: results from Welch-Yuen tests with 15% trimming for the primary (A), S-F (B), and S-L (C) surfaces.

	Primary surface (A)				**S-F surface (B)**				**S-L surface (C)**			
	Ft	*p*	nu1	nu2	*Ft*	*p*	nu1	nu2	*Ft*	*p*	nu1	nu2
Sa	5.831	**0.017**	3	9.160	10.275	**0.003**	3	9.205	4.840	**0.027**	3	9.453
Sdv	1.561	0.257	3	10.486	4.474	**0.035**	3	9.008	14.034	**0.001**	3	8.325
Shv	1.134	0.389	3	8.519	9.746	**0.003**	3	9.154	4.263	**0.044**	3	8.141
Smc	1.943	0.193	3	9.003	7.969	**0.006**	3	9.637	5.518	**0.019**	3	9.263
Spd	0.453	0.722	3	8.474	4.984	**0.029**	3	8.368	5.451	**0.020**	3	9.270
Sq	4.686	**0.033**	3	8.591	11.884	**0.003**	3	7.907	3.957	**4.5E-02**	3	9.340
Sxp	10.829	**0.002**	3	9.228	6.264	**0.013**	3	9.388	4.071	**0.042**	3	9.525
Vmc	22.410	**2.2E-04**	3	8.481	9.632	**0.003**	3	9.428	4.192	**0.040**	3	9.159
Vv	19.957	**2.3E-04**	3	9.240	8.310	**0.005**	3	9.625	4.071	**0.042**	3	9.525
Vvc	18.747	**4.4E-04**	3	8.439	9.075	**0.004**	3	9.692	3.611	0.055	3	9.613
Vvv	13.553	**0.001**	3	8.573	5.224	**0.022**	3	9.419	4.192	**0.040**	3	9.159
mev	2.034	0.182	3	8.660	2.493	0.126	3	9.080	10.211	**0.003**	3	8.621
medf	4.771	**0.028**	3	9.268	4.943	**0.027**	3	9.067	7.111	**8.3E-03**	3	9.602
metf	2.651	0.112	3	9.024	4.402	**0.034**	3	9.456	4.341	**3.5E-02**	3	9.529
Tr1R	8.534	**0.004**	3	10.510	2.097	0.170	3	9.065	2.097	0.170	3	9.065
IsT	5.007	**0.024**	3	9.608	9.205	**0.004**	3	8.839	9.729	**0.003**	3	9.028
FLTp	3.537	0.058	3	9.570	5.652	**0.017**	3	9.436	5.483	**0.018**	3	9.781
FLTq	5.522	**0.020**	3	9.108	6.239	**0.013**	3	9.605	3.274	0.075	3	8.736
FLTt	3.232	0.076	3	8.764	6.814	**0.013**	3	8.149	5.071	**0.023**	3	9.741

Values in bold indicate a significant difference ($p \leq 0.05$). *Ft* = test statistics; nu1 and nu2 = 1st and 2nd degree of freedom, respectively; *p* = significance level. Parameters: see Table 2.2. From Schulz *et al.* (submitted, table 3).

Table 3.3. List of parameters which return significant differences ($p \leq 0.05$) for both Dunnett and Cliff tests for the given pair of ungulate species for the primary (A), S-F (B), and S-L (C) surfaces.

	cotau dibic	*cotau eqgre*	*cotau gicam*	*dibic eqgre*	*dibic gicam*	*eqgre gicam*
Primary surface (A)	***Sa***, *Sq, Ssk, Std, Sv, Sxp, Vmc, Vv, Vvc, Vvv, FLTq, IsT, Tr1R*	*Ssk*	***Sa***, *Sq, Std, Sxp, Vmc, Vv, FLTq,* ***medf****, Tr1R*	***Sa***, *Sq, Ssk, Std, Sv, Sxp, Vmc, Vv, Vvc, Vvv, FLTq,* ***medf****,* ***IsT****, Tr1R*		*Std, Sxp, Vv,* ***medf****, Tr1R*
S-F surface (B)	***Sa***, *Smc, Spd, Sq, Sxp, Vmc, Vv, Vvc, Vvv, FLTp, FLTq, FLTt,* ***IsT***	***medf***	***Sa***, *Sdv, Shv, Smc, Spd, Sq, Sxp, Vmc, Vv, Vvc, Vvv, FLTp, FLTq, FLTt, metf,* ***IsT***	***Sa***, *Smc, Spd, Sq, Vmc, Vv, Vvc, Vvv, FLTp, FLTq, FLTt,* ***medf****, metf,* ***IsT***	*Sdv, Shv*	*Sdv, Shv, Smc, Sq, Sxp, Vmc, Vv, Vvc, FLTp, FLTq, FLTt,* ***medf****, metf,* ***IsT***
S-L surface (C)	*Sha, Spd, mev,* ***IsT***	*Sda, Sdv, Sha, Shv,* ***medf***	***Sa***, *Sdv , Shv, Spd,* ***IsT***	***Sa***, *Sda, Sdv, Sha, Shv, mev,* ***medf****,* ***IsT***	*Sdv, Shv*	***Sa***, *mev,* ***medf****,* ***IsT***

Values in bold indicate texture parameters providing stable patterns for the three surface types. Parameters: see Table 2.2. Species abbreviations as in Table 3.1. From Schulz *et al.* (submitted, table 4).

Figure 3.1. (next page, page 61) Boxplots of the inter-specific differences according to different polynomial orders for three parameters *Sa*, *medf*, and *IsT* of the primary surface (*white boxes*, A), the S-F surface (*light gray boxes*, B), and the S-L surface (*dark gray boxes*, C) for the four ungulate species. cotau = *Connochaetes taurinus*, dibic = *Diceros bicornis*, eqgre = *Equus grevyi*, gicam = *Giraffa camelopardalis*. Parameters: see Table 2.2. From Schulz *et al.* (submitted, fig. 3).

Figure 3.2. (page 62) Boxplots of the inter-specific differences on the S-F surfaces of the four ungulate species. Parameters: see Table 2.2. Species abbreviations: CT = *Connochaetes taurinus*, DB = *Diceros bicornis*, EG = *Equus grevyi*, GC = *Giraffa camelopardalis*. From Schulz *et al.* (submitted, fig. 4).

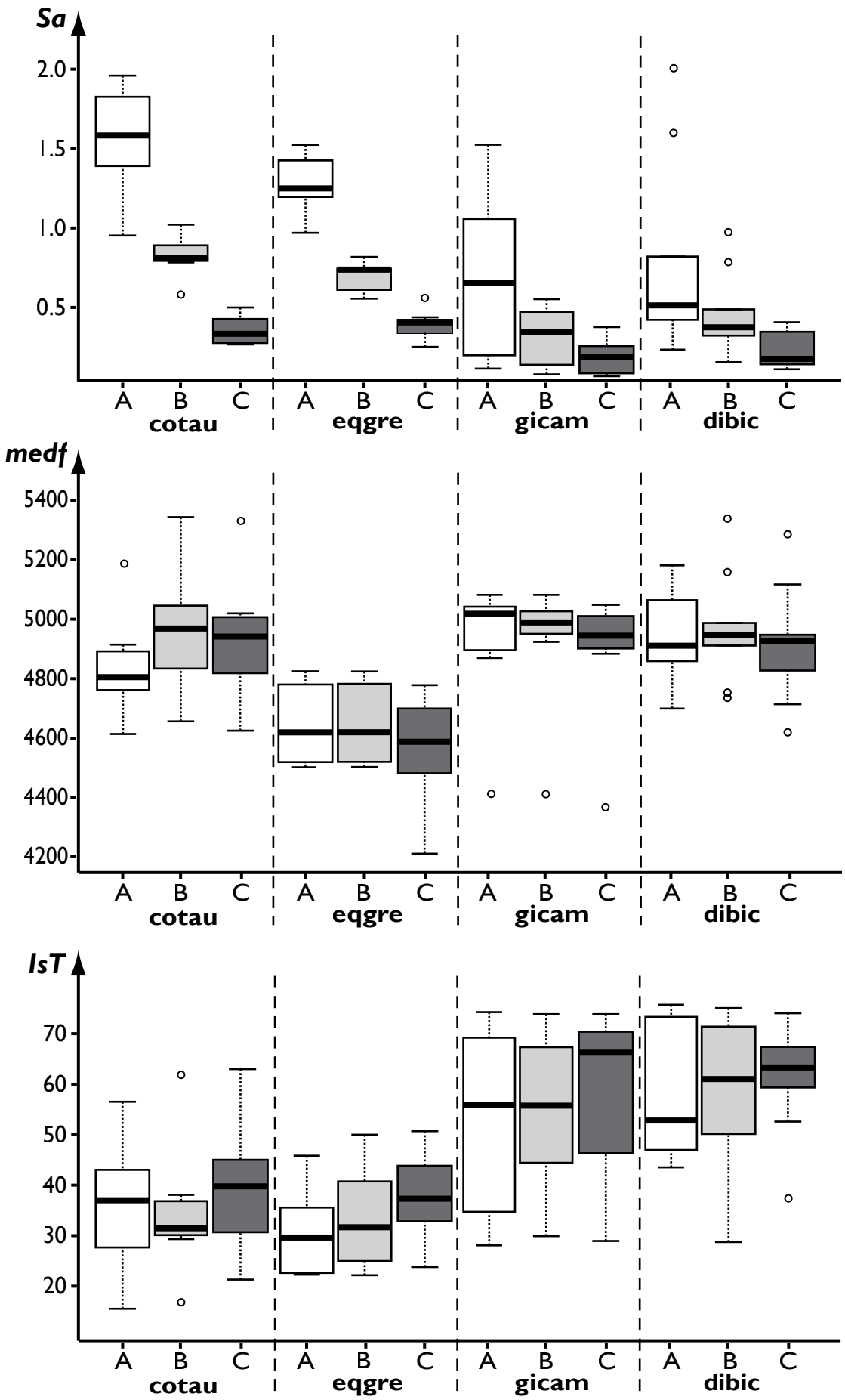
Sa
2.0
1.5
1.0
0.5
A B C A B C A B C A B C
cotau eqgre gicam dibic
medf
5400
5200
5000
4800
4600
4400
4200
A B C A B C A B C A B C
cotau eqgre gicam dibic
IsT
70
60
50
40
30
20
A B C A B C A B C A B C
cotau eqgre gicam dibic

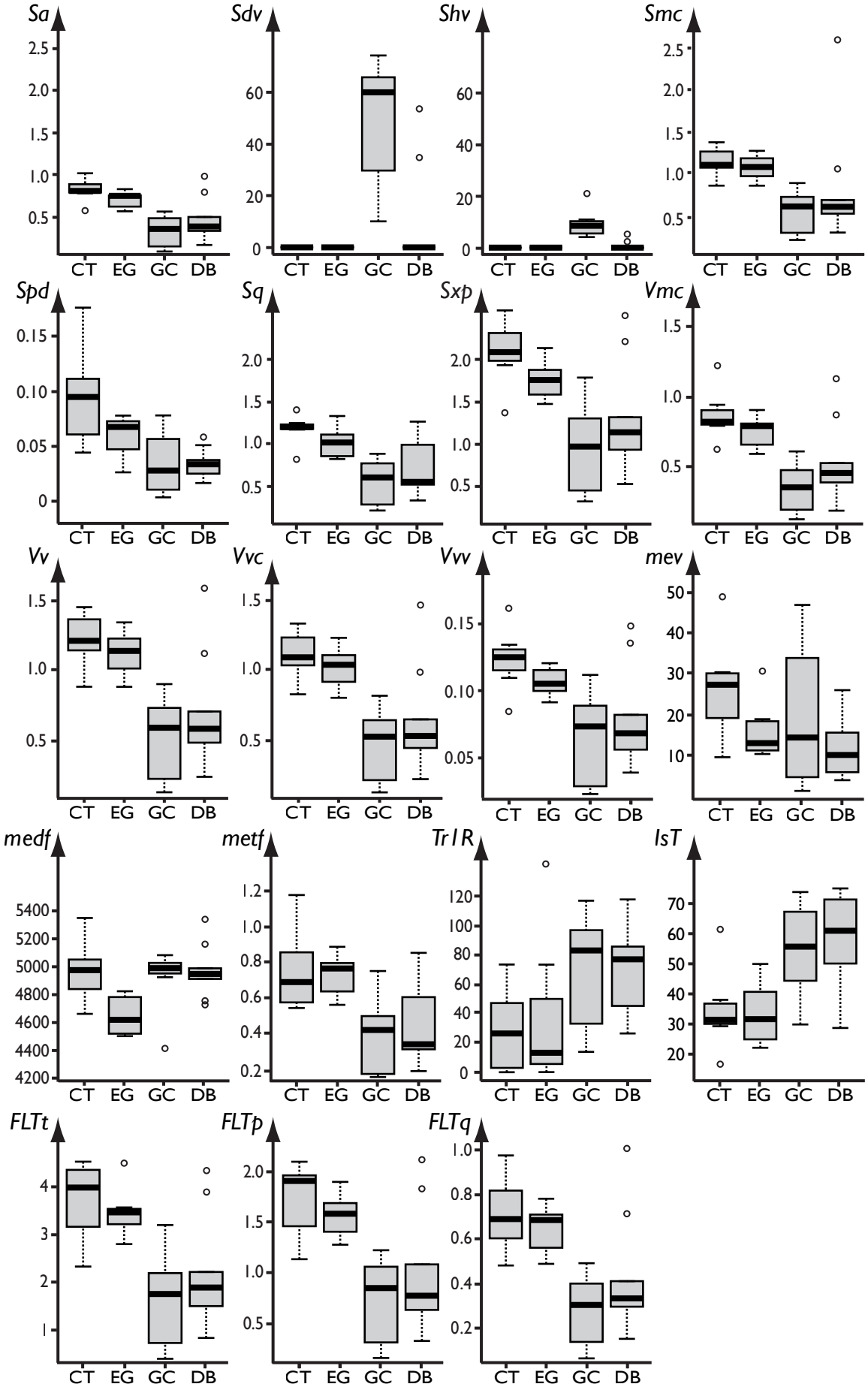
Sa
Sdv
Shv
Smc
Spd
Sq
Sxp
Vmc
Vv
Vvc
Vvv
mev
medf
metf
TrIR
IsT
FLTt
FLTp
FLTq
CT
EG
GC
DB

3.3 Primates

3.3.1 Primate diets assessed by the SSFA (hypothesis 3; Calandra *et al.* submitted)

Fruit proportion

There is a positive correlation between the complexity (*Asfc*) and the proportion of fruit in the diet (r_{pb} = 0.380, p = 0.032, 95% confidence interval = [0.029, 0.624]; Fig. 3.3a, Table 3.5). This correlation is negative and stronger for both $HAsfc_9$ (r_{pb} = -0.407, p = 0.006, 95% confidence interval = [-0.622, -0.120]; Fig. 3.3c) and $HAsfc_{81}$ (r_{pb} = -0.418, p = 0.005, 95% confidence interval = [-0.628, -0.115]; Fig. 3.3d). *Alouatta seniculus* and *Theropithecus gelada* fall above the regression lines for *Asfc*. The observed values for *Pongo abelii* are smaller than the estimated ones for *Asfc* and higher for both *HAsfc* parameters.

Consumption of hard items

No correlation is found between the textural fill volume (*Tfv*) and the proportion of fruit (r_{pb} =0.134, p=0.393, 95% confidence interval = [-0.195, 0.404]; Fig. 3.3b, Table 3.5).

Table 3.4. Descriptive statistics on primates.

Species	n	Stat	*Asfc*	*Tfv*	$HAsfc_9$	$HAsfc_{81}$	*epLsar*	*S5v*	*Sq*	*Vm*	*Spd*	*Sha*	*Sda*
A. seniculus	3	mean	144.531	43786.034	0.562	0.574	0.000309	5.345	1.057	0.101	0.084	0.324	0.432
		SD	59.917	16938.553	0.306	0.261	0.000187	2.084	0.468	0.062	0.036	0.025	0.319
G. gorilla	6	mean	60.524	40775.052	0.586	0.721	0.001361	3.038	0.660	0.039	0.037	2.209	2.323
		SD	42.281	6454.824	0.269	0.288	0.000406	2.488	0.415	0.036	0.024	3.593	3.337
L. albigena	7	mean	87.383	37257.314	0.711	1.045	0.000809	5.694	0.885	0.058	0.065	0.472	0.693
		SD	46.216	6118.501	0.421	0.609	0.000301	1.901	0.235	0.021	0.018	0.178	0.680
M. fascicularis	7	mean	140.863	37839.742	0.341	0.496	0.000537	5.080	1.092	0.093	0.105	0.300	0.178
		SD	28.000	10135.961	0.109	0.163	0.000157	1.705	0.351	0.037	0.045	0.157	0.242
P. abelii	7[a]	mean	27.461	28498.761	0.889	1.180	0.001177	2.232	0.426	0.020	0.024	1.636	0.867
		SD	13.485	6563.041	0.506	0.539	0.000612	1.395	0.128	0.012	0.014	1.379	0.418
P. cynocephalus	10	mean	47.802	33651.533	0.747	0.957	0.001398	2.782	0.667	0.034	0.031	1.246	4.128
		SD	14.703	4604.757	0.270	0.293	0.000845	0.749	0.198	0.012	0.012	0.744	5.179
P. troglodytes	5	mean	147.660	44178.380	0.389	0.462	0.000318	5.365	0.943	0.077	0.052	0.715	0.554
		SD	68.968	4766.154	0.178	0.207	0.000163	2.718	0.329	0.037	0.042	0.866	0.556
T. gelada	2	mean	110.602	37240.170	0.637	0.965	0.000846	4.643	0.778	0.070	0.075	0.386	1.234
		SD	53.366	6374.477	0.170	0.461	0.000331	0.716	0.366	0.040	0.010	0.150	0.235

n = number of individuals per species, SD = standard deviation. Parameters: see Tables 2.2-2.3. Species: *A. seniculus* = *Alouatta seniculus*, *G. gorilla* = *Gorilla gorilla*, *L. albigena* = *Lophocebus albigena*, *M. fascicularis* = *Macaca fascicularis*, *P. abelii* = *Pongo abelii*, *P. cynocephalus* = *Papio cynocephalus*, *P. troglodytes* = *Pan troglodytes*, *T. gelada* = *Theropithecus gelada*. [a] n = 6 for *Sda*.

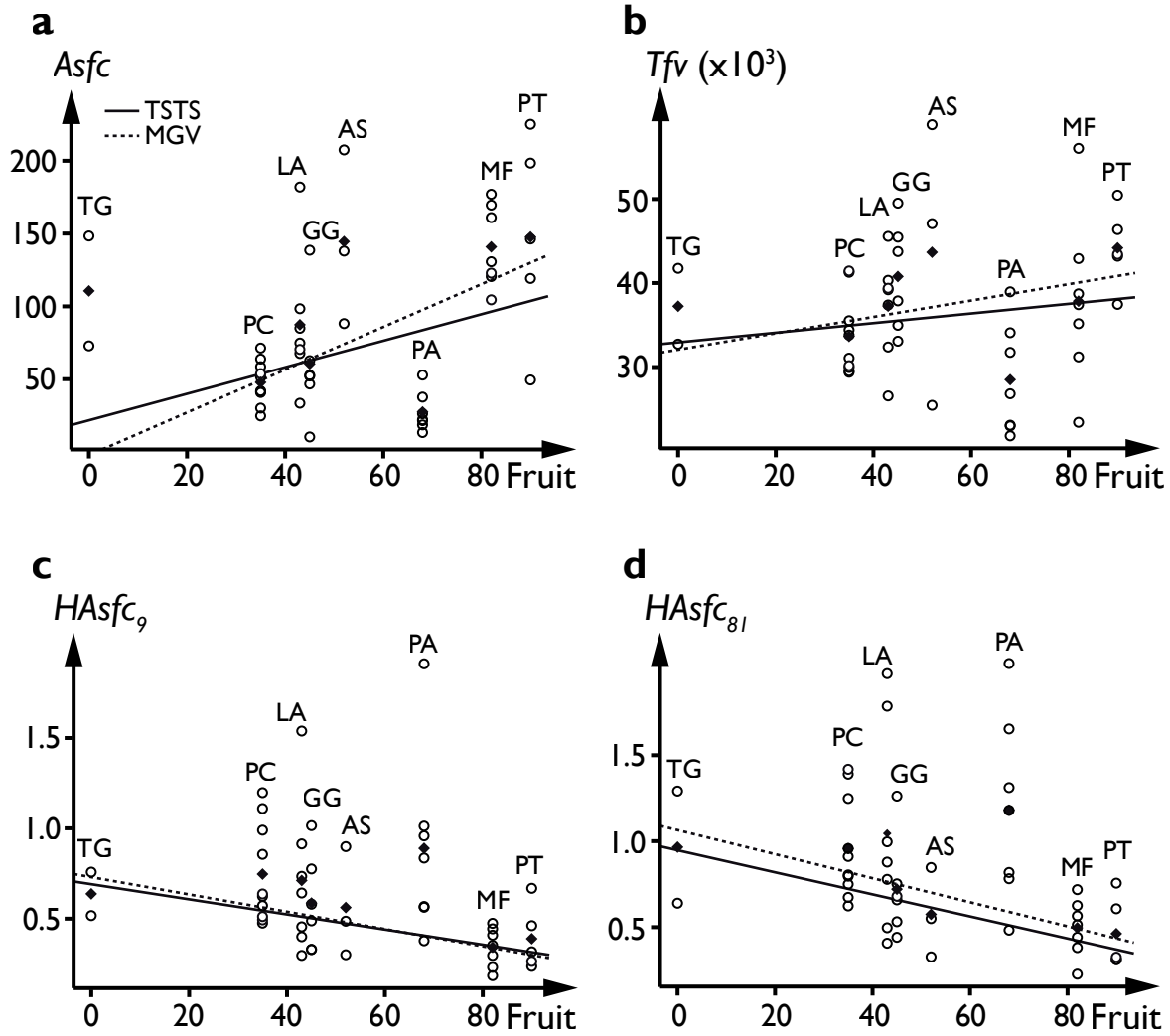

Figure 3.3. Regression based on two methods (TSTS and MGV) for four SSFA parameters (Table 2.3) against the mean annual proportion of fruits (in percent) in the diets of the eight primate species studied (Table 2.1). These parameters have no units. The regression equations and the correlation coefficients are given in Table 3.5. Unfilled dots represent all studied specimens; filled diamonds indicate the means for each species. Species abbreviations: AS = *Alouatta seniculus*, GG = *Gorilla gorilla*, LA = *Lophocebus albigena*, MF = *Macaca fascicularis*, PA = *Pongo abelii*, PC = *Papio cynocephalus*, PT = *Pan troglodytes*, TG = *Theropithecus gelada*.

Table 3.5. Analytical statistics on primates: regression equations and correlation coefficients.

	TSTS	MGV	r_{pb}	p	lower CI	upper CI
Asfc	Y = 21.7+91.1X	Y = -2.26+147X	0.380	0.032	0.029	0.624
Tfv	Y = 32900+5730X	Y = 32100+9740X	0.134	0.393	-0.195	0.404
$HAsfc_9$	Y = 0.691-0.418X	Y = 0.73-0.479X	-0.407	0.006	-0.622	-0.120
$HAsfc_{81}$	Y = 0.947-0.641X	Y = 1.06-0.699X	-0.418	0.005	-0.628	-0.115

Regression equations for the TSTS and MGV methods and percentage bend correlation coefficients (r_{pb}) with associated significance level (p) and 95% confidence interval (lower and upper CI) for four SSFA parameters against the mean annual proportion of fruits (in percent) in the diets of the eight primate species studied (see Fig. 3.3).

Dunnett and Cliff tests discriminate two groups of species according to *Tfv* (Fig. 3.4b, Tables 3.6-3.7, Appendices 4.2-4.3). The first group comprises *Pongo abelii* and *Papio cynocephalus*, which have very low and low values, respectively. The second group has moderate to high values. *Theropithecus gelada* could graphically belong to either group but could not be statistically analyzed because of the small sample size (Table 3.4, section 2.8.3).

Grass consumption

The anisotropy (*epLsar*) shows a grouping separating *Alouatta seniculus*, *Pan troglodytes*, *Macaca fascicularis* and *Lophocebus albigena* with low values on the one hand, and *Gorilla gorilla*, *Papio cynocephalus* and *Pongo abelii* with high values on the other (Fig. 3.4e, Tables 3.4, 3.6-3.7, Appendices 4.2-4.3). As for *Tfv*, the position of *Theropithecus gelada* is ambiguous.

Table 3.6. Analytical statistics on primates: results from Welch-Yuen tests with 0% (**a**) and 15% (**b**) trimming.

a. Trim 0%	*Ft*	*p*	nu1	nu2
Asfc	**15.121**	**0.000**	**6**	**12.150**
epLsar	**8.272**	**0.001**	**6**	**13.842**
HAsfc$_9$	**3.887**	**0.020**	**6**	**12.778**
HAsfc$_{81}$	**4.213**	**0.014**	**6**	**13.236**
Tfv	**4.043**	**0.017**	**6**	**12.702**
S5v	**4.356**	**0.014**	**6**	**12.069**
Sq	**6.012**	**0.004**	**6**	**12.474**
Vm	**6.049**	**0.004**	**6**	**12.163**
Spd	**6.234**	**0.003**	**6**	**12.270**
Sha	**3.959**	**0.014**	**6**	**15.485**
Sda	**2.961**	**0.047**	**6**	**13.170**

b. Trim 15%	*Ft*	*p*	nu1	nu2
Asfc	**14.353**	**0.000**	**6**	**10.811**
epLsar	**10.354**	**0.000**	**6**	**11.772**
HAsfc$_9$	2.988	0.054	6	11.276
HAsfc$_{81}$	2.996	0.053	6	11.308
Tfv	**3.683**	**0.029**	**6**	**11.095**
S5v	**4.644**	**0.015**	**6**	**10.565**
Sq	**8.410**	**0.001**	**6**	**10.919**
Vm	**4.557**	**0.016**	**6**	**10.457**
Spd	**6.220**	**0.005**	**6**	**10.529**
Sha	**5.246**	**0.007**	**6**	**12.316**
Sda	**4.367**	**0.017**	**6**	**10.796**

Values in bold indicate a significant difference ($p \leq 0.05$). Parameters: see Tables 2.2-2.3. Abbreviations as in Table 3.2.

Table 3.7. List of parameters which return significant differences ($p \leq 0.05$) for both Dunnett and Cliff tests for the given pair of primate species.

Species 1	**Species 2**	**Parameters**
A. seniculus	*P. cynocephalus*	*Asfc, epLsar, Sha*
*L. albige*na	*P. abel*ii	*Asfc, Spd*
L. albigena	*P. cynocephalus*	*S5v, Spd, Sha*
L. albigena	*P. troglodytes*	*epLsar*
M. fascicularis	*G. gorilla*	*Spd*
M. fascicularis	*P. abelii*	*Sq, Sha, Sda*
M. fascicularis	*P. cynocephalus*	*Asfc, epLsar, Vm, Spd, Sha*
P. cynocephalus	*P. troglodytes*	*Tfv, epLsar*
P. troglodytes	*P. abelii*	*Asfc, Tfv*

Parameters: see Tables 2.2-2.3. Species abbreviations: see Table 3.4.

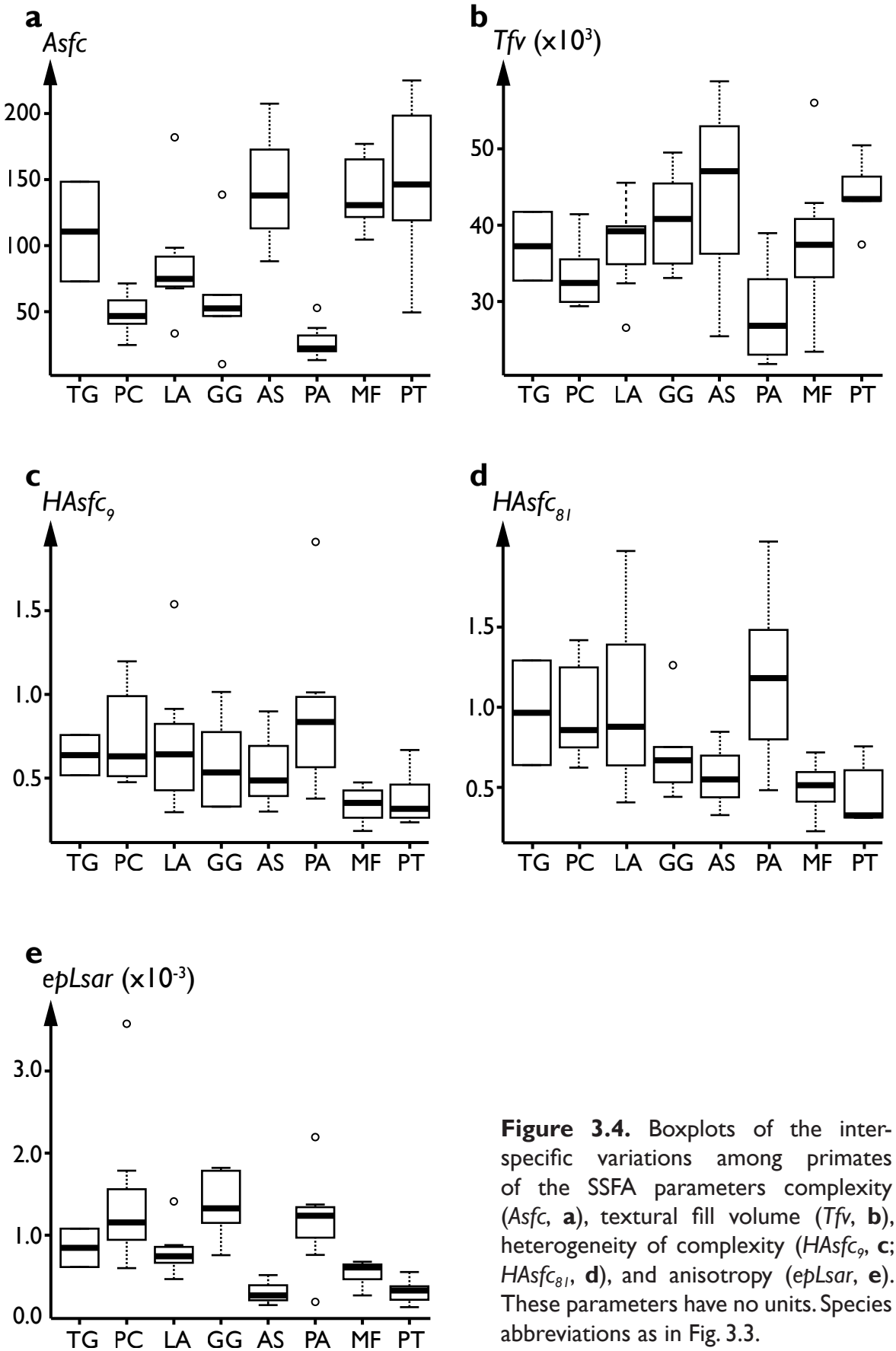

Figure 3.4. Boxplots of the inter-specific variations among primates of the SSFA parameters complexity (*Asfc*, **a**), textural fill volume (*Tfv*, **b**), heterogeneity of complexity ($HAsfc_9$, **c**; $HAsfc_{81}$, **d**), and anisotropy (*epLsar*, **e**). These parameters have no units. Species abbreviations as in Fig. 3.3.

3.3.2 DASTA, food biomechanics and tooth function of primates (hypothesis 4; Calandra *et al.* submitted)

Most of the differences in the ISO parameters *S5v*, *Sq* and *Vm* for the eight species are supported only by Dunnett tests (Appendices 4.2-4.3). This might imply that the differences are only indicative (Fig. 3.5). On the other hand, both Dunnett and Cliff tests distinguish differences between *Lophocebus albigena* and *Papio cynocephalus* (*S5v* and *Vm*) and between the former and *Pongo abelii* (*Sq*) (Table 3.7).

Two groups of species can be recognized from each of the six ISO parameters. The first group includes the two species with the largest consumption of fruits (*Pan troglodytes* and *Macaca fascicularis*, fruits > 80%), the only leaf-eater (*Alouatta seniculus*, tree leaves = 35%), and the hard-object feeder (*L. albigena*, fruits = 43%, seed destroying, insects = 36%, bark = 9%) (Table 2.1). *Theropithecus gelada* (grass = 100%) also seems to belong to this group. This group is characterized by enamel textures with deep valleys (high *S5v*), high amplitude in profile (high *Sq*), high material volume (high *Vm*), lots of peaks (high *Spd*), low values and narrow variations in hill (low *Sha*) and valley (low *Sda*) areas (Fig. 3.5, Table 3.4). The pattern is more complicated for *Spd*: the same grouping is actually more strongly supported (Table 3.7, Appendices 4.2-4.3), but *P. troglodytes* has intermediate values and is therefore not statistically different from any other species (Fig. 3.5d). The second group, composed of *Gorilla gorilla*, *P. cynocephalus* and *P. abelii*, has opposite values for all parameters. Enamel surfaces of the first group therefore have more and deeper but smaller and less variable (in area) valleys and hills/peaks as compared to the second group.

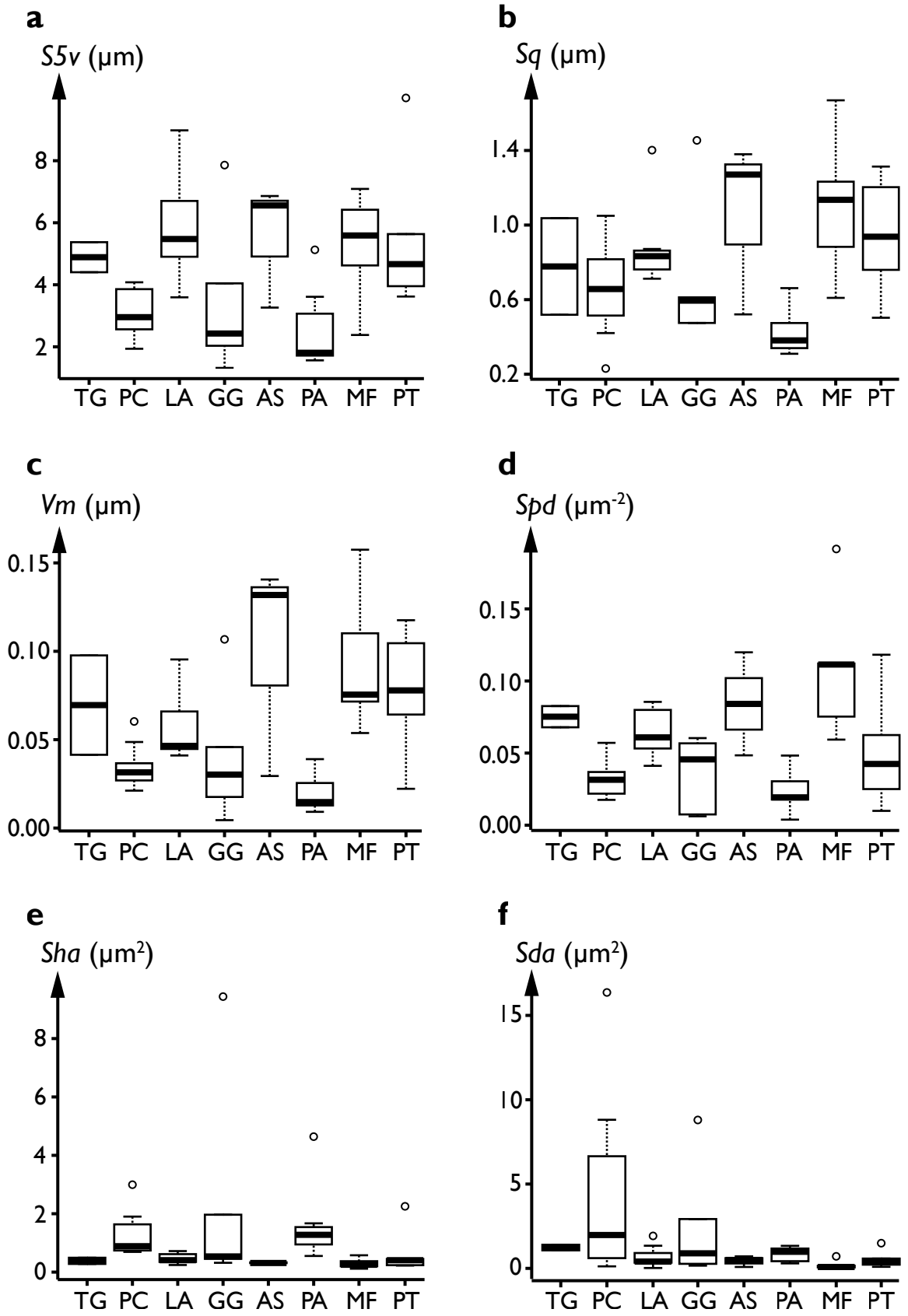

Figure 3.5. Boxplots representing the inter-specific variations among primates of the ISO parameters (Table 2.2) five point valley height (*S5v*, **a**), root mean square height (*Sq*, **b**), material volume (*Vm*, **c**), density of peaks (*Spd*, **d**), closed hill area (*Sha*, **e**), and closed dale area (*Sda*, **f**). Species abbreviations as in Figure 3.3.

Browse *versus* grass

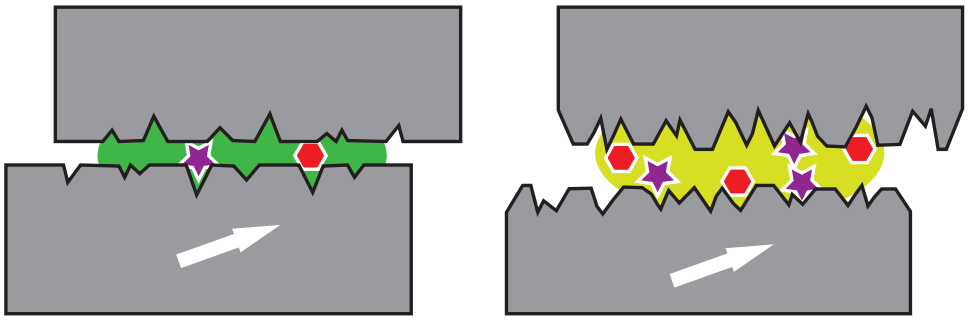

4. Discussion

4. Discussion

4.1 Tracing chewing mechanisms in ungulates: 3D tribology of enamel microtexture

Through the DASTA, two hypotheses have been tested on the ungulate dataset (Schulz *et al.* submitted) relating to wavelength filtering thresholds (hypothesis 1) and inter-specific differences in chewing mechanics (hypothesis 2).

4.1.1 Robustness of DASTA texture parameters across filtering thresholds (hypothesis 1)

Since the 3D ISO/FDIS 25178-2 (International Organization for Standardization 2010), the motif, furrow, and flatness analyses are available, new applications are rapidly being developed, but the practitioners have great difficulties to decide which wavelength filtering mode is most appropriate to apply on enamel surfaces. Here three different filters and their influence on the DASTA texture parameters extracted from the ungulate enamel surfaces have been tested (Schulz *et al.* submitted).

Arithmetical mean height

The arithmetical mean height (*Sa*) decreases when form (S-F surface, (B)) and waviness (S-L surface, (C)) are removed for each species. This indicates that the *Sa* is one of the few parameters which is *per se* sensitive to wavelength filtering (Schulz *et al.* submitted). This phenomenon illustrates a basic characteristic of wavelength filtering, which implies that long wavelength alterations are mostly associated with high peak values, while short wavelength alterations have low peak heights. Assuming that the steepness of flanks is constant within a surface, any surface will decrease in average peak height if long wavelength alterations are excluded and *vice versa* (Schulz *et al.* submitted).

Density of furrows

Mean density of the furrows (*medf*) is not affected by differing filtering algorithms. Since a furrow is about the smallest element of the texture pattern I expect it to be little affected by wavelength filtering and thus this result is not surprising. The density of furrows is therefore a robust parameter (Schulz *et al.* submitted).

Isotropy

Functional and structural isotropies are not necessarily coupled. Structural isotropy is related to the prism orientation in the enamel while functional isotropy is related to the chewing direction and to the direction of the food movements across the enamel facet (Schulz *et al.* submitted). Both elements of isotropy measured with the parameter isotropy (*IsT*) may be related to each other by the depth of evolutionary optimization. It is expected that optimization effects at a specific locus would be related to the diet and morphology of the tooth crown. Thus, if there was any evident interrelationship of both elements of isotropy, those elements should not be independent of dietary trait. Specifically, it is expected that excluding the structural wavelength would result in more fluctuation of the remaining features between the species due to their differences in diets (function). What we observe, however, is an increase in isotropy along the filtering gradient consistent for all species (Fig. 3.1). The results therefore suggest that (1) the structural isotropy is not filtered out because its wavelength is too large or too small, or that (2) no structural signal is involved at all. The latter explanation is more likely, since visual observations of the 3D surfaces show no sign of regularly oriented structures.

To conclude, hypothesis 1 has to be rejected (Schulz *et al.* submitted). No consistent wavelength filtering algorithm thresholds was found in the grazers and browsers selected. Instead species-independent patterns of effects induced by the filtering algorithms but not by the nature of the surface were found.

The largest number of inter-specific differences (n = 19) found on the S-F surface (B) as compared to the primary (A) and S-L (C) surfaces (Fig. 3.1, Table 3.3) indicates that the S-F surface is highly suited for inter-specific characterization (Schulz *et al.* submitted). The S-F surfaces have therefore been used to address hypotheses 2-4, as they relate to inter-specific comparisons.

4.1.2 Testing for characteristics of food and masticatory biomechanics through the DASTA (hypothesis 2)

Eleven (*Sa*, *Smc*, *Sxp*, *Vmc*, *Vv*, *Vvc*, *Vvv*, *IsT*, *FLTt*, *FLTp*, *FLTq*) out of nineteen significant surface texture parameters allow distinction between the dietary categories on the S-F surfaces of the four ungulate species (Fig. 3.2, Table 3.3). Summarizing the characteristics of the ISO/FDIS 25178, motif, furrow, isotropy, and flatness analyses, textures of the grazers are characterized as complex and anisotropic with large heights and volume, high ratios of peaks, and deep furrows (Fig. 4.1a; Schulz *et al.* submitted).

These characteristics relate to biomechanics of dietary components and chewing dynamics (Schulz *et al.* submitted), because significant impact of structural (morphology-related) low frequency alterations on the microtexture could be excluded (hypothesis 1, section 4.1.1). Since grass leaves tend to split along the parallel vascular strands, elongated particles result from comminution (Clauss *et al.* 2003). Chewing on browse, in particular on tree leaves which have polygonal vascular structures, thus results in polygonal and more compact particles. If dispersed in saliva, grass boli are supposed to bear a larger ratio of plant tissue to saliva as compared to browse boli. Together with the more fiber-mediated interconnection, a grass bolus should have higher viscosity as a result of its aeration. In terms of its tribology, this effect is similar to foam building in lubricating oils (Fowle 1981) and a grass bolus should thus have a similar tribologic effect. Both factors (aeration and fibers) should not apply to a browse-dominated bolus to the same extent (Schulz *et al.* submitted). This would result in a higher viscosity and flow resistance of the grass bolus (Fig. 4.1a) which would keep the occlusal gap larger as compared to the less viscous browse bolus (Fig. 4.1b), given that the same forces are applied (Schulz *et al.* submitted). Surface textures with more peaks (like a fakir bed of nails) as observed in the grazing *Connochaetes taurinus* and *Equus grevyi* would therefore increase friction between the surface and the bolus and fix particles to the surface. It is proposed that this increased friction provides a major element that allows shearing forces to rupture cell walls, which, after fermentation, constitute the main source of energy in grazers (Lechner-Doll *et al.* 1991; Van Soest 1994; Lucas 2004; Schulz *et al.* submitted).

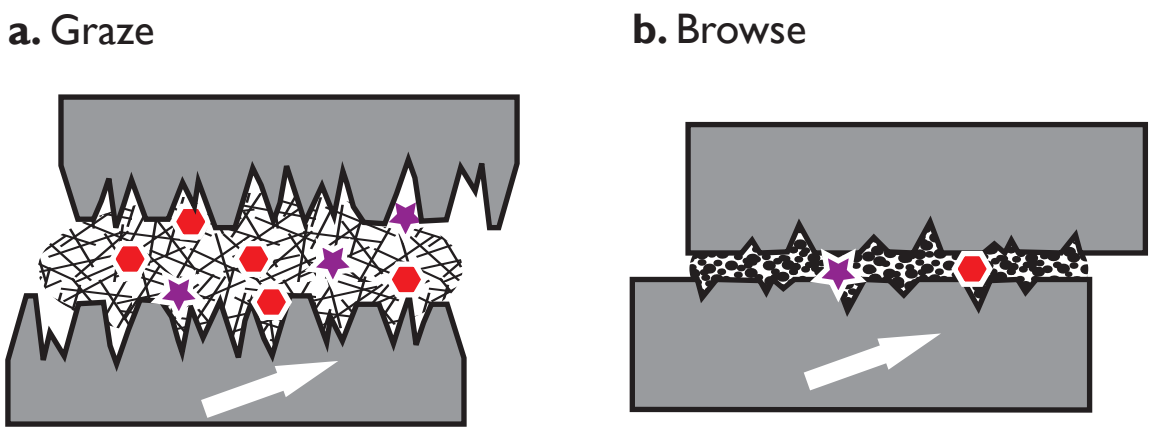

Figure 4.1. Characteristic models of the surface textures (viewed in profile) induced by a highly abrasive grazing diet (**a**) and a less abrasive browsing diet (**b**). *Purple starlets* = plant-based abrasives (phytoliths), *red hexagons* = exogenous abrasives (grit and dust), *white arrows* = movement of the lower jaw. From Schulz *et al.* (submitted, fig. 5).

Moreover, the higher abrasion of grass compared to browse material (Fortelius 1985; Janis & Fortelius 1988; Clauss *et al.* 2008) would create more relief and more anisotropy (Scott *et al.* 2006) in the microtexture of grazers' teeth.

Conversely in browsers (*Giraffa camelopardalis* and *Diceros bicornis*), less complex and more isotropic textures prevail, which have lower amplitudes in height, lower volume, and lower peak and furrow ratios (Fig. 3.2). Low peak densities would easily be explained by closer approaches of antagonistic dental faces, making the occlusal gap narrower (Schulz *et al.* submitted). Flattening caused by peak removal would be a necessary consequence (Kaiser & Brinkmann 2006). It is not generally proposed that attrition occurs more frequently in browsers than in grazers because it is unkown whether peak removal is the result of collision between antagonistic facets or of hydrodynamic pressures (see sections 1.2 and 1.5; Schulz *et al.* submitted).

In summary, this implies that more relief is created in grazers through abrasion and that the relief is flattened in browsers through peak removal (Schulz *et al.* submitted).

Texture patterns reflect geometric and dynamic mechanisms, that allow the distinction of major food sources according to the biomechanical properties relevant to comminution and chewing success (Schulz *et al.* submitted). Hypothesis 2 is thus accepted.

4.2 Teasing apart the contributions of hard dietary items on 3D dental microtextures in primates

This part concerns the primate dataset. First, the SSFA was used to assess the diets of the studied primates (hypothesis 3). The DASTA was then applied to understand the deformation and fracture mechanics of the enamel surfaces of these primates in relation to the food consumed (hypothesis 4).

4.2.1 Primate diets assessed by the SSFA (hypothesis 3)

Fruit proportion

As hypothesized, the consumption of fruits correlates positively with the complexity of facet surfaces (*Asfc*; Fig. 3.3a, Table 3.5) and negatively with the heterogeneity of complexity (*HAsfc*; Fig. 3.3c-d). Fruits include hard items, which fracture the enamel, so that a large consumption of fruits produces pitted, complex surfaces (high *Asfc*; Fig. 2.6, Table 2.3). Simultaneously, this complex pattern is homogeneous over the entire

surface (low $HAsfc_9$ and $HAsfc_{81}$). Taken together, parameters *Asfc* and *HAsfc* show a distinctive pattern related to the proportion of fruits in the diet of extant primates. The correlations thus show that it is possible to estimate the proportion of fruit components in extinct species, which is a big step forward in assessing the diets of Vertebrates. More precise estimations will come with larger data sets, on which different types of regression (non-linear) can be tested.

The complexity of the surfaces in *Alouatta seniculus* and *Theropithecus gelada* does not fit the regression (Fig. 3.3a). However, the heterogeneity values more closely correspond to their fruit proportions (Fig. 3.3c-d) indicating that this parameter is probably a better indicator of the fruit proportion than the complexity.

Pongo abelii, which consumes 68% of fruits (Table 2.1), clearly falls below the regression line for *Asfc* and above it for *HAsfc* (Fig. 3.3a, c-d). *P. abelii* is the only species from this dataset that clearly does not fit the regression. The regression is therefore considered to be supported by the data and the result for *P. abelii* are interpreted as pointing to yet unknown seasonal and/or dietary behavior not previously acknowledged (Table 2.1). Unfortunately, sampling dates are unavailable for the *P. abelii* specimens. Fruit is however a seasonal resource and the proportion of fruit in this species's diet can drop to less than 45% (Wich *et al.* 2006). Thus, seasons/years with low fruit availability were likely sampled. This point requires more detailed temporal data to clarify the meaning of these outliers.

Consumption of hard items

Since fruits include hard items, and since both the complexity (*Asfc*) and fill volume (textural fill volume, *Tfv*) have been found to indicate the consumption of fruit and hard items (Scott *et al.* 2006; Scott *et al.* 2009), it was expected that a correlation between the fill volume and the proportion of fruit would also be found (Fig. 3.3b, Table 3.5). But, if *Tfv* would reflect the amount of fruit consumed as *Asfc*/*HAsfc* do, one would expect to observe three groups: (1) *Pan troglodytes*, *Macaca fascicularis* and *Pongo abelii* with high *Tfv* values; (2) *Alouatta seniculus*, *Lophocebus albigena*, *Gorilla gorilla* and *Papio cynocephalus* with moderate to low *Tfv* values; and (3) *Theropithecus gelada* with very low *Tfv* values (Table 2.1). This partitioning, however, is not supported by Dunnett and Cliff tests (Fig. 3.4b, Tables 3.4 and 3.6-3.7, Appendices 3.3-3.4), indicating that complexity and textural fill volume are decoupled. The fill volume of a surface increases with the size (in area and depth) of the surface features. Other hard items can indent or fracture dental enamel in the same way fruits do. In addition to being related to the

amount of fruits consumed, the textural fill volume is more strongly impacted than complexity by the ingestion of other hard components of foods or environments. The processing of hard items thus results in larger and/or deeper enamel scar features, and in a larger volume that can fill this surface.

P. troglodytes and *M. fascicularis* are not known to include significant proportions of hard items besides fruits in their diets (Table 2.1). The large and deep features found on their facets thus result most likely only from the very large (> 80%) proportion of fruits in the diets of these two species.

L. albigena consumes 43% of fruits and its *Asfc* and *HAsfc* values fit the regressions (Fig. 3.3a, c-d). However, its surfaces have large and deep pits (high *Tfv*), most similar to *M. fascicularis* (Fig. 3.4b), which consumes almost twice as much fruit. This can be explained by the consumption of hard items other than fruits: *L. albigena* is primarily a seed destroyer, and insects and bark constitute a substantial part of its diet (36% and 9%, respectively; Table 2.1). This is consistent with my hypothesis that the fill volume (*Tfv*) and complexity (*Asfc*/*HAsfc*) are decoupled.

G. gorilla, which diet consists of about 45% fruit (Table 2.1), also fits the *Asfc*/*HAsfc* trends as related to the amount of fruit but has higher *Tfv* values than would be expected if fruits alone contributed to the fill volume (as high as *M. fascicularis* and *L. albigena*; Fig. 3.4b, Appendices 3.3-3.4). Based on the dietary information available (Table 2.1), *Gorilla* neither consumes the large amount of fruits of *M. fascicularis*, nor is it known to feed on other hard items (as *L. albigena* does). Following the hypothesis that the fill volume depends on the consumption of all hard items, the discrepancy between the expected and observed *Tfv* values in *G. gorilla* suggests that it does consume other hard items, which have not yet been recognized in its diet. One possible source of such hard particles is grass, which contains hard silica phytoliths (Baker *et al.* 1959). When grass is sheared, in order to extract the cell content from such tough tissues, phytoliths are known to scratch dental enamel (Lucas 2004; see also Sanson *et al.* 2007 and discussions in Merceron *et al.* 2007 and in Damuth & Janis 2011; section 1.4). When the food is crushed instead of sheared, phytoliths produce pits (Lucas 2004) similar to fruits. Facet #9 in primates has a major crushing component (Kay & Hiiemae 1974). Because dust on leaves can be excluded as having an impact because of the humid environment occupied by *G. gorilla* (Table 2.1), the excessive pitting observed is likely to derive from grass phytoliths. However, while phytoliths can produce pits on the facets (Gügel *et al.* 2001; Lucas 2004), it is still unclear as to what influence this pitting has on the fill volume relative to other pitting agents like fruits or grit (Solounias & Semprebon 2002; Merceron *et al.* 2004).

Similarly to *G. gorilla*, the *Tfv* values in *P. cynocephalus* (Fig. 3.4b) cannot be explained solely by the fruit proportion but indicate there are additional sources of pitting agents. Silica phytoliths in grass, dust on grass, and grit ingested together with food are all hard enough to indent crushing facets and so contribute to the larger fill volumes than would be expected if fruit was the only agent of hard particles in both species. *Theropithecus gelada* does not consume fruits but destroys the seeds of grass. Its seed treatment is in accordance with its high fill volume (Fig. 3.4b). In *Tfv*, the pattern is almost identical to *L. albigena*, and thus likely reflects a similar composition of hard objects in the diets of the two species. Additionally, as hypothesized for *G. gorilla* and *P. cynocephalus*, the consumption of grass and therefore the crushing of the phytoliths it contains and of the grit and dust that come with it probably also has an influence on the fill volume. *P. cynocephalus* and *T. gelada* both inhabit dry open environments, where they feed on the ground (Table 2.1). Grit and dust may therefore play a role in the large fill volumes observed in these primates.

A. seniculus feeds largely on soft but tough tree leaves, which largely lack phytoliths (Epstein 1999; Hodson *et al.* 2005; Piperno 2006). Moreover the species is arboreal in rain forests (Table 2.1). Endogenous and exogenous abrasives therefore cannot account for the large fill volume of its dental surfaces (Fig. 3.4b). The spread in *Tfv* of the three studied individuals is however very large, almost as large as all other species together (Fig. 3.4b, Table 3.4), making feasible explanations really difficult. More specimens of *A. seniculus* would allow for a better understanding of the mechanisms underlying the texture signal in this species.

In the previous subsection, it was noted that *P. abelii* has surfaces with a lower complexity than expected from the reported proportion of fruits in its diet (68%, Table 2.1; Fig. 3.3a, 3.4a). This surprising result suggested that the proportion of fruit consumed by this sample of *P. abelii* was smaller than generally reported in for this species. The same conclusion is suggested by the exceptionally flat surfaces as revealed by the low *Tfv* values (Fig. 3.3b, 3.4b).

Grass consumption

Scott *et al.* (2006) found that anisotropic (high *epLsar*) surfaces are produced by the consumption of abrasive food. The hard phytoliths in grass are one of the main abrasives that can impact enamel surfaces (Merceron *et al.* 2007; Sanson *et al.* 2007; Damuth & Janis 2011; see section 1.4). When grass is sheared, the abrasives leave scratches on the surface, which run roughly parallel to the direction of mastication and food flow (Mills

1955). This mechanism therefore results in surfaces with a preferred orientation, *i.e.* in anisotropic surface textures.

Results from Dunnett and Cliff tests show that both *Gorilla gorilla* and *Papio cynocephalus* that are known to consume grass in significant proportions (Table 2.1) have more anisotropic surfaces (higher *epLsar*) than the other primate species investigated (Fig. 3.4e, Tables 3.6-3.7, Appendices 3.3-3.4). *Theropithecus gelada* seems to fit this model.

Textures in *Pongo abelii* are unexpectedly anisotropic (Fig. 3.4e). Other SSFA parameters indicate that these individuals had eaten a lower proportion of fruits than reported (Table 2.1), so grass cannot be completely excluded as a possible, maybe seasonal, food resource of *P. abelii*.

In the *Gorilla* discussion it was noted that silica phytoliths in grass or grit and dust from grass, when crushed, indent the enamel to produce pits (Gügel *et al.* 2001; Lucas 2004) and therefore contribute to the fill volume. This does not contradict the hypothesis that grass induces anisotropy since grass is always subject to shearing action to a certain extent. Shearing is more likely to produce scratches than pits (Lucas 2004). This duality in the processing and texture manifestation of phytoliths and grit/dust can be used to further detail the assessment on diets. The fill volume (*Tfv*) indicates the consumption of hard items, but it does not distinguish between the components. Anisotropy on the other hand reveals the consumption of grass by high *epLsar* values. At least part of the hard items detected in the texture signatures must then be phytoliths or grit. Combined with evidence given by texture complexity (*Asfc*), fruits, grass (phytoliths, grit and dust), and other hard items can be discriminated.

To conclude, the SSFA can indeed infer key aspects of the diets of primates. In accordance with R. S. Scott *et al.* (2005), R. S. Scott *et al.* (2006), and J. R. Scott *et al.* (2009), it has been found that the consumption of hard items and grass can be revealed by the SSFA. This is however the first time that the proportion of fruit in the diets of primates can be estimated through the SSFA (Calandra *et al.* submitted). The hypothesis 3 is therefore accepted.

4.2.2 DASTA, food biomechanics and tooth function of primates (hypothesis 4)

The six selected ISO parameters reflect characteristics of the enamel facet textures different from those indicated by SSFA parameters as discussed above. ISO parameters characterize textures based on the general geometric properties: height amplitude of the surface (*Sq*), depth (*S5v*) and area of valleys (*Sda*), area of hills (*Sha*), volume of material (*Vm*), and density of peaks (*Spd*) on the surface (Table 2.2).

The more intense brittle fracture (*sensu* Lucas *et al.* 2008) of enamel from a substantial consumption of large hard particles (seeds from fruits, bark and potentially insect cuticles) results in greater texture relief, as indicated by high values in *S5v*, *Sq*, *Vm*, and *Spd* in *Pan troglodytes*, *Macaca fascicularis* and *Lophocebus albigena* (Fig. 4.2a, Table 2.1). Conversely, the mastication of small hard particles, like silica phytoliths and dust from grass, results in more plastic deformation ("wear" *sensu* Lucas *et al.* 2008) which generates flatter relief (Fig. 4.2b). These textural signals are evident in *Gorilla gorilla* and *Papio cynocephalus* (Table 2.1). These results lend support to the deformation and fracture theory as postulated by Lucas *et al.* (2008) in which the area of the contact between the indenter (food particle) and the surface (enamel) defines the transition boundary between plastic deformation and brittle fracturing. A small indenter deforms plastically the surface, whereas a large indenter fractures the surface (Lucas *et al.* 2008).

Lucas *et al.* (2008) considered both phytoliths and grit to be small particles (5-50 µm). Grit (soil particles) can be much larger, but dust deposited on leaves is more likely to fall in this small size range. Therefore, phytoliths and dust are considered as small hard particles.

The large variations observed in *Sha* and *Sda* (Fig. 3.5e-f) associated with the consumption of small hard particles can be explained as follows. Since large hard items fracture enamel more heavily, the wide valleys are unlikely to persist because they will soon be overlapped by new ones. Similarly, hill-like features tend to be smaller with large hard items comminuted because the persistence of large ones is less likely. On the other hand, when small hard particles are eaten, large valleys and hills will be more probable to persist (large *Sha*/*Sda*) and have higher likelihood of being overlapped by new features as well (small *Sha*/*Sda*).

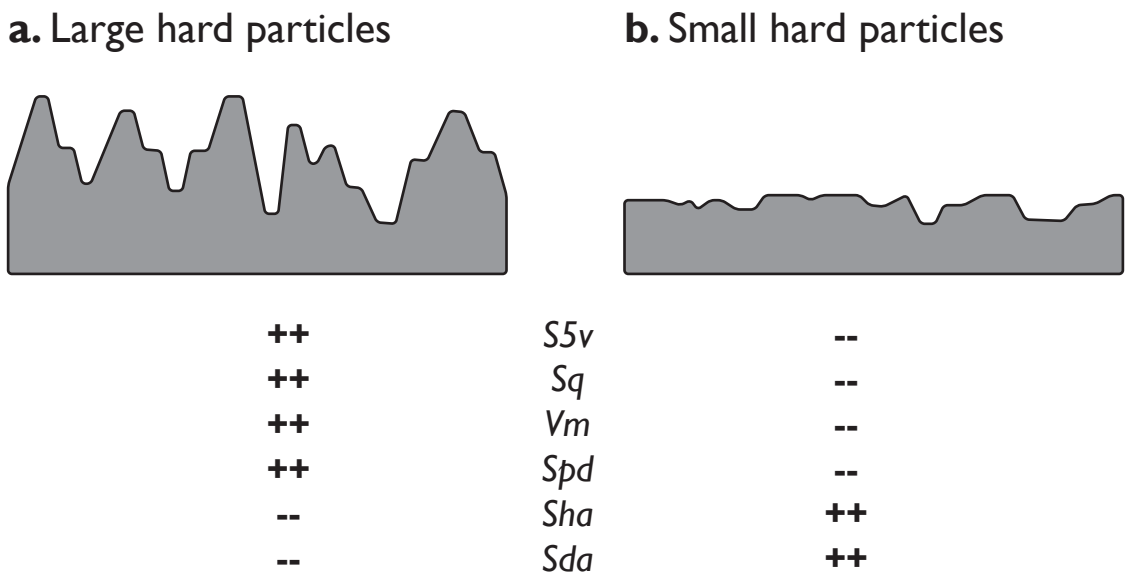

Figure 4.2. Schematic representation of the surface textures (viewed in profile) when dealing with large (**a**) and small (**b**) hard food items, and the qualitative influence on the six selected ISO parameters (Table 2.2).

With 68% of fruits in its diet (Table 2.1), *P. abelii* is expected to display the texture pattern of a "large hard object" feeder (Fig. 4.2a). However, ISO parameters do not match this expectation (Fig. 3.5). Consistently with the interpretation of the SSFA texture signature, these results are related to as yet unknown seasonal and/or dietary behavior, whereby less fruit is consumed, at least seasonally, than previously asserted in the species dietary dataset (Table 2.1).

T. gelada consumes 90% grass (Table 2.1). Its textural signal displays a "large hard object" pattern. The ISO texture model, however, suggests a "small hard object" pattern. As in *A. seniculus* it is not implied that the hypothesis concerning dietary traits need to be reconsidered, but rather argued that more samples are needed for more detailed investigation of these two species.

The results from the DASTA on this primate dataset support the deformation and fracture theory proposed by Lucas *et al.* (2008). The DASTA is therefore suitable for reconstructing the interaction between the physical properties of food and associated particles, and of tooth enamel facets (Calandra *et al.* submitted). This leads to the acceptance hypothesis 4.

4.3 Microtexture analyses with small sample sizes (hypothesis 5)

The data indicate that even small samples can resolve differences in the feeding behaviors and tooth biomechanics of ungulates and primates. Section 4.1.2 (hypothesis 2) showed that grazers and browsers can be clearly discriminated using the microtextural data with less than 10 specimens per species. Even subtler dietary assessments could be made on primates through the SSFA with $3 \leq n \leq 10$ (section 4.2.1, hypothesis 3). The DASTA is able to reconstruct precisely tooth-food interactions from the microtextures of a limited number of both ungulate and primate enamel facets (section 4.1.2, hypothesis 2 and section 4.2.2, hypothesis 4). I thus accept hypothesis 5.

The statistical tests used here are more robust than standard tests and thus can be applied on small samples of non-normal and heteroscedastic data. I therefore recommend the use of such tests, with large sample sizes as well.

4.4 General discussion

This section discusses the results in a larger context. First, I discuss the relevance of the DASTA relative to the SSFA. I then merge the results of the two taxonomic groups into a common model of microtexture formation. Last, I discuss questions related to the scaling of the microtexture patterns.

4.4.1 SSFA *versus* DASTA

The scale-sensitive fractal analysis (SSFA) is now a well-established method that can relate microtexture patterns to properties of the diets of extant and extinct organisms (section 1.3). The method is powerful enough not only to detect inter-specific differences (Scott *et al.* 2005; Scott *et al.* 2006; Ungar *et al.* 2007; Krueger *et al.* 2008; Scott *et al.* 2009; Schubert *et al.* 2010; Ungar *et al.* 2010), but also intra-specific (seasonal and sexual) differences (Merceron *et al.* 2010a) in the diets of ungulates, primates and carnivores. Section 4.2.1 also demonstrated the power of this method. A great deal of detail on the diet of primates can be inferred from the SSFA: amount of fruits consumed and ingestion of other hard items and of grass.

So why has the dental areal surface texture analysis (DASTA) been developed and what are its benefits for dental microwear/microtexture research? This section addresses these questions.

The SSFA parameters quantify complex characteristics of the texture (complexity, heterogeneity, textural fill volume and anisotropy) that are known to reflect properties of the diet (Scott *et al.* 2006). While the corresponding standardized parameters exist, other ISO parameters describe the basic geometry of the texture (International Organization for Standardization 2010): height difference between the lowest and highest point, height of the peaks only, depth of the troughs only, area of the hills, area of the valleys, density of peaks, volume of the material, void volume, shape of the peaks, and so on. Many parameters are available to quantify every single aspect of the texture.

All these parameters can either be interpreted separately to understand a specific property of the texture, or be integrated into a comprehensive representation of the surface texture and its functional unity. As shown in Figures 4.1-4.2, it is very straightforward to combine the significant parameters together and to get a representation relative to some feeding characteristics (Calandra *et al.* submitted; Schulz *et al.* 2009, 2010a, 2010b, submitted). In my opinion, this combination is more difficult with the SSFA parameters.

Moreover, this comprehensive representation allows functional inferences as it reflects direct interactions between food particles and enamel microtextures. These interactions relate specifically to the formation of dental microwear, *i.e.* how the microtexture forms as a result of contact between food particles and antagonistic dental surfaces. In this context, for instance, being able to analyze separately the size of the peaks, their density and their shape can help to understand better what kind of biomechanical properties of the food and of the tooth surface led to their formation or persistence.

Finally, standardized parameters (ISO and other norms; International Organization for Standardization 2010, 2011) are just beginning to be applied to biological systems. The results in section 4.1 already underlined that it will (soon) be possible to address unresolved research questions with such analyses.

In summary, the SSFA is probably the best tool to reconstruct diets, because the SSFA parameters were chosen in order to reflect diet-related microtexture (Scott *et al.* 2006), whereas the DASTA is more function-oriented and is still in its early stage of development. SSFA and DASTA are not competing but are complementary in that they focus on different questions, as shown in the sections 4.2.1-4.2.2. The following discussion (section 4.4.2) brings the DASTA one step further.

4.4.2 Taxon-independent characteristics of the microtexture relating to tooth function

As outlined in section 1.5, the processes and dynamics responsible for microwear formation on the enamel facets are not as yet clearly understood. Some theoretical work and modeling has been done (Lucas 2004), but teeth and enamel surfaces are much more complex than the models used to explain them. For example, Lucas *et al.* (2008) performed deformation and fracture experiments on glass domes with polymer resin back-fill to simulate tooth material. This type of experiment can explore the dynamics of the deformation and fracture occurring between the indenter and the surface. These materials are, however, isotropic and do not have the complex microstructure of enamel (e.g. enamel prisms, Schmelzmuster and Hunter-Schreger bands; Escala & Gállego 1977; Rensberger & von Koenigswald 1980; Young *et al.* 1987; von Koenigswald 2004a, b; Martin 2005). Even though the experiments are becoming more and more complex and thus simulate more closely the interactions between teeth and food, they are still simplifications of the real tooth tissues, food particle, and loads applied *in vivo*.

Microtexture on the other hand describes how the enamel surface looks like after being in contact with food and with the antagonistic surface *in vivo*. While the dynamics of mastication is lost, the microtexture is the end result of these dynamic interactions between food and enamel facet. By quantifying the geometry of the surface, the DASTA is a method that can complete the modeling approaches as it can test the predictions from these models in *in vivo* conditions.

The previous discussion (sections 4.1-4.2) was based on results from the DASTA and concerned very broad and contrasting categories of food items (grass/leaf browse for ungulates, fruits-hard items/grass for primates) and chewing mechanics (mainly crushing for primates, Kay & Hiiemae 1974; mainly shearing for ungulates, Fortelius 1985). It is difficult consistently to meld them into a general theory of microwear formation. They however constitute some initial elements of this theory.

It was demonstrated that ungulate grazers have more texture relief than ungulate leaf browsers (section 4.1.2). This is explained by there being relatively more peak removal in leaf browsers (as a result of either attrition or hydrodynamic pressures). In contrast, more relief is created in grazers through abrasion and this relief is maintained through larger occlusal gaps as a result of the physical properties of fibrous and gaseous grass boli. These characteristics of the textures are underlined by height (*Sa*, *Sxp*) and

volume (*Vmc*, *Vv*, *Vvc*, *Vvv*) parameters, by the density of peaks (*Spd*), and by isotropy (*IsT*). Some of these parameters (or similar ones) were also found to discriminate significantly between large (seeds, nuts, bark, and insects) and small (dust, phytoliths) hard item feeders in primates (section 4.2.2): height (*S5v*, *Sq*), volume (*Vm*), density of peaks (*Spd*), and anisotropy (SSFA parameter *epLsar*). The consumption of large hard items results in more relief through enamel fracture, whereas flatter reliefs are postulated to result from the plastic deformation of the surface from small hard items. This points to some common characteristics of the microtexture formation between the two groups of herbivorous mammals (ungulates and primates).

Many primates consume predominantly fruit, but those species which display the "small hard object" pattern are those that consume a significant amount of grass (Table 2.1). The consumption of grass in primates and in ungulates is not equivalent since it involves contrasting chewing dynamics between the two groups (Kay & Hiiemae 1974; Hiiemae 1978; Fortelius 1985). That being said, for the common parameters, we can observe that ungulate leaf browsers have similar values to primate "small hard object" feeders (ungulate browsers: *Sq* = 0.5-0.7 µm, *Spd* = 0.03 μm^{-2}, *Vm* = 0.3-0.5 $\mu m^3/\mu m^2$; primate "small hard object" feeders: *Sq* = 0.6-0.7 µm, *Spd* = 0.03 μm^{-2}, *Vmc* [about one order of magnitude lower than *Vm*] = 0.03-0.04 $\mu m^3/\mu m^2$; Tables 3.1 and 3.4). Ungulate grazers have similar values to primate "large hard object" feeders (ungulate grazers: *Sq* = 1.0-1.2 µm, *Spd* = 0.06-0.09 μm^{-2}, *Vm* = 0.7-0.9 $\mu m^3/\mu m^2$; primate "large hard object" feeders: *Sq* = 0.8-1.1 µm, *Spd* = 0.05-0.10 μm^{-2}, *Vmc* [about one order of magnitude lower than *Vm*] = 0.05-0.10 $\mu m^3/\mu m^2$).

If we speculate that grass is processed similarly in both groups, we can use the grass feeders as a standard reference point between the two groups. A gradient in microtexture relief then becomes apparent: leaf browsers have the flattest surfaces (Fig. 4.3a), large hard object feeders have the highest relief (Fig. 4.3c), and grazers have surfaces that are intermediate between these two extremes (Fig. 4.3b).

This potential gradient in texture relief underlines the significance of chewing mechanics and interactions between food particles and enamel facet surfaces.

(1) The tree leaves that are less abrasive create less texture relief from the shearing movements in ungulates (Fortelius 1985). The surfaces of leaf browsers will also undergo the highest amount of flattening through peak removal (being attrition or not), as seen in *Giraffa camelopardalis* and *Diceros bicornis*.

(2) Grazers will have higher relief than leaf browsers. In ungulates, where shearing

is dominant (Fortelius 1985), the consumption of abrasive grass will result in scratching of the surface, resulting in higher relief. Less peak removal will serve to maintain the higher relief (*Connochaetes taurinus* and *Equus grevyi*). In primates, on the other hand, crushing is dominant (Kay & Hiiemae 1974). So the higher relief in grazers relative to leaf browsers is a consequence of consumption of grass resulting in indentation from small hard particles such as dust and phytoliths (*Gorilla gorilla*, *Papio cynocephalus*) (Lucas *et al.* 2008).

(3) The consumption of large hard items (seeds, nuts, bark, insects) fractures the enamel surfaces generating even higher textural relief, as seen in the primates *Pan troglodytes*, *Macaca fascicularis* and *Lophocebus albigena* (Lucas *et al.* 2008).

This gradient in textural relief is a hypothesis that attempts to merge the results on the selected ungulates and primates into a common theory of microtexture formation. The hypothesis needs to be evaluated with more data. A first step would be to fill the gaps between the four ungulate species included in this work. For example, other ungulates (e.g. Camelidae, Suidae and Elephantidae) have other specific chewing mechanics (Butler 1952; Mills 1955; Lumsden & Osborn 1977; Hiiemae 1978; Fortelius 1985) and interactions with food particles. Similar chewing mechanics (groups) should be compared across diets, and *vice versa*. More primates, and especially more individuals of *Theropithecus gelada* and *Alouatta seniculus*, need to be included. The model also needs to be extended and further tested. Carnivores, for example, have further specific

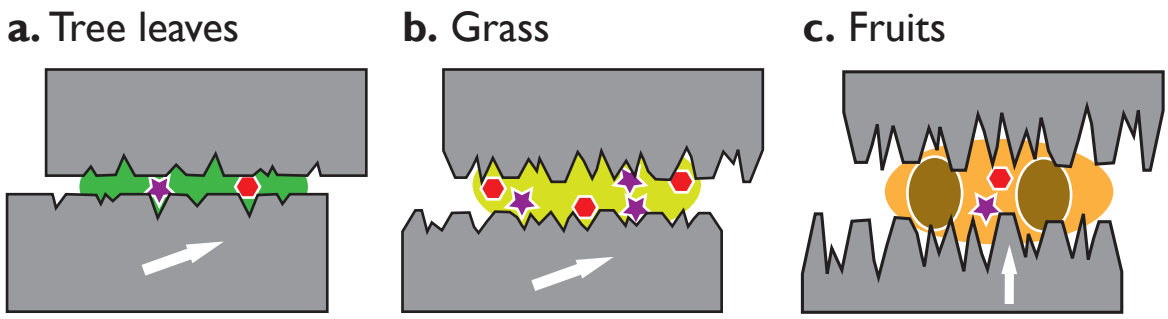

Figure 4.3. Schematic representation of the surface textures (view in profile) induced by the consumption of tree leaves (leaf browse, **a**), grass (**b**) and fruits and other large hard items (**c**). This represent a gradient from relatively flat (**a**) to high (**c**) texture reliefs.
Brown ellipses (small) = large hard items (seeds, nuts, bark), *green ellipse (large)* = leaf browse bolus, *orange ellipse (large)* = fruit bolus, *purple starlets* = plant-based abrasives (phytoliths), *red hexagons* = exogenous abrasives (grit and dust), *white arrows* = movement of the lower jaw, and *yellow ellipse (large)* = grass bolus.

masticatory functions related to specific food items. This work is already in progress (see section 5).

4.4.3 3D high-resolution scanning and microtextures

Traditionally, microwear has been analyzed at two spatial scales. The 2D method based on scanning electron microscopy (SEM) has taken microwear photographs at high magnifications: 100 to 500× (e.g. Walker *et al.* 1978; Solounias *et al.* 1988). 2D stereomicroscopy scoring methods have used lower magnifications: 30 to 35× (e.g. Solounias & Semprebon 2002; Merceron *et al.* 2005a). Both methods have proven power in inferring diets. The tandem scanning confocal microscopy employed by Ungar, Scott and coworkers (e.g. Ungar *et al.* 2003; Scott *et al.* 2006) and the present acquisition with the µsurf custom (section 2.4) have used magnifications similar to the SEM studies.

All methods can correctly assess diets, but because of large differences in magnification, they do not resolve similar scales of microwear/microtexture patterns. The principle of the SSFA itself demonstrates that the microtexture varies with the scale of measurement (Scott *et al.* 2006). So are the same processes responsible for microwear formation at all measurement scales? Is it possible to ignore scale and interpret what is observed at high magnification as comparable to what is observed at low magnification?

It is always assumed that food items and particles that come with food are the principle agents responsible for microwear (Dahlberg & Kinzey 1962; Gordon 1982). The enamel microstructure, however, probably also plays a role in microwear formation (e.g. Gordon 1982, 1988). As outlined in section 1.5, the processes of microwear formation in relation to enamel microstructure and biomechanics are not yet completely understood. 2D scoring methods (e.g. Walker *et al.* 1978; Solounias & Semprebon 2002; Merceron *et al.* 2005a; Rivals *et al.* 2007), whatever the magnification, analyze only supposedly diet-related features (pits, scratches…), which makes the inter-specific comparisons robust in terms of diet. On the other hand, 3D high magnification and resolution actually analyzes the whole texture, of which the enamel microstructure is a part.

The DASTA was developed in order to add information on tooth-food interactions and chewing function to the toolset of dental microtexture research. Hence, its primary goal is not to reconstruct the diet of extinct organisms in the first place.

The present thesis demonstrated that the microtexture pattern is related to the physical properties of the food items and to the chewing mechanics. It is, however, unknown whether the scale of observation (160 × 160 µm, x-y resolutions = 0.16 µm, z resolution = 0.06 µm; section 2.4) is the most appropriate to use. Lower magnification (20-50×), and hence lower resolution, might be of equal value in providing functional interpretations. Since there is no simple relationship between the size of the abrasive particle and the resulting wear feature (Dahlberg & Kinzey 1962), it is difficult to know which size of wear particle corresponds to which size and type of microtexture. The question is therefore to know which wear agent(s) produce the observed microtexture pattern. A correlation (as demonstrated herein) may not be taken as evidence for a causal relationship.

Such a cause-effect relationship between abrasive particles and microtexture is difficult to assess in the wild because too many factors come into play. Experiments are probably the best means. Two complementary types of experiments can be designed to understand this relationship. The first type is based on chewing machines, similar to the one that Gügel *et al.* (2001) built (see also Teaford & Oyen 1989c). This study represents a first step. The methodology can be developed further by using a design more similar to *in vivo* conditions: whole worn teeth with periodontal ligament, saliva, more complex chewing movements… Different types of abrasive particles would also need to be examined: grass, phytoliths, tree leaves, fruits with and without hard exocarp, fruits with and without seeds, bark, insects, grit, dust, and so on. While it would still be difficult to observe the dynamics of wear *in situ*, the controlled design allows the precise and exclusive identification of the wear agent(s) responsible for a given microtexture pattern and for the scale of this pattern. The second type of experiment is feeding experiments, as Kay & Covert (1983) and Teaford & Oyen (1989c) conducted. The chewing dynamics are not approximated with living animals as they are with chewing machines. But because of the complexity in chewing dynamics, it might be difficult to understand precisely the wear processes. Moreover, the molding of teeth from live animals is much more difficult than from dry skulls. As explained by Teaford (1988) and Teaford & Oyen (1989b), a pellicle of saliva coating the tooth surfaces can obscure the microwear pattern. Such saliva films were observed on the tooth casts from live goats, rendering the casts unusable for microtexture analyses (the experiments were conducted in Bonn, Germany, as part of the DFG research group 771; J. Hummel, E. Findeisen, E. Schulz, and me; coordination: J. Hummel and K.-H. Südekum, Institut für Tierwissenschaften, Bonn). In such experiments, different types of food should also be

tested on a range of mammalian species with different chewing dynamics (e.g. Equidae, Bovidae, Elephantidae, Primates, and Carnivores; Butler 1952; Mills 1955; Lumsden & Osborn 1977; Hiiemae 1978; Fortelius 1985). Moreover, it will be possible to assess whether pellicle formation is a universal phenomenon independent from food sources, or whether it is more related to the type of food eaten than to the taxonomic identity of the consumer. This field of research has not yet been developed.

As mentioned above, the principle of the SSFA (section 2.7; Scott *et al.* 2005; Scott *et al.* 2006) demonstrates that different aspects of the microtexture are measured depending on the scale of measurement. Low-magnification 2D scoring methods (e.g. Solounias & Semprebon 2002; Merceron *et al.* 2005a; Rivals *et al.* 2007) probably measure microwear left by the largest food particles (e.g. seeds, grit). The higher magnification 2D scoring methods (e.g. Walker *et al.* 1978; Gordon 1988; Pinto Llona 2006) are likely to relate to wear caused by smaller food particles such as phytoliths and dust. The high-resolution and the whole-surface quantification of the DASTA reach a scale where tribology, viscosity, enamel microstructure, and fracture and deformation mechanics come into play. Each measurement scale therefore reveals specific information on chewing mechanics. The combination and comparison of several scales can thus be very valuable in understanding different aspects of wear processes and of tooth-food interactions with even more precision.

Molding of the teeth on a living goat (Bonn)

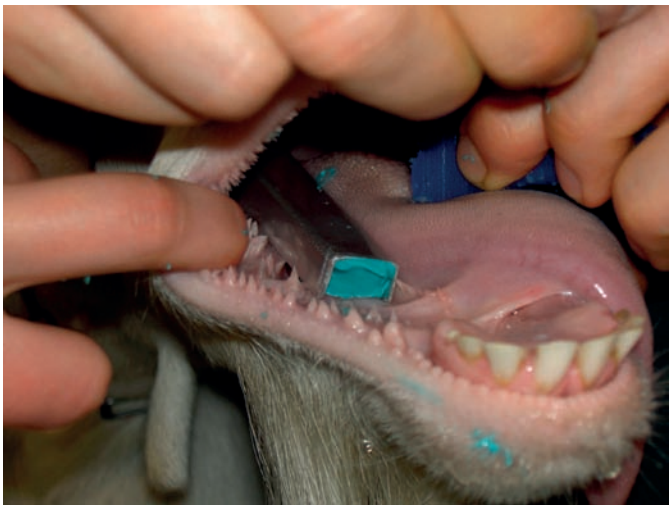

5. Conclusions and further perspectives

5. Conclusions and further perspectives

Teeth play an important role into the efficiency of energy uptake from the food. A variety of tooth-based methods have, therefore, been developed to decipher the interactions between teeth and food particles and the efficiency with which the mechanical processes of food reduction and of tooth wear take place.

The present Ph.D. thesis presented new developments in the dental microwear methodology. An automated dental microtexture analysis – the dental areal surface texture analysis (DASTA) – has been developed by taking advantage of the newly available 3D scanning and measuring devices (µsurf custom) and associated processing software packages (µsoft Analysis Premium) (Calandra *et al.* submitted; Schulz *et al.* 2010a, submitted). This analysis is based on standardized parameters (mainly, but not limited to, ISO/FDIS 25178-2; International Organization for Standardization 2010).

This method has been applied to two datasets: one composed of four ungulate model species, the second of eight primate species. The DASTA parameters have been found to provide a diagnostic tool set whereby characteristics at the enamel surface can be used to infer the masticatory function relevant to comminution and chewing success (Schulz *et al.* submitted). In particular, the higher viscosity and fiber content of grass boli as compared to browse boli produce more peaks and relief in ungulate grazers than in browsers (section 4.1). In primates, the size of the hard particles comminuted determines whether enamel is fractured or whether it plastically deforms (section 4.2).

As section 2 emphasized, work is still needed to overcome technical issues in order to reach the full potential of this approach. With the full-fledged method in hand, it might be possible to settle long-standing questions such as the grit and dust *vs.* phytoliths debate (section 1.4).

Now that the capacities of the method have been proven, it needs to be applied to many more species. The model of microwear/microtexture formation proposed in section 4.4.2 is still speculative. The inclusion of many more ungulate species (belonging to Bovidae, Camelidae, Cervidae, Elephantidae, Equidae, Hippopotamidae, Rhinocerotidae, Suidae and Tapiridae) will help close the gap between the ungulates and the primates that have been studied herein in terms of biomechanical properties of their food and tooth function (Butler 1952; Mills 1955; Lumsden & Osborn 1977; Hiiemae 1978; Fortelius 1985). Work in this direction is already in progress and microtexture data on these ungulate species have already been acquired.

Microtexture analysis is just one of several proxies of tooth function. Many other proxies have been used to understand chewing dynamics and efficiency.

Teeth display a wide range of morphologies (Hillson 2005). Each morphotype is capable of processing a limited range of food types with high efficiency. Each morphology represents a specific range of functional traits (e.g. shearing, crushing). Many authors have studied the tooth morphology to understand how teeth function, and how they reduce the food particles (Butler 1972; Rensberger 1973; Kay 1975; Fortelius 1985; Ungar & Williamson 2000; Pérez-Barbería & Gordon 2001; Archer & Sanson 2002; Kaiser 2002; Lucas 2004; Evans *et al.* 2007; Bunn & Ungar 2009; Gailer *et al.* 2010; Heywood 2010; Kaiser *et al.* 2010; Lazzari *et al.* 2010; Nieberg *et al.* 2010; von Koenigswald *et al.* 2010; Gailer & Kaiser in prep). These studies have relied on the adaptational signifance of the morphology reflected by cross morphologies: a given morphology is assumed to reflect adaptation to serve most efficiently a specific set of functional requirements. There is, however, no need for a specific morphology to fulfill a given function: it can but it does not have to. The 3D dental microtexture analysis on the other hand addresses the results of the functional interactions between the tooth facets and the food particles (Ungar *et al.* 2008) and thus reflects an integrated functional "interface" between the animal and its environment. It is, therefore, possible to discriminate between what an animal can eat (morphology) and what an animal has eaten (tooth wear proxies) (e.g. Merceron *et al.* 2006a; Ramdarshan *et al.* 2010). The combination of the microtexture analyses (e.g. Schulz *et al.* 2009, 2010a, 2010b; Calandra *et al.* submitted; Schulz *et al.* submitted) with the 3D occlusal topography (Nieberg *et al.* 2009; Gailer *et al.* 2010) will allow, for example, the distinction between the adaptive and non-adaptive functional characters in the tooth occlusal topography of bovids (Winkler *et al.* 2011; Gailer *et al.* in prep).

At a finer scale, the enamel microstructure also bears a functional signal (Maas 1993; von Koenigswald *et al.* 2011). The orientation of the enamel prisms and their patterns (Schmelzmuster, Hunter-Schreger bands) are important in regulating resistance to wear (e.g. Rensberger & von Koenigswald 1980; Xu *et al.* 1998). The microtexture quantifies the end result of these food-tooth interactions. The combination of these two approaches will help to refine our understanding of the deformation and fracture mechanics: Why do some teeth resist fracture more than others? Why does enamel fracture at some places but not others? How does enamel fracture depending on the underlying microstructure? What is the influence of the food consumed? What is the influence of the chewing mechanics in relation to prism orientation?

Chewing efficiency can be quantified by measuring the particle sizes in the faeces of a range of species. This is because the fragmentation of ingested particles occurs only by the mechanical action of chewing through the action of teeth in the mouth (see references in Pérez-Barbería & Gordon 1998a, and in Fritz *et al.* 2009). Fritz *et al.* (2009) for example showed that extant species of *Equus* comminute food particle more efficiently than other extant hindgut fermenters and related this higher efficiency to their more complex molar design. Ruminants were also found to have smaller faecal particles than non-ruminants, which was explained by the authors as resulting from sorting of the particles during rumination. When used in combination, analyses of faecal particle size, tooth functional morphology and dental microtexture analyses should make it possible to determine which traits make teeth efficient and how that efficiency is related to tooth morphology and to tooth-food interactions at the scale of contact.

As outlined in section 4.4.2, deformation and fracture experiments (Lucas *et al.* 2008) can describe the dynamics of wear. Finite element analyses (Macho *et al.* 2005; Lüpke *et al.* 2010; Benazzi *et al.* 2011) can estimate where the largest stress loads are applied and, therefore, where we expect the morphology to be adapted. Because of the complexity of the chewing and wear processes, the current models are only rough approximations of real teeth, of food particles and of chewing dynamics. As the results in sections 4.2.2 showed, the microtexture analyses can test the predictions of such simulations. As the modeling becomes closer and closer to reality, the simulations will yield more detailed predictions of the chewing mechanics that can be critically evaluated to the end result of these processes as described through microtexture analyses.

The combination of these approaches has much more power than any single method as several aspects can be addressed simultaneously. This is the goal of the DFG research cluster 771 "Function and performance enhancement in the mammalian dentition – phylogenetic and ontogenetic impact on the masticatory apparatus". Each project within this cluster focuses on one of the approaches described above. By merging the results from these projects (e.g. Hummel *et al.* 2011; Gailer *et al.* in prep), tooth and chewing function will become better understood.

6. References

Anders U, von Koenigswald W, Ruf I, Smith BH (2011). Generalized individual dental age stages for fossil and extant placental mammals. *Paläontolgische Zeitschrift* **Online First**.

Anderson TW, Darling DA (1952). Asymptotic Theory of Certain "Goodness of Fit" Criteria Based on Stochastic Processes. *The Annals of Mathematical Statistics* **23**(2): 193-212.

Anderson TW, Darling DA (1954). A Test of Goodness of Fit. *Journal of the American Statistical Association* **49**(268): 765-769.

Archer D, Sanson G (2002). Form and function of the selenodont molar in southern African ruminants in relation to their feeding habits. *Journal of Zoology* **257**(01): 13-26.

Baker G, Jones LHP, Wardrop ID (1959). Cause of Wear in Sheep's Teeth. *Nature* **184**: 1583-1584.

Benazzi S, Kullmer O, Grosse IR, Weber GW (2011). Using occlusal wear information and finite element analysis to investigate stress distributions in human molars. *Journal of Anatomy* **219**: 259-272.

Bengtsson H (2010). R.utils: Various programming utilities. http://CRAN.R-project.org/package=R.utils. Downloaded on 01.06.2010.

Born M, Wolf E (1999). Principles of Optics: Electromagnetic theory of propagation, interference and diffraction of light, 7th ed. Cambridge University Press, Cambridge.

Boubli J-P, Di Fiore A, Rylands AB, Mittermeier RA (2008). *Alouatta seniculus*. In: IUCN 2010. IUCN Red List of Threatened Species. Version 2010.4. www.iucnredlist.org. Downloaded on 21.02.2011.

Boyde A (1984). Dependence of rate of physical erosion on orientation and density in mineralised tissues. *Anatomy and Embryology* **170**: 57-62.

Brown MB, Forsythe AB (1974). The Small Sample Behavior of Some Statistics Which Test the Equality of Several Means. *Technometrics* **16**(1): 129-132.

Bunn JM, Ungar PS (2009). Dental topography and diets of four old world monkey species. *American Journal of Primatology* **71**(6): 466-477.

Butler PM (1952). The milk-molars of Perissodactyla with remarks on molar occlusion. *Proceedings of the Zoological Society of London* **121**: 777-817.

Butler PM (1972). Some functional aspects of molar evolution. *Evolution* **26**: 474-483.

Calandra I, Göhlich UB, Merceron G (2008). How could sympatric megaherbivores coexist? Example of niche partitioning within a proboscidean community from the Miocene of Europe. *Naturwissenschaften* **95**(9): 831-838.

Calandra I, Göhlich UB, Merceron G (2010). Feeding preferences of *Gomphotherium subtapiroideum* (Proboscidea, Mammalia) from the Miocene of Sandelzhausen (Northern Alpine Foreland Basin, southern Germany) through life and geological time: evidence from dental microwear analysis. *Paläontologische Zeitschrift* **84**(1): 205-215.

Calandra I, Schulz E, Pinnow M, Krohn S, Kaiser TM (submitted). Teasing Apart the Contributions of Hard Items on 3D Dental Microtextures in Primates. *Journal of Human Evolution*.

Cawthon Lang KA (2005a). Primate Factsheets: Gorilla (*Gorilla*) Taxonomy, Morphology, & Ecology. http://pin.primate.wisc.edu/factsheets/entry/gorilla. Downloaded on 02.02.2011.

Cawthon Lang KA (2005b). Primate Factsheets: Orangutan (*Pongo*) Taxonomy, Morphology, & Ecology. http://pin.primate.wisc.edu/factsheets/entry/orangutan. Downloaded on 02.02.2011.

Cawthon Lang KA (2006a). Primate Factsheets: Chimpanzee (*Pan troglodytes*) Taxonomy, Morphology, & Ecology. http://pin.primate.wisc.edu/factsheets/entry/chimpanzee. Downloaded on 02.02.2011.

Cawthon Lang KA (2006b). Primate Factsheets: Long-tailed macaque (*Macaca fascicularis*) Taxonomy, Morphology, & Ecology. http://pin.primate.wisc.edu/factsheets/entry/long-tailed_macaque/taxon. Downloaded on 28.04.2011.

Cawthon Lang KA (2006c). Primate Factsheets: Yellow baboon (*Papio cynocephalus*) Taxonomy, Morphology, & Ecology. http://pin.primate.wisc.edu/factsheets/entry/yellow_baboon. Downloaded on 02.02.2011.

Charles C, Jaeger J-J, Michaux J, Viriot L (2007). Dental microwear in relation to changes in the direction of mastication during the evolution of Myodonta (Rodentia, Mammalia). *Naturwissenschaften* **94**: 71-75.

Chauncey HH, Henriques BL, Tanzer JM (1963). Comparative Enzyme Activity of Saliva from the Sheep, Hog, Dog, Rabbit, Rat, and Human. *Archives of Oral Biology* **8**: 615-627.

Clauss M, Lechner-Doll M, Streich WJ (2003). Ruminant diversification as an adaptation to the physiomechanical characteristics of forage. A reevaluation of an old debate and a new hypothesis. *Oikos* **102**: 253-262.

Clauss M, Kaiser T, Hummel J (2008). The Morphophysiological Adaptations of Browsing and Grazing Mammals. In: *The Ecology of Browsing and Grazing*, Gordon IJ, Prins HHT (Eds.). Springer, pp. 47-88.

Cliff N (1996). Ordinal Methods for Behavioral Data Analysis, Erlbaum, Mahwah, New Jersey.

Corlett RT, Lucas PW (1990). Alternative seed-handling strategies in primates: seed-spitting by long-tailed macaques (*Macaca fascicularis*). *Oecologia* **82**(2): 166-171.

Cotterill JV, Watkins RW, Brennon CB, Cowan DP (2007). Boosting silica levels in wheat leaves reduces grazing by rabbits. *Pest Management Science* **63**: 247-253.

Dahlberg AA, Kinzey W (1962). Etude microscopique de l'abrasion et de l'attrition sur la surface des dents. *Bulletin du Groupement international pour la recherche scientifique en stomatologie* **5**: 242-251.

Damuth J, Janis CM (2011). On the relationship between hypsodonty and feeding ecology in ungulate mammals, and its utility in palaeoecology. *Biological Reviews* **86**: 733-758.

Darras L, Purnell MA, Hart PJB, Turingan RG (2010). Investigating the Diet of Extant and Fossil Fishes Through Microtextural Analysis of Teeth. *International Palaeontological Congress 3*, London, UK. Programme & Abstract Volume: p. 137.

Diaspro A (2002). Confocal and two-photon microscopy: foundations, applications, and advances. Wiley, New York, 567 p.

Dunnett CW (1980). Pairwise multiple comparisons in the unequal variance case. *Journal of the American Statistical Association* **75**(372): 796-800.

East R (1984). Rainfall, soil nutrient status and biomass of large African savanna mammals. *African Journal of Ecology* **22**: 245-270.

Ego WK, Mbuvi DM, Kibet PFK (2003). Dietary composition of wildebeest (*Connochaetes taurinus*), kongoni (*Alcephalus buselaphus*) and cattle (*Bos indicus*), grazing on a common ranch in south-central Kenya. *African Journal of Ecology* **41**: 83-92.

Epstein E (1999). Silicon. *Annual Review of Plant Physiology and Plant Molecular Biology* **50**: 641-664.

Escala MC, Gállego L (1977). Systematic Usefulness of Lower Incisor Enamel in Muridae (Rodentia). *Journal of Mammalogy* **58**(1): 25-31.

Evans AR, Wilson GP, Fortelius M, Jernvall J (2007). High-level similarity of dentitions in carnivorans and rodents. *Nature* **445**(7123): 78-81.

Every RG (1960). The significance of extreme mandibular movements. pp. 37-39.

Every RG (1970). Sharpness of teeth in man and other primates. *Postilla* **143**: 1-30.

Every RG (1975). Significance of tooth sharpness for mammalian, especially primate, evolution. In: *Approaches to primate paleobiology*, Szalay FS (Ed.). Karger, Basel, pp. 293-325.

Fennessy J, Brown D (2010). *Giraffa camelopardalis*. In: IUCN 2011, IUCN Red List of Threatened Species, Version 2011.1. www.iucnredlist.org. Downloaded on 02.08.2011.

Ferigolo J (1985). Evolutionary Trends of the Histological Pattern in the Teeth of Edentata (Xenarthra). *Archives of Oral Biology* **30**(1): 71-82.

Fortelius M (1985). Ungulate cheek teeth: developmental, functional, and evolutionary interrelations. *Acta Zoologica Fennica* **180**: 1-76.

Fortelius M, Solounias N (2000). Functional characterization of Ungulate molars using the abrasion-attrition wear gradient: A new method for reconstructing palaeodiets. *American Museum Novitates* **3301**: 1-36.

Fowle TI (1981). Aeration in lubricated oils. *Tribology International* **14**(3): 151-157.

Fritz J, Hummel J, Kienzle E, Arnold C, Nunn C, Clauss M (2009). Comparative chewing efficiency in mammalian herbivores. *Oikos* **118**(11): 1623-1632.

Gagnon M, Chew AE (2000). Dietary preferences in extant African Bovidae. *Journal of Mammalogy* **81**(2): 490-511.

Gailer JP, Calandra I, Kaiser TM (2010). Three-dimensional Functional Quantification of Ruminant Occlusal Patterns - An Approach Using Industrial Metrology Systems. *International Palaeontological Congress 3*, London, UK. Programme & Abstract Volume: p. 174.

Gailer JP, Calandra I, Schulz E, Kaiser TM (in prep). Do Bovids really eat what they are best adapted to?

Gailer JP, Kaiser TM (in prep). Three-dimensional Functional Quantification of Ruminant Occlusal Patterns - An Approach Using Industrial Metrology Systems.

Gippoliti S, Hunter C (2008). *Theropithecus gelada*. In: IUCN 2010. IUCN Red List of Threatened Species. Version 2010.4. www.iucnredlist.org. Downloaded on 21.02.2011.

Goillot C, Blondel C, Peigné S (2009). Relationships between dental microwear and diet in Carnivora (Mammalia)--Implications for the reconstruction of the diet of extinct taxa. *Palaeogeography, Palaeoclimatology, Palaeoecology* **271**(1-2): 13-23.

Gomes Rodrigues H, Merceron G, Viriot L (2009). Dental microwear patterns of extant and extinct Muridae (Rodentia, Mammalia): ecological implications. *Naturwissenschaften* **96**(4): 537-542.

Gordon KD (1982). A Study of Microwear on Chimpanzee Molars: Implications for Dental Microwear Analysis. *American Journal of Physical Anthropology* **59**: 195-215.

Gordon KD (1984). The assessment of jaw movement direction from dental microwear. *American Journal of Physical Anthropology* **63**: 77-84.

Gordon KD (1988). A review of methodology and quantification in dental microwear analysis. *Scanning Microscopy* **2**: 1139-1147.

Goswami A, Flynn JJ, Ranivoharimanana L, Wyss AR (2005). Dental Microwear in Triassic Amniotes: Implications for Paleoecology and Masticatory Mechanics. *Journal of Vertebrate Paleontology* **25**(2): 320-329.

Green JL, Semprebon GM, Solounias N (2005). Reconstructing the palaeodiet of Florida *Mammut americanum* via low-magnification stereomicroscopy. *Palaeogeography, Palaeoclimatology, Palaeoecology* **223**: 34-48.

Green JL (2009). Dental microwear in the orthodentine of the Xenarthra (Mammalia) and its use in reconstructing the palaeodiet of extinct taxa: the case study of *Nothrotheriops shastensis* (Xenarthra, Tardigrada, Nothrotheriidae). *Zoological Journal of Linnean Society* **156**: 201-222.

Grine FE (1986). Dental evidence for dietary differences in *Australopithecus* and *Paranthropus*: a quantitative analysis of permanent molar microwear. *Journal of Human Evolution* **15**: 783-822.

Grine FE, Ungar PS, Teaford MF (2002). Error Rates in Dental Microwear Quantification Using Scanning Electron Microscopy. *Scanning* **24**: 144-153.

Gron KJ (2007). Primate Factsheets: Red howler (*Alouatta seniculus*) Taxonomy, Morphology, & Ecology. http://pin.primate.wisc.edu/factsheets/entry/red_howler. Downloaded on 02.02.2011.

Gron KJ (2008). Primate Factsheets: Gelada baboon (*Theropithecus gelada*) Taxonomy, Morphology, & Ecology. http://pin.primate.wisc.edu/factsheets/entry/gelada_baboon. Downloaded on 02.02.2011.

Gügel IL, Grupe G, Kunzelmann K-H (2001). Simulation of Dental Microwear: Characteristic Traces by Opal Phytoliths Give Clues to Ancient Human Dietary Behavior. *American Journal of Physical Anthropology* **114**: 124-138.

Healy WB, Ludwig TG (1965). Wear of sheep's teeth: I The role of ingested soil. *New Zealand Journal of Agricultural Research* **8**: 737-752.

Heywood JJN (2010). Functional anatomy of bovid upper molar occlusal surfaces with respect to diet. *Journal of Zoology* **281**(1): 1-11.

Hiiemae KM (1978). Mammalian Mastication: a review of the activity of the jaw muscles and the movements they produce in chewing. In: *Development, Function and Evolution of Teeth*, Butler PM, Joysey KA (Eds.). Academic Press, New York, pp. 359-398.

Hillson S (2005). Teeth. Cambridge University Press, Cambridge.

Hochberg Y (1988). A sharper Bonferroni procedure for multiple tests of significance. *Biometrika* **75**(4): 800-802.

Hodson MJ, White PJ, Mead A, Broadley MR (2005). Phylogenetic Variation in the Silicon Composition of Plants. *Annals of Botany* **96**: 1027-1046.

Højsgaard S, Wright K, Leidi AA (2010). doBy: Groupwise computations of summary statistics, general linear contrasts and other utilities. http://CRAN.R-project.org/package=doBy. Downloaded on 01.06.2010.

Hummel J, Findeisen E, Südekum KH, Ruf I, Kaiser TM, Bucher M, Clauss M, Codron D (2011). Another one bites the dust: faecal silica levels in large herbivores correlate with high-crowned teeth. *Proceedings of the Royal Society B: Biological Sciences* **278**(1712): 1742-1747.

International Organization for Standardization (2010). ISO/FDIS 25178-2 – Geometrical product specifications (GPS) – Surface texture: Areal – Part 2: Terms, definitions and surface texture parameters.

International Organization for Standardization (2011). ISO 12781-2 Geometrical product specification (GPS) - Flatness - Part 2: Specific operators.

Jacobsen N, Lyche Melvaer K, Hensten-Pettersen A (1972). Some Properties of Salivary Amylase: A Survey of the Literature and Some Observations. *Journal of Dental Research* **51**(suppl. 2): 381-388.

Janis CM, Fortelius M (1988). On the means whereby mammals achieve increased functional durability of their dentitions, with special reference to limiting factors. *Biological Reviews* **63**(2): 197-230.

Joubert E, Eloff FC (1971). Notes on the Ecology and Behaviour of the Black Rhinoceros *Diceros bicornis* Linn. 1758 in South West Africa. *Madoqua* **1**(3): 5-53.

Kaiser TM (2002). Functional significance of ontogenetic gradients in the enamel ridge pattern of the upper cheek dentition of the Miocene hipparionin horse *Cormohipparion occidentale* (Equidae, Perissodactyla). *Senckenbergiana lethaea* **82**(1): 167-180.

Kaiser TM, Brinkmann G (2006). Measuring dental wear equilibriums — the use of industrial surface texture parameters to infer the diets of fossil mammals. *Palaeogeography, Palaeoclimatology, Palaeoecology* **239**: 221-240.

Kaiser TM, Fickel J, Streich WJ, Hummel J, Clauss M (2010). Enamel ridge alignment in upper molars of ruminants in relation to their natural diet. *Journal of Zoology* **281**(1): 12-25.

Kalthoff DC (2011). Microstructure of Dental Hard Tissues in Fossil and Recent Xenarthrans (Mammalia: Folivora and Cingulata). *Journal of Morphology* **272**: 641-661.

Kay RF, Hiiemae KM (1974). Jaw movement and tooth use in recent and fossil primates. *American Journal of Physical Anthropology* **40**(2): 227-256.

Kay RF (1975). The functional adaptations of primate molar teeth. *American Journal of Physical Anthropology* **43**: 195-216.

Kay RF (1981). The Nut-Crackers – A New Theory of the Adaptations of the Ramapithecinae. *American Journal of Physical Anthropology* **55**: 141-151.

Kay RF, Covert HH (1983). True grit: A microwear experiment. *American Journal Physical Anthropology* **61**: 33-38.

Keselman HJ, Huberty CJ, Lix LM, Olejnik S, Cribbie RA, Donahue B, Kowalchuk RK, Lowman LL, Petoskey MD, Keselman JC, Levin JR (1998). Statistical Practices of Educational Researchers: An Analysis of Their ANOVA, MANOVA, and ANCOVA Analyses *Review of Educational Research* **68**(3): 350-386.

King T, Andrews P, Boz B (1999). Effect of Taphonomic Processes on Dental Microwear. *American Journal of Physical Anthropology* **108**: 359-373.

Kingdon J, Butynski TM, De Jong Y (2008). *Papio cynocephalus*. In: IUCN 2010. IUCN Red List of Threatened Species. Version 2010.4. www.iucnredlist.org. Downloaded on 21.02.2011.

Klingel H (1974). Soziale Organisation und Verhalten des Grevy-Zebras *(Equus grevyi*). *Zeitschrift für Tierpsychologie* **36**: 37-70.

Krueger KL, Scott JR, Kay RF, Ungar PS (2008). Technical Note: Dental Microwear Textures of "Phase I" and "Phase II" Facets. *American Journal of Physical Anthropology* **137**(4): 485-490.

Krueger KL, Ungar PS (2010). Incisor Microwear Textures of Five Bioarcheological Groups. *International Journal of Osteoarchaeology* **20**: 549-560.

Kruskal WH, Wallis WA (1952). Use of ranks in one-criterion variance analysis. *Journal of the American Statistical Association* **47**(260): 583-621.

Lambert JE, Garber PA (1998). Evolutionary and ecological implications of primate seed dispersal. *American Journal of Primatology* **45**(1): 9-28.

Lambert JE, Chapman CA, Wrangham RW, Conklin Brittain NL (2004). Hardness of cercopithecine foods: implications for the critical function of enamel thickness in exploiting fallback foods. *American Journal of Physical Anthropology* **125**(4): 363-368.

Lazzari V, Schultz JA, Tafforeau P, Martin T (2010). Occlusal Pattern in Paulchoffatiid Multituberculates and the Evolution of Cusp Morphology in Mammaliamorphs with Rodent-like Dentitions. *Journal of Mammalian Evolution* **17**: 177-192.

Lechner-Doll M, Kaske M, Engelhardt WV (1991). Factors affecting the mean retention time of particles in the forestomach of ruminants and camelids. pp. 455-482.

Leuthold BM, Leuthold W (1972). Food habits of giraffe in Tsavo National Park, Kenya. *East African Wildlife Journal* **10**: 129-141.

Levene H (1960). Robust tests for equality of variance. In: *Contributions to Probability and Statistics*, Olkin I (Ed.). Stanford University Press, Palo Alto, California, pp. 278-292.

Lucas P (2004). Dental functional morphology. How teeth work. Cambridge University Press, Cambridge, 355 p.

Lucas P, Constantino P, Wood B, Lawn B (2008). Dental enamel as a dietary indicator in mammals. *BioEssays* **30**(4): 374-385.

Lucas PW, Corlett RT (1998). Seed dispersal by long-tailed macaques. *American Journal of Primatology* **45**(1): 29-44.

Luciani TJ (2009). RSvgDevice: An R SVG graphics device. http://www.darkridge.com/~jake/RSvg/. Downloaded on 01.06.2010.

Lumsden AGS, Osborn JW (1977). The evolution of chewing: a dentist's view of palaeontology. *Journal of Dentistry* **5**(4): 269-287.

Lüpke M, Gardemin M, Kopke S, Seifert H, Staszyk C (2010). Finite element analysis of the equine periodontal ligament under masticatory loading. *Wiener Tierärztliche Monatsschrift* **97**(3-4): 101-106.

Maas MC (1993). Enamel Microstructure and Molar Wear in the Greater Galago, *Otolemur crassicaudatus* (Mammalia, Primates). *American Journal of Physical Anthropology* **92**(2): 217-233.

Macho GA, Shimizu D, Jiang Y, Spears IR (2005). *Australopithecus anamensis*: A Finite-Element Approach to Studying the Functional Adaptations of Extinct Hominins. *The Anatomical Record Part A* **283A**: 310-318.

Mainland IL (2000). A Dental Microwear Study of Seaweed-Eating and Grazing Sheep from Orkney. *International Journal of Osteoarchaeology* **10**: 93-107.

Mainland IL (2003). Dental microwear in grazing and browsing Gotland sheep (*Ovis aries*) and its implications for dietary reconstruction. *Journal of Archaeological Science* **30**(11): 1513-1527.

Mann HB, Whitney DR (1947). On a test of whether one of two random variables is stochastically larger than the other. *Annals of Mathematical Statistics* **18**: 50-60.

Markowski CA, Markowski EP (1990). Conditions for the Effectiveness of a Preliminary Test of Variance. *The American Statistician* **44**(4): 322-326.

Martin LB, Olejniczak AJ, Maas MC (2003). Enamel thickness and microstructure in pitheciin primates, with comments on dietary adaptations of the middle Miocene hominoid *Kenyapithecus*. *Journal of Human Evolution* **45**(5): 351-367.

Martin T (2005). Incisor Schmelzmuster Diversity in South America's Oldest Rodent Fauna and Early Caviomorph History. *Journal of Mammalian Evolution* **12**(3/4): 405-417.

Martin T (2007). Incisor Enamel Microstructure and the Concept of Sciuravida. *Bulletin of Carnegie Museum of Natural History* **39**: 127-140.

Massey FP, Ennos AR, Hartley SE (2006). Silica in grasses as a defence against insect herbivores: contrasting effects on folivores and a phloem feeder. *Journal of Animal Ecology* **75**: 595-603.

Massey FP, Hartley SE (2006). Experimental demonstration of the antiherbivore effects of silica in grasses: impacts on foliage digestibility and vole growth rates. *Proceedings of the Royal Society B: Biological Sciences* **273**: 2299-2304.

Massey FP, Ennos AR, Hartley SE (2007). Grasses and the resource availability hypothesis: the importance of silica-based defences. *Journal of Ecology* **95**(3): 414-424.

Massey FP, Massey K, Roland Ennos A, Hartley SE (2009). Impacts of silica-based defences in grasses on the feeding preferences of sheep. *Basic and Applied Ecology* **10**(7): 622-630.

Mau M, Südekum K-H, Johann A, Sliwa A, Kaiser TM (2009). Saliva of the graminivorous *Theropithecus gelada* lacks proline-rich proteins and tannin-binding capacity. *American Journal of Primatology* **71**(8): 663-669.

Mau M, Südekum K-H, Johann A, Sliwa A, Kaiser TM (2010). Indication of higher salivary α-amylase expression in hamadryas baboons and geladas compared to chimpanzees and humans. *Journal of Medical Primatology* **39**: 187-190.

Mendoza M, Palmqvist P (2008). Hypsodonty in ungulates: an adaptation for grass consumption or for foraging in open habitat? *Journal of Zoology* **274**: 134-142.

Merceron G, Blondel C, Brunet M, Sen S, Solounias N, Viriot L, Heintz E (2004). The Late Miocene paleoenvironment of Afghanistan as inferred from dental microwear in artiodactyls. *Palaeogeography, Palaeoclimatology, Palaeoecology* **207**: 143-163.

Merceron G, Blondel C, De Bonis L, Koufos GD, Viriot L (2005a). A New Method of Dental Microwear Analysis: Application to Extant Primates and *Ouranopithecus macedoniensis* (Late Miocene of Greece). *Palaios* **20**(6): 551-561.

Merceron G, De Bonis L, Viriot L, Blondel C (2005b). Dental microwear of fossil bovids from northern Greece: paleoenvironmental conditions in the eastern Mediterranean during the Messinian. *Palaeogeography, Palaeoclimatology, Palaeoecology* **217**(3-4): 173-185.

Merceron G, Taylor S, Scott R, Chaimanee Y, Jaeger J-J (2006a). Dietary characterization of the hominoid *Khoratpithecus* (Miocene of Thailand): evidence from dental topographic and microwear texture analyses. *Naturwissenschaften* **93**: 329-333.

Merceron G, Zazzo A, Spassov N, Geraads D, Kovachev D (2006b). Bovid paleoecology and paleoenvironments from the Late Miocene of Bulgaria: Evidence from dental microwear and stable isotopes. *Palaeogeography, Palaeoclimatology, Palaeoecology* **241**: 637-654.

Merceron G, Schulz E, Kordos L, Kaiser TM (2007). Paleoenvironment of *Dryopithecus brancoi* at Rudabánya, Hungary:evidence from dental meso- and micro-wear analyses of large vegetarian mammals. *Journal of Human Evolution* **53**: 331-349.

Merceron G, Scott J, Scott RS, Geraads D, Spassov N, Ungar PS (2009). Folivory or fruit/seed predation for *Mesopithecus*, an earliest colobine from the late Miocene of Eurasia? *Journal of Human Evolution* **57**(6): 732-738.

Merceron G, Escarguel G, Angibault J-M, Verheyden-Tixier H (2010a). Can Dental Microwear Textures Record Inter-Individual Dietary Variations? *PLoS ONE* **5**(3): e9542.

Merceron G, Kaiser TM, Kostopoulos DS, Schulz E (2010b). Ruminant diets and the Miocene extinction of European great apes. *Proceedings of the Royal Society B* **277**: 3105-3112.

Mills JRE (1955). Ideal Dental Occlusion In The Primates. *Dental Practitioner* **6**(2): 47-63.

Moscovice LR, Issa MH, Petrzelkova KJ, Keuler NS, Snowdon CT, Huffman MA (2007). Fruit availability, chimpanzee diet, and grouping patterns on Rubondo Island, Tanzania. *American Journal of Primatology* **69**(5): 487-502.

Moser BK, Stevens GR, Watts CL (1989). The Two-sample t Test Versus Satterthwaite's Approximate F Test. *Communications in Statistics - Theory and Methods* **18**(11): 3963-3975.

Mukinya JG (1977). Feeding and drinking habits of the black rhinoceros in Masai Mara Game Reserve. *African Journal of Ecology* **15**(2): 125-138.

Murray CG, Sanson GD (1998). Thegosis - A critical review. *Australian Dental Journal* **43**(3): 192-198.

Nelson S, Badgley C, Zakem E (2005). Microwear in Modern Squirrels in Relation to Diet. *Palaeontologia Electronica* **8**(1): 14A.

Nieberg C, Gailer JP, Kaiser TM (2009). Quantifying functional traits in the ungulate dentition. *Terra Nostra* **3**: 83.

Nieberg C, Schwitzer S, Kaiser TM (2010). Quantifying occlusal topography and complexity in non-ruminating mammals. *Mammalian Biology* **75**: 19.

Norton GW, Rhine RJ, Wynn GW, Wynn RD (1987). Baboon Diet: A Five-Year Study of Stability and Variability in the Plant Feeding and Habitat of the Yellow Baboons (*Papio cynocephalus*) of Mikumi National Park, Tanzania. *Folia Primatologica* **48**(1-2): 78-120.

Oates JF, Groves CP, Ehardt C (2008a). *Lophocebus albigena*. In: IUCN 2010. IUCN Red List of Threatened Species. Version 2010.4. www.iucnredlist.org. Downloaded on 21.02.2011.

Oates JF, Tutin CEG, Humle T, Wilson ML, Baillie JEM, Balmforth Z, Blom A, Boesch C, Cox D, Davenport T, Dunn A, Dupain J, Duvall C, Ellis CM, Farmer KH, Gatti S, Greengrass E, Hart J, Herbinger I, Hicks C, Hunt KD, Kamenya S, Maisels F, Mitani JC, Moore J, Morgan BJ, Morgan DB, Nakamura M, Nixon S, Plumptre AJ, Reynolds V, Stokes EJ, Walsh PD (2008b). *Pan troglodytes*. In: IUCN 2010. IUCN Red List of Threatened Species. Version 2010.4. www.iucnredlist.org. Downloaded on 21.02.2011.

Oloo TW, Brett R, Young TP (1994). Seasonal variation in the feeding ecology of black rhinoceros (*Diceros bicornis* L.) in Laikipia, Kenya. *African Journal of Ecology* **32**(2): 142-157.

Ong P, Richardson M (2008). *Macaca fascicularis*. In: IUCN 2010. IUCN Red List of Threatened Species. Version 2010.4. www.iucnredlist.org. Downloaded on 21.02.2011.

Osborn JW, Lumsden AGS (1978). An alternative to "thegosis" and a re-examination of the ways in which mammalian molars work. *Neues Jahrbuch für Geologie und Paläontologie, Monatshefte* **156**(3): 371-392.

Owaga ML (1975). The feeding ecology of wildebeest and zebra in Athi-Kaputei plains. *East African Wildlife Journal* **13**: 375-383.

Owen-Smith N, Robbins CT, Hagerman AE (1993). Browse and Browsers: Interactions Between Woody Plants and Mammalian Herbivores. *Trends in Ecology & Evolution* **8**(5): 158-160.

Palacios E, Rodriguez A (2001). Ranging pattern and use of space in a group of red howler monkeys (*Alouatta seniculus*) in a southeastern Colombian rainforest. *American Journal of Primatology* **55**(4): 233-251.

Palombo MR, Filippi ML, Iacumin P, Longinelli A, Barbieri M, Maras A (2005). Coupling tooth microwear and stable isotope analyses for palaeodiet reconstruction: the case study of Late Middle Pleistocene *Elephas* (*Palaeoloxodon*) *antiquus* teeth from Central Italy (Rome area). *Quaternary International* **126-128**: 153-170.

Peigné S, Goillot C, Germonpre M, Blondel C, Bignon O, Merceron G (2009). Predormancy omnivory in European cave bears evidenced by a dental microwear analysis of *Ursus spelaeus* from Goyet, Belgium. *Proceedings of the National Academy of Science* **106**(36): 15390-15393.

Pellew RA (1984). The feeding ecology of a selective browser, the giraffe (*Giraffa camelopardalis tippelkirchi*). *Journal of Zoology* **201**(1): 57-81.

Pérez-Barbería FJ, Gordon IJ (1998a). The influence of molar occlusal surface area on the voluntary intake, digestion, chewing behaviour and diet selection of red deer (*Cervus elaphus*). *Journal of Zoology* **245**(03): 307-316.

Pérez-Barbería FJ, Gordon IJ (1998b). Factors affecting food comminution during chewing in ruminants: A review. *Biological Journal of the Linnean Society* **63**: 233-256.

Pérez-Barbería FJ, Gordon IJ (2001). Relationships between oral morphology and feeding style in the Ungulata: a phylogenetically controlled evaluation. *Proceedings of the Royal Society of London B* **268**: 1023–1032.

Pinto Llona AC (2006). Comparative dental microwear analysis of cave bears *Ursus spelaeus* Rosenmüller, 1794 and brown bears *Ursus arctos* Linnaeus, 1758. *Scientific Annals* **98**(Special Volume): 103-108.

Piperno DR (2006). Phytoliths. A comprehensive Guide for Archaeologists and Paleoecologists. Altamira Press, Oxford, 238 p.

Popowics TE, Rensberger JM, Herring SW (2001). The fracture behaviour of human and pig molar cusps. *Archives of Oral Biology* **46**(1): 1-12.

Prinz JF, Lucas PW (1997). An optimization model for mastication and swallowing in mammals. *Proceedings of the Royal Society B: Biological Sciences* **264**: 1715-1721.

Prinz JF (2004). Abrasives in foods and their effect on intra-oral processing: a two-colour chewing gum study. *Journal of Oral Rehabilitation* **31**: 968-971.

Purnell MA (1995). Microwear on conodont elements and macrophagy in the first vertebrates. *Nature* **374**: 798-800.

Quade J, Cerling TE, Barry JC, Morgan ME, Pilbeam DR, Chivas AR, Lee-Thorp JA, van der Merwe NJ (1992). A 16-Ma record of paleodiet using carbon and oxygen isotopes in fossil teeth from Pakistan. *Chemical Geology* **94**: 183-192.

R Development Core Team (2010). R: A language and environment for statistical computing. R Foundation for Statistical Computing, Vienna, Austria. http://www.R-project.org. Downloaded on 28.04.2010.

Ramdarshan A, Merceron G, Tafforeau P, Marivaux L (2010). Dietary reconstruction of the Amphipithecidae (Primates, Anthropoidea) from the Paleogene of South Asia and paleoecological implications. *Journal of Human Evolution* **59**: 96-108.

Remis MJ, Dierenfeld ES, Mowry CB, Carroll RW (2001). Nutritional Aspects of Western Lowland Gorilla (*Gorilla gorilla gorilla*) Diet during Seasons of Fruit Scarcity at Bai Hokou, Central African Republic. *International Journal of Primatology* **22**(5): 807-836.

Rensberger JM (1973). An occlusion model for mastication and dental wear in herbivorous mammals. *Journal of Paleontology* **47**(3): 515-528.

Rensberger JM (1978). Scanning Electron Microscopy of Wear and Occlusal Events in Some Small Herbivores. In: *Development, Function and Evolution of Teeth*, Butler PM, Joysey KA (Eds.). Academic Press, New York, pp. 415-438.

Rensberger JM, von Koenigswald W (1980). Functional and phylogenetic interpretation of enamel microstructure in rhinoceroses. *Palaeobiology* **6**(4): 477-495.

Rensberger JM, Forsten A, Fortelius M (1984). Functional evolution of the cheek tooth pattern and chewing direction in Tertiary horses. *Paleobiology* **10**(4): 439-452.

Rensberger JM (1995). Determination of stresses in mammalian dental enamel and their relevance to the interpretation of feeding behaviors in extinct taxa. In: *Functional morphology in vertebrate paleontology*, Thomason JJ (Ed.). Press Syndicate of the University of Cambrigde, Cambridge, pp. 151-172.

Rivals F, Solounias N, Mihlbachler MC (2007). Evidence for geographic variation in the diets of late Pleistocene and early Holocene Bison in North America, and differences from the diets of recent Bison. *Quaternary Research* **68**: 338-346.

Rivals F, Schulz E, Kaiser TM (2009a). A new application of dental wear analyses: estimation of duration of hominid occupations in archaeological localities. *Journal of Human Evolution* **56**(4): 329-339.

Rivals F, Schulz E, Kaiser TM (2009b). Late and middle Pleistocene ungulates dietary diversity in Western Europe indicate variations of Neanderthal paleoenvironments through time and space. *Quaternary Science Reviews* **28**(27-28): 3388-3400.

Rowen M, Ginsberg G (1992). Grevyi's Zebra (*Equus grevyi* Oustalet). In: *Zebras, Asses and Horses. An Action Plan for the Conservation of Wild Equids*, Duncan P (Ed.). IUCN, Gland, pp. 10-12.

Rubenstein DI (1986). Ecology and Sociality in Horses and Zebras. In: *Ecological Aspects of Social Evolution. Birds and Mammals*, Rubenstein DI, Wrangham RW (Eds.). Princeton University Press, New Jersey, pp. 282-302.

Sanson GD, Kerr SA, Gross KA (2007). Do silica phytoliths really wear mammalian teeth? *Journal of Archaeological Science* **34**(4): 526-531.

Schubert BW, Ungar P, DeSantis LRG (2010). Carnassial microwear and dietary behaviour in large carnivorans. *Journal of Zoology* **280**: 257-263.

Schulz E, Calandra I, Kaiser T (2009). Three-Dimension Microtexture Analysis - A New Approach for Dietary Reconstruction. *Journal of Vertebrate Paleontology* **29**(Suppl. 3): 178A.

Schulz E, Calandra I, Kaiser TM (2010a). Applying tribology to teeth of hoofed mammals. *Scanning* **32**(4): 162-182.

Schulz E, Calandra I, Kaiser TM (2010). Tracing chewing mechanisms in hoofed mammals: 3D tribology of enamel wear. *Mammalian Biology* **75S**: 24-25.

Schulz E, Piotrowski V, Clauss M, Merceron G, Kaiser TM (2011). Where do all the pits come from? – The effect of abrasive silica particles on tooth wear and its implication for paleodietary interpretations. *71st Annual Meeting of the Society of Vertebrate Paleontology*, Las Vegas.

Schulz E, Calandra I, Kaiser TM (submitted). Tracing chewing mechanisms in hoofed mammals: 3D tribology of enamel wear. *Journal of The Royal Society Interface*.

Scott JR, Godfrey LR, Jungers WL, Scott RS, Simons EL, Teaford MF, Ungar PS, Walker A (2009). Dental microwear texture analysis of two families of subfossil lemurs from Madagascar. *Journal of Human Evolution* **56**: 405-416.

Scott RS, Ungar PS, Bergstrom TS, Brown CA, Grine FE, Teaford MF, Walker A (2005). Dental microwear texture analysis shows within-species diet variability in fossil hominins. *Nature* **436**: 693-695.

Scott RS, Ungar PS, Bergstrom TS, Brown CA, Childs BE, Teaford MF, Walker A (2006). Dental microwear texture analysis: technical considerations. *Journal of Human Evolution* **51**: 339-349.

Semprebon G, Godfrey LR, Solounias N, Sutherland MR, Jungers WL (2004a). Can low-magnification stereomicroscopy reveal diet? *Journal of Human Evolution* **47**: 115-144.

Semprebon G, Janis C, Solounias N (2004b). The diets of the Dromomerycidae (Mammalia: Artiodactyla) and their response to Miocene vegetational change. *Journal of Vertebrate Paleontology* **24**(2): 427-444.

Sen PK (1968). Estimates of the Regression Coefficient Based on Kendall's Tau. *Journal of the American Statistical Association* **63**(324): 1379-1389.

Shapiro SS, Wilk MB (1965). An analysis of variance test for normality (complete samples). *Biometrika* **52**(3-4): 591-611.

Shimada T (2006). Salivary Proteins as a Defense Against Dietary Tannins. *Journal of chemical ecology* **32**: 1149-1163.

Singleton I, Wich SA, Griffiths M (2008). *Pongo abelii*. In: IUCN 2010. IUCN Red List of Threatened Species. Version 2010.4. www.iucnredlist.org. Downloaded on 21.02.2011.

Skinner JD, Smithers RHN (1990). The mammals of the southern African subregion. University of Pretoria, Pretoria, 771 p.

Solounias N, Teaford MF, Walker A (1988). Interpreting the diet of extinct ruminants: the case of a non-browsing giraffid. *Palaeobiology* **14**: 287-300.

Solounias N, Fortelius M, Freeman P (1994). Molar wear rates in ruminants: A new approach. *Annales Zoologici Fennici* **31**(2): 219-227.

Solounias N, Semprebon G (2002). Advances in the reconstruction of ungulate ecomorphology and application to early fossil equids. *American Museum Novitates* **3366**(1): 1-49.

Solounias N, Rivals F, Semprebon GM (2010). Dietary interpretation and paleoecology of herbivores from Pikermi and Samos (late Miocene of Greece). *Paleobiology* **36**(1): 113-136.

Suter H-P (2010). xlsReadWrite: Natively read and write Excel files. http://CRAN.R-project.org/package=xlsReadWrite. Downloaded on 01.06.2010.

Taylor AB (2006). Feeding behavior, diet, and the functional consequences of jaw form in orangutans, with implications for the evolution of *Pongo*. *Journal of Human Evolution* **50**: 377-393.

Teaford MF, Walker A (1983). Prenatal Jaw Movements in the Guinea Pig, *Cavia porcellus*; Evidence from Patterns of Tooth Wear. *Journal of Mammalogy* **64**(3): 534-536.

Teaford MF (1988). Scanning electron microscope diagnosis of wear patterns versus artifacts on fossil teeth. *Scanning Microscopy* **2**: 1167-1175.

Teaford MF, Byrd KE (1989). Differences in tooth wear as an indicator of changes in jaw movement in the guinea pig Cavia porcellus. *Archives of Oral Biology* **34**(12): 926-936.

Teaford MF, Oyen OJ (1989a). Differences in Rate of Molar Wear between Monkeys Raised on Different Diets. *Journal of Dental Research* **68**(11): 1513-1518.

Teaford MF, Oyen OJ (1989b). Live Primates and dental replication: New problems and new techniques. *American Journal of Physical Anthropology* **80**: 73-81.

Teaford MF, Oyen OJ (1989c). In Vivo and In Vitro Turnover in Dental Microwear. *American Journal of Physical Anthropology* **80**: 447-460.

Teaford MF, Robinson JG (1989). Seasonal or ecological zone differences in diet and molar microwear in *Cebus nigrivittatus*. *American Journal of Physical Anthropology* **80**: 391-401.

Theil H (1950). A rank-invariant method of linear and polynomial regression analysis. *Indagationes Mathematicae* **12**: 85-91.

Thenius E (1989). Zähne und Gebiss der Säugetiere. Walter de Gruyter, Berlin, New York.

Thomas TR (1991). Rough Surfaces. Imperial College Press, London, 278 p.

Tweheyo M, Lye KA, Weladji RB (2004). Chimpanzee diet and habitat selection in the Budongo Forest Reserve, Uganda. *Forest Ecology and Management* **188**: 267-278.

Ungar P, Williamson M (2000). Exploring the effects of tooth wear on functional morphology: a preliminary study using dental topographic analysis. *Palaeontologia Electronica* **3**(1): 1-18.

Ungar P, Teadford M, Kay R (2004). Molar microwear and shearing crest development in Miocene catarrhines. *Anthropology* **XLII**(1): 21-35.

Ungar P, Merceron G, Scott R (2007). Dental Microwear Texture Analysis of Varswater Bovids and Early Pliocene Paleoenvironments of Langebaanweg, Western Cape Province, South Africa. *Journal of Mammalian Evolution* **14**(3): 163-181.

Ungar P (2008). Materials science: Strong teeth, strong seeds. *Nature* **452**(7188): 703-705.

Ungar PS, Simon J-C, Cooper JW (1991). A Semiautomated Image Analysis Procedure for the Quantification of Dental Microwear. *Scanning* **13**: 31-36.

Ungar PS (1995). A Semiautomated Image Analysis Procedure for the Quantification of Dental Microwear II. *Scanning* **17**(1): 57-59.

Ungar PS, Brown CA, Bergstrom TS, Walker A (2003). Quantification of Dental Microwear by Tandem Scanning Confocal Microscopy and Scale-Sensitive Fractal Analyses. *Scanning* **25**(4): 185-193.

Ungar PS (2005). Dental evidence for the diets of fossil primates from Rudabánya, northeastern Hungary with comments on extant primate analogs and “noncompetitive” sympatry. *Palaeontographia Italica* **90**: 97-111.

Ungar PS, Grine FE, Teaford MF (2008). Dental Microwear and Diet of the Plio-Pleistocene Hominin *Paranthropus boisei*. *PLoS ONE* **3**(4): e2044.

Ungar PS, Scott JR, Schubert BW, Stynder DD (2010). Carnivoran dental microwear textures: comparability of carnassial facets and functional differentiation of postcanine teeth. *Mammalia* **74**(2): 219–224.

Van Soest PJ (1994). Nutritional ecology of the ruminant, 2 ed. Cornell University Press, New York, 476 p.

van Valkenburgh BV (1996). Feeding behaviour in free-ranging, large African carnicores. p. 240_254.

von Koenigswald W (2004a). The three basic types of schmezmuster in fossil and extant rodent molars and their distribution among rodent clades. *Palaeontographica Abteilung A* **270**: 95-131.

von Koenigswald W (2004b). Enamel Microstructure of Rodent Molars, Classification, and Parallelisms, with a Note on the Systematic Affiliation of the Enigmatic Eocene Rodent *Protoptychus*. *Journal of Mammalian Evolution* **11**(2): 127-142.

von Koenigswald W, Anders U, Engels S, Schultz JA, Ruf I (2010). Tooth Morphology in Fossil and Extant Lagomorpha (Mammalia) Reflects Different Mastication Patterns. *Journal of Mammalian Evolution* **17**: 275-299.

von Koenigswald W, Holbrook LT, Rose KD (2011). Diversity and evolution of Hunter-Schreger Band configuration in tooth enamel of perissodactyl mammals. *Acta Palaeontologica Polonica* **56**(1): 11-32.

Walker A, Hoeck HN, Perez L (1978). Microwear of Mammalian Teeth as an Indicator of Diet. *Science* **201**: 908-910.

Walker PL (1976). Wear striations on the incisors of ceropithecoid monkeys as an index of diet and habitat preference. *American Journal of Physical Anthropology* **45**(2): 299-307.

Walsh PD, Tutin CEG, Oates JF, Baillie JEM, Maisels F, Stokes EJ, Gatti S, Bergl RA, Sunderland-Groves J, Dunn. A (2008). *Gorilla gorilla*. In: IUCN 2010. IUCN Red List of Threatened Species. Version 2010.4. www.iucnredlist.org. Downloaded on 21.02.2011.

Wang Y, Cerling TE (1994). A model of fossil tooth and bone diagenesis: implications for paleodiet reconstruction from stable isotopes. *Palaeogeography, Palaeoclimatology, Palaeoecology* **107**: 281-289.

Welch BL (1938). The significance of the difference between two means when the population variances are unequal. *Biometrika* **29**(3-4): 350-362.

Wich SA, Fredriksson G, Sterck EHM (2002). Measuring fruit patch size for three sympatric Indonesian primate species. *Primates* **43**(1): 19-27.

Wich SA, Utami-Atmoko SS, Mitra Setia T, Djoyosudharmo S, Geurts ML (2006). Dietary and energetic responses of *Pongo abelii* to fruit availability fluctuations. *International Journal of Primatology* **27**(6): 1535-1550.

Wilcox RR, Charlin VL, Thompson KL (1986). New Monte-Carlo Results on the Robustness of the ANOVA F, W and F* Statistics. *Communications in Statistics - Simulation and Computation* **15**(4): 933-943.

Wilcox RR (1994). The percentage bend correlation coefficient. *Psychometrika* **59**(4): 601-616.

Wilcox RR (2003). Applying Contemporary Statistical Techniques. Academic Press, San Diego, 608 p.

Wilcox RR (2005). Introduction to Robust Estimation and Hypothesis Testing, 2nd ed. Elsevier Academic Press, Burlington, San Diego, London, 588 p.

Wilcox RR, Schönbrodt FD (2010). The WRS package for robust statistics in R. http://r-forge.r-project.org/projects/wrs/. Downloaded on 27.04.2011.

Wilcoxon F (1945). Individual comparison by ranking methods. *Biometrics Bulletin* **1**: 80-83.

Williams SD (2002). Status and Action Plan for Grevyi Zebra (*Equus grevyi*). In: *Equids: Zebras, Asses and Horses. Status Survey and Conservation Action Plan*, Moehlman PD (Ed.). UCN/SCC Equid Specialist Group, IUCN (The World Conservation Union), Gland, Switzerland and Cambridge, UK, pp. 11-27.

Williams VS, Barrett PM, Purnell MA (2009). Quantitative analysis of dental microwear in hadrosaurid dinosaurs, and the implications for hypotheses of jaw mechanics and feeding. *Proceedings of the National Academy of Sciences* **106**(27): 11194-11199.

Winkler DE, Schulz E, Kaiser TM (2011). No Grass Today: Dietary Reconstruction and Dental Evolution of the Balearic Cave Goat *Myotragus* (Plio-Holocene, Spain). *71st Annual Meeting of the Society of Vertebrate Paleontology*, Las Vegas, USA.

Xu HHK, Smith DT, Jahanmir S, Romberg E, Kelly JR, Thompson VP, Rekow ED (1998). Indentation Damage and Mechanical Properties of Human Enamel and Dentin. *Journal of Dental Research* **77**(3): 472-480.

Young WG, McGowan M, Daley TJ (1987). Tooth enamel structure in the koala, *Phascolarctos cinereus*: - Some functional interpretations. *Scanning Microscopy* **1**(4): 1925-1934.

Young WG, Robson SK (1987). Jaw movements from microwear on the molar teeth of the koala *Phascolarctus cinereus*. *Journal of Zoology* **213**: 51-61.

Yuen KK (1974). The two-sample trimmed *t* for unequal population variances. *Biometrika* **61**(1): 165-170.

7. Appendices

Appendix 2.1. Ungulate specimens included in the sample.

Species	Specimen	Tooth	Locality	Country
Connochaetes taurinus	ZMH-5670	M1	Chimporo	Angola
	ZMH-6774	M2	Kajado	Kenya
	ZMH-7939	M2	Kirawira, Serengeti plain	Tanzania
	ZMH-8010	M2		Angola
	ZMB-unknown	M1	Ngorongoro	Tanzania
	ZMB-unknown	M2	Okavango	Namibia
	ZMH-6776	M2	Narok-Massai-Mara	Kenya
Equus grevyi	ZMH-7205	M1	Wamba	Kenya
	ZMH-7196	M2	Wamba	Kenya
	ZMH-7201	M2	Wamba	Kenya
	ZMH-7204	M2	Wamba	Kenya
	ZMH-6749	M2	Isiolo	Kenya
	ZMH-9385	M2	Wamba	Kenya
	ZMH-9386	M1	Wamba	Kenya
Giraffa camelopardalis	ZMB-15552	M1	Capland	South Africa
	ZMB-84948	M1	Kilimandscharo	Tanzania
	ZMB-84954	M1	Uhehe, Udschungwe Mountains	Tanzania
	ZMB-32372	M2	Kilimandscharo, El Oldorobo, E of Tawata	Kenya
	ZMB-84955	M2		Kenya
	ZMB-17391	M2	Nguru mountains	Tanzania
	ZMH-9426	M2		Tanzania
Diceros bicornis	ZMB-35746	M2	SE, An. Luijana	Angola
	ZMB-40053	M2	Umbulu, Engotiek	Tanzania
	ZMB-41480	M2	Cerere, near lake Maujara	Tanzania
	ZMB-46166	M2	Engaruka	Tanzania
	ZMB-83230	M2	Ukerewe, Neuwied	Tanzania
	ZMH-1865	M1		Tanzania/Kenya
	ZMH-2553	M2	Hluluwe reservation	South Africa
	ZMH-9378	M2	Wamba	Kenya
	ZMH-9379	M2	Wamba	Kenya

Upper first (M1) and second (M2) molars analyzed from the mammal collections of the Museum für Naturkunde Berlin (ZMB) and the Zoologisches Museum Hamburg (ZMH). From Schulz *et al.* (submitted, table 1).

Appendix 2.2. Primate specimens included in the sample.

Family	Species	n	Number [a]	Side [b]	Type [c]	Locality	Country	Continent
Atelidae	*Alouatta seniculus*	3	SMF-979	L	Cast	St. Catharina	Brazil	S. America
			SMF-985	L	Cast	St. Catharina	Brazil	S. America
			SMF-4991	L	Cast	St. Catharina	Brazil	S. America
Cercopithecidae	*Lophocebus albigena*	7	SMF-4113	R	Cast	Bange-Urwald	Republic of Cameroon	Africa
			SMF-4116	L	Cast		Democratic Republic of the Congo	Africa
			SMF-59239	L	Cast	Irangi	Democratic Republic of the Congo	Africa
			ZMB-A60.05	L	Cast		Republic of Cameroon	Africa
			ZMB-1090	L	Cast	Avakubi	Democratic Republic of the Congo	Africa
			ZMB-18441	R	Cast	Sarvi, Deng Deng	Former Neukamerun	Africa
			ZMB-18526	R	Cast	Edea	Republic of Cameroon	Africa
Cercopithecidae	*Macaca fasciularis*	7	AIMUG-13.1.4	L	Cast		Sumatra?	Indonesia
			AIMUG-13.1.16	R	Cast		Sumatra?	Indonesia
			AIMUG-13.2.22	L	Cast		Sumatra?	Indonesia
			AIMUG-13.2.25	L	Cast		Sumatra?	Indonesia
			AIMUG-13.2.29	L	Cast		Sumatra?	Indonesia
			AIMUG-13.2.38	L	Cast		Sumatra?	Indonesia
			AIMUG-13.3.74	R	Cast		Sunda Islands	Indonesia
Cercopithecidae	*Papio cynocephalus*	10	ZMH-6788	R	Orig	Lake Baringo	Kenya	Africa
			ZMH-6789	R	Orig	Lake Baringo	Kenya	Africa
			ZMH-6790	R	Orig	Lake Baringo	Kenya	Africa
			ZMH-6791	R	Orig	Lake Baringo	Kenya	Africa
			ZMH-6792	R	Orig	Lake Baringo	Kenya	Africa
			ZMH-6793	L	Orig	Lake Baringo	Kenya	Africa
			ZMH-6795	L	Orig	Lake Baringo	Kenya	Africa
			ZMH-6800	L	Orig	Gilgil	Kenya	Africa
			ZMH-6801	L	Orig	Elementaita, Gilgil	Kenya	Africa
			ZMH-6802	L	Orig	Elementaita, Gilgil	Kenya	Africa
Cercopithecidae	*Theropithecus gelada*	2	SMF-1011	L	Cast		Ethiopia	Africa
			ZMB-72127	L	Cast	Shoa	Ethiopia	Africa

Appendix 2.2. (continued)

Family	Species	n	Number [a]	Side [b]	Type [c]	Locality	Country	Continent
Hominidae	*Gorilla gorilla gorilla*	6	ZMH-6992	L	Orig	Kangula by Kinshasa	Democratic Republic of the Congo	Africa
			ZMH-6993	L	Orig	Kelle district by Brazzaville	Republic of the Congo	Africa
			ZMH-7113	L	Orig	Sanga	Republic of the Congo	Africa
			ZMH-7902	L	Orig	Evonmitok	Gabon	Africa
			ZMH-8024	L	Orig	Jaunde	Republic of Cameroon	Africa
			ZMH-8192	L	Orig	Jaunde	Republic of Cameroon	Africa
Hominidae	*Pan troglodytes*	5	SMF-4107	L	Cast	N'ginda	Republic of Cameroon	Africa
			SMF-15817	L	Cast	Bibundi	Republic of Cameroon	Africa
			AIMUG-15.5.12	L	Cast		Republic of Cameroon	Africa
			AIMUG-15.5.13	L	Cast		Republic of Cameroon	Africa
			AIMUG-15.5.14	L	Cast		Republic of Cameroon	Africa
Hominidae	*Pongo abelii*	7	SMF-1120	L	Cast	Deli	Sumatra	Indonesia
			SMF-6716	L	Cast	Medan	Sumatra	Indonesia
			SMF-59140	L	Cast	Bezirk Atjeh	Sumatra	Indonesia
			SMF-59147	L	Cast	Bezirk Atjeh	Sumatra	Indonesia
			SMF-59148	L	Cast	Bezirk Atjeh	Sumatra	Indonesia
			AIMUG-15.4.2	L	Cast		Sumatra	Indonesia
			AIMUG-15.4.7	L	Cast		Sumatra	Indonesia

[a] Museum abbreviations: AIMUG, Anatomische Sammlung des Institutes für Anatomie und Zellbiologie der Universität Greifswald; SMF, Senckenberg Forschungsinstitut und Museum Frankfurt am Main; ZMB, Museum für Naturkunde Berlin; ZMH, Zoologisches Museum Hamburg. [b] L, left; R, right. [c] Cast, molded from cast; Orig, molded directly from original; see text for explanations.

Appendix 2.3. R scripts

These appendices present some of the scripts I have written to run my analyses in R. They can be run readily in R for Windows. Few modifications relative to data import and export are required to run the scripts in Appendices 2.1 and 2.4 on MacOS because package xlsReadWrite is not available (yet) on this platform. Package xlsx [Dragulescu AA (2011). xlsx: Read, write, format Excel 2007 and Excel 97/2000/XP/2003 files. v. 0.3.0. http://CRAN.R-project.org/pakcage=xlsx] offers alternatives but was not used at the time of these studies.

I wrote these scripts so that anyone in the team with a basic knowledge of the R programming language could use them (more than just a basic knowledge is necessary to understand them though!). The amount of modifications required to adjust them to specific data sets is therefore kept to a minimum (usually in step 2). The comments appear in green and are preceded by the symbol '#'.

Appendix 2.3.1: Data import and preparation

```
#1. import libraries
#2. import data from xls
#3. select measurements
#4. compute median for numerical variables
#5. reorder the level if needed (for plots only)
#6. check data objects
#7. save data objects
#8. export objects to xls
#ALL STEPS NEED TO BE ADJUSTED!

#1. load libraries
library(xlsReadWrite)
library(doBy)
library(R.utils)

#2. define the modes of the columns in "vect_mode" and import data into "primate"
vect_mode <- c(rep("factor",6), rep("numeric",30))
primates <- read.xls(file=file.choose(), colNames=TRUE, sheet=1, type="data.frame",
                 from=1, rowNames=FALSE, checkNames=TRUE, colClasses=vect_mode)
str(primates)
```

```
#3. if needed: select data where SEL_MEAS=1
primates_sel <- primates[primates$SEL_MEAS==1,]
str(primates_sel)
#4. column statistics:
#when all the values for SPECSHOR, SPEC_ID, BONE, TO_POS, and SIDE are equal,
#computes the median for all numeric variables (see ".")
#removes MEASUREM, SEL_FAC and SEL_MEAS from data.frame
primates_med <- summaryBy(.~SPECSHOR+SPEC_ID+BONE+TO_POS+SIDE,
                    data=subset(primates_sel,select=-c(MEASUREM,SEL_MEAS)),
                    FUN=median)
str(primates_med)

#5. reorder the levels of TO_POS and SPECSHOR into primate_med_order
#NOT FOR STATISTICAL TESTS
primates_med_order <- primates_med
primates_med_order$SPECSHOR <- factor(primates_med_order$SPECSHOR, levels
                                      =c("thgel","pacyn","loalb","gogor","alsen","poabe",
                                      "mafas","patro"))
str(primates_med_order)

#6. save objects to Binary files
saveObject(primates, file="primates.Rbin")
saveObject(primates_sel, file="primates_sel.Rbin")
saveObject(primates_med, file="primates_med.Rbin")
saveObject(primates_med_order, file="primates_med_order.Rbin")

#7. export as xls file
write.xls(primates_med, file="primates_med.xls", colNames=TRUE, sheet="primates_
          med", rowNames=FALSE)
```

Appendix 2.3.2: Descriptive statistics

```
#computes the n, mean, and standard deviation
#for each group for all numeric variables
#Step 1 need to be run only once at the beginning
#Step 2 NEEDS TO BE MODIFIED FOR EVERY RUN
#Steps 3-5 need to be run everytime, but without modifications
#step 5: choose between 5c and 5d

#1. load libraries, external package and data
library(R.utils)
library(doBy)
library(xlsReadWrite)
primates <- loadObject("primates.Rbin")

#2. set variables to be used
datobj <- primates  #data object to use
selvarind1 <- NA    #column index of 1st selection variable, WRITE 'NA' (without
                    quotes) IF YOU DON'T NEED IT
selvarind2 <- NA    #column index of 2nd selection variable, WRITE 'NA' (without
                    quotes) IF YOU DON'T NEED IT
selvarstr <- "NS"   #names of the levels to select from selvarind1 and selvarind2: the
                    1st value of selvarstr must correspond to selvarind1
                    #WRITE "NS" (with quotes), i.e. "no subset", IF YOU DON'T NEED
                    IT
seq.num <- 7:36     #column indexes to be used as numerical variables
cat <- 1            #column index(es) to be used as categorical variable(s)

#3. select data
    #3a. subset depending on your selecting variable(s)
    select <- sub2var(dat=datobj, sel1=selvarind1, sel2=selvarind2, selstr=selvarstr)
    #3b. create a character scalar for name of the file
    filename <- paste("summary", paste(names(datobj)[cat], collapse="_"),
              paste(selvarstr,collapse="_"), sep="_")
    #3c. subset only the columns for the categorical variable (cat) and numeric
      variables   (seq.num) to be used
    select_numvar <- select[, c(cat, seq.num)]
    #3d. display your selections
    select[,1:3]
    select_numvar[,1:3]

#4. Compute the function desc.stat.4 for each level of datobj[cat]
    #4a. Computation
    data_summary <- summaryBy(as.formula(paste(".~",paste(names(datobj)[cat],
                    collapse="+"))), data=select_numvar, FUN=desc.stat.3)
```

```
    #4b. Rename the columns
    vect_var <- names(datobj)[seq.num]
    names(data_summary)[-seq_along(cat)] <- sapply(vect_var, FUN=paste, desc.
                                                   stat.3.names, sep="_")

#5. prepare data and export to xls file
    #5a. create a sequence of the numbers of the columns that you don't want/need to
      export
    #delete every 3 columns from column 5 to the last (all "n" columns except the
      first))
    seq_delete <- seq.int(length(cat)+4,3*length(seq.num),3)
    #5b. prepare the data to export
    if (any(sapply(data_summary[,seq_delete], FUN=identical, data_summary[,length(
                    cat)+1])==FALSE)){
        data_export <- data_summary
    } else {
        data_export <- data_summary[,-seq_delete]
        names(data_export)[length(cat)+1] <- "n"
    }

    #5c. export to xls with variables in columns
    # MAX 256 COLUMNS
    write.xls(data_export, file=paste(filename,".xls",sep=""), colNames=TRUE,
                    sheet=filename, rowNames=FALSE)
    #5d. transpose data_export and export to xls with variables in rows
    t_data <- t(data_export)
    write.xls(t_data, file=paste(filename,"_t.xls",sep=""), colNames=FALSE,
                    sheet=filename, rowNames=TRUE)
```

Appendix 2.3.3: Plots

Boxplots

```
#boxplots for all numerical variables by 1 categorical variable
#save as *.svg
#Step 1 needs to be run only once
#Step 2 NEEDS TO BE MODIFIED FOR EVERY RUN
#Step 3 needs to be run everytime, but without modifications
#Step 4: choose between vertical (boxvert()) and horizontal (boxhoriz()) boxes

#1. load data and required libraries to export as .svg
library(R.utils)
library(RSvgDevice)
primates_med_order <- loadObject("primates_med_order.Rbin")

#2. set variables to be used
datobj <- primates_med_order    #data object to use
selvarind1 <- NA                #column index of 1st selection variable, WRITE 'NA'
                                (without quotes) IF YOU DON'T NEED IT
selvarind2 <- NA                #column index of 2nd selection variable, WRITE 'NA'
                                (without quotes) IF YOU DON'T NEED IT
selvarstr <- "NS"               #names of the levels to select from selvarind1 and
                                selvarind2: the 1st value of selvarstr must correspond
                                to selvarind1
                                #WRITE "NS" (with quotes), i.e. "no subset", IF YOU
                                DON'T NEED IT
seq.num <- 6:38                 #column indexes to be used as numerical variables
cat <- 1                        #column index to be used as categorical variable
ax.range <- NULL                #range of the x- or y-axis for all boxplots, WRITE
                                'NULL' (without quotes) FOR AN AUTOMATIC RANGE

#3. select data
    #3a. subset depending on your selecting variable(s)
    select <- sub2var(dat=datobj, sel1=selvarind1, sel2=selvarind2, selstr=selvarstr)
    #3b. create a character vector for name of the file
    filenames <- paste("boxplot", names(datobj)[cat], names(datobj)[seq.num],
                    paste(selvarstr,collapse="_"), sep="_")
    filenames <- gsub(".median", "", filenames)
    #3c. display your selection
    select[,1:5]

#4. boxplots on select with select[[cat]] as category and select[[seq.num[i]]] as
    numeric variable
for(i in seq_along(seq.num)) {
    devSVG(file=paste(filenames[i], ".svg", sep=""))
    boxvert(dat=select, x=cat, y=seq.num[i], nt=filenames[i], yr=ax.range)
    dev.off()
}
```

Regression

```
#Robust regressions and correlation for selected numerical variables
#by 1 categorical variable
#save as *.svg
#Step 1 needs to be run only once
#Step 2 NEEDS TO BE MODIFIED FOR EVERY RUN
#Steps 3&5 need to be run everytime, but without modifications
#Step 4: if x is discrete, do 4a; if x is continuous, do 4b

#1. load data and required libraries
library(R.utils)
library(RSvgDevice)
library(doBy)
source("~/Rallfun-v12_Wilcox")
primate_med <- loadObject("primate_med.Rbin")

#2. set variables to be used
datobj <- primate_med     #data object to use
selvarind1 <- NA          #column index of 1st selection variable, WRITE 'NA' (without
                          quotes) IF YOU DON'T NEED IT
selvarind2 <- NA          #column index of 2nd selection variable, WRITE 'NA'
                          (without quotes) IF YOU DON'T NEED IT
selvarstr <- "NS"         #names of the levels to select from selvarind1 and
                          selvarind2: the 1st value of selvarstr must correspond to
                          selvarind1
                          #WRITE "NS" (with quotes), i.e. "no subset", IF YOU DON'T
                          NEED IT
seq.yvar <- c(5,12,8,9)   #column indexes to be used as y-variables, NOT MORE THAN
                          4 AT ONCE
ind.xvar <- 4             #column index to be used as x-variable

#3. select data
    #3a. subset depending on your selecting variable(s)
    select <- sub2var(dat=datobj, sel1=selvarind1, sel2=selvarind2, selstr=selvarstr)
    #3b. create a character scalar for name of the file
    filename <- paste("regression", names(datobj)[ind.xvar], paste(names(datobj)[seq.
                yvar],collapse="_"), paste(selvarstr,collapse="_"), sep="_")
    filename <- gsub(".median", "", filename)
    #3c. display your selection
    select[,1:3]

#4. choose whether to compute the means by group of ind.xvar
    #4a. ind.xvar is discrete
    # compute the means for every numerical variable by ind.xvar (here PROP_FRUIT)
    select_mean <- summaryBy(as.formula(paste(".~",names(select)[ind.xvar])),
                  data=select, FUN=mean)
```

```
    #4b. ind.xvar is continuous
    # you don't want to compute the means
    select_mean <- NULL

#5. compute and plot regression lines
    #5a. open svg file to plot
    devSVG(file=paste(filename, ".svg", sep=""))
    par(mfrow=c(2,2))
    diff_len <- length(select)-length(select_mean)
    #5b. compute and plots 2 regressions (tstsreg() and mgvreg())
    # and correlation (pbcor() and corb())
    # everything done by custom two_reg()
    for (i in seq_along(seq.yvar)){
        k <- seq.yvar[i]
        plot(select[[k]]~select[[ind.xvar]], type="p", pch=1, xlab=names(select)[ind.
            xvar], ylab=names(select)[k], las=1)
        points(select_mean[[ind.xvar-diff_len]], select_mean[[k-diff_len]], pch=18,
            cex=2)
        two_reg(dat=select, xvar=ind.xvar, yvar=k)
    }
    #5c. close connection to svg file
    dev.off()
```

Appendix 2.3.4: Analytical statistics

Preparation

```
#Prepares the data objects for Wilcox's functions
#all numeric variables, 1 list per variable
#Step 1 needs to be run only once at the beginning, path needs to be adjusted
#Step 2 NEEDS TO BE MODIFIED FOR EVERY RUN
#Steps 3&4 need to be run everytime, but without modifications

# 1. load data and libraries, and source external packages
library(R.utils)
source("~/Rallfun-v12_Wilcox")
primates <- loadObject("primates_med.Rbin")


#2. set variables to be used
datobj <- primates  #data object to use
selvarind1 <- NA    #column index of 1st selection variable, WRITE 'NA' (without
                    quotes) IF YOU DON'T NEED IT
selvarind2 <- NA    #column index of 2nd selection variable, WRITE 'NA' (without
                    quotes) IF YOU DON'T NEED IT
selvarstr <- "NS"   #names of the levels to select from selvarind1 and selvarind2: the
                    1st value of selvarstr must correspond to selvarind1
                    #WRITE "NS" (with quotes), i.e. "no subset", IF YOU DON'T NEED
                    IT
seq.num <- 6:38     #column indexes to be used as numerical variables
cat <- 1            #column index to be used as categorical variable

#3. select data
    #3a. subset depending on your selecting variable(s)
    select <- sub2var(dat=datobj, sel1=selvarind1, sel2=selvarind2, selstr=selvarstr)
    #3b. create a character vector for names of the files
    filenames <- paste(names(datobj)[cat], names(datobj)[seq.num],
                    paste(selvarstr,collapse="_"), sep="_")
    filenames <- gsub(".median", "", filenames)
    #3c. display your selection
    select[,1:5]

#4. Split the data from select[,seq.num[i]] into groups from select[cat]
#store into list "temp"
#save as objects into Rbin files
for(i in seq_along(seq.num)) {
    temp <- fac2list(select[,seq.num[i]], select[cat])
    names(temp) <- levels(select[[cat]])
    print(filenames[i])
    assign(filenames[i], temp)
    saveObject(object=temp, file=paste(filenames[i],".Rbin",sep=""))
}
```

Tests

```
#runs t1way(), lincon() and cidmulv2() on all objects (from *.Rbin) in the specified folder
#with or without trimming
#Step 1 needs to be run only once at the beginning
#Step 2 needs to be run every time, adjust the amount of trimming
#Step 3 needs to be run every time, adjust the path
#Steps 4-9 need to be run every time, but without modifications
#STEP 5 TAKES SOME TIME, LET IT RUN UNTIL THE END BEFORE GOING TO STEP 6

#1. source external packages and load libraries
source("~/Rallfun-v12_Wilcox")
library(xlsReadWrite)
library(R.utils)

#2. define the amount of trimming for t1way() and lincon()
trimming <- 0.15

#3. set the path for where to get the files
# and get the names of files with *.Rbin as extension
# "cat" should be the name of the last subfolder, the one directly containing the *.Rbin files
# "fpath" therefore does not include the whole path, but only until "cat"
cat <- "SPECSHOR"
fpath <- "D:/Pro/R/Data/Primates/Output/lists_Rbin"
listnames <- list.files(path=paste(fpath,cat,sep="/"), pattern="^.*\\.Rbin$", full.
                names=FALSE)

#4. defines the object for the outputs of t1way (test1),
#lincon (test2 and test3) and cidmulv2 (test4)
test1 <- dataFrameIC(colClasses=rep("numeric",4), colnames=c("Ft","nu1","nu2",
          "p.value"), nrow=length(listnames))
test2 <- vector(mode="list", length=length(listnames))
test3 <- vector(mode="list", length=length(listnames))
test4 <- vector(mode="list", length=length(listnames))

#5. Run t1way, lincon and cidmulv2 for all lists and export as xls and csv
for (i in seq_along(listnames)) {
    #5a. load the .Rbin files (objects)
    z1 <- loadObject(paste(fpath, cat, listnames[i], sep="/"))
    #5b. remove ".Rbin" and ".median"
    filename <- gsub(".Rbin", "", listnames[i])
    filename2 <- gsub(".median", "", filename)
    #5c. Remove NAs
    z2 <- list_noNA(z1, filename2)
    #5d. Check if any level has 2 or less elements; if yes, remove the level from z
    z3 <- list_morethan2(z2, filename2)
```

```
    #5e. t1way
    test1[i,] <- as.data.frame(t1way(z3, tr=trimming))
    row.names(test1)[i] <- filename2
    #5f. complete lincon
    print("Lincon test:")
    test2[[i]] <- as.data.frame(lincon(z3,tr=trimming,alpha=0.05))[-c(7,8)]
    names(test2)[i] <- filename2
    #5g. select useful columns of lincon (Groups, Test, p-value, and df)
    test3[[i]] <- test2[[i]][c(1:3,10,6)]
    names(test3[[i]]) <- c("Group1", "Group2", "Test", "p.value", "df")
    names(test3)[i] <- filename2
    #5h. Perform Cliff's method for all pairs of J independent groups.
    #The familywise type I error probability is controlled via Hochberg's method
    Temp <- as.data.frame(cidmulv2(z3)[[1]])
    names(temp)[c(1,2,6)] <- c("Group1", "Group2", "p.value")
    temp$p.compare <- ifelse(temp$p.value<=temp$p.crit, 1, 0)
    test4[[i]] <- temp
    names(test4)[i] <- filename2
    #5i. make sure that it prints during process
    flush.console()
}

#6. export t1way to xls (and reorder the columns)
expfile_name1 <- paste("t1way_", cat, "_tr", trimming, sep="")
write.xls(test1[c(1,4,2,3)], file=paste(expfile_name1,".xls",sep=""), colNames=TRUE,
          rowNames=TRUE, sheet=expfile_name1)

#7. export complete lincon to csv
expfile_name2 <- paste("lincon_", cat, "_tr", trimming, "_raw", sep= "")
lincon_raw_f <- file(paste(expfile_name2,".csv",sep=""), open="a")
for (i in seq_along(test2)){
    write.table(names(test2)[i], file=lincon_raw_f, sep=",", dec=".", quote=FALSE, col.
            names=FALSE, row.names=FALSE)
    write.table(test2[[i]], file=lincon_raw_f, sep=",", dec=".", quote=FALSE, col.
            names=TRUE, row.names=FALSE)
 }
close(lincon_raw_f)

#8. export useful columns of lincon to xls or csv
    #8a. create a sequence of column indexes to delete if all values are equal
    seq_delete3a <- seq.int(6,5*length(listnames),5)
    seq_delete3b <- seq.int(7,5*length(listnames),5)
    seq_delete3 <- sort(c(seq_delete3a, seq_delete3b))
    #8b. export to xls/csv depending on the structure of the output from lincon
    expfile_name3 <- paste("lincon_", cat, "_tr", trimming, sep="")
    exp_xls(dat=test3, fname=expfile_name3, del=seq_delete3)
```

```
#9. export cidmulv2 to xls or csv
    #9a. create a sequence of column indexes to delete if all values are equal
    seq_delete4a <- seq.int(9,8*length(listnames),8)
    seq_delete4b <- seq.int(10,8*length(listnames),8)
    seq_delete4 <- sort(c(seq_delete4a, seq_delete4b))
    #9b. export to xls/csv depending on the structure of the output from cidmulv2
    expfile_name4 <- paste("cidmulv2", cat, sep="_")
    exp_xls(dat=test4, fname=expfile_name4, del=seq_delete4)
```

Appendix 2.3.5: Custom functions

These functions are included in a script that is source()d at the beginning of an R session, so that all functions are loaded in the workspace (*i.e.* "available").

```
#sub2var()
#Subset dataset based on 0 to 2 selection variables

#Argument description
#dat: data.frame, data object to use
#sel1: integer, column index of 1st selection variable
#sel2: integer, column index of 2nd selection variable
#selstr: character vector, level to select from sel1 and sel2, in this order

sub2var <- function(dat, sel1, sel2, selstr) {
    if (is.na(sel1)==TRUE){
        select_fun <- dat
        print("no subsetting: everything will be used")
    } else {
        if (is.na(sel2)==TRUE){
        select_fun <- dat[dat[[sel1]]==selstr, ]
        print("data subset based on 1 variable")
    } else {
            select_fun <- dat[dat[[sel1]]==selstr[1] & dat[[sel2]]==selstr[2], ]
        print("data subset based on 2 variables")
        }
    }
    return(select_fun)
}
```

```
############################

#list_noNA()
#remove NAs recursively from each element of a list

#Argument description
#dat: list, data object to use
#fname: character scalar, name of data object used

list_noNA <- function(dat, fname) {
    temp <- vector(mode="list", length=length(dat))
    names(temp) <- names(dat)
    for (xx in seq_along(dat)) {
        dat_NA <- dat[[xx]][is.na(dat[[xx]])]
        dat_noNA <- dat[[xx]][!is.na(dat[[xx]])]
        print(paste("test NA: ", fname, "; ", names(dat)[xx], "; n(NA)=", length(dat_NA),
            ";    n=", length(dat_noNA), sep=""))
        temp[[xx]] <- dat_noNA
    }
    return(temp)
}

############################

#list_morethan2()
#keep elements from a list with strictly more than 2 sub-elements

#Argument description
#dat: list, data object to use
#fname: character scalar, name of data object used

list_morethan2 <- function(dat, fname) {
    if (any(lapply(dat, FUN=length)<=2)==TRUE) {
        toosmall <- which(lapply(dat, FUN=length)<=2)
        print(paste("test length: ", fname, "; ", names(toosmall), " removed", sep=""))
        temp <- dat[-toosmall]
    } else {
        temp <- dat
        print(paste("test length: ", fname, "; GOOD, all levels contain at least 3
            elements", sep=""))
    }
    return(temp)
}

############################
```

```
#exp_xls()
#Export output from lincon() or cidmulv2() to csv or xls
#depending on the structure of the output (number and order of pairwise comparison
for all variables)
#load wlsReadWrite on Windows

#Argument description
#dat: data.frame, data object to use
#fname: character scalar, name of the output file (without extension)
#del: integer vector, indexes of the columns to be deleted if identical

exp_xls <- function(dat, fname, del) {
    if (all(sapply(dat, FUN=function(x) nrow(dat[[1]][1])==nrow(x[1])))==FALSE){
    exp_f <- file(paste(fname,".csv",sep=""), open="a")
    for (i in seq_along(dat)){
            write.table(names(dat)[i], file=exp_f, sep=",", dec=".", quote=FALSE, col.
                names=FALSE, row.names=FALSE)
            write.table(dat[[i]], file=exp_f, sep=",", dec=".", quote=FALSE, col.
                names=TRUE, row.names=FALSE)
    }
    close(exp_f)
    } else {
        if (all(sapply(dat, FUN=function(x) identical(x[,1:2], dat[[1]][,1:2])))==TRUE){
        df_out <- as.data.frame(dat)[-del]
        } else {
        df_out <- as.data.frame(dat)
        }
        if (.Platform$OS.type=="windows"){
    require(xlsReadWrite)
    write.xls(df_out, file=paste(fname,".xls",sep=""), colNames=TRUE,
            rowNames=FALSE, sheet=fname)
        } else {
        write.csv(df_out, file=paste(fname,".csv",sep=""), quote=FALSE, row.
                names=FALSE)
        }
    }
}

###########################

#dataFrameIC()
#modified from R.utils::dataFrame()
#create an empty data.frame

#Argument description
#colClasses: character vector, modes of the columns; length(colClasses) defines the
number of columns; "factor" is not allowed
#colnames: character vector, names of the columns; length(colnames) should be equal
```

```
to length(colClasses)
#nrow: integer, number of rows

dataFrameIC <- function (colClasses, colnames, nrow=1) {
    if(length(colClasses)!=length(colnames)) warning("the number of columns
        (colClasses) don't match the number of names (colnames)")
    df <- vector("list", length(colClasses))
    names(df) <- colnames
    for (kk in seq(along = df)) {
        df[[kk]] <- vector(colClasses[kk], nrow)
    }
    attr(df, "row.names") <- seq(length = nrow)
    class(df) <- "data.frame"
    return(df)
}

############################

#desc.stat.3()
#Computes the n [length()], mean(),
#and standard deviation [sd()=sqrt(variance)]
#removes NAs before calculations

#Arguments description
#x: numerical vector

desc.stat.3 <- function(x) {
    y <- x[!is.na(x)]
    n_test <- length(y)
    mean_test <- mean(y)
    sd_test <- sd(y)
    return(c(n_test, mean_test, sd_test))
}
desc.stat.3.names <- c("n", "Mean", "SD")

############################

#boxvert()
#Boxplots, with vertical boxes

#Arguments description
#dat: data.frame, data object to use
#x: integer, index column of the categorical variable
#y: integer, index column of the numerical variable
#nt: character scalar, title of the boxplot
#yr: numerical vector of length 2, range of the y-axis. For automatic range, set as
NULL
```

```
boxvert <- function(dat, x, y, nt, yr) {
    boxplot(dat[[y]]~dat[[x]], main=nt, xlab=names(dat)[x], ylab=names(dat)[y],
        ylim=yr, las=1, horizontal=FALSE, cex.axis=0.8)
}

############################

#two_reg()
#Regression lines

#Arguments description
#dat: data.frame, data object where the values come from
#xvar: integer, index of the x-variable
#yvar: integer, index of the y-variable
#col1: character scalar, color for the TSTS line (default="red")
#col2: character scalar, color for the MGV line (default="green")
#name.dat: character scalar, name of the data object used to plot (default="dat")

two_reg <- function(dat,xvar,yvar,col1="red",col2="green", name.dat=
            deparse(substitute(dat))){
    # compute 2 regressions (tstsreg() and mgvreg()) and correlation (pbcor() and
            corb())
    tsts <- tstsreg(dat[[xvar]],dat[[yvar]])
    tsts_inter <- signif(tsts$coef[1], digits=3)
    tsts_slope <- signif(tsts$coef[2], digits=3)
    mgv <- mgvreg(as.matrix(dat[[xvar]]), as.matrix(dat[[yvar]]))
    mgv_inter <- signif(mgv$coef[1], digits=3)
    mgv_slope <- signif(mgv$coef[2], digits=3)
    corb_out <- corb(dat[[xvar]], dat[[yvar]], corfun=pbcor, nboot=2000)
    corb_out_cor <- round(corb_out$cor.est, digits=3)
    corb_out_p <- round(corb_out$p.value,digits=3)
    corb_out_ci <- paste(round(corb_out$cor.ci, digits=3), collapse=",")
    #plot them
    abline(tsts$coef, lty="longdash", col=col1)
    abline(mgv$coef, lty="dotted", col=col2)
    legend(x="topleft", legend=c(paste("TSTS ", name.dat, ": Y=", tsts_inter, "+", tsts_
            slope, "X", sep=""),paste("MGV ", name.dat, ": Y=", mgv_inter, "+", mgv_slope,
            "X", sep="")), lty=c("longdash","dotted"), col=c(col1,col2))
    text(x=max(range(dat[[xvar]])), pos=2, offset=5, y=max(range(dat[[yvar]])),
            labels=paste(name.dat,": rpb=",corb_out_cor,"  p=",corb_out_p,"  0.95CI=[",
            corb_out_ci, "]", sep=""))
}
```

Appendix 3.1. Analytical statistics on ungulates: results from Dunnett test with 15% trimming for the primary (A), the S-F (B), and the S-L (C) surfaces for a given pair of species.

		Primary surface (A)						S-F surface (B)						S-L surface (C)					
	Stat	cotau dibic	cotau eqgre	cotau gicam	dibic eqgre	dibic gicam	eqgre gicam	cotau dibic	cotau eqgre	cotau gicam	dibic eqgre	dibic gicam	eqgre gicam	cotau dibic	cotau eqgre	cotau gicam	dibic eqgre	dibic gicam	eqgre gicam
Sa	Test	**3.552**	2.068	**3.419**	**2.578**	0.148	2.508	**3.876**	2.401	**4.619**	**2.489**	0.690	3.261	1.892	0.516	**2.492**	**2.828**	0.738	**3.412**
	p	**0.006**	0.080	**0.015**	**0.035**	0.886	0.057	**0.006**	0.048	**0.007**	**0.037**	0.507	0.020	0.089	0.623	**0.038**	**0.019**	0.480	**0.014**
	df	**9.011**	6.565	**5.861**	**7.294**	9.056	4.711	**7.029**	6.883	**4.639**	**8.226**	9.391	5.458	9.570	6.478	**7.866**	**9.251**	8.936	**5.994**
Sda	Test	1.567	0.468	1.857	1.275	1.895	1.870	0.760	1.382	1.527	0.756	1.422	1.527	1.959	**9.759**	1.916	**9.747**	1.915	0.900
	p	0.171	0.653	0.122	0.244	0.117	0.120	0.476	0.204	0.201	0.478	0.226	0.201	0.091	**0.001**	0.128	**0.001**	0.128	0.418
	df	5.681	7.481	5.005	6.799	5.001	5.003	6.000	7.997	4.000	6.000	4.123	4.000	7.059	**4.000**	4.000	**4.000**	4.000	4.086
Sdv	Test	0.448	1.122	1.786	1.443	1.787	1.782	0.742	0.369	**3.837**	0.742	**3.079**	**3.837**	1.847	**4.610**	**2.992**	**4.610**	**2.992**	0.517
	p	0.664	0.294	0.134	0.186	0.134	0.135	0.486	0.723	**0.019**	0.486	**0.021**	**0.019**	0.100	**0.010**	**0.040**	**0.010**	**0.040**	0.620
	df	9.999	8.111	5.000	8.148	5.000	5.000	6.000	7.227	**4.000**	6.000	**6.086**	**4.000**	8.432	**4.000**	**4.000**	**4.000**	**4.000**	7.601
Sha	Test	0.349	0.964	0.973	1.897	0.996	0.900	0.767	0.233	2.819	0.766	2.525	2.819	**2.811**	**4.263**	2.657	**4.241**	2.652	1.617
	p	0.740	0.359	0.402	0.112	0.393	0.434	0.472	0.821	0.048	0.473	0.057	0.048	**0.021**	**0.013**	0.057	**0.013**	0.057	0.174
	df	5.298	9.667	3.021	5.434	3.001	3.014	6.000	7.822	4.000	6.000	4.579	4.000	**8.500**	**4.000**	4.000	**4.000**	4.000	4.436
Shv	Test	0.396	0.786	1.537	1.071	1.552	1.518	0.742	0.058	**5.739**	0.742	**5.238**	**5.739**	0.975	**5.675**	**3.961**	**5.675**	**3.961**	0.339
	p	0.701	0.460	0.199	0.327	0.196	0.204	0.486	0.955	**0.005**	0.486	**0.004**	**0.005**	0.352	**0.005**	**0.017**	**0.005**	**0.017**	0.745
	df	9.197	6.427	4.004	5.787	4.008	4.001	6.000	7.719	**4.000**	6.000	**4.832**	**4.000**	9.942	**4.000**	**4.000**	**4.000**	**4.000**	6.726
Smc	Test	2.305	1.351	0.945	1.706	1.329	1.068	**3.848**	0.688	**4.061**	**3.082**	0.512	**3.374**	1.479	0.883	2.198	2.395	0.882	2.986
	p	0.053	0.212	0.398	0.139	0.252	0.345	**0.004**	0.512	**0.007**	**0.012**	0.621	**0.012**	0.170	0.405	0.065	0.039	0.403	0.025
	df	7.330	8.339	4.047	5.938	4.190	4.018	**9.284**	7.672	**6.022**	**9.908**	8.933	**6.821**	9.998	7.530	6.850	9.537	8.302	5.890
Spd	Test	0.433	0.992	0.939	0.832	0.746	0.085	**3.128**	1.425	**2.532**	**3.088**	0.039	1.816	**3.277**	1.500	**2.708**	2.313	0.133	1.666
	p	0.677	0.357	0.382	0.427	0.481	0.935	**0.028**	0.207	**0.036**	**0.017**	0.970	0.118	**0.023**	0.178	**0.027**	0.060	0.899	0.137
	df	7.859	6.527	6.410	8.991	6.829	5.443	**4.741**	5.620	**7.761**	**7.307**	5.057	6.211	**4.821**	6.815	**7.808**	5.977	5.127	7.425
Sq	Test	**3.014**	1.593	**3.200**	**2.406**	0.364	2.641	**3.911**	2.566	**4.647**	**1.914**	0.844	**2.754**	1.728	0.149	2.415	1.793	0.662	2.561
	p	**0.014**	0.168	**0.018**	**0.048**	0.724	0.052	**0.007**	0.057	**0.009**	**0.086**	0.420	**0.031**	0.115	0.886	0.042	0.104	0.524	0.037
	df	**9.324**	5.322	**6.158**	**6.732**	9.083	4.398	**6.241**	4.395	**4.130**	**9.519**	9.108	**6.378**	9.866	7.411	7.938	9.743	9.590	7.076
Ssk	Test	**2.449**	**3.099**	1.444	**2.720**	1.780	2.158	1.339	0.296	0.883	1.450	1.077	1.452	2.633	0.458	0.804	2.232	1.096	0.566
	p	**0.050**	**0.014**	0.218	**0.034**	0.115	0.094	0.224	0.776	0.404	0.195	0.320	0.186	0.033	0.661	0.461	0.054	0.303	0.594
	df	**6.051**	**8.538**	4.240	**6.040**	7.596	4.189	6.741	6.830	7.582	6.312	6.464	7.697	7.189	6.839	4.541	8.558	8.529	5.271
Std	Test	**5.545**	0.426	**3.535**	**5.281**	0.001	**3.391**	2.080	0.018	1.624	1.983	0.091	1.587	2.080	0.018	1.624	1.984	0.091	1.587
	p	**0.003**	0.681	**0.015**	**0.003**	0.999	**0.017**	0.072	0.986	0.146	0.086	0.931	0.152	0.072	0.986	0.146	0.086	0.931	0.152
	df	**4.854**	8.558	**5.407**	**5.054**	8.079	**5.508**	7.762	7.942	7.450	7.272	6.311	7.719	7.763	7.942	7.450	7.272	6.311	7.719
Sv	Test	**3.859**	0.375	1.583	**6.038**	0.639	1.559	1.930	1.146	2.301	0.744	0.508	1.191	2.744	1.113	1.309	2.144	0.647	0.648
	p	**0.008**	0.723	0.162	**2.5E-04**	0.552	0.188	0.084	0.285	0.051	0.475	0.624	0.268	0.024	0.304	0.233	0.058	0.541	0.544
	df	**6.324**	5.078	6.316	**8.403**	4.774	4.350	9.527	7.992	7.891	9.392	8.948	7.940	8.473	6.790	6.876	9.993	6.179	5.339

Appendix 3.1. (continued)

		Primary surface (A)						S-F surface (B)						S-L surface (C)					
	Stat	cotau dibic	cotau eqgre	cotau gicam	dibic eqgre	dibic gicam	eqgre gicam	cotau dibic	cotau eqgre	cotau gicam	dibic eqgre	dibic gicam	eqgre gicam	cotau dibic	cotau eqgre	cotau gicam	dibic eqgre	dibic gicam	eqgre gicam
Sxp	Test	**4.933**	1.086	**3.389**	**4.767**	0.262	**2.876**	**3.080**	2.346	**4.024**	1.858	0.810	**2.879**	1.988	0.082	2.316	3.216	0.586	3.496
	p	**0.001**	0.313	**0.011**	**0.001**	0.802	**0.028**	**0.014**	0.050	**0.007**	0.103	0.438	**0.035**	0.091	0.937	0.054	0.009	0.573	0.011
	df	**7.626**	7.132	**7.446**	**9.609**	6.207	**6.051**	**8.734**	7.177	**5.931**	7.515	9.492	**5.001**	6.396	5.226	6.910	9.860	8.718	6.570
Vmc	Test	**7.421**	1.984	**3.485**	**6.700**	0.751	2.443	**3.302**	1.618	**5.050**	**2.281**	0.969	**3.801**	1.491	1.010	2.097	2.634	0.858	2.982
	p	**2.4E-04**	0.086	**0.012**	**1.9E-04**	0.488	0.056	**0.012**	0.148	**0.004**	**0.050**	0.356	**0.008**	0.167	0.347	0.076	0.028	0.416	0.030
	df	**6.332**	7.224	**6.289**	**7.621**	4.801	5.242	**7.332**	7.204	**5.171**	**8.434**	9.940	**6.194**	9.975	6.699	6.644	8.842	7.783	5.148
Vv	Test	**6.635**	1.361	**3.948**	**6.532**	0.483	**3.271**	**3.954**	0.994	**4.171**	**3.046**	0.508	**3.352**	1.550	0.824	2.275	2.554	0.852	3.210
	p	**4.1E-04**	0.214	**0.004**	**2.1E-04**	0.645	**0.013**	**0.003**	0.350	**0.006**	**0.013**	0.624	**0.014**	0.153	0.437	0.055	0.030	0.417	0.019
	df	**6.465**	7.222	**8.497**	**7.723**	6.562	**7.186**	**8.984**	7.745	**5.791**	**9.656**	8.975	**6.445**	9.891	7.014	7.444	9.363	8.686	5.944
Vvc	Test	**6.033**	1.393	2.223	**6.815**	2.034	1.456	**4.054**	0.997	**4.429**	**3.225**	0.559	**3.654**	1.439	0.874	2.259	2.357	0.942	3.086
	p	**0.001**	0.210	0.060	**1.6E-04**	0.098	0.201	**0.003**	0.348	**0.004**	**0.010**	0.590	**0.009**	0.181	0.409	0.058	0.041	0.372	0.021
	df	**5.738**	6.366	7.345	**7.755**	4.973	5.372	**9.342**	7.957	**6.227**	**9.599**	9.157	**6.508**	9.983	7.584	7.105	9.675	8.527	6.174
Vvv	Test	**5.074**	0.583	1.991	**5.615**	1.900	1.698	**2.893**	2.141	**3.233**	**1.952**	0.533	2.402	2.178	0.410	2.136	3.017	0.199	2.626
	p	**0.003**	0.577	0.083	**0.001**	0.114	0.136	**0.022**	0.065	**0.025**	**0.091**	0.607	0.066	0.069	0.698	0.068	0.013	0.847	0.040
	df	**5.731**	7.335	7.722	**7.089**	5.185	6.582	**7.446**	7.897	**4.768**	**7.167**	8.945	4.612	6.477	5.182	7.468	9.773	7.952	5.956
FLTp	Test	0.720	1.515	3.403	0.162	1.321	2.524	**3.014**	1.119	**3.617**	**2.499**	0.533	**3.152**	1.551	1.361	2.866	2.726	1.165	4.032
	p	0.495	0.168	0.017	0.876	0.218	0.048	**0.014**	0.300	**0.010**	**0.038**	0.607	**0.024**	0.152	0.211	0.022	0.021	0.272	0.004
	df	6.790	7.963	5.343	6.902	9.440	5.526	**9.284**	7.079	**6.470**	**7.857**	9.527	**5.266**	9.994	7.981	7.694	9.994	9.692	7.820
FLTq	Test	**3.474**	2.081	**3.295**	**2.515**	0.101	2.395	**2.864**	0.668	**3.689**	**2.674**	0.751	**3.618**	1.867	1.253	2.362	2.395	0.900	2.785
	p	**0.007**	0.079	**0.017**	**0.039**	0.922	0.066	**0.017**	0.526	**0.006**	**0.025**	0.471	**0.010**	0.102	0.262	0.071	0.038	0.396	0.030
	df	**8.910**	6.467	**5.787**	**7.177**	9.069	4.647	**9.987**	6.979	**7.811**	**9.066**	9.634	**6.359**	7.432	5.408	4.462	9.996	7.466	6.312
FLTt	Test	2.677	1.150	2.390	2.296	0.324	1.978	**2.978**	1.131	**3.846**	**2.781**	0.771	**3.834**	1.571	1.199	2.747	2.667	1.138	3.819
	p	0.023	0.298	0.052	0.053	0.755	0.111	**0.014**	0.314	**0.006**	**0.030**	0.459	**0.016**	0.147	0.265	0.027	0.024	0.284	0.006
	df	9.993	5.452	6.318	7.494	7.436	4.478	**9.895**	4.566	**7.316**	**6.454**	9.579	**4.302**	9.999	7.974	7.454	9.962	9.306	7.246
FLTv	Test	**3.949**	0.582	2.131	**4.506**	0.443	1.931	**2.572**	0.856	3.844	**2.409**	1.031	3.999	1.554	0.715	2.452	2.582	1.065	3.484
	p	**0.006**	0.579	0.071	**0.001**	0.676	0.107	**0.028**	0.428	0.005	**0.045**	0.327	0.010	0.154	0.497	0.040	0.027	0.315	0.010
	df	**6.499**	6.807	6.993	**8.989**	5.150	5.426	**9.990**	5.415	7.803	**7.305**	9.840	5.043	9.068	7.289	7.985	10.000	8.831	7.124
mev	Test	2.130	2.301	0.541	0.317	1.313	1.302	2.674	2.571	0.646	0.691	0.631	0.377	**5.188**	0.525	2.339	**3.919**	0.707	**2.345**
	p	0.062	0.063	0.603	0.761	0.231	0.257	0.024	0.040	0.547	0.507	0.555	0.724	**0.001**	0.617	0.057	**0.010**	0.510	**0.047**
	df	9.081	5.697	8.421	6.314	6.846	4.418	9.550	6.397	5.025	9.190	5.027	4.346	**7.874**	6.330	6.091	**5.369**	5.203	**7.967**
medf	Test	1.495	2.006	**2.436**	**2.913**	0.413	**3.711**	0.030	**3.051**	0.550	**3.081**	0.512	**4.123**	0.147	**3.829**	0.525	**3.445**	0.642	**4.839**
	p	0.172	0.089	**0.041**	**0.018**	0.690	**0.009**	0.976	**0.017**	0.604	**0.014**	0.622	**0.009**	0.886	**0.005**	0.616	**0.007**	0.537	**0.002**
	df	8.284	6.352	**7.992**	**8.486**	8.400	**6.473**	9.589	**7.640**	5.627	**8.449**	8.272	**5.074**	9.968	**7.810**	6.987	**9.553**	9.155	**6.366**

Appendix 3.1. (continued)

		Primary surface (A)						S-F surface (B)						S-L surface (C)					
	Stat	cotau dibic	cotau eqgre	cotau gicam	dibic eqgre	dibic gicam	eqgre gicam	cotau dibic	cotau eqgre	cotau gicam	dibic eqgre	dibic gicam	eqgre gicam	cotau dibic	cotau eqgre	cotau gicam	dibic eqgre	dibic gicam	eqgre gicam
metf	Test	1.335	0.810	1.446	2.349	0.217	2.341	1.947	0.128	**2.416**	**2.696**	0.595	**3.218**	1.538	0.616	2.195	2.688	0.819	3.397
	p	0.215	0.446	0.188	0.048	0.834	0.060	0.084	0.902	**0.042**	**0.023**	0.566	**0.016**	0.161	0.558	0.060	0.023	0.434	0.011
	df	8.993	6.543	7.595	7.621	8.415	5.707	8.717	6.142	**7.941**	**9.544**	9.190	**6.467**	8.421	6.573	7.903	9.949	9.055	7.016
IsT	Test	**2.803**	0.755	1.466	**3.866**	0.384	1.972	**4.830**	0.078	**3.261**	**3.688**	0.541	**2.708**	**4.233**	0.040	**2.478**	**4.956**	0.346	**2.617**
	p	**0.019**	0.473	0.194	**0.003**	0.714	0.106	**0.001**	0.941	**0.024**	**0.005**	0.602	**0.028**	**0.004**	0.969	**0.043**	**0.001**	0.742	**0.040**
	df	**9.929**	7.530	5.824	**9.865**	6.416	4.977	**7.838**	5.218	**4.820**	**9.466**	8.368	**7.687**	**7.177**	7.522	**6.966**	**8.685**	5.481	**5.981**
Tr	Test	0.228	0.019	3.020	0.234	2.954	2.864	0.757	0.724	0.883	0.014	1.753	1.665	3.002	0.169	2.349	3.649	0.137	2.519
	p	0.824	0.985	0.015	0.819	0.013	0.019	0.472	0.490	0.403	0.989	0.120	0.136	0.017	0.871	0.049	0.004	0.895	0.048
	df	9.997	7.891	8.810	9.898	10.802	8.990	7.740	7.757	7.992	8.800	7.552	7.668	7.904	6.738	7.403	9.972	6.357	5.684
Tr1R	Test	**4.159**	0.426	**3.535**	**3.942**	0.485	**3.391**	2.080	0.018	1.624	1.983	0.091	1.587	**2.080**	0.018	**1.624**	**1.984**	0.091	**1.587**
	p	**0.004**	0.681	**0.015**	**0.005**	0.639	**0.017**	0.072	0.986	0.146	0.086	0.931	0.152	**0.072**	0.986	**0.146**	**0.086**	0.931	**0.152**
	df	**6.992**	8.558	**5.407**	**7.216**	9.217	**5.508**	7.762	7.942	7.450	7.272	6.311	7.719	**7.763**	7.942	**7.450**	**7.272**	6.311	**7.719**

Values in bold indicate a significant difference ($p \leq 0.05$).
df = degree of freedom, p = significance level, Test = test statistics. Species abbreviations as in Table 3.1. From Schulz *et al.* (submitted, appendix 2).

Appendix 3.2. Analytical statistics on ungulates: results from Cliff tests for the primary (A), the S-F (B), and the S-L (C) surfaces.

		Primary surface (A)						S-F surface (B)						S-L surface (C)					
	Stat	cotau dibic	cotau eqgre	cotau gicam	dibic eqgre	dibic gicam	eqgre gicam	cotau dibic	cotau eqgre	cotau gicam	dibic eqgre	dibic gicam	eqgre gicam	cotau dibic	cotau eqgre	cotau gicam	dibic eqgre	dibic gicam	eqgre gicam
Sa	ph	0.175	0.245	**0.102**	0.778	0.444	0.184	0.127	0.184	**0**	0.794	0.381	0.000	0.238	0.592	**0.143**	0.857	0.365	0.082
	pl	0.044	0.069	**0.020**	0.436	0.188	0.040	0.028	0.043	**0**	0.461	0.153	0.000	0.078	0.282	**0.032**	0.573	0.138	0.014
	pu	0.494	0.588	**0.386**	0.941	0.734	0.548	0.426	0.527	**0.348**	0.945	0.677	0.348	0.534	0.843	**0.455**	0.964	0.674	0.354
	p	0.046	0.160	**0.008**	0.120	0.750	0.091	0.016	0.072	**0.008**	0.085	0.470	0.008	0.084	0.610	**0.026**	0.015	0.430	0.004
	pc	0.010	0.025	**0.008**	0.017	0.050	0.013	0.013	0.017	**0.010**	0.025	0.050	0.008	0.017	0.050	**0.013**	0.010	0.025	0.008
Sda	ph	0.333	0.469	0.571	0.683	0.741	0.571	0.889	0.735	1.000	0.206	0.889	1.000	0.825	1.000	1.000	1.000	1.000	0.633
	pl	0.119	0.197	0.253	0.386	0.432	0.253	0.627	0.393	0.652	0.062	0.611	0.652	0.542	0.652	0.652	0.717	0.717	0.313
	pu	0.650	0.762	0.840	0.880	0.915	0.840	0.974	0.922	1.000	0.506	0.976	1.000	0.950	1.000	1.000	1.000	1.000	0.867
	p	0.330	0.870	0.710	0.250	0.130	0.710	0.005	0.190	0.008	0.055	0.008	0.008	0.025	0.008	0.008	0.002	0.002	0.460
	pc	0.013	0.050	0.025	0.010	0.008	0.017	0.008	0.050	0.017	0.025	0.013	0.010	0.025	0.017	0.013	0.010	0.008	0.050
Sdv	ph	0.375	0.611	0.583	0.729	0.604	0.500	0.810	0.633	1.000	0.302	0.921	1.000	0.746	1.000	1.000	1.000	1.000	0.388
	pl	0.138	0.280	0.238	0.398	0.265	0.173	0.508	0.293	0.652	0.102	0.679	0.652	0.441	0.652	0.652	0.717	0.717	0.145
	pu	0.693	0.864	0.863	0.916	0.866	0.827	0.946	0.878	1.000	0.622	0.984	1.000	0.916	1.000	1.000	1.000	1.000	0.703
	p	0.480	0.560	0.690	0.190	0.600	0.990	0.045	0.490	0.008	0.240	0.002	0.008	0.120	0.008	0.008	0.002	0.002	0.530
	pc	0.010	0.013	0.025	0.008	0.017	0.050	0.017	0.050	0.013	0.025	0.008	0.010	0.025	0.017	0.013	0.010	0.008	0.050
Sha	ph	0.542	0.694	0.625	0.771	0.563	0.417	0.905	0.551	1.000	0.143	0.889	1.000	0.905	1.000	1.000	1.000	1.000	0.816
	pl	0.218	0.328	0.261	0.415	0.213	0.115	0.646	0.248	0.652	0.036	0.620	0.652	0.656	0.652	0.652	0.717	0.717	0.505
	pu	0.834	0.914	0.887	0.941	0.859	0.796	0.980	0.820	1.000	0.425	0.975	1.000	0.979	1.000	1.000	1.000	1.000	0.951
	p	0.840	0.330	0.560	0.150	0.780	0.730	0.004	0.780	0.008	0.015	0.006	0.008	0.003	0.008	0.008	0.002	0.002	0.047
	pc	0.050	0.010	0.013	0.008	0.025	0.017	0.008	0.050	0.017	0.025	0.010	0.013	0.013	0.025	0.017	0.010	0.008	0.050
Shv	ph	0.438	0.611	0.567	0.604	0.525	0.567	0.667	0.510	1.000	0.317	0.984	1.000	0.651	1.000	1.000	1.000	1.000	0.531
	pl	0.180	0.265	0.198	0.282	0.181	0.198	0.370	0.226	0.652	0.116	0.829	0.652	0.349	0.652	0.652	0.717	0.717	0.241
	pu	0.733	0.873	0.874	0.856	0.847	0.874	0.872	0.788	1.000	0.623	0.999	1.000	0.867	1.000	1.000	1.000	1.000	0.801
	p	0.720	0.580	0.780	0.570	0.920	0.780	0.290	0.960	0.008	0.260	0.000	0.008	0.360	0.008	0.008	0.002	0.002	0.860
	pc	0.013	0.010	0.025	0.008	0.050	0.017	0.025	0.050	0.013	0.017	0.008	0.010	0.025	0.017	0.013	0.010	0.008	0.050
Smc	ph	0.188	0.306	0.595	0.750	0.696	0.595	0.127	0.367	0.020	0.857	0.429	0.041	0.317	0.633	0.245	0.778	0.381	0.163
	pl	0.047	0.091	0.259	0.392	0.348	0.259	0.025	0.137	0.002	0.538	0.180	0.005	0.114	0.313	0.063	0.481	0.150	0.036
	pu	0.520	0.658	0.861	0.933	0.908	0.861	0.454	0.680	0.210	0.969	0.719	0.277	0.626	0.867	0.608	0.930	0.682	0.508
	p	0.066	0.310	0.630	0.190	0.300	0.630	0.026	0.440	0.000	0.029	0.670	0.001	0.270	0.460	0.180	0.067	0.480	0.056
	pc	0.008	0.017	0.050	0.010	0.013	0.025	0.013	0.025	0.008	0.017	0.050	0.010	0.017	0.025	0.013	0.010	0.050	0.008
Spd	ph	0.563	0.444	0.556	0.313	0.333	0.500	0.063	0.286	0.143	0.841	0.444	0.265	0.063	0.204	0.082	0.825	0.460	0.224
	pl	0.227	0.157	0.213	0.106	0.073	0.155	0.011	0.086	0.034	0.542	0.172	0.080	0.011	0.056	0.014	0.527	0.183	0.066
	pu	0.849	0.774	0.853	0.637	0.759	0.845	0.294	0.629	0.444	0.960	0.755	0.602	0.294	0.524	0.354	0.953	0.765	0.542
	p	0.770	0.790	0.800	0.280	0.520	0.990	0.001	0.240	0.021	0.027	0.770	0.190	0.001	0.070	0.004	0.033	0.830	0.090
	pc	0.013	0.017	0.025	0.008	0.010	0.050	0.008	0.025	0.010	0.013	0.050	0.017	0.008	0.017	0.010	0.013	0.050	0.025
Sq	ph	0.159	0.286	**0.102**	0.778	0.429	0.184	0.127	0.245	**0.020**	0.778	0.349	0.041	0.254	0.490	**0.143**	0.730	0.317	0.102
	pl	0.039	0.088	**0.020**	0.436	0.175	0.040	0.028	0.063	**0.002**	0.475	0.131	0.005	0.083	0.210	**0.034**	0.431	0.113	0.020
	pu	0.464	0.624	**0.386**	0.941	0.726	0.548	0.426	0.608	**0.210**	0.931	0.657	0.277	0.561	0.776	**0.444**	0.906	0.628	0.386
	p	0.030	0.230	**0.008**	0.120	0.680	0.091	0.016	0.180	**1.0E-04**	0.073	0.370	0.001	0.120	0.960	**0.021**	0.140	0.270	0.008
	pc	0.010	0.025	**0.008**	0.017	0.050	0.013	0.013	0.025	**0.008**	0.017	0.050	0.010	0.013	0.050	**0.010**	0.017	0.025	0.008
Ssk	ph	**0.952**	**0.071**	0.673	**0**	0.270	**0.929**	**0.683**	**0.531**	0.653	**0.365**	0.492	**0.673**	**0.873**	**0.510**	0.633	**0.206**	0.270	**0.571**
	pl	**0.745**	**0.010**	0.322	**0**	0.094	**0.655**	**0.372**	**0.225**	0.334	**0.147**	0.227	**0.353**	**0.603**	**0.221**	0.317	**0.063**	0.089	**0.267**
	pu	**0.993**	**0.379**	0.900	**0.283**	0.567	**0.989**	**0.887**	**0.815**	0.876	**0.658**	0.762	**0.886**	**0.969**	**0.793**	0.865	**0.501**	0.584	**0.830**
	p	**2.0E-04**	**0.009**	0.370	**0.002**	0.140	**0.004**	**0.270**	**0.870**	0.380	**0.400**	0.970	**0.320**	**0.009**	**0.960**	0.450	**0.051**	0.160	**0.690**
	pc	**0.008**	**0.017**	0.050	**0.010**	0.025	**0.013**	**0.008**	**0.025**	0.013	**0.017**	0.050	**0.010**	**0.008**	**0.050**	0.017	**0.010**	0.013	**0.025**

Appendix 3.2. (continued)

		Primary surface (A)						S-F surface (B)						S-L surface (C)					
	Stat	cotau dibic	cotau eqgre	cotau gicam	dibic eqgre	dibic gicam	eqgre gicam	cotau dibic	cotau eqgre	cotau gicam	dibic eqgre	dibic gicam	eqgre gicam	cotau dibic	cotau eqgre	cotau gicam	dibic eqgre	dibic gicam	eqgre gicam
Std	ph	**1.000**	0.667	**0.972**	**0**	0.429	**0.967**	**0.873**	0.531	**0.796**	**0.206**	0.524	**0.755**	**0.873**	0.531	**0.796**	**0.206**	0.524	**0.755**
	pl	**0.652**	0.307	**0.733**	**0**	0.154	**0.695**	**0.584**	0.235	**0.476**	**0.050**	0.235	**0.412**	**0.584**	0.235	**0.476**	**0.050**	0.235	**0.412**
	pu	**1.000**	0.900	**0.998**	**0.348**	0.756	**0.997**	**0.971**	0.806	**0.944**	**0.564**	0.798	**0.931**	**0.971**	0.806	**0.944**	**0.564**	0.798	**0.931**
	p	**0.008**	0.410	**0.001**	**0.008**	0.720	**0.002**	**0.013**	0.870	**0.070**	**0.120**	0.900	**0.160**	**0.013**	0.870	**0.070**	**0.120**	0.900	**0.160**
	pc	**0.017**	0.025	**0.008**	**0.013**	0.050	**0.010**	**0.008**	0.025	**0.010**	**0.013**	0.050	**0.017**	**0.008**	0.025	**0.010**	**0.013**	0.050	**0.017**
Sv	ph	**0.071**	0.388	0.245	**0.982**	0.518	0.306	**0.238**	0.265	0.204	**0.683**	0.429	0.347	**0.175**	0.347	0.245	**0.778**	0.540	0.408
	pl	**0.012**	0.137	0.075	**0.811**	0.211	0.088	**0.075**	0.083	0.050	**0.381**	0.180	0.122	**0.050**	0.124	0.075	**0.483**	0.247	0.155
	pu	**0.322**	0.716	0.565	**0.999**	0.812	0.668	**0.548**	0.591	0.558	**0.883**	0.719	0.670	**0.458**	0.666	0.565	**0.929**	0.807	0.722
	p	**0.002**	0.550	0.130	**1.0E-04**	0.930	0.330	**0.100**	0.170	0.110	**0.250**	0.670	0.390	**0.025**	0.380	0.130	**0.066**	0.820	0.610
	pc	**0.010**	0.025	0.013	**0.008**	0.050	0.017	**0.008**	0.013	0.010	**0.017**	0.050	0.025	**0.008**	0.017	0.013	**0.010**	0.050	0.025
Sxp	ph	**0.079**	0.327	**0.102**	**0.937**	0.524	0.184	**0.175**	0.245	**0.041**	**0.778**	0.349	0.102	**0.206**	0.429	**0.122**	**0.873**	0.365	0.122
	pl	**0.015**	0.107	**0.020**	**0.674**	0.231	0.040	**0.045**	0.067	**0.005**	**0.436**	0.133	0.019	**0.063**	0.164	**0.026**	**0.588**	0.138	0.026
	pu	**0.322**	0.663	**0.386**	**0.991**	0.801	0.548	**0.489**	0.593	**0.277**	**0.941**	0.652	0.402	**0.503**	0.742	**0.425**	**0.971**	0.674	0.425
	p	**0.002**	0.350	**0.008**	**0.003**	0.900	0.091	**0.043**	0.160	**0.001**	**0.120**	0.360	0.011	**0.053**	0.700	**0.016**	**0.012**	0.430	0.016
	pc	**0.008**	0.025	**0.013**	**0.010**	0.050	0.017	**0.013**	0.025	**0.008**	**0.017**	0.050	0.010	**0.017**	0.050	**0.013**	**0.008**	0.025	0.010
Vmc	ph	**0**	0.245	**0.102**	**1.000**	0.592	0.163	**0.175**	0.245	**0**	**0.794**	0.333	0.020	**0.317**	0.673	**0.224**	**0.857**	0.365	0.163
	pl	**0**	0.069	**0.019**	**0.652**	0.266	0.036	**0.045**	0.075	**0**	**0.461**	0.124	0.002	**0.114**	0.345	**0.057**	**0.573**	0.136	0.036
	pu	**0.348**	0.588	**0.402**	**1.000**	0.853	0.508	**0.489**	0.565	**0.348**	**0.945**	0.639	0.210	**0.626**	0.890	**0.579**	**0.964**	0.677	0.508
	p	**0.008**	0.160	**0.011**	**0.008**	0.630	0.056	**0.043**	0.130	**0.008**	**0.085**	0.310	0.000	**0.270**	0.330	**0.140**	**0.015**	0.430	0.056
	pc	**0.010**	0.025	**0.013**	**0.008**	0.050	0.017	**0.013**	0.025	**0.010**	**0.017**	0.050	0.008	**0.017**	0.025	**0.013**	**0.008**	0.050	0.010
Vv	ph	**0**	0.286	**0.048**	**1.000**	0.500	0.119	**0.143**	0.347	**0.020**	**0.857**	0.429	0.041	**0.317**	0.633	**0.184**	**0.825**	0.349	0.143
	pl	**0**	0.093	**0.006**	**0.652**	0.184	0.022	**0.031**	0.124	**0.002**	**0.538**	0.180	0.005	**0.114**	0.313	**0.045**	**0.535**	0.128	0.031
	pu	**0.348**	0.610	**0.309**	**1.000**	0.816	0.448	**0.462**	0.666	**0.210**	**0.969**	0.719	0.277	**0.626**	0.867	**0.520**	**0.951**	0.663	0.466
	p	**0.008**	0.210	**0.002**	**0.008**	0.990	0.024	**0.029**	0.380	**1.0E-04**	**0.029**	0.670	0.001	**0.270**	0.460	**0.066**	**0.029**	0.380	0.031
	pc	**0.013**	0.025	**0.008**	**0.010**	0.050	0.017	**0.017**	0.025	**0.008**	**0.013**	0.050	0.010	**0.017**	0.050	**0.013**	**0.008**	0.025	0.010
Vvc	ph	**0**	0.306	0.143	**1.000**	0.800	0.286	**0.127**	0.327	0.000	**0.857**	0.413	0.041	**0.317**	0.612	0.204	**0.810**	0.349	0.163
	pl	**0**	0.102	0.029	**0.652**	0.387	0.079	**0.025**	0.114	0.000	**0.538**	0.171	0.005	**0.114**	0.297	0.051	**0.521**	0.130	0.036
	pu	**0.348**	0.631	0.483	**1.000**	0.962	0.651	**0.454**	0.647	0.348	**0.969**	0.705	0.277	**0.626**	0.855	0.552	**0.943**	0.658	0.508
	p	**0.008**	0.260	0.040	**0.008**	0.170	0.280	**0.026**	0.320	0.008	**0.029**	0.600	0.001	**0.270**	0.530	0.097	**0.036**	0.370	0.056
	pc	**0.010**	0.025	0.013	**0.008**	0.017	0.050	**0.013**	0.025	0.010	**0.017**	0.050	0.008	**0.017**	0.050	0.013	**0.008**	0.025	0.010
Vvv	ph	**0.063**	0.347	0.200	**0.968**	0.756	0.257	**0.190**	0.204	0.061	**0.778**	0.381	0.102	**0.206**	0.429	0.163	**0.857**	0.365	0.143
	pl	**0.011**	0.115	0.047	**0.773**	0.395	0.055	**0.049**	0.048	0.009	**0.436**	0.147	0.019	**0.063**	0.164	0.041	**0.556**	0.138	0.032
	pu	**0.293**	0.685	0.560	**0.996**	0.936	0.672	**0.516**	0.564	0.309	**0.941**	0.687	0.402	**0.503**	0.742	0.471	**0.966**	0.674	0.455
	p	**0.001**	0.410	0.110	**1.0E-04**	0.180	0.290	**0.063**	0.120	0.002	**0.120**	0.490	0.011	**0.053**	0.700	0.033	**0.021**	0.430	0.026
	pc	**0.010**	0.050	0.013	**0.008**	0.017	0.025	**0.013**	0.025	0.008	**0.017**	0.050	0.010	**0.017**	0.050	0.013	**0.008**	0.025	0.010
FLTp	ph	0.333	0.286	0.102	0.651	0.317	0.184	0.159	0.306	0.041	0.794	0.429	0.000	0.302	0.755	0.184	0.825	0.365	0.122
	pl	0.114	0.093	0.016	0.334	0.117	0.040	0.038	0.097	0.005	0.461	0.180	0.000	0.108	0.423	0.040	0.535	0.136	0.023
	pu	0.659	0.610	0.446	0.874	0.620	0.548	0.476	0.644	0.277	0.945	0.719	0.348	0.606	0.928	0.548	0.951	0.677	0.450
	p	0.350	0.210	0.025	0.380	0.260	0.091	0.035	0.290	0.001	0.085	0.670	0.008	0.220	0.140	0.091	0.029	0.430	0.025
	pc	0.025	0.013	0.008	0.050	0.017	0.010	0.013	0.025	0.008	0.017	0.050	0.010	0.025	0.017	0.013	0.010	0.050	0.008
FLTq	ph	0.159	0.224	**0.102**	0.778	0.444	0.184	0.175	0.408	**0.020**	0.810	0.365	0.020	0.317	0.714	**0.245**	0.857	0.317	0.143
	pl	0.039	0.063	**0.020**	0.436	0.188	0.045	0.044	0.159	**0.002**	0.485	0.144	0.002	0.115	0.381	**0.063**	0.573	0.109	0.031
	pu	0.464	0.555	**0.386**	0.941	0.734	0.520	0.494	0.715	**0.210**	0.950	0.663	0.210	0.625	0.910	**0.608**	0.964	0.639	0.466
	p	0.030	0.110	**0.008**	0.120	0.750	0.066	0.046	0.600	**1.0E-04**	0.062	0.410	0.000	0.260	0.230	**0.180**	0.015	0.290	0.031
	pc	0.010	0.017	**0.008**	0.025	0.050	0.013	0.013	0.050	**0.010**	0.017	0.025	0.008	0.025	0.017	**0.013**	0.008	0.050	0.010

Appendix 3.2. (continued)

		Primary surface (A)						S-F surface (B)						S-L surface (C)					
	Stat	cotau dibic	cotau eqgre	cotau gicam	dibic eqgre	dibic gicam	eqgre gicam	cotau dibic	cotau eqgre	cotau gicam	dibic eqgre	dibic gicam	eqgre gicam	cotau dibic	cotau eqgre	cotau gicam	dibic eqgre	dibic gicam	eqgre gicam
FLTt	ph	0.190	0.306	**0.143**	0.778	0.397	0.163	0.111	0.408	**0.061**	0.810	0.381	0.020	0.270	0.673	**0.184**	0.841	0.333	0.122
	pl	0.053	0.097	**0.034**	0.467	0.156	0.041	0.025	0.155	**0.009**	0.484	0.153	0.002	0.094	0.353	**0.040**	0.564	0.119	0.023
	pu	0.497	0.644	**0.444**	0.933	0.700	0.471	0.380	0.722	**0.309**	0.951	0.677	0.210	0.569	0.886	**0.548**	0.956	0.649	0.450
	p	0.048	0.290	**0.021**	0.081	0.550	0.033	0.006	0.610	**0.002**	0.063	0.470	0.000	0.140	0.320	**0.091**	0.017	0.330	0.025
	pc	0.013	0.025	**0.008**	0.017	0.050	0.010	0.013	0.050	**0.010**	0.017	0.025	0.008	0.017	0.025	**0.013**	0.008	0.050	0.010
FLTv	ph	0.127	0.388	0.163	0.873	0.508	0.184	0.159	0.429	0.102	0.810	0.333	0.122	0.254	0.612	0.163	0.762	0.317	0.143
	pl	0.028	0.143	0.041	0.546	0.215	0.048	0.039	0.170	0.019	0.484	0.124	0.020	0.086	0.297	0.036	0.463	0.113	0.027
	pu	0.426	0.707	0.471	0.975	0.795	0.504	0.464	0.733	0.402	0.951	0.639	0.494	0.552	0.855	0.508	0.922	0.630	0.496
	p	0.016	0.530	0.033	0.026	0.970	0.053	0.030	0.690	0.011	0.063	0.310	0.047	0.110	0.530	0.056	0.087	0.270	0.048
	pc	0.008	0.025	0.013	0.010	0.050	0.017	0.010	0.050	0.008	0.017	0.025	0.013	0.017	0.050	0.010	0.013	0.025	0.008
mev	ph	0.208	0.167	0.367	0.625	0.675	0.571	0.143	0.286	0.327	0.698	0.540	0.490	0.111	0.592	0.204	0.921	0.556	0.204
	pl	0.059	0.038	0.113	0.311	0.347	0.200	0.036	0.086	0.110	0.398	0.244	0.198	0.018	0.282	0.050	0.629	0.257	0.053
	pu	0.527	0.503	0.725	0.860	0.890	0.877	0.427	0.629	0.655	0.890	0.810	0.789	0.454	0.843	0.558	0.988	0.819	0.538
	p	0.074	0.052	0.520	0.470	0.320	0.770	0.015	0.240	0.330	0.210	0.830	0.960	0.027	0.610	0.110	0.007	0.760	0.084
	pc	0.010	0.008	0.025	0.017	0.013	0.050	0.008	0.013	0.017	0.010	0.025	0.050	0.010	0.025	0.017	0.008	0.050	0.013
medf	ph	0.714	0.224	0.714	**0.054**	0.536	0.857	0.476	0.102	0.531	**0.079**	0.587	0.857	0.460	0.061	0.531	**0.079**	0.540	0.878
	pl	0.395	0.066	0.359	**0.007**	0.247	0.462	0.209	0.020	0.235	**0.016**	0.290	0.462	0.205	0.008	0.238	**0.016**	0.260	0.506
	pu	0.906	0.542	0.918	**0.305**	0.802	0.977	0.757	0.386	0.806	**0.321**	0.832	0.977	0.739	0.338	0.803	**0.321**	0.796	0.980
	p	0.200	0.090	0.260	**0.002**	0.840	0.078	0.890	0.008	0.870	**0.002**	0.610	0.078	0.810	0.004	0.870	**0.002**	0.810	0.047
	pc	0.017	0.013	0.025	**0.008**	0.050	0.010	0.050	0.010	0.025	**0.008**	0.017	0.013	0.025	0.010	0.050	**0.008**	0.017	0.013
metf	ph	0.286	0.633	0.286	0.786	0.411	0.224	0.206	0.551	0.122	0.825	0.381	0.102	0.270	0.612	0.163	0.810	0.365	0.122
	pl	0.093	0.309	0.095	0.461	0.160	0.063	0.062	0.243	0.023	0.532	0.147	0.020	0.094	0.293	0.038	0.511	0.138	0.026
	pu	0.611	0.869	0.604	0.940	0.719	0.555	0.505	0.825	0.450	0.952	0.687	0.386	0.569	0.857	0.490	0.945	0.674	0.425
	p	0.210	0.460	0.200	0.086	0.610	0.110	0.055	0.790	0.025	0.031	0.490	0.008	0.140	0.530	0.044	0.043	0.430	0.016
	pc	0.017	0.025	0.013	0.008	0.050	0.010	0.017	0.050	0.010	0.013	0.025	0.008	0.017	0.050	0.013	0.010	0.025	0.008
IsT	ph	**0.889**	0.357	0.714	**0.037**	0.381	0.833	**0.841**	0.490	0.837	**0.095**	0.413	0.857	**0.889**	0.510	0.837	**0.063**	0.492	0.816
	pl	**0.605**	0.125	0.390	**0.004**	0.147	0.510	**0.533**	0.210	0.510	**0.020**	0.175	0.556	**0.617**	0.226	0.519	**0.009**	0.214	0.480
	pu	**0.977**	0.683	0.907	**0.260**	0.687	0.960	**0.961**	0.776	0.962	**0.353**	0.699	0.966	**0.975**	0.788	0.961	**0.326**	0.775	0.955
	p	**0.009**	0.430	0.210	**4.0E-04**	0.480	0.044	**0.031**	0.960	0.044	**0.004**	0.590	0.021	**0.007**	0.960	0.038	**0.003**	0.970	0.066
	pc	**0.010**	0.025	0.017	**0.008**	0.050	0.013	**0.013**	0.050	0.017	**0.008**	0.025	0.010	**0.010**	0.025	0.013	**0.008**	0.050	0.017
Tr	ph	0.444	0.531	0.833	0.556	0.889	0.881	0.381	0.347	0.653	0.508	0.778	0.796	0.794	0.510	0.796	0.127	0.524	0.837
	pl	0.195	0.238	0.497	0.271	0.573	0.572	0.152	0.126	0.334	0.238	0.480	0.476	0.473	0.221	0.476	0.028	0.241	0.519
	pu	0.725	0.803	0.962	0.808	0.979	0.976	0.680	0.662	0.876	0.774	0.930	0.944	0.943	0.793	0.944	0.426	0.792	0.961
	p	0.730	0.870	0.052	0.740	0.017	0.017	0.470	0.370	0.380	0.970	0.068	0.070	0.074	0.960	0.070	0.016	0.890	0.038
	pc	0.017	0.050	0.013	0.025	0.010	0.008	0.025	0.013	0.017	0.050	0.008	0.010	0.017	0.050	0.013	0.008	0.025	0.010
Tr1R	ph	**1.000**	0.667	**0.972**	**0**	0.519	**0.967**	**0.873**	0.531	**0.796**	**0.206**	0.524	**0.755**	**0.873**	0.531	**0.796**	**0.206**	0.524	**0.755**
	pl	**0.717**	0.307	**0.733**	**0**	0.224	**0.695**	**0.584**	0.235	**0.476**	**0.050**	0.235	**0.412**	**0.584**	0.235	**0.476**	**0.050**	0.235	**0.412**
	pu	**1.000**	0.900	**0.998**	**0.283**	0.801	**0.997**	**0.971**	0.806	**0.944**	**0.564**	0.798	**0.931**	**0.971**	0.806	**0.944**	**0.564**	0.798	**0.931**
	p	**0.002**	0.410	**0.001**	**0.002**	0.920	**0.002**	**0.013**	0.870	**0.070**	**0.120**	0.900	**0.160**	**0.013**	0.870	**0.070**	**0.120**	0.900	**0.160**
	pc	**0.017**	0.025	**0.008**	**0.013**	0.050	**0.010**	**0.008**	0.025	**0.010**	**0.013**	0.050	**0.017**	**0.008**	0.025	**0.010**	**0.013**	0.050	**0.017**

Values in bold indicate a significant difference ($p \leq pc \leq 0.05$) for the parameters for the given pair of species. Statistics abbreviations: ph = test statistics $\hat{P}$; pl = lower 95% confidence interval of $\hat{P}$; pu = upper 95% confidence interval of $\hat{P}$; *p* = significance level, not adjusted for family-wise error (FWE); *pc* = critical significance level, adjusted for FWE. Species abbreviations as in Table 3.1. From Schulz *et al.* (submitted, appendix 3).

Appendix 3.3. Analytical statistics on primates: results from Dunnett test with 0% (**a-b**) and 15% (**c-d**) trimming for the parameters.

a. SSFA, trimming 0%

		Afsc			*Tfv*			*epLsar*			*HAsfc9*			*HAsfc81*		
Group1	Group2	Test	*p*	df	Test	*p*	df	Test	*p*	df	Test	*p*	df	Test	*p*	df
A. seniculus	***G. gorilla***	2.173	0.117	3.044	0.297	0.791	2.296	**5.321**	**0.001**	**6.996**	0.118	0.912	3.620	0.767	0.481	4.508
A. seniculus	***L. albigena***	1.475	0.234	3.083	0.650	0.577	2.228	**3.186**	**0.018**	**6.336**	0.629	0.555	5.381	1.712	0.126	7.896
A. seniculus	*M. fascicularis*	0.101	0.927	2.385	0.566	0.616	2.640	1.857	0.152	3.289	1.212	0.338	2.223	0.483	0.666	2.704
A. seniculus	***P. abelii***	3.348	0.074	2.087	1.515	0.255	2.263	**3.400**	**0.010**	**7.784**	1.257	0.252	6.471	**2.391**	**0.046**	**7.574**
A. seniculus	***P. cynocephalus***	2.771	0.105	2.073	1.025	0.409	2.089	**3.779**	**0.003**	**10.870**	0.942	0.416	3.006	2.166	0.102	3.683
A. seniculus	*P. troglodytes*	0.068	0.949	4.897	0.039	0.972	2.192	0.068	0.949	3.858	0.889	0.443	2.839	0.635	0.564	3.546
G. gorilla	***L. albigena***	1.094	0.298	10.931	1.003	0.338	10.485	**2.746**	**0.022**	**9.140**	0.648	0.531	10.269	1.255	0.242	8.816
G. gorilla	***M. fascicularis***	**3.968**	**0.004**	**8.468**	0.631	0.542	10.264	**4.680**	**0.003**	**6.270**	2.088	0.079	6.415	1.695	0.130	7.659
G. gorilla	*P. abelii*	1.837	0.117	5.873	**3.392**	**0.006**	**10.752**	0.645	0.533	10.437	1.374	0.201	9.374	1.953	0.081	9.400
G. gorilla	*P. cynocephalus*	0.712	0.505	5.735	**2.366**	**0.045**	**8.100**	0.118	0.908	13.626	1.154	0.274	10.715	1.580	0.143	10.825
G. gorilla	***P. troglodytes***	**2.465**	**0.046**	**6.396**	1.004	0.342	8.914	**5.757**	**0.001**	**6.812**	1.453	0.182	8.662	1.730	0.118	8.866
L. albigena	***M. fascicularis***	**2.618**	**0.026**	**9.882**	0.130	0.899	9.860	2.114	0.064	9.017	2.248	0.060	6.806	2.306	0.055	6.860
L. albigena	***P. abelii***	**3.293**	**0.013**	**7.014**	**2.583**	**0.024**	**11.941**	1.429	0.188	8.745	0.714	0.489	11.616	0.440	0.668	11.829
L. albigena	***P. cynocephalus***	2.190	0.066	6.857	1.319	0.215	10.591	2.029	0.065	11.975	0.195	0.850	9.428	0.354	0.732	7.963
L. albigena	***P. troglodytes***	1.700	0.136	6.530	2.201	0.053	9.856	**3.625**	**0.005**	**9.534**	1.809	0.105	8.581	**2.351**	**0.047**	**7.794**
M. fascicularis	***P. abelii***	**9.654**	**0.000**	**8.641**	2.047	0.067	10.279	**2.679**	**0.033**	**6.780**	**2.798**	**0.028**	**6.559**	**3.212**	**0.015**	**7.091**
M. fascicularis	***P. cynocephalus***	**8.051**	**0.000**	**8.333**	1.022	0.338	7.751	**3.145**	**0.011**	**9.868**	**4.269**	**0.001**	**12.671**	**4.144**	**0.001**	**14.487**
M. fascicularis	***P. troglodytes***	0.208	0.843	4.952	1.446	0.182	8.996	**2.332**	**0.046**	**8.519**	0.530	0.615	6.141	0.304	0.770	7.377
P. cynocephalus	***P. abelii***	**2.948**	**0.011**	**13.779**	1.791	0.103	10.052	0.624	0.542	14.949	0.681	0.514	8.406	0.996	0.347	8.490
P. cynocephalus	***P. troglodytes***	**3.201**	**0.031**	**4.183**	**4.078**	**0.004**	**7.845**	**3.898**	**0.003**	**10.268**	**3.058**	**0.010**	**11.628**	**3.781**	**0.003**	**11.078**
P. troglodytes	***P. abelii***	**3.845**	**0.017**	**4.219**	**4.794**	**0.001**	**9.975**	**3.540**	**0.009**	**7.150**	**2.412**	**0.043**	**7.910**	**3.207**	**0.012**	**8.206**

Appendix 3.3. (continued)

b. ISO, trimming 0%

		S5v			*Sq*			*Vm*		
Group1	Group2	Test	*p*	df	Test	*p*	df	Test	*p*	df
A. seniculus	***G. gorilla***	1.465	0.204	4.876	1.246	0.287	3.657	1.593	0.219	2.701
A. seniculus	***L. albigena***	0.249	0.817	3.532	0.605	0.597	2.447	1.172	0.352	2.205
A. seniculus	*M. fascicularis*	0.195	0.857	3.224	0.117	0.914	3.021	0.202	0.854	2.635
A. seniculus	***P. abelii***	2.370	0.104	2.807	2.302	0.140	2.129	2.244	0.150	2.065
A. seniculus	***P. cynocephalus***	2.090	0.162	2.157	1.409	0.283	2.219	1.844	0.204	2.045
A. seniculus	*Pa. troglodytes*	0.012	0.991	5.369	0.370	0.734	3.221	0.593	0.596	2.902
G. gorilla	***L. albigena***	2.134	0.061	9.313	1.177	0.274	7.646	1.112	0.299	7.851
G. gorilla	***M. fascicularis***	1.697	0.125	8.665	2.010	0.073	9.903	**2.655**	**0.023**	**10.781**
G. gorilla	*P. abelii*	0.704	0.502	7.597	1.330	0.233	5.814	1.256	0.256	5.956
G. gorilla	*P. cynocephalus*	0.245	0.815	5.549	0.036	0.972	6.393	0.312	0.767	5.674
G. gorilla	***P. troglodytes***	1.469	0.179	8.301	1.263	0.238	8.992	1.715	0.122	8.503
L. albigena	***M. fascicularis***	0.636	0.537	11.860	1.298	0.222	10.485	2.186	0.055	9.581
L. albigena	***P. abelii***	**3.884**	**0.003**	**11.008**	**4.544**	**0.001**	**9.264**	**4.110**	**0.002**	**9.481**
L. albigena	***P. cynocephalus***	**3.848**	**0.006**	**7.316**	2.012	0.068	11.543	**2.628**	**0.028**	**8.685**
L. albigena	***P. troglodytes***	0.233	0.823	6.737	0.338	0.745	6.842	1.054	0.333	5.850
M. fascicularis	***P. abelii***	**3.420**	**0.005**	**11.547**	**4.725**	**0.002**	**7.566**	**4.982**	**0.001**	**7.256**
M. fascicularis	***P. cynocephalus***	**3.346**	**0.011**	**7.637**	**2.904**	**0.018**	**8.688**	**4.047**	**0.005**	**6.893**
M. fascicularis	***P. troglodytes***	0.207	0.842	6.237	0.752	0.471	9.122	0.717	0.492	8.698
P. cynocephalus	***P. abelii***	0.953	0.367	8.437	**3.046**	**0.008**	**14.955**	**2.465**	**0.028**	**13.052**
P. cynocephalus	***P. troglodytes***	2.086	0.100	4.307	1.731	0.139	5.500	2.502	0.061	4.416
P. troglodytes	***P. abelii***	2.365	0.060	5.517	**3.343**	**0.021**	**4.871**	**3.317**	**0.024**	**4.595**

Appendix 3.3. (continued)

b. ISO, trimming 0%

		Spd			*Sha*			*Sda*		
Group1	Group2	Test	*p*	df	Test	*p*	df	Test	*p*	df
A. seniculus	***G. gorilla***	2.058	0.132	2.975	1.285	0.255	5.001	1.376	0.225	5.181
A. seniculus	***L. albigena***	0.891	0.452	2.433	2.146	0.072	6.533	0.826	0.434	7.669
A. seniculus	*M. fascicularis*	0.794	0.464	4.853	0.401	0.701	6.674	1.232	0.305	3.045
A. seniculus	***P. abelii***	2.823	0.092	2.275	**2.515**	**0.046**	**6.009**	1.732	0.140	5.326
A. seniculus	***P. cynocephalus***	2.518	0.120	2.132	**3.912**	**0.004**	**9.069**	2.243	0.051	9.223
A. seniculus	*Pa. troglodytes*	1.165	0.297	4.987	1.008	0.370	4.011	0.397	0.705	5.988
G. gorilla	***L. albigena***	**2.321**	**0.045**	**9.001**	1.183	0.290	5.021	1.176	0.289	5.356
G. gorilla	***M. fascicularis***	**3.484**	**0.006**	**9.513**	1.301	0.250	5.016	1.571	0.176	5.045
G. gorilla	*P. abelii*	1.153	0.283	7.768	0.368	0.725	6.260	1.061	0.336	5.157
G. gorilla	*P. cynocephalus*	0.530	0.614	6.433	0.648	0.544	5.259	0.847	0.411	13.838
G. gorilla	***P. troglodytes***	0.687	0.517	6.164	0.985	0.365	5.687	1.277	0.254	5.332
L. albigena	***M. fascicularis***	2.229	0.057	7.834	1.920	0.079	11.815	1.888	0.098	7.498
L. albigena	***P. abelii***	**4.771**	**0.001**	**11.452**	2.214	0.067	6.200	0.563	0.586	10.099
L. albigena	***P. cynocephalus***	**4.372**	**0.002**	**9.693**	**3.165**	**0.010**	**10.429**	2.072	0.067	9.440
L. albigena	***P. troglodytes***	0.661	0.538	5.019	0.618	0.568	4.243	0.387	0.707	9.715
M. fascicularis	***P. abelii***	**4.591**	**0.002**	**7.192**	**2.547**	**0.043**	**6.155**	**3.558**	**0.008**	**7.757**
M. fascicularis	***P. cynocephalus***	**4.275**	**0.004**	**6.589**	**3.902**	**0.003**	**10.120**	**2.408**	**0.039**	**9.056**
M. fascicularis	***P. troglodytes***	2.123	0.062	9.102	1.060	0.347	4.188	1.420	0.214	5.093
P. cynocephalus	***P. abelii***	1.133	0.280	11.445	0.681	0.514	8.458	1.981	0.078	9.194
P. cynocephalus	***P. troglodytes***	1.056	0.346	4.317	1.172	0.279	7.068	2.157	0.058	9.409
P. troglodytes	***P. abelii***	1.413	0.221	4.653	1.418	0.187	9.919	1.035	0.334	7.345

Appendix 3.3. (continued)

c. SSFA, trimming 15%

		Afsc			*Tfv*			*epLsar*		
Group1	Group2	Test	*p*	df	Test	*p*	df	Test	*p*	df
A. seniculus	***G. gorilla***	2.173	0.117	3.044	0.297	0.791	2.296	**5.321**	**0.001**	**6.996**
A. seniculus	***L. albigena***	1.844	0.195	2.190	0.607	0.602	2.157	**3.504**	**0.029**	**3.658**
A. seniculus	*M. fascicularis*	0.098	0.929	2.566	0.661	0.569	2.304	1.990	0.124	3.677
A. seniculus	***P. abelii***	3.419	0.072	2.070	1.574	0.238	2.349	**4.713**	**0.003**	**5.996**
A. seniculus	***P. cynocephalus***	2.769	0.105	2.086	1.063	0.393	2.142	**4.933**	**0.001**	**8.373**
A. seniculus	*P. troglodytes*	0.068	0.949	4.897	0.039	0.972	2.192	0.068	0.949	3.858
G. gorilla	***L. albigena***	0.995	0.354	6.762	0.930	0.377	8.681	**3.366**	**0.013**	**6.623**
G. gorilla	***M. fascicularis***	**3.734**	**0.005**	**8.729**	0.982	0.352	8.856	**4.438**	**0.003**	**6.641**
G. gorilla	***P. abelii***	1.977	0.098	5.691	**3.348**	**0.009**	**8.669**	0.851	0.417	9.000
G. gorilla	***P. cynocephalus***	0.711	0.504	5.862	**2.358**	**0.042**	**9.417**	0.602	0.559	11.237
G. gorilla	***P. troglodytes***	**2.465**	**0.046**	**6.396**	1.004	0.342	8.914	**5.757**	**0.001**	**6.812**
L. albigena	***M. fascicularis***	**4.143**	**0.005**	**6.437**	0.197	0.849	7.274	1.980	0.083	8.000
L. albigena	***P. abelii***	**6.155**	**0.001**	**6.614**	**2.893**	**0.023**	**7.013**	**2.542**	**0.046**	**5.649**
L. albigena	***P. cynocephalus***	**3.487**	**0.009**	**7.566**	1.701	0.120	9.864	**2.819**	**0.019**	**9.478**
L. albigena	***P. troglodytes***	2.155	0.090	4.471	2.240	0.056	7.923	**4.374**	**0.002**	**7.970**
M. fascicularis	***P. abelii***	**8.478**	**0.000**	**4.995**	**2.383**	**0.044**	**7.964**	**3.722**	**0.011**	**5.667**
M. fascicularis	***P. cynocephalus***	**6.745**	**0.001**	**5.258**	1.195	0.268	7.653	**3.977**	**0.003**	**9.501**
M. fascicularis	***P. troglodytes***	0.202	0.847	5.349	2.073	0.074	7.618	**2.443**	**0.040**	**7.975**
P. cynocephalus	***P. abelii***	**3.306**	**0.007**	**10.654**	1.609	0.150	7.240	0.255	0.804	10.304
P. cynocephalus	***P. troglodytes***	**3.197**	**0.031**	**4.216**	**3.904**	**0.003**	**9.207**	**5.399**	**0.000**	**9.720**
P. troglodytes	***P. abelii***	**3.927**	**0.016**	**4.176**	**4.603**	**0.002**	**7.391**	**5.172**	**0.002**	**5.842**

Appendix 3.3. (continued)

d. ISO, trimming 15%

		S5v			*Sq*			*Vm*		
Group1	Group2	Test	*p*	df	Test	*p*	df	Test	*p*	df
A. seniculus	***G. gorilla***	1.465	0.204	4.876	1.246	0.287	3.657	1.593	0.219	2.701
A. seniculus	***L. albigena***	0.132	0.902	3.429	0.886	0.467	2.049	1.277	0.317	2.266
A. seniculus	*M. fascicularis*	0.020	0.985	3.135	0.055	0.960	2.918	0.334	0.763	2.669
A. seniculus	***P. abelii***	2.623	0.086	2.753	2.388	0.132	2.131	2.279	0.144	2.107
A. seniculus	***P. cynocephalus***	2.060	0.164	2.195	1.468	0.267	2.234	1.888	0.197	2.042
A. seniculus	*P. troglodytes*	0.012	0.991	5.369	0.370	0.734	3.221	0.593	0.596	2.902
G. gorilla	***L. albigena***	2.010	0.077	8.535	0.910	0.402	5.312	0.833	0.429	8.113
G. gorilla	***M. fascicularis***	1.906	0.093	8.100	1.950	0.084	8.756	**2.366**	**0.042**	**8.922**
G. gorilla	***P. abelii***	0.988	0.355	7.295	1.465	0.195	5.811	1.327	0.229	6.498
G. gorilla	***P. cynocephalus***	0.219	0.835	5.676	0.058	0.955	6.464	0.416	0.693	5.622
G. gorilla	***P. troglodytes***	1.469	0.179	8.301	1.263	0.238	8.992	1.715	0.122	8.503
L. albigena	***M. fascicularis***	0.222	0.830	7.892	1.963	0.114	4.442	2.006	0.086	6.776
L. albigena	***P. abelii***	**4.124**	**0.004**	**7.292**	**7.250**	**0.000**	**6.652**	**3.259**	**0.015**	**6.782**
L. albigena	***P. cynocephalus***	**3.592**	**0.015**	**5.120**	**2.344**	**0.042**	**9.562**	2.100	0.087	5.295
L. albigena	***P. troglodytes***	0.117	0.910	6.448	0.845	0.442	4.332	1.246	0.258	6.203
M. fascicularis	***P. abelii***	**4.180**	**0.003**	**7.686**	**4.923**	**0.004**	**5.144**	**4.479**	**0.006**	**5.273**
M. fascicularis	***P. cynocephalus***	**3.667**	**0.013**	**5.418**	**2.967**	**0.025**	**6.093**	**3.696**	**0.017**	**4.518**
M. fascicularis	***P. troglodytes***	0.034	0.974	6.014	0.669	0.523	7.841	0.477	0.647	7.831
P. cynocephalus	***P. abelii***	1.550	0.171	6.130	**3.059**	**0.011**	**11.000**	2.134	0.070	7.127
P. cynocephalus	***P. troglodytes***	2.056	0.103	4.379	1.829	0.121	5.575	2.598	0.055	4.385
P. troglodytes	***P. abelii***	**2.616**	**0.044**	**5.390**	**3.494**	**0.018**	**4.866**	**3.340**	**0.021**	**4.958**

Appendix 3.3. (continued)

d. ISO, trimming 15%

		Spd			*Sha*			*Sda*		
Group1	Group2	Test	*p*	df	Test	*p*	df	Test	*p*	df
A. seniculus	***G. gorilla***	2.058	0.132	2.975	1.285	0.255	5.001	1.376	0.225	5.181
A. seniculus	***L. albigena***	0.831	0.471	2.790	1.822	0.138	4.277	0.465	0.658	6.000
A. seniculus	*M. fascicularis*	0.531	0.625	3.755	0.748	0.492	4.514	1.762	0.212	2.145
A. seniculus	***P. abelii***	2.899	0.092	2.165	**4.323**	**0.012**	**4.037**	1.732	0.140	5.326
A. seniculus	***P. cynocephalus***	2.601	0.116	2.093	**3.870**	**0.006**	**7.075**	1.907	0.097	7.242
A. seniculus	*P. troglodytes*	1.165	0.297	4.987	1.008	0.370	4.011	0.397	0.705	5.988
G. gorilla	***L. albigena***	2.114	0.064	8.998	1.185	0.289	5.028	1.256	0.261	5.368
G. gorilla	***M. fascicularis***	**3.580**	**0.008**	**7.681**	1.314	0.246	5.015	1.631	0.164	5.007
G. gorilla	***P. abelii***	1.285	0.242	6.651	0.646	0.546	5.212	1.061	0.336	5.157
G. gorilla	***P. cynocephalus***	0.683	0.520	6.000	0.751	0.485	5.185	0.400	0.697	11.733
G. gorilla	***P. troglodytes***	0.687	0.517	6.164	0.985	0.365	5.687	1.277	0.254	5.332
L. albigena	***M. fascicularis***	1.952	0.092	6.964	1.954	0.090	7.302	1.813	0.142	4.142
L. albigena	***P. abelii***	**4.249**	**0.006**	**5.627**	**3.443**	**0.018**	**5.032**	0.913	0.391	7.084
L. albigena	***P. cynocephalus***	**3.717**	**0.014**	**4.980**	**2.944**	**0.017**	**8.924**	1.785	0.115	7.493
L. albigena	***P. troglodytes***	0.661	0.534	5.751	0.625	0.563	4.320	0.073	0.944	7.978
M. fascicularis	***P. abelii***	**5.220**	**0.004**	**4.747**	**4.387**	**0.009**	**4.551**	**4.398**	**0.006**	**5.417**
M. fascicularis	***P. cynocephalus***	**4.837**	**0.006**	**4.431**	**3.944**	**0.004**	**8.074**	2.162	0.067	7.009
M. fascicularis	***P. troglodytes***	1.966	0.088	7.275	1.109	0.327	4.169	1.805	0.143	4.158
P. cynocephalus	***P. abelii***	1.291	0.231	8.296	0.529	0.608	9.748	1.598	0.153	7.211
P. cynocephalus	***P. troglodytes***	1.140	0.315	4.223	0.877	0.413	6.148	1.807	0.111	7.444
P. troglodytes	***P. abelii***	1.478	0.207	4.391	1.213	0.269	6.235	1.035	0.334	7.345

Values in bold indicate a significant difference ($p \leq 0.05$). Parameters: see Tables 2.2-2.3. Statistics abbreviations as in Appendix 3.1. Species abbreviations: see Table 3.4.

Appendix 3.4. Analytical statistics on primates: results from Cliff tests.

		Asfc					*Tfv*					*HAsfc9*					*HAsfc81*				
Group 1	Group 2	ph	pl	pu	*p*	*pc*	ph	pl	pu	*p*	*pc*	ph	pl	pu	*p*	*pc*	ph	pl	pu	*p*	*pc*
A. seniculus	*G. gorilla*	0.111	0.015	0.513	0.058	0.005	0.389	0.070	0.842	0.730	0.017	0.611	0.192	0.912	0.690	0.010	0.611	0.192	0.912	0.690	0.013
A. seniculus	*L. albigena*	0.143	0.025	0.523	0.067	0.005	0.333	0.047	0.836	0.630	0.010	0.571	0.213	0.868	0.750	0.017	0.762	0.364	0.947	0.220	0.006
A. seniculus	*M. fascicularis*	0.476	0.111	0.868	0.940	0.050	0.333	0.061	0.794	0.570	0.008	0.190	0.027	0.670	0.240	0.004	0.429	0.105	0.827	0.800	0.025
A. seniculus	*P. abelii*	0.000	0.000	0.348	0.008	0.003	0.190	0.027	0.670	0.240	0.004	0.762	0.328	0.955	0.270	0.004	0.810	0.401	0.964	0.150	0.004
A. seniculus	***P. cynocephalus***	**0.000**	**0.000**	**0.259**	**0.001**	**0.003**	0.333	0.046	0.837	0.640	0.013	0.733	0.278	0.952	0.370	0.006	0.833	0.378	0.976	0.170	0.005
A. seniculus	*P. troglodytes*	0.533	0.168	0.866	0.900	0.025	0.400	0.075	0.845	0.760	0.025	0.267	0.051	0.712	0.360	0.006	0.267	0.053	0.702	0.340	0.006
G. gorilla	*L. albigena*	0.762	0.394	0.940	0.180	0.007	0.381	0.136	0.706	0.520	0.007	0.548	0.244	0.819	0.800	0.025	0.667	0.325	0.892	0.370	0.007
G. gorilla	*M. fascicularis*	0.905	0.560	0.986	0.023	0.004	0.381	0.137	0.705	0.520	0.006	0.190	0.045	0.542	0.086	0.003	0.238	0.067	0.577	0.140	0.004
G. gorilla	*P. abelii*	0.238	0.056	0.620	0.200	0.010	0.095	0.017	0.392	0.010	0.003	0.690	0.352	0.902	0.300	0.005	0.810	0.461	0.955	0.083	0.003
G. gorilla	*P. cynocephalus*	0.417	0.167	0.719	0.630	0.013	0.167	0.045	0.458	0.026	0.003	0.683	0.363	0.891	0.290	0.005	0.767	0.439	0.932	0.120	0.004
G. gorilla	*P. troglodytes*	0.833	0.448	0.969	0.092	0.006	0.633	0.284	0.883	0.510	0.006	0.200	0.043	0.579	0.130	0.003	0.233	0.052	0.630	0.210	0.005
L. albigena	*M. fascicularis*	0.857	0.462	0.977	0.078	0.006	0.449	0.184	0.746	0.770	0.050	0.163	0.041	0.471	0.033	0.003	0.184	0.045	0.520	0.066	0.003
L. albigena	***P. abelii***	**0.041**	**0.005**	**0.277**	**0.001**	**0.002**	0.143	0.034	0.444	0.021	0.003	0.633	0.320	0.863	0.440	0.007	0.592	0.285	0.841	0.600	0.010
L. albigena	*P. cynocephalus*	0.143	0.030	0.474	0.035	0.004	0.329	0.119	0.640	0.310	0.005	0.586	0.282	0.836	0.620	0.008	0.500	0.220	0.780	0.990	0.050
L. albigena	***P. troglodytes***	0.771	0.374	0.950	0.200	0.008	0.829	0.472	0.963	0.072	0.003	0.229	0.059	0.581	0.140	0.004	0.114	0.021	0.443	0.023	0.003
M. fascicularis	*P. abelii*	0.000	0.000	0.348	0.008	0.003	0.204	0.056	0.524	0.070	0.003	0.939	0.662	0.992	0.004	0.003	0.918	0.606	0.988	0.011	0.003
M. fascicularis	***P. cynocephalus***	**0.000**	**0.000**	**0.259**	**0.001**	**0.003**	0.314	0.111	0.626	0.260	0.005	**1.000**	**0.741**	**1.000**	**0.001**	**0.002**	**0.957**	**0.765**	**0.994**	**0.000**	**0.002**
M. fascicularis	*P. troglodytes*	0.543	0.200	0.849	0.850	0.017	0.800	0.434	0.954	0.120	0.004	0.571	0.242	0.848	0.720	0.013	0.429	0.141	0.774	0.740	0.017
P. cynocephalus	*P. abelii*	0.129	0.030	0.412	0.012	0.003	0.271	0.088	0.589	0.170	0.004	0.529	0.255	0.786	0.860	0.050	0.614	0.316	0.846	0.490	0.008
P. cynocephalus	***P. troglodytes***	0.900	0.548	0.985	0.027	0.004	**0.960**	**0.724**	**0.995**	**0.001**	**0.002**	0.120	0.018	0.501	0.051	0.003	0.060	0.008	0.340	0.004	0.003
P. troglodytes	***P. abelii***	**0.029**	**0.002**	**0.273**	**0.001**	**0.003**	**0.029**	**0.002**	**0.273**	**0.001**	**0.003**	0.886	0.554	0.980	0.024	0.003	0.943	0.651	0.993	0.005	0.003

Appendix 3.4. (continued)

		epLsar					*S5v*					*Sq*					*Vm*				
Group1	Group2	ph	pl	pu	*p*	*pc*	ph	pl	pu	*p*	*pc*	ph	pl	pu	*p*	*pc*	ph	pl	pu	*p*	*pc*
A. seniculus	*G. gorilla*	1.000	0.607	1.000	0.016	0.004	0.222	0.047	0.623	0.190	0.005	0.333	0.079	0.744	0.490	0.007	0.167	0.022	0.639	0.190	0.006
A. seniculus	*L. albigena*	0.952	0.613	0.996	0.011	0.003	0.524	0.150	0.873	0.930	0.050	0.429	0.091	0.849	0.820	0.025	0.333	0.047	0.836	0.630	0.013
A. seniculus	*M. fascicularis*	0.881	0.509	0.981	0.045	0.006	0.429	0.114	0.814	0.780	0.013	0.476	0.119	0.860	0.940	0.050	0.429	0.091	0.849	0.820	0.050
A. seniculus	*P. abelii*	0.905	0.535	0.987	0.033	0.004	0.095	0.011	0.499	0.050	0.003	0.095	0.011	0.499	0.050	0.003	0.095	0.011	0.499	0.050	0.003
A. seniculus	*P. cynocephalus*	**1.000**	**0.741**	**1.000**	**0.001**	**0.003**	0.133	0.018	0.558	0.093	0.004	0.233	0.034	0.726	0.350	0.006	0.167	0.024	0.622	0.170	0.004
A. seniculus	*P. troglodytes*	0.533	0.168	0.866	0.900	0.050	0.467	0.108	0.863	0.910	0.025	0.333	0.064	0.784	0.560	0.010	0.267	0.038	0.772	0.450	0.010
G. gorilla	*L. albigena*	0.119	0.024	0.428	0.017	0.004	0.833	0.451	0.968	0.089	0.004	0.833	0.407	0.973	0.140	0.004	0.762	0.379	0.944	0.200	0.006
G. gorilla	*M. fascicularis*	0.000	0.000	0.348	0.008	0.003	0.762	0.386	0.942	0.190	0.005	0.833	0.451	0.968	0.089	0.004	0.881	0.504	0.982	0.048	0.003
G. gorilla	*P. abelii*	0.429	0.163	0.743	0.700	0.017	0.405	0.146	0.730	0.610	0.007	0.286	0.079	0.650	0.280	0.005	0.310	0.092	0.664	0.330	0.007
G. gorilla	*P. cynocephalus*	0.417	0.175	0.707	0.610	0.013	0.617	0.274	0.873	0.560	0.006	0.600	0.292	0.845	0.570	0.013	0.550	0.243	0.823	0.790	0.025
G. gorilla	*P. troglodytes*	0.000	0.000	0.393	0.016	0.003	0.800	0.427	0.956	0.120	0.004	0.733	0.347	0.934	0.260	0.005	0.767	0.387	0.945	0.190	0.005
L. albigena	*M. fascicularis*	0.184	0.045	0.520	0.066	0.007	0.469	0.197	0.762	0.870	0.017	0.673	0.337	0.893	0.350	0.006	0.816	0.480	0.955	0.066	0.004
L. albigena	*P. abelii*	0.714	0.371	0.914	0.240	0.010	0.082	0.014	0.354	0.004	0.003	0.000	0.000	0.348	0.008	0.003	0.000	0.000	0.348	0.008	0.003
L. albigena	***P. cynocephalus***	0.814	0.517	0.947	0.039	0.006	**0.043**	**0.006**	**0.262**	**0.000**	**0.002**	0.200	0.062	0.488	0.042	0.003	0.129	0.031	0.404	0.010	0.003
L. albigena	*P. troglodytes*	**0.029**	**0.002**	**0.273**	**0.001**	**0.002**	0.400	0.128	0.752	0.640	0.008	0.571	0.226	0.859	0.740	0.017	0.686	0.301	0.917	0.390	0.008
M. fascicularis	***P. abelii***	0.857	0.462	0.977	0.078	0.008	0.082	0.014	0.354	0.004	0.003	**0.020**	**0.002**	**0.210**	**0.000**	**0.002**	0.000	0.000	0.348	0.008	0.003
M. fascicularis	***P. cynocephalus***	**0.943**	**0.700**	**0.992**	**0.002**	**0.003**	0.143	0.027	0.504	0.053	0.003	0.143	0.036	0.427	0.015	0.003	**0.014**	**0.001**	**0.157**	**0.000**	**0.002**
M. fascicularis	*P. troglodytes*	0.143	0.029	0.480	0.038	0.005	0.429	0.148	0.764	0.730	0.010	0.371	0.122	0.715	0.510	0.008	0.429	0.152	0.758	0.720	0.017
P. cynocephalus	***P. abelii***	0.457	0.206	0.732	0.790	0.025	0.271	0.080	0.614	0.210	0.006	0.129	0.029	0.419	0.014	0.003	0.200	0.051	0.537	0.082	0.004
P. cynocephalus	*P. troglodytes*	**0.000**	**0.000**	**0.259**	**0.001**	**0.003**	0.900	0.621	0.980	0.007	0.003	0.760	0.393	0.939	0.180	0.004	0.820	0.375	0.972	0.180	0.005
P. troglodytes	***P. abelii***	0.886	0.520	0.982	0.039	0.005	0.086	0.012	0.417	0.016	0.003	0.057	0.007	0.356	0.006	0.003	0.057	0.007	0.356	0.006	0.003

Appendix 3.4. (continued)

		Spd					*Sha*					*Sda*				
Group1	Group2	ph	pl	pu	*p*	*pc*	ph	pl	pu	*p*	*pc*	ph	pl	pu	*p*	*pc*
A. seniculus	*G. gorilla*	0.167	0.022	0.639	0.190	0.004	0.944	0.573	0.995	0.021	0.003	0.667	0.256	0.921	0.490	0.006
A. seniculus	*L. albigena*	0.333	0.076	0.754	0.510	0.013	0.810	0.432	0.960	0.120	0.004	0.476	0.145	0.829	0.930	0.050
A. seniculus	*M. fascicularis*	0.619	0.193	0.917	0.670	0.050	0.429	0.149	0.763	0.730	0.050	0.238	0.056	0.624	0.200	0.004
A. seniculus	*P. abelii*	0.000	0.000	0.348	0.008	0.003	1.000	0.652	1.000	0.008	0.003	0.778	0.362	0.956	0.210	0.005
A. seniculus	*P. cynocephalus*	**0.033**	**0.003**	**0.301**	**0.002**	**0.003**	**1.000**	**0.741**	**1.000**	**0.001**	**0.003**	0.833	0.489	0.963	0.058	0.003
A. seniculus	*P. troglodytes*	0.200	0.035	0.635	0.200	0.005	0.600	0.210	0.894	0.690	0.025	0.533	0.149	0.882	0.910	0.025
G. gorilla	*L. albigena*	0.833	0.510	0.960	0.044	0.004	0.357	0.122	0.690	0.440	0.010	0.405	0.146	0.731	0.620	0.010
G. gorilla	*M. fascicularis*	**0.952**	**0.688**	**0.995**	**0.002**	**0.003**	0.143	0.031	0.468	0.032	0.004	0.095	0.017	0.392	0.010	0.003
G. gorilla	*P. abelii*	0.310	0.088	0.676	0.340	0.007	0.667	0.298	0.904	0.420	0.007	0.472	0.173	0.793	0.900	0.017
G. gorilla	*P. cynocephalus*	0.383	0.120	0.740	0.580	0.025	0.683	0.297	0.917	0.400	0.006	0.600	0.310	0.834	0.540	0.008
G. gorilla	*P. troglodytes*	0.633	0.275	0.887	0.520	0.017	0.233	0.052	0.629	0.210	0.006	0.333	0.103	0.686	0.400	0.006
L. albigena	*M. fascicularis*	0.796	0.448	0.949	0.097	0.004	0.224	0.066	0.542	0.090	0.004	0.224	0.056	0.585	0.140	0.004
L. albigena	*P. abelii*	**0.041**	**0.005**	**0.277**	**0.001**	**0.003**	0.939	0.662	0.992	0.004	0.003	0.619	0.288	0.867	0.530	0.007
L. albigena	***P. cynocephalus***	**0.029**	**0.003**	**0.208**	**0.000**	**0.002**	**0.971**	**0.789**	**0.997**	**0.000**	**0.003**	0.757	0.467	0.917	0.083	0.003
L. albigena	*P. troglodytes*	0.343	0.095	0.721	0.470	0.010	0.400	0.127	0.754	0.640	0.013	0.429	0.152	0.758	0.720	0.013
M. fascicularis	***P. abelii***	0.000	0.000	0.348	0.008	0.003	**0.980**	**0.790**	**0.998**	**0.000**	**0.002**	**0.952**	**0.691**	**0.994**	**0.002**	**0.003**
M. fascicularis	***P. cynocephalus***	**0.000**	**0.000**	**0.259**	**0.001**	**0.003**	**1.000**	**0.741**	**1.000**	**0.001**	**0.003**	**0.929**	**0.702**	**0.986**	**0.001**	**0.002**
M. fascicularis	*P. troglodytes*	0.229	0.050	0.627	0.200	0.005	0.657	0.300	0.896	0.430	0.008	0.829	0.478	0.962	0.067	0.003
P. cynocephalus	***P. abelii***	0.300	0.105	0.610	0.220	0.006	0.571	0.284	0.818	0.670	0.017	0.300	0.110	0.597	0.200	0.004
P. cynocephalus	*P. troglodytes*	0.660	0.281	0.906	0.460	0.008	0.180	0.028	0.625	0.180	0.005	0.200	0.058	0.504	0.054	0.003
P. troglodytes	***P. abelii***	0.286	0.076	0.660	0.290	0.006	0.829	0.389	0.973	0.160	0.005	0.700	0.307	0.925	0.360	0.005

Values in bold indicate a significant difference ($p \leq pc \leq 0.05$) for the parameters.
Parameters: see Tables 2.2-2.3. Statistics abbreviations as in Appendix 3.2. Species abbreviations: see Table 3.4.

SCANNING VOL. 32, 162–182 (2010)

Applying Tribology to Teeth of Hoofed Mammals

Ellen Schulz, Ivan Calandra, and Thomas M. Kaiser

Biocenter Grindel and Zoological Museum, University of Hamburg, Hamburg, Germany

Summary: Mammals inhabit all types of environments and have evolved chewing systems capable of processing a huge variety of structurally diverse food components. Surface textures of cheek teeth should thus reflect the mechanisms of wear as well as the functional traits involved. We employed surface textures parameters from ISO/DIS 25178 and scale-sensitive fractal analysis (SSFA) to quantify dental wear in herbivorous mammals at the level of an individual wear enamel facet. We evaluated cheek dentitions of two grazing ungulates: the Blue Wildebeest (*Connochaetes taurinus*) and the Grevy's Zebra (*Equus grevyi*). Both inhabit the east African grassland savanna habitat, but they belong to fundamentally different taxonomic units. We tested the hypothesis that the foregut fermenting wildebeest and the hindgut fermenting zebra show functional traits in their dentitions that relate to their specific mode of food-composition processing and digestion. In general, surface texture parameters from SSFA as well as ISO/DIS 25178 indicated that individual enamel ridges acting as crushing blades and individual wear facets of upper cheek teeth are significantly different in surface textures in the zebra when compared with the wildebeest. We interpreted the complexity and anisotropy signals to be clearly related to the brittle, dry grass component in the diet of the zebra, unlike the wildebeest, which ingests a more heterogeneous diet including fresh grass and herbs. Thus, SSFA and ISO parameters allow distinctions within the subtle dietary strategies that evolved in herbivorous ungulates with fundamentally different systematic affinities but which exploit a similar dietary niche. SCANNING 32: 162–182, 2010. © 2010 Wiley Periodicals, Inc.

Key words: dental microtexture, *Equus*, *Connochaetes*, diet

Introduction

Wear analyses in mammalian teeth are applied to reconstruct jaw movements or dietary behaviors, and thus to infer habitat and climate preferences of extant and extinct species. During the last two decades, the various qualitative and quantitative microwear approaches focusing on 2D microscopic inspection of enamel facets became powerful tools, especially in paleoecology (Walker *et al.* 1978; Solounias *et al.* 1988; Teaford 1993; Ungar 1996; Mainland 1998; Rivals and Deniaux 2003; Merceron *et al.* 2004; for a detailed review, see Kaiser and Brinkmann 2006).

Nevertheless, the mastication process is a 3D process, and Ungar *et al.* (2003) pioneered the 3D fractal analysis of dental microwear as a quantitative approach in wear analysis, using confocal microscopy. On the basis of high degree of correspondence between industrial-machined surfaces and tooth enamel surfaces, Kaiser and Brinkmann (2006) applied 2D surface roughness parameters and found them to reflect the dental wear equilibrium of food/tooth wear (abrasion) and tooth/tooth wear (attrition). In addition, Kaiser and Brinkmann (2006) pointed out that much more biological information could be retrieved from dental wear facet surface data using standardized approaches. Therefore, when the ISO/DIS 25178 became available (ISO/DIS 25178–2 2007), we decided to combine the approaches of Ungar *et al.* (2003) and Kaiser and Brinkmann (2006), applying the 3D surface texture parameters to mammalian tooth enamel wear surfaces.

Contract grant sponsor: Deutsche Forschungsgemeinschaft; Contract grant number: KA 1525/8-1.

Address for reprints: Ellen Schulz, Biocenter Grindel and Zoological Museum, University of Hamburg, Martin-Luther-King-Platz 3, 20146 Hamburg, Germany
E-mail: ellen.schulz@uni-hamburg.de

Received 17 December 2009; Accepted with revision 23 March 2010

DOI 10.1002/sca.20181
Published online 28 April 2010 in Wiley Online Library (wiley onlinelibrary.com)

In African ungulates, for example, two feeding categories are widely employed in dietary reconstructions that refer to physiological grazing or browsing adaptations of the digestive system (Hofmann 1989) or to the observed proportion of certain major groups of food plants (monocotyledonous/dicotyledonous) in the diet of the species under consideration (Gagnon and Chew 2000). As Ungar *et al.* (2007) pointed out, there is no one-to-one correspondence between diet and habitat, but a reasonable association exists between grazing and grass availability, as well as browsing and the presence of woody cover. They found strong evidence that dental microwear texture analysis is useful to distinguish extant African ruminant grazers from browsers; additionally, it was found that the method has a high potential for identifying fine-scale dietary differences. We therefore decided to address the question relating to the fine-scale diet differences within the grazer guild, combining the approaches of Ungar *et al.* (2003) with the ISO/DIS 25178 parameters (ISO/DIS 25178–2 2007). Two model organisms, the Grevy's Zebra (*Equus grevyi*) and the Blue Wildebeest (*Connochaetes taurinus*), were selected because they represent medium-sized, extant grazing ungulates inhabiting the grassland ecosystem of East Africa. Both species have a similar dietary trait but different post-oral digestive physiology. The Blue Wildebeest is a ruminant and thus a foregut fermenter, whereas the Grevy's Zebra, as a perissodactyl, is a hindgut fermenter. We would expect fundamental differences in the mode of occlusion to affect the texture signature and selected these two species because both have (convergently) reduced the bimodal chewing mode and have developed a similarly unimodal occlusion, with predominantly transversal chewing action (Janis and Fortelius 1988). This measure was taken to reduce the potential of occlusion-related distortion of the data due to the fundamentally different evolutionary history in the two model organisms selected (Fortelius 1985).

In ruminants, forage is not chewed extensively during ingestion (reviewed in Janis *et al.* 2010); the majority of particle size reduction in ruminants does not take place during ingestive chewing but during rumination (McLeod and Minson 1988). Ruminants and camelids are characterized by a unique sorting mechanism in their forestomach, which selectively retains large particles, and leads to their regurgitation and further communition via rumination (Clauss *et al.* 2010). This sorting mechanism is based on particle density rather than particle size (Lechner-Doll *et al.* 1991), but due to the correlation of particle size and density in the rumen ingests, the result is a discrimination not only according to density but also to size. The rumen contents are stratified in ruminants to varying degrees (Clauss *et al.* 2010), with particles being immersed in a fluid phase. In some ruminants, even a distinct "mud" or "sludge" layer can be observed at the bottom of the rumen (Hofmann 1973; Hummel *et al.* 2009), indicating a collection of high-density material. Material that is regurgitated for rumination, however, is recruited from the low-density material floating in the fluid layer of the rumen. We hypothesize that any grit adhering to the forage ingested by a ruminant will be washed off the forage and aggregate in this sludge layer. We therefore put forward the hypothesis that cud should be significantly less abrasive when compared with first ingested foods. In addition, we would expect cud chewing to more noticeably affect the distal part of the dentition, while the mesial cheek teeth should be slightly more confronted with grit-loaded first ingests. This might result in a mesio-distal wear gradient, with first ingests producing coarser wear signatures in the mesial part of the dentition.

The nonruminant *E. grevyi* relies on first ingests only, which subsequently have to be comminuted to particles small enough to make cell wall components available to bacterial fermentation in the hindgut. No cud washing takes place, and contaminated first ingests will be chewed.

The Model Organisms

E. grevyi prefers the semi-arid grass/shrub land where permanent sources of water are available (Klingel 1974; Rubenstein 1986; Rowen and Ginsberg 1992). It is predominantly a grazer, although browsing can make up to 30% of its diet during times of drought or in those areas that have been highly transformed through overgrazing (Codron *et al.* 2007; Moehlman *et al.* 2008). The specimen investigated was collected from lowlands with semi-arid grassland characteristics (Keast 1965). It was donated by Prof. H. Klingel in person and thus has good environmental data attached. It is indicated from observations and stomach contents of individuals from the Wamba region that their diet was strictly composed of grazed materials (Klingel 1974). Furthermore, Klingel (1974) suggests that even in the dry seasons the individuals preferred tough and brittle grass to the softer leaves of bushes. Additional soil eating was also observed.

The wildebeest (*C. taurinus)* inhabits the short-grass plains and requires water at least every day or two in the dry season (IUCN SSC Antelope Specialist Group 2008). Besides the grazing component, which consists mainly of fresh short grasses, up to 12% of materials from browsing can be included in the diet, depending on the season (Ego *et al.* 2003;

Gagnon and Chew 2000; Owaga 1975; Skinner and Smithers 1990).

Aim of the Study

The major aim of this study was to test functional parameters as specified in ISO/DIS 25178-2 and parameters derived from scale-sensitive fractal analysis (SSFA) as tools to functionally characterize complex dental surfaces (hypothesis 1 and 4). A second aim of the study was to differentially investigate the power of 3D-texture parameters and ISO/DIS 25178-2 and SSFA as toolsets for dental functional evaluation. The study however did not aim to test the power of those parameters to discriminate for specific dietary traits across the broad range of feeding types in ungulates (microwear texture approach; Merceron *et al.* 2010; Scott *et al.* 2005, 2006, 2009; Ungar *et al.* 2003) but focused on the functional signal (hypothesis 2).

We also proposed to test a very fundamental biomechanical mechanism that we expect to control dental wear and function to a very significant extent. Chewing action is the application of forces to anisotropic food components (Lucas 1982; Lucas *et al.* 2008). Applying forces always requires structures that hinder food from following pressure gradients and escaping from functional surfaces. As a consequence, central surfaces should thus in general encounter higher food pressure when compared with surfaces bordering the tooth at the buccal or lingual side; and higher pressures should, in turn, induce more abrasive wear due to more intimate food/tooth contacts. The signatures of abrasive wear along a bucco-lingual gradient were thus a subject of testing hypothesis 3.

Subsequently, we tested the following hypotheses:

Hypothesis 1: Nonruminating and ruminating physiological pathways should result in specific longitudinal functional gradients along the cheek tooth row. In particular, it would be expected that the unidirectional food passage in the nonruminating *E. grevyi* contrasts with the bi-directional food passage in the ruminating *C. taurinus*. The cause would be the likely separation of grit during gravity sorting in the rumen.

Hypothesis 2: Teeth receive their load from chewing forces that may act along three major vectors: (1) ortal, (2) transversal (bucco-lingual), and (3) propalinal (mesio-distal). Transversally oriented tooth relief features are thus loaded when mesio-distal components of the chewing force are applied. Wear-induced surface textures should thus reflect the specific mesio-distal loading pattern as a differential signal of the mesial and distal facets of each cusp. As cheek dentitions in both species have different curvatures, we would further expect this to be reflected in texture directions.

Hypothesis 3: Because both species chew in a unimodal pattern, the power stroke involves a chewing motion that is generally directed from buccal to lingual in the upper and from lingual to buccal in the lower dentition (Fortelius 1985). We would thus expect that central enamel ridges encounter more abrasion (tooth-food contacts) when compared with buccal and lingual enamel ridges, because they should be subjected to attritional (tooth/tooth) contacts to a lesser extent when compared with the buccal and the lingual enamel ridges (ectoloph). This functional difference should result in a gradient of surface textures of the four enamel ridges of the upper cheek dentition.

Hypothesis 4: Both parameters implemented in SSFA, as well as in industrial ISO/DIS 25178–2 3D surface texture parameters, quantify dental wear features (Leach *et al.* 2009), which originate from the processing of food by teeth. When applied to the same set of tooth facets, both sets of parameters should equally be capable of indicating subtle species-specific patterns in dietary traits, as has been shown for SSFA parameters by Ungar *et al.* (2003), Scott *et al.* (2005, 2006) and 2D parameters by Kaiser and Brinkmann (2006).

Materials and Methods

Materials

Upper and lower cheek dentitions of the two grazing ungulates, the Blue Wildebeest (*C. taurinus* BURCHELL, 1823; Bovidae, Cetartiodactyla; from Kajiado in Kenya, collected in September 1968) and the Grevy's Zebra (*E. grevyi* OUSTALET, 1882, Equidae, Perissodactyla; from Wamba in Kenya, collected in December 2002) were evaluated. All specimens analyzed are curated at the Zoological Museum of the University of Hamburg (ZMH). The second, third, and fourth premolar (P2, P3, and P4) and the first, second, and third molars (M1, M2, and M3) of the upper (tx) and lower (tm) tooth rows were examined. Sixteen well-defined wear facets per tooth were measured (Fig. 1).

Molding

After cleaning the tooth rows with ethanol, each facet was individually molded using the high-resolution silicone-A dental impression material Provil novo Light C.D. fast set EN ISO 4823, type 3, light (Heraeus Kulzer GmbH, Dormagen, Germany). To allow precise reconstruction of the orientation of

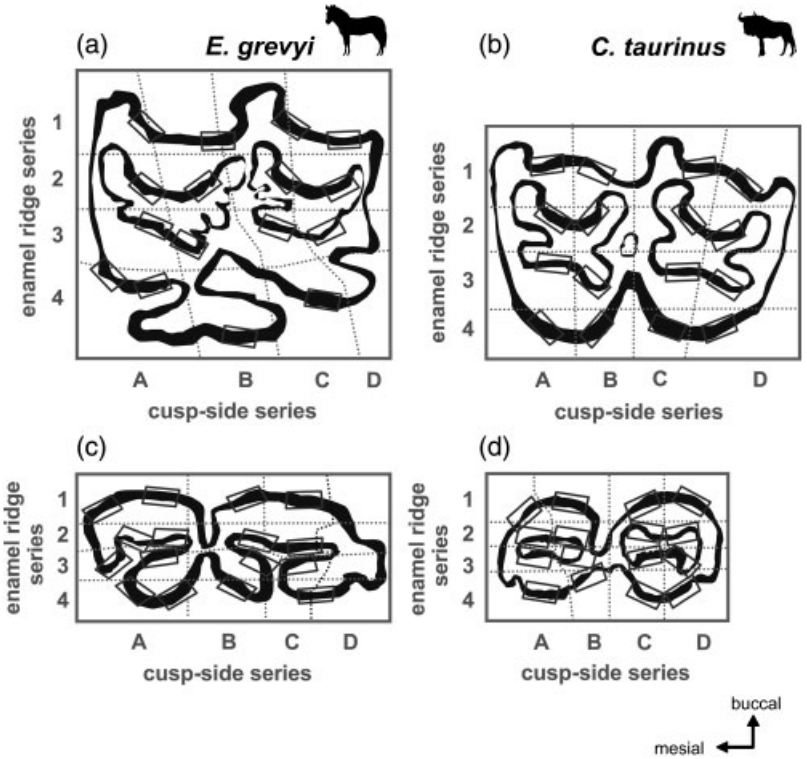

Fig 1. Occlusal enamel ridge pattern of the right upper (**a**) and lower (**c**) molar of *E. grevyi* [ZMH 9386] and *C. taurinus* [ZMH 6775] (**b** and **d**), specimens from the Zoological Museum Hamburg. Enamel facets are indicated by rectangles. The numbering of enamel ridges series counts from buccal to lingual (1–4). The numbering of the cusp-side series counts from mesial to distal, respectively, on the two cusps of the tooth (mesial spots A and C, distal spots D and B). Three to four measurements per facet were defined on each of the 16 facets. Taken together, one tooth may have up to 64 measurements.

the molds, a rectangular, bent copper wire (2×5 mm) was inserted in the mold so as to indicate the mesial and buccal directions of the tooth row in relation to the saggital plane of the skull (Fig. 2(a,b)). Microtiter plates with 96 wells (Carl Roth GmbH+Co KG, Karlsruhe, Germany) were used as specimen holders (Fig. 2(c,d)) of facet molds. Surface measurements were then taken directly on the mold, and data were reversed afterwards. This procedure was selected to avoid another step of casting and reversing the mold with resin.

Data Acquisition and Classification

The high-resolution disk scanning confocal microscope µsurf Custom (NanoFocus AG, Oberhausen, Germany), set to a $100 \times$ long distance objective, was used to acquire surface data, with a resolution in x, $y = 0.16\,\mu$m and $z = 0.06\,\mu$m, and a field of view of $160 \times 160\,\mu$m. When possible, four measurement fields per facet were collected to increase the sampling area. Measurements with less than 95% surface points captured and surface areas with defects, such as adherent dust particles and with a vertical displacement range $\delta z > 40\,\mu$m, were abolished, and measurements were repeated at a slightly different location on the same facet, if possible. 3D surface models were analyzed using two different methods.

The first approach is SSFA, as introduced into dental wear research by Scott *et al.* (2005, 2006). This approach uses SFrax and Toothfrax software packages (Surfract, www.surfract.com), based on the principle that a dimensional measurement (i.e., length, area, volume) of a rough surface is larger at fine scales than at coarser ones. Six SSFA parameters (Appendix A) were thus used to describe a wear surface: (1) complexity (*Asfc*), (2) scale of maximum complexity (*Smc*), (3) anisotropy (*epLsar*), (4) textural fill volume on a coarse scale (*Tfv*), (5) textural fill volume on a fine scale (*Ftfv*), and (6) heterogeneity (*HAsfc*, one feature per splitting).

The second approach applied is based on 3D industrial areal surface texture standards (ISO/DIS 25178–2 2007), using the same surface models. To generate parameters, we employed µsoft analysis premium v. 5.0 software (NanoFocus AG, Oberhausen, Germany; a derivative of Mountains® Analysis software by Digital Surf, Besançon, France). The following classes of ISO/DIS 25178 parameters were employed: (1) standardized height, (2) spatial, (3) hybrid, (4) functional, and (5) segmentation (ISO/DIS 25178-2 2007).

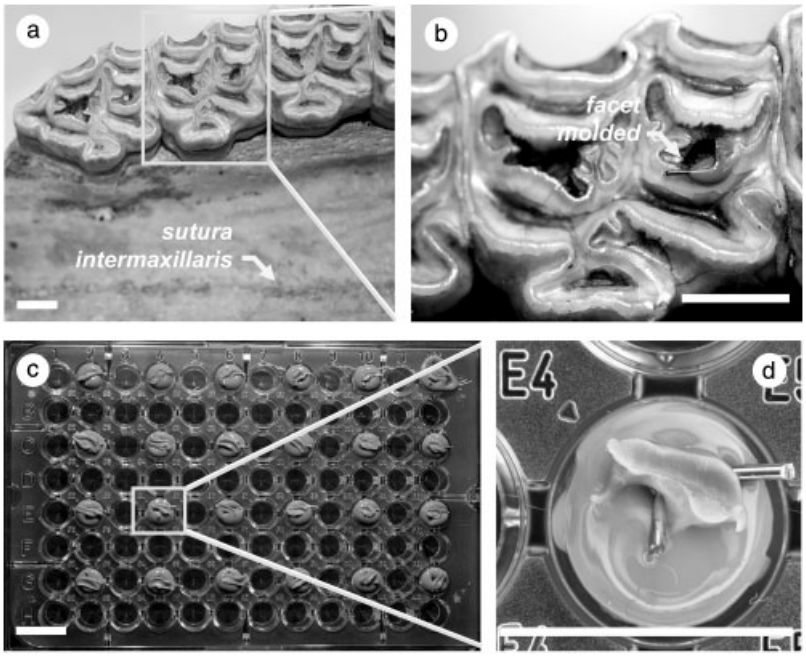

Fig 2. Molding and measuring facets. (**a**,**b**) The high-resolution impression-molding material is applied on the tooth facet of the third upper premolar. The copper wire is added on the molding material, orientated parallel to the sutura intermaxillaris, thereby indicating the mesio-distal and bucco-lingual directions of the tooth row. (**c**) A microtiter plate is used to arrange twenty-four tooth facet molds of *E. grevyi* for measurement. (**d**) The facet is turned upside down and mounted in the well E4 of the upper third premolar enamel ridge 3 and cusp-side series C. Scale bars = 10 mm.

Statistics

Subsequent statistical analysis was carried out using SYSTAT 12 (Systat Software, Inc., Chicago, IL), and predictions were tested using the following categorical variables: (1) tooth position, (2) cusp-side series—mesial and distal spots of the mesial and distal side of the cusp of each tooth, adopted from the numbering of phase I facets, according to Janis (1990) and Kaiser and Brinkmann (2006), (3) enamel ridge series (the position of the enamel ridge 1 to 4 as counted bucco-lingually, and (4) species (Fig. 1). Upper and lower tooth rows were analyzed separately. Each categorical variable can be divided into levels: (1) tooth position—second, third, and fourth premolar (P2, P3, and P4)—, and the first, second, and third molar (M1, M2, and M3), (2) cusp-side series—mesial side = series A and C and distal side = series B and D, (3) enamel ridge—four series counted from buccal to lingual, and (4) species—*E. grevyi* and *C. taurinus*. The categorical variables and their levels were used in the SSFA as well as in the discriminant analyses.

Scale-Sensitive Fractal Analysis

The SSFA analysis was done mainly according to Scott *et al.* (2006). But, we modified the statistical treatment and worked with parametric values and not with rank-transformed values as did by Scott *et al.* (2006), because Lix *et al.* (1996), Oshima and Algina (1992), and Tomarken and Serlin (1986) pointed out that even though nonparametric ranking procedures are independent of the normality assumptions, they are still affected by violations of the homogeneity of variances. Moreover, these procedures test for the equality of the distributions and not for the equality of the means, as in the *F*-test of variances (analysis of variance (ANOVA)).

Therefore, we tested each distribution first for the assumptions of normality and homogeneity of variances and secondly for the between-group differences on the SSFA parameters, using ANOVA (see Results: SSFA parameter selection). The violation of these assumptions can significantly increase type-I (probability to detect a false difference) and type-II (probability to not detect a genuine difference, related to the power of the test) errors (e.g., Keselman *et al.* 1998).

The parameters were first logarithmically transformed ($\log_{10}[1+\text{parameter}]$). The outliers were then identified for both original and log-transformed variables according to their Studentized residual values (absolute value greater than 3) and removed from the data set. Finally, we tested the distributions to identify those variables that would not violate the ANOVA assumptions. The normality assumption was tested using the Shapiro-Wilk, and Anderson-Darling test (Table I, Appendices B and C). Levene's (1960) tests were used to test for equality of the

TABLE I. Basic statistics of the SSFA parameters (*Asfc* = area-scale fractal complexity, *epLsar* = exact proportion length-scale anisotropy, log(*Tfv*) = $\log_{10}(1+Tfv)$ = textural fill volume) of both species

		E. grevyi			*C. taurinus*		
SSFA parameters	Tooth row[a]	LS Mean	SEM	*N*	LS Mean	SEM	*N*
Asfc	tx	177.199	7.349	63	206.078	14.273	39
	tm	126.664087	7.794777	56	190.180886	15.516816	33
epLsar	tx	0.001198	0.000042	63	0.001003	0.000050	39
	tm	0.001157	0.000045	56	0.000931	0.000054	33
log(*Tfv*)	tx	4.481	0.006	64	4.497	0.009	39
	tm	4.454	0.007	58	4.476	0.010	32
		tx			tm		
SSFA parameter	Species[b]	LS Mean	SEM	*N*	LS Mean	SEM	*N*
Asfc	*E. grevyi*	177.199	9.336	63	126.664	9.119	56
	C. taurinus	206.077839	11.865915	39	190.180886	11.879351	33
epLsar	*E. grevyi*	0.001198	0.000042	63	0.001157	0.000042	56
	C. taurinus	0.001003	0.000054	39	0.000931	0.000055	33
log(*Tfv*)	*E. grevyi*	4.481	0.006	64	4.454	0.007	58
	C. taurinus	4.497	0.008	39	4.476	0.009	32
		E. grevyi, tx			*C. taurinus*, tx		
SSFA parameter	Tooth position[c]	LS Mean	SEM	*N*	LS Mean	SEM	*N*
Asfc	P2	195.628	20.639	7			0
	P3	144.095	15.763	12	122.915	39.830	5
	P4	184.375	16.464	11	263.769	33.663	7
	M1	206.054	16.464	11	238.972	29.688	9
	M2	188.073	16.464	11	209.367	31.489	8
	M3	154.683	16.464	11	175.039	28.164	10
epLsar	P2	0.001110	0.000134	7			0
	P3	0.001185	0.000103	12	0.001182	0.000125	5
	P4	0.001104	0.000107	11	0.000935	0.000106	7
	M1	0.001136	0.000107	11	0.000897	0.000093	9
	M2	0.001162	0.000107	11	0.001067	0.000099	8
	M3	0.001463	0.000107	11	0.001005	0.000089	10
log(*Tfv*)	P2	4.481	0.018	8			0
	P3	4.473	0.014	12	4.461	0.025	5
	P4	4.479	0.015	11	4.519	0.021	7
	M1	4.488	0.015	11	4.518	0.019	9
	M2	4.498	0.015	11	4.481	0.020	8
	M3	4.469	0.015	11	4.493	0.018	10
		E. grevyi, tm			*C. taurinus*, tm		
SSFA parameter	Tooth position[c]	LS Mean	SEM	*N*	LS Mean	SEM	*N*
Asfc	P2	125.491	24.856	6			0
	P3	134.138	18.357	11	174.345	57.171	2
	P4	142.163	19.253	10	182.816	33.008	6
	M1	139.158	20.295	9	164.246	40.426	4
	M2	105.697	18.357	11	168.541	24.378	11
	M3	114.222	20.295	9	231.945	25.568	10
epLsar	P2	0.001232	0.000122	6			0
	P3	0.001138	0.000090	11	0.000807	0.000257	2
	P4	0.001008	0.000095	10	0.000880	0.000148	6
	M1	0.001248	0.000100	9	0.000999	0.000182	4
	M2	0.001169	0.000090	11	0.000995	0.000110	11
	M3	0.001191	0.000100	9	0.000887	0.000115	10
log(*Tfv*)	P2	4.490	0.022	5			0
	P3	4.478	0.014	13	4.496	0.036	2
	P4	4.446	0.016	10	4.441	0.021	6
	M1	4.441	0.016	9	4.485	0.023	5
	M2	4.450	0.015	11	4.467	0.017	9
	M3	4.427	0.016	10	4.498	0.016	10

TABLE I. Continued

		E. grevyi, tx			*C. taurinus*, tx		
SSFA parameter	Cusp side[d]	LS Mean	SEM	*N*	LS Mean	SEM	*N*
Asfc	A	171.507	13.960	15	199.161	25.141	13
	B	181.269	12.744	18	201.396	26.168	12
	C	206.600	13.517	16	168.944	30.216	9
	D	144.465	14.450	14	302.140	40.539	5
epLsar	A	0.001132	0.000095	15	0.000956	0.000080	13
	B	0.001170	0.000087	18	0.001031	0.000083	12
	C	0.001206	0.000092	16	0.001062	0.000096	9
	D	0.001297	0.000098	14	0.000951	0.000129	5
log(*Tfv*)	A	4.490	0.013	15	4.485	0.016	13
	B	4.482	0.012	18	4.521	0.016	12
	C	4.477	0.012	16	4.484	0.019	9
	D	4.476	0.013	15	4.494	0.025	5

		E. grevyi, tm			*C. taurinus*, tm		
SSFA parameter	Cusp side[d]	LS Mean	SEM	*N*	LS Mean	SEM	*N*
Asfc	A	103.698	19.824	9	196.927	27.448	9
	B	113.581	15.895	14	163.733	24.828	11
	C	141.532	14.424	17	211.878	29.113	8
	D	135.234	14.868	16	201.508	36.825	5
epLsar	A	0.001198	0.000101	9	0.000880	0.000118	9
	B	0.001107	0.000081	14	0.000925	0.000107	11
	C	0.001167	0.000073	17	0.001050	0.000125	8
	D	0.001167	0.000076	16	0.000843	0.000159	5
log(*Tfv*)	A	4.460	0.016	11	4.497	0.016	10
	B	4.453	0.014	14	4.452	0.016	10
	C	4.450	0.013	17	4.488	0.019	7
	D	4.454	0.013	16	4.468	0.023	5

		E. grevyi, tx			*C. taurinus*, tx		
SSFA parameter	Enamel ridge[e]	LS Mean	SEM	*N*	LS Mean	SEM	*N*
Asfc	1	179.761	13.518	18	195.778	30.834	10
	2	167.527	13.910	17	196.805	29.400	11
	3	193.890	14.338	16	255.331	43.607	5
	4	164.805	16.557	12	202.904	27.044	13
epLsar	1	0.001013	0.000082	18	0.000910	0.000087	10
	2	0.001334	0.000085	17	0.001152	0.000083	11
	3	0.001242	0.000087	16	0.000947	0.000123	5
	4	0.001226	0.000101	12	0.000969	0.000076	13
log(*Tfv*)	1	4.466	0.011	18	4.491	0.017	10
	2	4.481	0.011	17	4.474	0.016	11
	3	4.513	0.011	16	4.548	0.024	5
	4	4.463	0.013	13	4.502	0.015	13

		E. grevyi, tm			*C. taurinus*, tm		
SSFA parameter	Enamel ridge[e]	LS Mean	SEM	*N*	LS Mean	SEM	*N*
Asfc	1	97.776	16.392	13	215.116	27.451	9
	2	133.936	13.559	19	156.763	33.621	6
	3	132.833	20.896	8	185.422	31.127	7
	4	138.416	14.775	16	191.036	24.831	11
epLsar	1	0.001075	0.000079	13	0.000868	0.000115	9
	2	0.001258	0.000066	19	0.000911	0.000141	6
	3	0.000978	0.000101	8	0.001125	0.000131	7
	4	0.001193	0.000072	16	0.000869	0.000104	11

TABLE I. Continued

		E. grevyi, tm			*C. taurinus*, tm		
SSFA parameter	Enamel ridge[e]	LS Mean	SEM	*N*	LS Mean	SEM	*N*
log(*Tfv*)	1	4.431	0.014	13	4.480	0.017	9
	2	4.447	0.011	19	4.505	0.023	5
	3	4.466	0.017	9	4.478	0.020	7
	4	4.472	0.012	17	4.460	0.016	11

LS Mean, least square mean; *N*, number of facets measured, SEM, standard error of the mean.
[a]Categorical variable = upper/lower dentition (tm = teeth mandibular = lower dentition; tx = teeth maxillary = upper dentition).
[b]Categorical variable = species (*Connochaetes taurinus*, *Equus grevyi*).
[c]Categorical variable = tooth position (the second, third, and fourth premolar (P2, P3, and P4) and the first, second, and third molars (M1, M2, and M3).
[d]Categorical variable = cusp side (mesio-distally counted A, B, C, and D).
[e]Categorical variable = enamel ridge (bucco-lingually counted 1, 2, 3, and 4).

variances. A p-value smaller than 0.05 indicates non-normal distribution or heterogeneous variances.

Scott *et al*. (2006) found the SSFA parameters to be weakly correlated with each other and concluded that they can be treated as independent variables in future analyses. We concurred with their findings and performed five sets of one-way ANOVA instead of a MANOVA. The first set tested for differences between the upper and lower tooth rows of both species. As significant differences were found in *E. grevyi* (Appendix C), the upper and lower tooth rows were separately analyzed in the ANOVA. We subsequently tested for differences between the two species; between the six tooth positions, between the four cusp-side series, and between the four enamel ridge series within a single species on each tooth row. When the ANOVA was found significant, two post-hoc tests, Fisher's least significance difference (Fisher's LSD) and Tukey's honestly significance difference (Tukey's HSD), were performed to determine the source of significant variation (Table II).

TABLE II. Post-hoc tests summary

	E. grevyi, tx				*E. grevyi*, tm	
Cusp side	B	C	D	Enamel ridge	2	3	4
A				1	***log(Tfv)***		
B				2	log(*Tfv*)		
D		***Asfc***		3			***log(Tfv)***

Only significant results according to the SSFA parameters *Asfc* and log(*Tfv*) are shown for the cusp-side and enamel ridge series on the upper (tx) and lower (tm) tooth row; p-values lower than 0.05 are indicated in regular case for Fisher's LSD and in bold italic case for both Fisher's LSD and Tukey's HSD tests.

3D Areal Surface Texture Standards (ISO/DIS 25178-2 2007)

The following tools of the µsoft analysis premium software were applied on the original 3D-surface models before using the built-in "texture direction standard" and the ISO/DIS 25178 standards: (1) mirroring in x and z, leveling (least square plane by subtraction), (2) spatial filtering (denoising median 5×5 filter size and Gaussian 3×3 filter size), (3) erasing nonmeasured points (a selection dependent value = mean), and (4) form removal (polynomial of increasing power = 2).

A total of 16 discriminant analyses were performed (run ♯1–16, Table III) to test the potential of the metric parameters (ISO/DIS 25178–2 2007) to separate levels on the base of the predefined categorical variables used in the SSFA analyses ((1) tooth position, (2) cusp-side series, (3) enamel ridge; and (4) species). In all discriminant analyses performed, we employed the incremental forward-stepping algorithm. The default settings of SYSTAT 12 were used to generate *F*-ratios to rank metric parameters. In this way, those parameters were identified that allow best discrimination of levels within the categorical variables and being further discussed.

The 16 discriminant analyses can be divided into 5 sets (Table III); all sets differentiate between upper and lower teeth. In the first set (run ♯1–4), tooth position was used as a categorical variable. The second set (run ♯5–8) was undertaken to test whether the two mesial and two distal cusp sides are different in their surface texture within the species *E. grevyi* and *C. taurinus*. The aim of the third set (run ♯9–12) was to test whether the enamel ridges as defined in Figure 1 are different within the two species. The fourth set (run ♯13–14) was performed with species as the categorical variable. Additionally, runs ♯15–16 were performed with species as the categorical variable, including only the five most powerful surface parameters (*Sal*, *Std*, *Shv*, *Spd*, and *Sq*). Eigenvalues, Wilks' lambda, approximate *F*-ratio, degree of freedom (df), p-value, and the percentage of jackknifed classification matrices are given for each set in Table III. The entire set of the 30 surface texture parameters (ISO/DIS 25178–2 2007) were used as metric variables to compute the discriminant function.

TABLE III. Discriminant analysis performed using the surface texture parameters (according to ISO/DIS 25178-2) as metric variables

Run ♯	Metric variable	Categorial variable	Species	Tooth row	Eigenvalue	Wilks' lambda	Approx. *F*-ratio	df		p-value	JCM
1	30 parameters	Tooth position	*E. grevyi*	tx	0.306	0.766	4714	5	77	0.001	22
2	30 parameters	Tooth position	*E. grevyi*	tm	0.162	0.861	2398	5	74	0.045	24
3	30 parameters	Tooth position	*C. taurinus*	tx	2.293	0.234	4128	20	150	0	24
4	30 parameters	Tooth position	*C. taurinus*	tm	NA	NA	NA	NA	NA	NA	NA
5	30 parameters	Cusp side	*E. grevyi*	tx	0.215	0.714	3102	9	172	0.002	43
6	30 parameters	Cusp side	*E. grevyi*	tm	0.134	0.833	2398	6	150	0.031	36
7	30 parameters	Cusp side	*C. taurinus*	tx	0.262	0.745	2589	6	98	0.023	44
8	30 parameters	Cusp side	*C. taurinus*	tm	0.161	0.861	2358	3	44	0.085	21
9	30 parameters	Enamel ridge	*E. grevyi*	tx	0.425	0.638	6554	6	156	0	51
10	30 parameters	Enamel ridge	*E. grevyi*	tm	0.521	0.4	3618	21	198	0	54
11	30 parameters	Enamel ridge	*C. taurinus*	tx	0.369	0.657	3813	6	98	0.002	43
12	30 parameters	Enamel ridge	*C. taurinus*	tm	0.316	0.647	3487	6	86	0.004	46
13	30 parameters	Species	All	tx	0.399	0.715	23313	10	584	0	74
14	30 parameters	Species	All	tm	0.108	0.903	13379	4	496	0	62
15	*Sq*, *Sal*, *Shv*	Species	All	tx	0.301	0.769	59940	3	597	0	72
16	*Spd*, *Std*	Species	All	tm	0.077	0.929	19.535	2	508	0	60

Run ♯ = identification number of the data set grouped by categorical variables (tooth position, cusp side, enamel ridge, and species (*Equus grevyi* and *Connochaetes taurinus*)), JCM = Jackknifed classification matrix (%total correct classification). NA = data not available, insufficient variables in the model.

Results

SSFA Parameter Selection

Normality and homogeneity tests led to the observation that only parameters *Asfc*, *epLsar,* and log(*Tfv*) met the normality and homogeneity conditions in both species (Appendix B). This appears to reflect an issue of critically low sample size in some categorical variables. Most likely, this is due to the smaller numbers of homologue facets in *C. taurinus* when compared with *E. grevyi* and also to the fact that lower teeth are narrower and thus *per se* have fewer homologous facets than upper cheek teeth.

Testing for mesio-distal gradients along the tooth row (hypothesis 1)

Scale-sensitive fractal analysis: No significance was found in inter-tooth variation; however, we found a decrease in texture fill volumes (*Tfv*) toward the distal pole of the *E. grevyi* cheek tooth row. In *C. taurinus*, this gradient was not evident (Fig. 3(a,b)).

3D areal surface texture standards (ISO/DIS 25178): The autocorrelation length parameter (*Sal*) shows another gradient in *C. taurinus* cheek dentition (Fig. 3(d)). This parameter is a measure of the wavelength of surface texture and indicates that mesial teeth in *C. taurinus* have longer wavelength textures in contrast to distal teeth. *E. grevyi* did not show such gradient in *Sal* (Fig. 3(c)). Both species investigated show a remarkable difference in the curvature of their cheek tooth rows (Fig. 3). Texture directions in *C. taurinus* dentition show an inclination toward the saggital plane from mesial to distal, with the smallest angles being on the distal teeth and the largest angles being on the mesial teeth (Fig. 3(f)). *E. grevyi* dentition lacks such gradient (Fig. 3(e)). Using "tooth position" as a categorical variable results in eigenvalues ranging from 0.162 in the lower tooth row of *E. grevyi* to 2.293 in the upper tooth row of *C. taurinus*. The correctly classified cases give the lowest values (22–24%, run ♯1–4, Table III) when compared with the other categorical variables (cusp-side series, enamel ridge, tooth position, and species; see below).

Testing for mesio-distal gradients within cusps (hypothesis 2)

Scale-sensitive fractal analysis: In mesial and distal cusp sides of *E. grevyi* upper cheek teeth, only the mesial facets of the metacone and metaloph (cusp-side series C; Fig. 4(a), Tables I and II, Appendix C) display significantly higher texture complexity (*Asfc*) than the distal facets of the metacone, metaloph, and hypocone (cusp-side series D; Fig. 4(a), Tables I and II, Appendix C). *C. taurinus* does not show significant differences in textures of cusp-side series although there are high values of texture complexity in the cusp-side series D (Fig. 4(b)). The *Tfv* values (textural fill volume, in log scale) did not display significant differences in both species (Fig. 5). We therefore saw no sufficient indication for the presence of a mesio-distal gradient in surface texture signatures within a tooth.

3D areal surface texture standards (ISO/DIS 25178): To test for intra-tooth variation along the upper or lower teeth, ISO/DIS 25178 parameters were tested using discriminant analysis. Bar charts using the

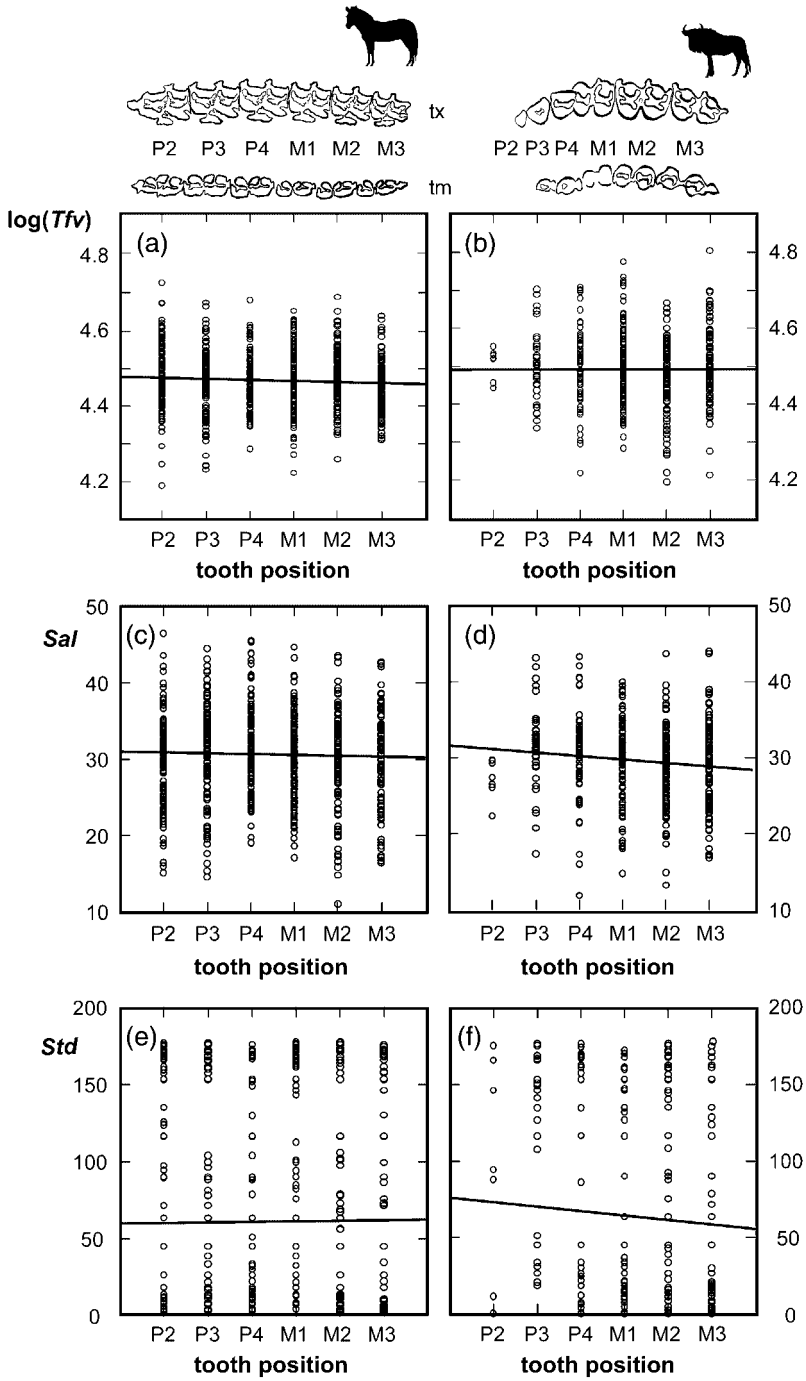

Fig 3. Scatter plots indicating values of the SSFA parameter *Tfv* = texture fill volume (in log scale), ISO/DIS 25178 parameters autocorrelation length (*Sal* in μm), and texture direction (*Std* in °) of upper (tx) and lower (tm) teeth, sorted according to tooth position (second, third, and fourth premolar = P2, P3, and P4; first, second, and third molar = M1, M2, and M3) for *E. grevyi* (**a**, **c** and **e**) and *C. taurinus* (**b**, **d**, and **f**).

autocorrelation length (*Sal*) and texture direction (*Std*) parameters, depending of the cusp-side series, are given in Figs. 6 and 7, respectively. Investigating cusp-side series (A–D) as a categorical variable to test for mesio-distal gradients within all six tooth positions of a tooth row (upper/lower, respectively) results in generally low eigenvalues, ranging between 0.134 in the lower tooth row of *E. grevyi* and 0.262 in the upper tooth row of *C. taurinus*. Hence, the percentage of correctly classified cases is very low (21–44%, run ♯5–8, Table III). This indicates that textures are not different in the four cusp-side series of the two species.

Testing for bucco-lingual gradients (hypothesis 3)

Scale-sensitive fractal analysis: The third enamel ridge has a significantly higher textural fill volume (*Tfv* in log scale) compared with the remaining three

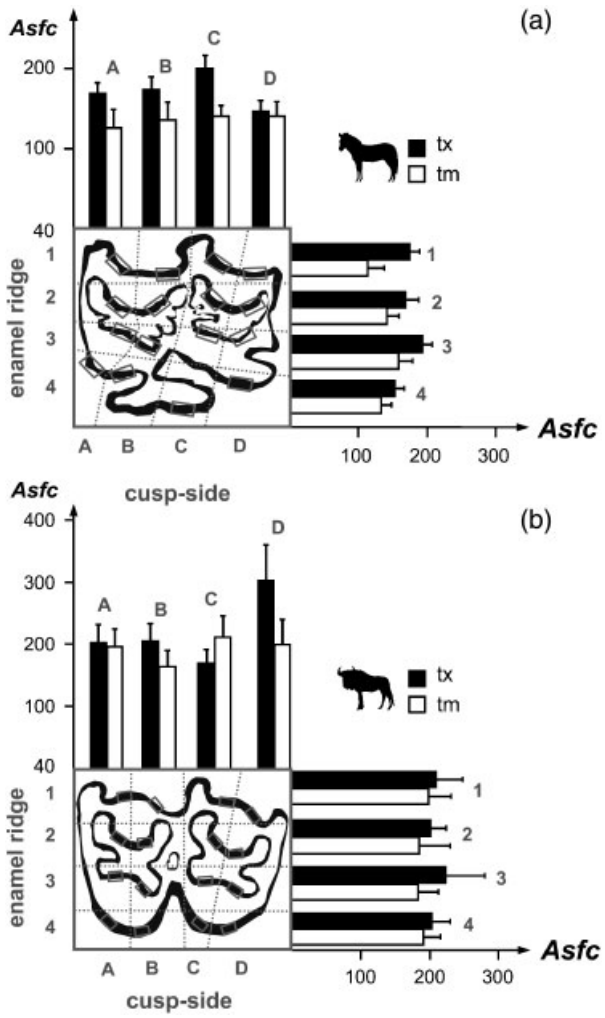

Fig 4. Bar charts indicating mean and standard error of the mean of the SSFA parameter *Asfc* = area-scale fractal complexity; values of the upper (tx) and lower (tm) teeth sorted according to cusp-side series (A–D) and enamel ridge (1–4) for *E. grevyi* (**a**) and *C. taurinus* (**b**). The enamel ridges and cusp sides of a second upper molar are shown exemplarily to display the enamel ridge and cusp-side series.

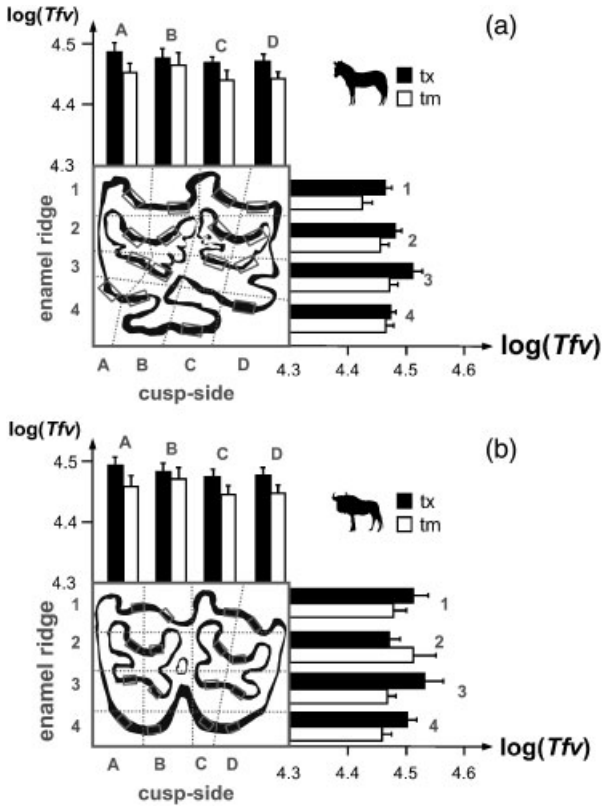

Fig 5. Bar charts indicating mean and standard error of the mean of the SSFA parameter *Tfv* = texture fill volume values of the upper (tx) and lower (tm) teeth, according to cusp- side series (A–D) and enamel ridge (1–4) for *E. grevyi* (**a**) and *C. taurinus* (**b**).

upper tooth enamel ridges of *E. grevyi* (Fig. 5(a), Tables I and II, Appendix C). In *C. taurinus,* no signal is evident (Fig. 5(b))

3D areal surface texture standards (ISO/DIS 25178): Investigating enamel ridges (1–4) as categorical variables results in generally low eigenvalues, ranging between 0.316 in the lower tooth row of *C. taurinus* and 0.521 in lower tooth row of *E. grevyi*. The low eigenvalues in the discriminant function, using the ISO/DIS parameters, indicate that the enamel ridges have very similar surface textures in both species. Nevertheless, we noted some variability between the enamel ridges using the parameters *Sal* and *Std* (Figs. 6 and 7). In particular, the third upper enamel ridge displays the highest value for *Sal* in *C. taurinus* only. But correctly classified cases are as low as 43–54% (run ♯9–12, Table III). This indicates again that the four enamel ridges are only slightly more variant (>9%) in their textures than the cusp-side series. Textures cannot be employed as a predictor.

Testing for resolution in dietary reconstruction (hypothesis 4)

Scale-sensitive fractal analysis: *E. grevyi* has higher *epLsar* values (exact proportion length-scale anisotropy) than *C. taurinus* on both upper and lower tooth rows (Fig. 8(c), Tables I and II, Appendix C). The latter has higher *Asfc* values (area-scale fractal complexity) and *Tfv* values (textural fill volume in log scale) than has *E. grevyi* on the lower tooth row (Fig. 8(a,b)). Thus, a higher complexity of surface features is observed in *C. taurinus* in contrast to *E. grevyi*. We interpreted this as a species-specific feature. A typical facet surface texture is shown as photo simulation and meshed axiomatic 3D model in Figure 9.

3D areal surface texture standards (ISO/DIS 25178): Testing for species discrimination results in the most distinct pattern, using 3D surface texture parameters as metric variables. Upper tooth rows of *E. grevyi* and *C. taurinus* result in an eigenvalue of 0.399 at a percentage of 74% correctly classified cases (run ♯13, Table III) and gives the highest values, compared with the remaining categorical variables.

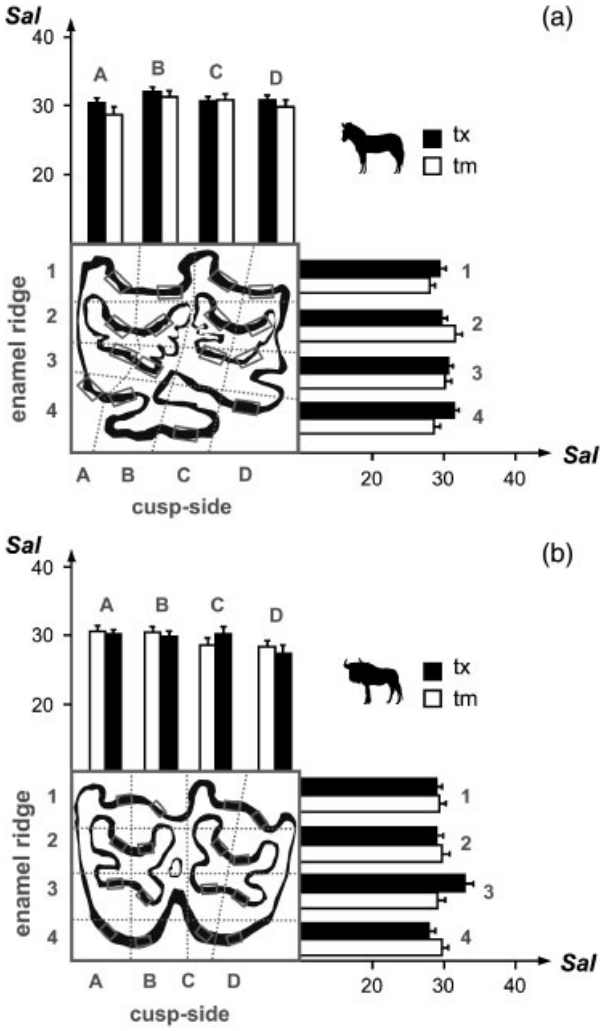

Fig 6. Bar charts indicating mean and standard error of the mean of the surface texture parameter autocorrelation length (*Sal* in μm, ISO/DIS 25178), identified as separating the two extant species with the highest degree of probability. The bar charts show the *Sal* values of the upper (tx) and lower (tm) teeth, sorted according to cusp-side series (A–D) and enamel ridge (1–4) for *E. grevyi* (**a**) and *C. taurinus* (**b**).

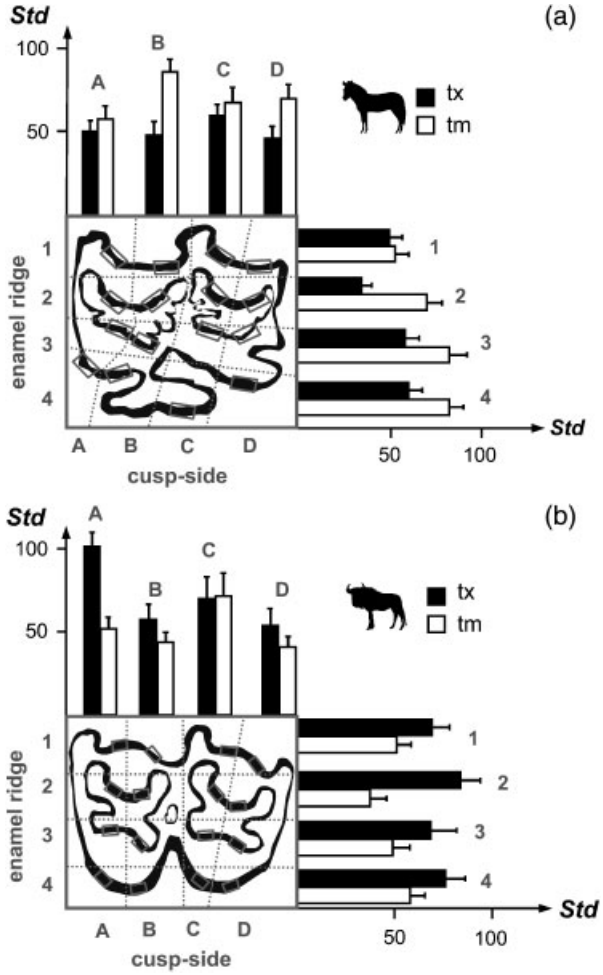

Fig 7. Bar charts indicating mean and standard error of the mean of the surface texture parameter texture direction (*Std* in °, ISO/DIS 25178), identified as separating the two extant species with the highest degree of probability. The bar charts show the *Std* values sorted according to cusp-side series (A–D) and enamel ridge (1–4) for *E. grevyi* (**a**) and *C. taurinus* (**b**).

Lower tooth rows of both species are signified in less correctly classified cases (62%, run ♯14, Table III). On the basis of these two analyses, we identified five 3D texture parameters to allow discrimination of the two species investigated with the best probability: (1) *Sq* (F-to-enter/remove = 115.381), (2) *Sal* (F-to-enter/remove = 28.576), (3) *Spd* (F-to-enter/remove = 25.391), (4) *Shv* (F-to-enter/remove = 24.648), and (5) *Std* (F-to-enter/remove = 12.934). Inclusion of only those five parameters decreases the percentage of correctly classified cases by only 2% in both upper and lower tooth rows (run ♯15–16, Table III).

Compiling all categorical variables employed to classify facet loci of molars and premolars in the two ungulate species, 18 of the set of thirty tested parameters (Appendix D) have a significant *F*-to-enter/remove values ($P<0.05$). Those parameters are the most powerful and are listed in Table IV. Of these 18 parameters, we identified only two (*Sal*, autocorrelation length and *Std*, texture direction) that result in significant F-to-enter in each categorical variable (Table IV). Therefore, both *Sal* and *Std* are further discussed and used for plotting charts (Figs. 5, 6 and 8(d,e)).

Sal-Parameter (*autocorrelation length*): The *Sal* is only slightly variable and ranges around 30 μm in the cusp-side series of both species (Figs. 6 and 8(d)). *Sal* does not significantly indicate differences in textures in the six tooth positions (P2–M3; Fig. 3(c,d)) nor does it indicate that mesial or distal facets on a given cusp, or buccal and lingual facets along the tooth row, are different in their textures (Fig. 6). This applies to both species. Upper teeth have slightly higher autocorrelation lengths compared with lower teeth in *E. grevyi* (Fig. 6(a)). In *C. taurinus*,

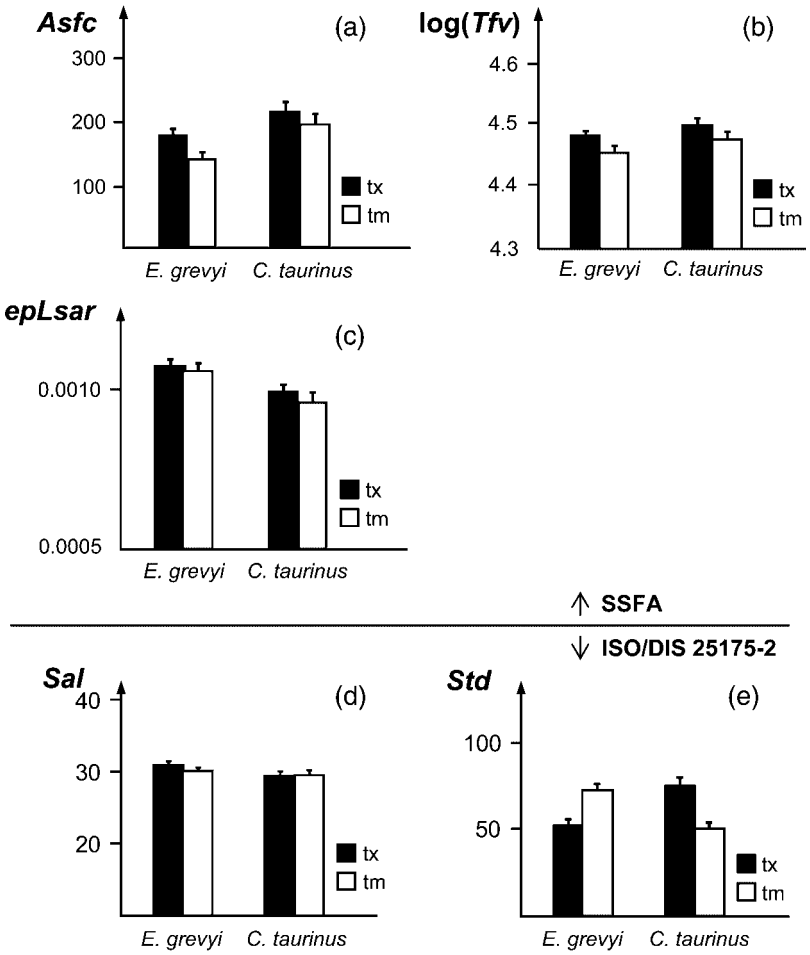

Fig 8. Bar charts indicating mean and standard error of the mean of the SSFA parameter (**a**) *Asfc* = area-scale fractal complexity, (**b**) *Tfv* = texture fill volume (in log scale), (**c**) *epLsar* = exact proportion length-scale anisotropy; and the ISO/DIS 25178 parameters (**d**) autocorrelation length (*Sal*), and (**e**) texture direction (*Std*,); values of the upper (tx) and lower (tm) teeth for *E. grevyi* and *C. taurinus*.

the opposite is observed; lower teeth have slightly higher *Sal* values (Fig. 6(b)).

Std-Parameter (*texture direction*):*Std* is found to be more heterogeneous than the *Sal* in each of the categorical variables tested (Figs. 6 and 7). Both species *Std* values range between 30° and 145°. In *E. grevyi,* lower teeth *Std* exceeds values of upper teeth (Fig. 7(a)). In *C. taurinus*, we found an exactly reverse pattern, in which the upper teeth *Std* exceeds values of the lower teeth (with the exception of the upper P2; Fig. 7(b)).

Discussion

Testing for mesio-distal gradients along the tooth row (hypothesis 1)

Along the cheek tooth row (upper and lower), we found a mesio-distal gradient in textural fill volumes (*Tfv*) for *E. grevyi* and in auto correlation length (*Sal*) and texture direction (*Std*) for *C. taurinus* (Fig. 3). Textural fill volumes decrease in the distal-tooth positions in *E. grevyi* (Fig. 3(a)). *E. grevyi* accomplishes all comminution on first ingestion of foods, which leads to a unidirectional food passage along the oral cavity (as in most animals). Grit-contaminated foods will thus always first contact the mesial teeth initially although distal teeth will contribute in comminution. This will also result in coarse-grit contamination, which will more severely affect mesial teeth; distal teeth will encounter reduced particle sizes of such abrasive agents. Coarse particles should produce coarser scars and thus more volume in texture signatures. The slightly reduced particle size experienced by the distal portion of the cheek dentition can then explain their smaller texture fill volumes. In *C. taurinus*, this gradient is not evident (Fig. 3(b)). Although this species also ingests grit-contaminated grass forage, the regurgitation process causes a bi-directional food passage in *C. taurinus*'s mouth. Cud, on the other hand, will

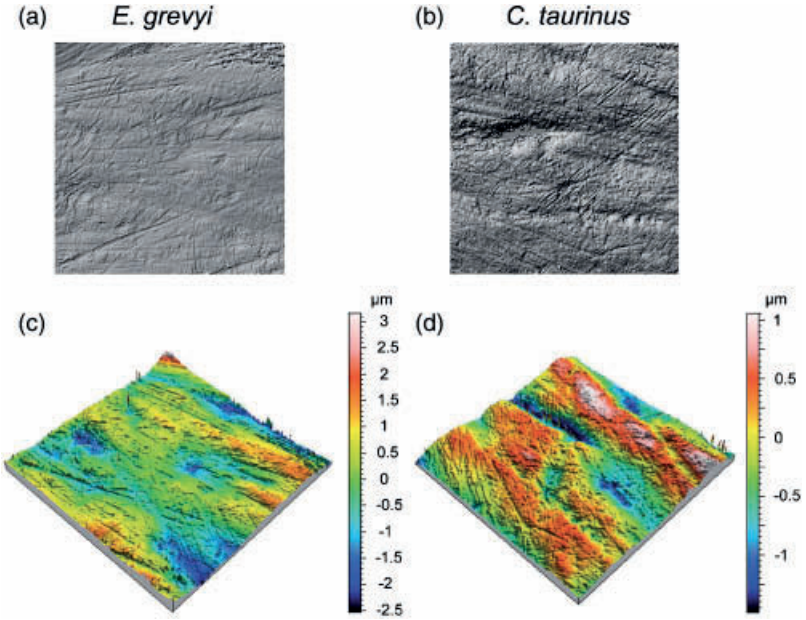

Fig 9. Photo simulations and meshed axiomatic 3D models of tooth enamel surfaces of *E. grevyi* (**a** and **c**) and *C. taurinus* (**b** and **d**). Each picture represents a field of view of 160 × 160 µm of the facet at the second upper molar, cusp-side A, enamel ridge 2.

TABLE IV. Occurrence of the 18 surface texture parameters (according to ISO/DIS 25178-2), identified as separating the extant species with the best probability using the discriminant analyses

Run#	Categorial variable	Tooth row	Species	*Sal*	*Std*	*Sda*	*Shv*	*S5v*	*Sku*	*Str*	*Spd*	*Vvc*	*Vm*	*Sa*	*Sha*	*Sdv*	*Sq*	*Sv*	*Sxp*	*Vmc*	*Vvv*
1	Tooth position	tx	*E. grevyi*									1									
2	Tooth position	tm	*E. grevyi*	1																	
3	Tooth position	tx	*C. taurinus*				1			1		1		1							1
4	Tooth position	tm	*C. taurinus*		1					1											
5	Cusp side	tx	*E. grevyi*					1							1	1					
6	Cusp side	tm	*E. grevyi*				1		1												
7	Cusp side	tx	*C. taurinus*		1				1												
8	Cusp side	tm	*C. taurinus*			1															
9	Enamel ridge	tx	*E. grevyi*		1			1													
10	Enamel ridge	tm	*E. grevyi*	1		1		1			1		1					1		1	
11	Enamel ridge	tx	*C. taurinus*	1									1								
12	Enamel ridge	tm	*C. taurinus*			1													1		
13	Species	tx	All	1			1										1				
14	Species	tm	All		1						1										
			n_occurrence	4	4	3	3	3	2	2	2	2	2	1	1	1	1	1	1	1	1

n_occurence = occurrence of the surface texture parameter with the best probability within the datasets employed in the discriminant analyses; for parameter description see Appendix D.

always be far less loaded with abrasive grit when compared with first ingest. We would therefore suggest that chewing cud will level the texture gradient caused on first ingestion and result in a less pronounced mesio-distal gradient in texture fill volumes.

Another gradient is evident in autocorrelation length parameter (*Sal*) in *C. taurinus* cheek dentition (Fig. 3(d)). This parameter is a measure of the wavelength of surface texture and indicates that mesial teeth in *C. taurinus* have longer wavelength textures in comparison to distal teeth. We interpreted this signal to reflect the "washing effect" experienced by the distal portion of *C. taurinus*'s dentition due to cud chewing. Unlike the texture fill volume parameter, the autocorrelation length parameter seems to capture this functional gradient as proposed by our hypothesis 1. *E. grevyi*, which lacks rumination, does not show a similar gradient but displays a constant autocorrelation length signature along the entire tooth row (Fig. 3(c)).

Both species investigated show a remarkable difference in the curvature of their cheek tooth rows (Fig. 3). Compared with *C. taurinus*, the tooth row of *E. grevyi* is rather straight and far less curved. With the saggital plane as reference, we would expect the curvature to be reflected by the direction of texture. In fact, observations support this hypothesis. Texture directions in *C. taurinus* dentition show an inclination toward the saggital plane from mesial to distal, with the smallest angles existing on the distal teeth and the largest angles arising on the mesial teeth. Our hypothesis is further supported by the lack of such gradient in *E. grevyi* dentition, which is far less curved.

Testing for mesio-distal gradients within cusps (hypothesis 2)

Differences between textures of mesial and distal cusp sides (mesial facets A and C and distal facets B and D; Fig. 1) are only evident in the upper cheek dentition of *E. grevyi*. In this study, mesial facets of the metacone and metaloph (C) are more complex in texture, as indicated by the parameter *Asfc* in SSFA (Fig. 4(a)). The lower cheek dentition of *E. grevyi* and the upper and the lower dentition of *C. taurinus* do not show such signals (Fig. 4(b)). ISO/DIS parameters, however, do not indicate differential textures in either species (Figs. 6 and 7).

We therefore concluded that mesial and distal facets in the two grazing ungulates have the same texture signature, which would indicate the same functional trait. This finding does not support our hypothesis 2, which suggests that mesial and distal facets should have different textures because they receive their occlusal load from different vectors of the chewing motion. Assuming a mesowear profile as suggested by Fortelius and Solounias (2000), and assuming the capability to perform mesio-distally oriented jaw movements to a certain degree, distal facets of upper cheek teeth should be loaded by distal chewing force vectors and vice versa. In the two grazers investigated, however, the mesowear profile is dominated by low reliefs and blunt cusps (Fortelius and Solounias 2000) and thus, antagonistic facets would not produce reactive forces. The lack of mesio-distally oriented forces in a flat post-canine dentition would then account for functional homogeneity of mesial and distal cusp faces. We thus would interpret the lack of differential textural signals as rather to signify the grazing niche and would, in turn, expect more variant textures in those species exhibiting more occlusal relief, which is commonly related to a more browse-dependent feeding trait (Fortelius and Solounias 2000).

Testing for bucco-lingual gradients (hypothesis 3)

The third enamel ridge has a significantly higher textural fill volume (*Tfv* in log scale; one of the SSFA parameters) when compared with the remaining three upper tooth enamel ridges of *E. grevyi* (Fig. 5(a), Tables I and II, Appendix C). In *C. taurinus*, however, no signal is evident (Fig. 5(b)). We would relate this to the width of the respective enamel ridges, of which the third is the narrowest and the ectoloph, the thickest. This applies to both enamel ridges of the ectoloph (the mesial and the distal). Although we are aware of the limited sample in this study, we got the impression that both the buccal and the lingual ectoloph have the lowest fill volumes, which immediately translates into a smoother surface texture. Smooth surface textures, however, have been shown to be indicative of a more attrition-dominated wear (Kaiser and Brinkmann 2006), in comparison to the more centrally oriented enamel ridges (2 and 3). We thus found this to be a strong argument for our hypothesis that central enamel ridges should encounter less attrition and more abrasion, because peripheral ridges function as guidance structures that encounter significant attrition but leave pure abrasional contacts to the more central ridges of a tooth

Testing for resolution in dietary reconstruction (hypothesis 4)

Compared with *C. taurinus*, *E. grevyi* is consistently regarded as a pure grazer. Besides what it grazes, *C. taurinus* eats up to 12% of browse (Gagnon and Chew 2000). *E. grevyi*'s diet consists of long and dry grass, which is even preferred when fresh grass is available (Klingel 1974). This forage is more brittle than the short but predominantly fresh and green lawn-like grassland forage of *C. taurinus* (Skinner and Smithers 1990). In addition, eating long grass involves less feeding close to the ground and thus less contamination with soil and ground-born grit in *E. grevyi*'s diet. The lower complexity (*Asfc*) in textures (Fig. 8(a)) and the lower textural fill volume (log(*Tfv*); Fig. 8(b)) found in *E. grevyi*'s diet impressively reflect the lack of deep gouges and scars on the tooth surface, produced by coarse ground-born grit and sand grains, which *C. taurinus* obviously can not avoid ingesting. The higher anisotropy (*epLsar*; Fig. 8(c)) in *E. grevyi* indicates a more structured orientation of scars. The scars are initially oriented more or less parallel to each other and also parallel to the saggital axes of the mouth. We would interpret this as reflecting the distinctive wear pattern

that must result from chewing long grass. In general, Ungar *et al*. (2007) also found high anisotropy and low complexity in wear textures of extant grazers with SSFA; however, no subtle signatures within different grazing traits could be resolved. The signatures we found in upper cheek teeth of both species are also consistently observed in lower cheek teeth (Figs. 4–8). This consistency is a strong indication that this is a species-specific dietary signature. We would thus interpret the shift within texture signatures observed between the two species as precisely reflecting the different dietary strategy of the two taxa, within the general niche of a grazer. The ISO/DIS 25178-2 parameter *Sal* (autocorrelation length; Fig. 8(d)) does not seem to capture those subtle traits, as is being indicated by the similarly low wavelength, which we tentatively would interpret as signifying a rather robust general grazing signal.

Conclusion

The SSFA as well as ISO/DIS 25178 parameters are found to be very promising tools in standardized and quantitative analyses of tooth enamel facets of extant ungulates. On the one hand, strong arguments are found that central enamel ridges encounter less attrition and more abrasion, because peripheral ridges function as guiding structures that encounter significant attrition but leave pure abrasional contacts to the more central ridges of a tooth. On the other hand, functional mesio-distal gradients in the enamel surface textures were not detected. Furthermore, SSFA and ISO parameters allow distinctions among the subtle dietary strategies that evolved in herbivorous ungulates with fundamentally different systematic affinities but which exploit a similar dietary niche.

Acknowledgements

This research was supported by the "Deutsche Forschungsgemeinschaft" (DFG, German Research Foundation, KA 1525/8-1) and is publication no. 12 of the DFG Research Unit 771 "Function and performance enhancement in the mammalian dentition—phylogenetic and ontogenetic impact on the masticatory apparatus". E. Schulz and T. M. Kaiser are very grateful to P. S. Ungar and J. R. Scott (both at the University of Arkansas) for the fruitful discussions about microwear texture as well as their warm welcome and hospitality during the visit at the University of Arkansas in 2008. We acknowledge A. Roeder and M. Skiba (both at the University of Hamburg) for assistance in operating the disk scanning confocal microscope and M. Clauss (University of Zürich) for discussion about digestive strategies in ruminants. The authors thank the reviewers for their constructive and helpful comments that improved the manuscript.

Appendix A

TABLE A1. Description and example case of the SSFA parameters according to Scott *et al*. (2005, 2006)

Parameter	Name	Description	Example
Afsc	Area-scale fractal complexity	Change of the surface roughness with scale	A surface with pits and scratches of different sizes would have a high *Asfc*
Smc	Scale of maximum complexity	The scale at which *Asfc* is the largest	Less wear at fine scales and/or more at coarse scales, e.g. large pits without fine scratches, results in greater *Smc* values
epLsar	Exact proportion length-scale anisotropy	A measure of the orientation of the surface wear features	A surface characterized by the scratches running in the same direction is expected to have high *epLsar* values
Tfv/*Ftfv*	Textural fill volume	Computed by filling a surface with square cuboids of a given scale. The surface waviness is removed so that only the roughness is examined	A surface showing many wear features at the computational scale is expected to have a high *Tfv*/*Ftfv*
HAsfc	Heterogeneity of area-scale fractal complexity	Calculated by splitting a surface into smaller sections with equal numbers of rows and columns. *Asfc* for each section and its median for each surface is then calculated	A surface with variations of features across the area would have a high *HAsfc* *HAsfc*9, for example, is the heterogeneity associated with a 3×3 splitting of the surface

Appendix B

TABLE B1. Normality and variance homogeneity tests summary

SSFA parameter	Species	Tooth row	Tooth						Cusp side						Enamel ridge					
			LEV		SW		AD		LEV		SW		AD		LEV		SW		AD	
			Test	p	Test	p	Test	p	Test	p	Test	p	Test	p	Test	p	Test	p	Test	p
Asfc	*E. grevyi*	tx	1.898	0.109	0.982	0.490	0.353	>0.15	0.603	0.615	0.989	0.839	0.260	>0.15	1.026	0.388	0.984	0.571	0.334	>0.15
	E. grevyi	tm	1.470	0.216	0.970	0.168	0.545	>0.15	0.535	0.661	0.964	0.095	0.611	0.107	0.249	0.861	0.969	0.166	0.391	>0.15
	C. taurinus	tx	2.566	0.056	0.969	0.360	0.425	>0.15	1.216	0.318	0.958	0.157	0.592	0.116	1.476	0.238	0.947	0.065	0.613	0.103
	C. taurinus	tm	1.141	0.358	0.984	0.888	0.194	>0.15	0.054	0.983	0.958	0.226	0.484	>0.15	0.297	0.827	0.954	0.178	0.43	>0.15
epLsar	*E. grevyi*	tx	0.720	0.611	0.985	0.616	0.361	>0.15	1.247	0.301	0.972	0.166	0.606	0.110	0.951	0.422	0.982	0.508	0.378	>0.15
	E. grevyi	tm	1.832	0.124	0.982	0.544	0.339	>0.15	0.895	0.450	0.975	0.294	0.373	>0.15	1.696	0.179	0.989	0.877	0.213	>0.15
	C. taurinus	tx	0.657	0.626	0.980	0.695	0.246	>0.15	0.769	0.519	0.977	0.603	0.283	>0.15	0.085	0.968	0.979	0.654	0.273	>0.15
	C. taurinus	tm	1.937	0.132	0.964	0.324	0.342	>0.15	0.953	0.428	0.982	0.858	0.192	>0.15	0.358	0.783	0.953	0.166	0.441	>0.15
log(*Tfv*)	*E. grevyi*	tx	0.691	0.633	0.989	0.831	0.195	>0.15	1.280	0.290	0.989	0.856	0.121	>0.15	2.135	0.105	0.984	0.578	0.233	>0.15
	E. grevyi	tm	1.657	0.162	0.986	0.757	0.229	>0.15	0.702	0.555	0.983	0.595	0.208	>0.15	0.489	0.691	0.975	0.277	0.453	>0.15
	C. taurinus	tx	0.065	0.992	0.961	0.196	0.467	>0.15	1.402	0.259	0.974	0.483	0.349	>0.15	0.257	0.856	0.974	0.484	0.270	>0.15
	C. taurinus	tm	1.058	0.396	0.926	**0.030**	0.799	**0.034**	2.225	0.107	0.954	0.183	0.512	>0.15	1.753	0.179	0.977	0.694	0.302	>0.15

LEV = Levene's test for homogeneity of variances; AD = Anderson-Darling, and SW = Shapiro-Wilk tests for assessing normality. Only normally distributed and homoscedastic parameters from the SSFA are shown. Probability values lower than 0.05 are indicated in bold case. *Asfc* = area-scale fractal complexity, *epLsar* = exact proportion length-scale anisotropy, log (*Tfv*) = $\log_{10}(1+Tfv)$ = textural fill volume.

Appendix C

TABLE C1. ANOVA summary

SSFA parameter	Tooth row (a)	*E. grevyi* SS	df	MS	*F*	p	*C. taurinus* SS	df	MS	*F*	p
Asfc	Effect	75713.157	1	75713.157	22.252	**0.000**	4517.247	1	4517.247	0.569	0.453
	Error	398090.056	117	3402.479			556182.329	70	7945.462		
epLsar	Effect	≈0	1	≈0	0.453	0.502	≈0	1	≈0	0.959	0.331
	Error	0.000013	117	≈0			0.000007	70	≈0		
log(*Tfv*)	Effect	0.023	1	0.023	9.210	0.003	0.007	1	0.007	2.506	0.118
	Error	0.300	120	0.003			0.205	69	0.003		
		tx					tm				
SSFA parameter	Species (b)	SS	df	MS	*F*	p	SS	df	MS	*F*	p
Asfc	Effect	20088.742	1	20088.742	3.658	0.059	83770.126	1	83770.126	17.988	**0.000**
	Error	549119.800	100	5491.198			405152.585	87	4656.926		
epLsar	Effect	0.000001	1	0.000001	8.241	**0.005**	0.000001	1	0.000001	10.733	**0.002**
	Error	0.000011	100	≈0			0.000009	87	≈0		
log(*Tfv*)	Effect	0.006	1	0.006	2.236	0.138	0.011	1	0.011	4.017	**0.048**
	Error	0.272	101	0.003			0.233	88	0.003		
		E. grevyi, tx					*E. grevyi*, tm				
SSFA parameter	Tooth postion (c)	SS	df	MS	*F*	p	SS	df	MS	*F*	p
Asfc	Effect	32129.630	5	6425.926	2.155	0.072	10658.751	5	2131.750	0.575	0.719
	Error	169955.698	57	2981.679			185345.977	50	3706.920		
epLsar	Effect	0.000001	5	≈0	1.557	0.187	≈0	5	≈0	0.771	0.575
	Error	0.000007	57	≈0			0.000004	50	≈0		
log(*Tfv*)	Effect	0.006	5	0.001	0.486	0.785	0.023	5	0.005	1.913	0.108
	Error	0.144	58	0.002			0.127	52	0.002		
		C. taurinus, tx					*C. taurinus*, tm				
SSFA parameter	Tooth postion (c)	SS	df	MS	*F*	p	SS	df	MS	*F*	p
Asfc	Effect	77337.120	4	19334.280	2.437	0.066	26110.579	4	6527.645	0.999	0.425
	Error	269697.352	34	7932.275			183037.278	28	6537.046		
epLsar	Effect	≈0	4	≈0	1.036	0.403	≈0	4	≈0	0.245	0.910
	Error	0.000003	34	≈0			0.000004	28	≈0		
log(*Tfv*)	Effect	0.016	4	0.004	1.287	0.295	0.014	4	0.004	1.387	0.265
	Error	0.106	34	0.003			0.069	27	0.003		
		E. grevyi, tx					*E. grevyi*, tm				
SSFA parameter	Cusp side (d)	SS	df	MS	*F*	p	SS	df	MS	*F*	p
Asfc	Effect	29615.902	3	9871.967	3.377	0.024	12076.148	3	4025.383	1.138	0.342
	Error	172469.426	59	2923.211			183928.579	52	3537.088		
epLsar	Effect	≈	3	≈0	0.541	0.656	≈0	3	≈0	0.195	0.899
	Error	0.000008	59	≈0			0.000005	52	≈0		
log(*Tfv*)	Effect	0.002	3	0.001	0.255	0.857	0.001	3	≈0	0.084	0.969
	Error	0.148	60	0.002			0.150	54	0.003		
		C. taurinus, tx					*C. taurinus*, tm				
SSFA parameter	Cusp side (d)	SS	df	MS	*F*	p	SS	df	MS	*F*	p
Asfc	Effect	59434.720	3	19811.573	2.411	0.083	12511.483	3	4170.494	0.615	0.611
	Error	287599.751	35	8217.136			196636.374	29	6780.565		
epLsar	Effect	≈0	3	≈0	0.334	0.801	≈0	3	≈0	0.465	0.709
	Error	0.000003	35	≈0			0.000004	29	≈0		
log(*Tfv*)	Effect	0.010	3	0.003	1.042	0.386	0.012	3	0.004	1.525	0.230
	Error	0.112	35	0.003			0.071	28	0.003		
		E. grevyi, tx					*E. grevyi*, tm				
SSFA parameter	Enamel ridge (e)	SS	df	MS	*F*	p	SS	df	MS	*F*	p
Asfc	Effect	8009.399	3	2669.800	0.812	0.493	14367.811	3	4789.270	1.371	0.262
	Error	194075.929	59	3289.423			181636.916	52	3493.018		
epLsar	Effect	0.000001	3	≈0	2.660	0.056	0.000001	3	≈0	2.267	0.092

TABLE C1. Continued

SSFA parameter	Enamel ridge (e)	*E. grevyi*, tx SS	df	MS	*F*	p	*E. grevyi*, tm SS	df	MS	*F*	p
	Error	0.000007	59	≈0			0.000004	52	≈0		
log(*Tfv*)	Effect	0.025	3	0.008	3.998	0.012	0.015	3	0.005	1.979	0.128
	Error	0.125	60	0.002			0.136	54	0.003		

SSFA parameter	Enamel ridge (e)	*C. taurinus*, tx SS	df	MS	*F*	p	*C. taurinus*, tm SS	df	MS	*F*	p
Asfc	Effect	14266.990	3	4755.663	0.500	0.685	12462.913	3	4154.304	0.613	0.612
	Error	332767.481	35	9507.642			196684.944	29	6782.239		
epLsar	Effect	≈0	3	≈0	1.604	0.206	≈0	3	≈0	0.953	0.428
	Error	0.000003	35	≈0			0.000003	29	≈0		
log(*Tfv*)	Effect	0.019	3	0.006	2.197	0.106	0.007	3	0.002	0.923	0.443
	Error	0.102	35	0.003			0.075	28	0.003		

df = degree of freedom, *F* = value of the *F*-test, MS = mean squares, SS = sum of squares. Only the results from the SSFA parameters *Asfc* = area-scale fractal complexity, *epLsar* = exact proportion length-scale anisotropy, log (*Tfv*) = $\log_{10}(1+Tfv)$ = textural fill volume are shown. Probability values lower than 0.05 are indicated in bold case.

Appendix D

TABLE D1 Description of the 18 surface texture parameters (according to ISO/DIS 25178-2), identified as separating the extant species with the best probability, using the discriminant analyses

Parameter	Group	Name	Description
S5v	Feature	Five point pit height	Average value of the heights of the five pits with the largest global pit height, within the definition area
Sa	Height	Arithmetical mean height	Mean surface roughness
Sal	Spatial	Auto-correlation length	Horizontal distance of the autocorrelation function (tx, ty) which has the fastest decay to a specified value s, with $0<s<1$. The default value for s in the software is 0.2. This parameter expresses the content in wavelength of the surface. A high value indicates that the surface has mainly high wavelengths (low frequencies)
Sda	Feature	Closed dale area	Average area of dales connected to the edge at height c
Sdv	Feature	Closed dale volume	Average volume of dales connected to the edge at height c
Sha	Feature	Closed hill area	Average area of dales connected to the edge at height c
Shv	Feature	Closed hill volume	Average volume of hills connected to the edge at height c
Sku	Height	Kurtosis	Kurtosis of the height distribution
Spd	Feature	Density of peaks	Number of peaks per unit area
Sq	Height	Root mean square height	Standard deviation of the height distribution, or RMS surface roughness
Std	Spatial	Texture direction	This parameter calculates the main angle for the texture of the surface, given by the maximum of the polar spectrum. This parameter has a meaning if *Str* (see below) is lower than 0.5. If the surface has a circular texture (turning, sawing), this parameter will give a wrong direction near to the tangential of the circle. In case the surface has two or more main directions, the *Std* parameter will give the angle of the main direction. The angle is given between 0° and 360° counterclockwise, from a reference angle. The reference angle may be set to another value than 0°
Str	Spatial	Texture-aspect ratio	This is the ratio of the shortest decrease length at 0.2 from the autocorrelation, on the greatest length. This parameter has a result between 0 and 1. If the value is near 1, we can say that the surface is isotropic, i.e. has the same characteristics in all directions. If the value is near 0, the surface is anisotropic, i.e. has an oriented and/or periodical structure
Sv	Height	Maximum pit height	Depth between the mean plane and the deepest valley
Sxp	Functional	Extreme peak height	Difference in height between q% and p% material ratio. This parameter must be configured with two thresholds entered in %
Vm	Volume	Material volume	Volume of the material at a material ratio p (in %)
Vmc	Volume	Core material volume of the scale limited surface	Volume of material in the core or kernel, between two material ratios p and q (in %), calculated in the zone between c1 and c2
Vvc	Volume	Core void volume of the scale limited surface	Volume of void in the core or kernel, between two material ratios p and q (in %), calculated in the zone between c1 and c2
Vvv	Volume	Pit void volume of the scale limited surface	Volume of void in the valleys, between a material ratio p (in %) and 100% material ratio, calculated in the zone below c2

References

Clauss M, Hume D, Hummel J: Evolutionary adaptations of ruminants and their potential relevance for modern production systems. *Animal* (2010). DOI: 10.1017/S1751731110000388.

Codron D, Codron J, Lee-Thorp JA, Sponheimer M, de Ruiter D, *et al.*: Diets of savanna ungulates from stable carbon isotope composition of faeces. *J Zool* **273**, 21–29 (2007).

Ego WK, Mbuvi DM, Kibet PFK: Dietary composition of wildebeest (*Connochaetes taurinus*) kongoni (*Alcephalus buselaphus*) and cattle (*Bos indicus*), grazing on a common ranch in south-central Kenya. *Afr J Ecol* **41**, 83–92 (2003).

Fortelius M: Ungulate cheek teeth: developmental, functional, and evolutionary interrelations. *Acta Zool Fennica* **180**, 1–76 (1985).

Fortelius M, Solounias N: Functional characterization of Ungulate molars using the abrasion-attrition wear gradient: a new method for reconstructing palaeodiets. *Am Museum Novitates* **3301**, 1–36 (2000).

Gagnon M, Chew AE: Dietary preferences in extant African Bovidae. *J Mammal* **81**, 490–511 (2000).

Hofmann RR: The Ruminant Stomach: Stomach Structure and Feeding Habits of East African Game Ruminants. East African Monographs in Biology 2. East African Literature Bureau, Nairobi, 1–354 (1973).

Hofmann RR: Evolutionary steps of ecophysiological adaptation and diversification of ruminants: a comparative view of their digestive system. *Oecologia* **78**, 443–457 (1989).

Hummel J, Südekum K-H, Bayer D, Ortmann S, Streich WJ, *et al.*: Physical characteristics of reticuloruminal contents of cattle in relation to forage type and time after feeding. *J Anim Physiol Anim Nutr* **93**, 209–220 (2009).

International Organization for Standardization: Geometrical product specifications (GPS)—Surface texture: Areal—Part 2: Terms, definitions and surface texture parameters. p. 1–42 (2007).

IUCN SSC Antelope Specialist Group. *Connochaetes taurinus*. In *IUCN 2009*. IUCN Red List of Threatened Species. Version 2009.2. Available at www.iucnredlist.org. Downloaded on November 20, 2009 (2008).

Janis CM: The correlation between diet and dental wear in herbivorous mammals, and its relationship to the determination of diets of extinct species. In *Evolutionary Paleobiology of Behavior and Coevolution* (Boucot AJ, Ed.), Elsevier Science Publishers B. V., Amsterdam, 241–272 (1990).

Janis CM, Fortelius M: On the means whereby mammals achieve increased functional durability of their dentitions, with special reference to limiting factors. *Biol Rev* **63**, 197–230 (1988).

Janis CM, Constable EC, Houpt KA, Streich WJ, Clauss M: Comparative ingestive mastication in domestic horses and cattle: a pilot investigation. *J Anim Physiol Anim Nutr* (2010).

Kaiser TM, Brinkmann G: Measuring dental wear equilibriums-the use of industrial surface texture parameters to infer the diets of fossil mammals. *Palaeogeogr Palaeoclimatol Palaeoecol* **239**, 221–240 (2006).

Keast A: Interrelationships of Two zebra species in an overlap zone. *J Mammal* **46**, 53–66 (1965).

Keselman HJ, Huberty CJ, Lix LM, Olejnik S, Cribbie RA, *et al.*: Statistical practices of educational researchers: an analysis of their ANOVA, MANOVA, and ANCOVA analyses. *Rev Educ Res* **68**, 350–386 (1998).

Klingel H: Soziale Organisation und Verhalten des Grevy-Zebras (*Equus grevyi*). *Zeitschrift für Tierpsychologie* **36**, 37–70 (1974).

Leach RK, Flack DR, Hughes EB, Jones CW: Development of a new traceable areal surface texture measuring instrument. *Wear* **266**, 552–554 (2009).

Lechner-Doll M, Kaske M, Engelhardt W: Factors affecting the mean retention time of particles in the forestomach of ruminants and camelids. In *Physiological Aspects of Digestion and Metabolism in Ruminants* (Tsuda T, Sasaki Y, Kawashima R, Eds.), Academic Press, San Diego, 455–482 (1991).

Levene H: Robust tests for equality of variance. In *Contributions to Probability and Statistics* (Olkin I, Ed.), Stanford University Press, Palo Alto, California, 278–292 (1960).

Lix LM, Keselman JC, Keselman HJ: Consequences of assumption violations revisited: a quantitative review of alternatives to the one-way analysis of variance F test. *Rev Educ Res* **66**, 579–619 (1996).

Lucas PW: Basic principles of tooth design. In *Teeth*: *Form*, *Function and Evolution* (Kurten B, Ed.), Columbia University Press, New York, 154–162 (1982).

Lucas P, Constatino P, Wood B, Lawn B: Dental enamel as a dietary indicator in mammals. *BioEssays* **30**, 374–385 (2008).

Mainland IL: Dental microwear and diet in domestic sheep (*Ovis aries*) and goats (*Capra hircus*): distinguishing grazing and fooder-fed Ovicaprids using a quantitative analytical approach. *J Archaeological Sci* **25**, 1259–1271 (1998).

McLeod MN, Minson DJ: Large particle breakdown by cattle eating ryegrass and alfalfa. *J Anim Sci* **66**, 992–999 (1988).

Merceron G, Blondel C, Brunet M, Sen S, Solounias N, *et al.*: The Late Miocene paleoenvironment of Afghanistan as inferred from dental microwear in artiodactyls. *Palaeogeogr Palaeoclimatol Palaeoecol* **207**, 143–163 (2004).

Merceron G, Escarguel G, Angibault J-M, Verheyden-Tixier H: Can dental microwear textures record inter-individual dietary variations? *PLoS One* **5**, 1–9 (2010).

Moehlman PD, Rubenstein DI, Kebede F: *Equus grevyi*. In *IUCN 2009*. IUCN Red List of Threatened Species. Version 2009.2. Available at: www.iucnredlist.org. Downloaded on November 20, 2009 (2008).

Oshima TC, Algina J: Type I error rates for James's second-order test and Wilcox's Hm test under heteroscedasticity and non-normality. *Br J Math Stat Psychol* **42**, 255–263 (1992).

Owaga ML: The feeding ecology of wildebeest and zebra in Athi-Kaputei plains. *East Afr Wildl J* **13**, 375–383 (1975).

Rivals F, Deniaux B: Dental microwear analysis for investigating the diet of an argali population (*Ovis ammon antiqua*) of mid-Pleistocene age, Caune de l'Arago cave, eastern Pyrenees, France. *Palaeogeogr Palaeoclimatol Palaeoecol* **193**, 443–455 (2003).

Rowen M, Ginsberg G: Grevyi's Zebra (*Equus grevyi* Oustalet). In *Zebras*, *Asses and Horses*. *An Action Plan for the Conservation of Wild Equids* (Duncan P, Ed.), IUCN, Gland, 10–12 (1992).

Rubenstein DI: Ecology and sociality in horses and zebras. In *Ecological Aspects of Social Evolution*. *Birds and Mammals* (Rubenstein DI, Wrangham RW, Eds.), Princeton University Press, New Jersey, 282–302 (1986).

Skinner JD, Smithers RHN: The mammals of the southern African subregion. University of Pretoria, Pretoria (1990).

Scott RS, Ungar PS, Bergstrom TS, Brown CA, Grine FE, *et al.*: Dental microwear texture analysis shows within-species

diet variability in fossil hominins. *Nature* **436**, 693–695 (2005).

Scott RS, Ungar PS, Bergstrom TS, Brown CA, Childs BE, *et al*.: Dental microwear texture analysis: technical considerations. *J Hum Evol* **51**, 339–349 (2006).

Scott JR, Godfrey LR, Jungers WL, Scott RS, Simons EL, *et al*.: Dental microwear texture analysis of two families of subfossil lemurs from Madagascar. *J Hum Evol* **56**, 405–416 (2009).

Solounias N, Teaford MF, Walker A: Interpreting the diet of extinct ruminants: the case of a non-browsing giraffid. *Palaeobiology* **14**, 287–300 (1988).

Teaford MF: Dental microwear and diet in extant and extinct Theropithecus: preliminary analyses. In *Theropithecus: The Life and Death of a Primate Genus* (Jablonski NG, Ed.), Cambridge University Press, Cambridge, 331–349 (1993).

Tomarken AJ, Serlin RC: Comparison of ANOVA alternatives under variance heterogeneity and specific noncentrality structures. *Psychol Bull* **99**, 90–99 (1986).

Ungar PS: Dental microwear of European miocene catarrhines: evidence for diets and tooth use. *J Hum Evol* **31**, 335–366 (1996).

Ungar PS, Brown CA, Bergstrom TS, Walker A: Quantification of dental microwear by tandem scanning confocal microscopy and scale-sensitive fractal analyses. *Scanning* **25**, 185–193 (2003).

Ungar PS, Merceron G, Scott RS: Dental microwear texture analysis of varswater bovids and early pliocene paleoenvironments of Langebaanweg, Western Cape Province, South Africa. *J Mamm Evol* (2007).

Walker A, Hoeck HN, Perez L: Microwear of mammalian teeth as an indicator of diet. *Science* **201**, 908–910 (1978).

Tooth function and dietary reconstruction in ungulates using 2D and 3D methods – a review

Ellen Schulz[1], Ivan Calandra[2] and Thomas M. Kaiser[3]

Biocenter Grindel and Zoological Museum, University of Hamburg, Martin-Luther-King-Platz 3, 20146 Hamburg, Germany; emails: ellen.schulz@uni-hamburg.de[1], ivan.calandra@uni-hamburg.de[2], thomas.kaiser@uni-hamburg.de[3]

For the last four decades methods of dental wear evaluation have been applied to infer dietary traits of both extant and extinct mammals. Recent developments add a new functional aspect to these routinely used semiquantitative 2D approaches and open the field for the three-dimensional understanding of the chewing process based on tooth surface micro-topography. Key aspects are different scales of wear analyses. The levels of resolution in each approach are a crucial issue and need evaluation. Testing research hypotheses related to dental wear largely depends on the scaling of wear evaluation which thus needs to be discussed in order to better understand opportunities and limitations of individual approaches. In order to overcome limitations related to observer specific scoring setups, a new standard of dental wear evaluation is strictly based on industrial 3D surface texture parameters as defined by the International Standardization Organization (ISO). These parameters are initially developed and widely applied in engineering applications related to bearing wear and surface quality evaluation of machined products. Surface texture parameters encapsulate a wide range of surface characteristics including lay and orientations measures of features. In order to apply such tools of topographic quantification to dental tissues, three dimensional topographic models of standardized tooth occlusal surfaces are acquired using a high resolution confocal topometric system. Based on these models fully quantitative 3D parameters and functional indices are computed and for the first time linked to functional aspects of dental wear. Sixteen newly defined standard measuring sites on upper and lower herbivorous premolars and molars are being tested in terms of their potential to discriminate functional as well as dietary traits.

Talk presented at the 79th Annual Meeting of the German Paleontological Society in Bonn (DE) in 2009. Abstract published in: *Terra Nostra* **3** – Schriften der GeoUnion Alfred-Wegener-Stiftung, Paläontologie Schlüssel zur Evolution, Kurzfassung und Tagungsbeiträge der 79. Jahrestagung der Paläontologischen Gesellschaft, p. 112.

Technical Session VII, Thursday 3:00

THREE-DIMENSIONAL MICROTEXTURE ANALYSIS - A NEW APPROACH FOR DIETARY RECONSTRUCTION

SCHULZ, Ellen, Biocenter Grindel and Zoological Museum, Hamburg, Germany;
CALANDRA, Ivan, Biocenter Grindel and Zoological Museum, Hamburg, Germany;
KAISER, Thomas, Biocenter Grindel and Zoological Museum, Hamburg, Germany

A diverse set of two dimensional analytic tools has been so far successfully applied to analyze tooth enamel wear facets and infer dietary traits of extant and fossil herbivorous mammals at different levels of resolution. The chewing process in mammals is functionally complex and not yet understood in detail. Taking into account that chewing function always involves surface interaction dominated by wear, established technical standards in quantifying wear are proposed to allow inference on both dental function at the level of an individual wear facet and diet at the level of an individual animal. For the first time, we therefore establish a system of dental wear evaluation strictly based on industrial engineering standards and parameters set by the International Standardization Organization (ISO). 2D and 3D-ISO roughness parameters are computed using metrology software as is the standard in technical protocols. We link these parameters with dental wear using 3D-topographic models of tooth enamel wear surfaces acquired with a high resolution confocal surface measuring system. As a fully quantitative approach to dental wear evaluation, we find ISO-roughness parameters particular robust as no intra- nor inter- observer errors are involved. Extant ungulates representing different well known dietary traits are analyzed for intra-facet, intra-tooth and inter-species tooth enamel surface variations. Sixteen well defined tooth enamel facets of upper and lower premolars and molars are tested for each species and new functional indices are identified.

Talk presented at the 69th Annual Meeting of the Society of Vertebrate Paleontology in Bristol (UK) in 2009. Abstract published in: *Journal of Vertebrate Paleontology* **29**(Suppl. 3), p. 178A.

Tracing chewing mechanisms in hoofed mammals: 3D tribology of enamel wear

E. SCHULZ, I. CALANDRA, T. M. KAISER, [1]Biocenter Grindel and Zoological Museum, University of Hamburg, Martin-Luther-King-Platz 3, 20146 Hamburg, Germany, e-mail: ellen.schulz@uni-hamburg.de

Mammals inhabit all types of environments and have evolved chewing systems capable of processing a huge variety of structurally diverse food components. Since the permanent dentition of mammals can not be replaced or repaired in a natural setting, functional changes in surfaces induced by wear play a major role in the evolution of functionally durable teeth. In general chewing function involves surface interaction which includes two components of wear, attrition (tooth-tooth wear) and abrasion (tooth-food wear). Wear analyses in mammalian teeth are applied to reconstruct jaw movements or dietary behaviours, and thus to infer habitat and climate preferences of extant and extinct species. During the last two decades the various qualitative and quantitative microwear approaches focusing on 2D microscopic inspection of enamel facets became powerful tools in dietary reconstruction. Nevertheless the mastication process is a three-dimensional process and the 3D fractal analysis of dental microwear as a quantitative approach was developed. Based on the high degree of correspondence between industrial machined surfaces and the tooth enamel surfaces, we decided to combine the advantages of 3D fractal analysis with standardised industrial tribology. We developed a new 3D microtexture method using the industriaI surface texture parameters to quantify attritional and abrasional wear as well as functional traits involved. 3D topographic models of the mammalian tooth enamel wear surfaces are acquired using a high resolution disk scanning confocal measurement system. Industrial 3D standards like surface textures parameters after ISO/DIS 25178-2 and Scale-Sensitive Fractal Analysis (SSFA) are applied to quantify dental wear in herbivorous ungulates. We evaluate cheek dentitions of two grazing ungulates, *Connochaetes taurinus* (Bovidae, Cetartiodactyla) and *Equus grevyi* (Equidae, Perissodactyla), and of two browsing ungulates, *Giraffa camelopardalis* (Giraffidae, Cetartiodactyla) and *Diceros bicornis* (Rhinocerotidae, Perissodactyla). These species inhabit a similar habitat in East Africa representing two opposite dietary adaptations characterised by fundamentally different digestive strategies within the two orders. We test the hypothesis that the four species show functional traits along mesio-distal and bucco-lingual gradients within a tooth row that relate to their specific food composition, and modes of processing and digestion. The SSFA as well as ISO/DIS 25178-2 parameters are found to be very promising tools in standardized and quantitative analyses of tooth enamel facets. We find that industrial standards have the potential to distinguish subtle dietary preferences, for instance between the two grazers. Strong arguments are found that central enamel ridges encounter less attrition and more abrasion, because peripheral ridges function as guiding structures that encounter significant attrition but leave pure abrasional contacts to the more central ridges of a tooth. Furthermore, SSFA and ISO parameters allow distinctions among the subtle dietary strategies that evolved in herbivorous ungulates with fundamentally different systematic affinities but which exploit a similar dietary niche. The analyses also point to species-specific metabolic traits, reflecting their respective digestive strategies.

Talk presented at the 84th Annual Meeting of the German Society of Mammalogy in Berlin (DE) in 2010. Abstract published in: *Mammalian Biology* **75S**, p. 24-25.

Poster MO.29

Functional morphology at the intersection between biology and engineering: 3D tribologies of enamel wear of hoofed mammals

ELLEN SCHULZ[1], IVAN CALANDRA[1], THOMAS M. KAISER[1]

[1] Biozentrum Grindel und Zoologisches Museum, Universität Hamburg

Mammals inhabit all types of environments and evolved chewing systems capable of processing a variety of structurally diverse food components. Since the permanent dentition of mammals is not replaced or repaired, functional changes in surfaces induced by wear play a major role in the evolution of functionally durable teeth. Surface textures of cheek teeth should thus reflect the mechanisms of wear as well as functional traits. We employ industrial 3D surface texture parameters after ISO 25178-2 and Scale-Sensitive Fractal Analysis to quantify wear. 3D topographic models of facets are acquired using a high resolution confocal microscope. We evaluate cheek dentitions of two grazers, *Connochaetes taurinus* (Bovidae, Cetartiodactyla) and *Equus grevyi* (Equidae, Perissodactyla), and of two browsers, *Giraffa camelopardalis* (Giraffidae, Cetartiodactyla) and *Diceros bicornis* (Rhinocerotidae, Perissodactyla). They inhabit a similar habitat in East Africa but represent two opposite diets and fundamentally different digestive strategies. We test the hypothesis that they show mesio-distal and bucco-lingual gradients within a tooth row related to their food composition. Industrial parameters of enamel surfaces distinguish subtle dietary preferences, even among grazers. We also found attrition-dominated peripheral ridges to function as guidance structures in non-ruminants. Besides of indicators of diet, surface textures are thus reflecting basic functional traits of the mammal dentition.

Poster presented at the 103rd Annual Meeting of the German Society of Zoology in Hamburg (DE) in 2010. Abstract Volume p. 163.

S17 - DENTAL FUNCTIONAL MORPHOLOGY OF HOOFED MAMMALS: INSIGHTS FROM 3-D MICROTEXTURE ANALYSIS

Calandra, Ivan, Schulz, Ellen and Kaiser, Thomas M.

Biocenter Grindel and Zoological Museum, University of Hamburg, Martin-Luther-King-Platz 3, D-20146 Hamburg, Germany

e-mail: *ivan.calandra@uni-hamburg.de*

Mammals inhabit all types of environments and evolved chewing systems capable of processing a huge variety of structurally diverse food components. Since the permanent dentition of mammals is not replaced or repaired in a natural setting, functional changes in surfaces induced by wear play a major role in the evolution of functionally durable teeth. Surface textures of cheek teeth should thus reflect the mechanisms of wear as well as functional traits. We employ industrial three-dimensional (3D) surface texture parameters after ISO/DIS 25178 and Scale-Sensitive Fractal Analysis to quantify dental wear in herbivorous ungulates at the level of a single wear enamel facet. 3D topographic models of the facets are acquired using a high resolution confocal surface measurement system. We evaluate cheek dentitions of two grazing ungulates, *Connochaetes taurinus* (Bovidae, Cetartiodactyla) and *Equus grevyi* (Equidae, Perissodactyla), and of two browsing ungulates, *Giraffa camelopardalis* (Giraffidae, Cetartiodactyla) and *Diceros bicornis* (Rhinocerotidae, Perissodactyla). These species inhabit a similar habitat in East Africa and represent two opposite diets and two fundamentally different digestive strategies within the two orders. We test the hypothesis that the four species show mesiodistal and bucco-lingual gradients within a tooth row that relate to their specific food composition. Industrial standards applied on the enamel surfaces distinguish subtle dietary preferences, even between grazers. Furthermore functional traits along the tooth rows are retrieved. We found that attrition-dominated peripheral ridges function as guidance structures in non-ruminants. Therefore surface textures are additionally interpreted as indicators of chewing mechanisms and occlusal function.

Talk presented at the International Palaeontological Congress 3 in London in 2010. Abstract Volume p. 110.

Fruit proportion and consumption of hard items in the diets of Primates correlate with 3D microwear textures

Calandra I [1]*, Schulz E [1], Pinnow M [1], Krohn S [1], Kaiser TM [1]

[1]University of Hamburg, Biocentre Grindel and Zoological Museum, Martin-Luther-King-Platz 3, 20146 Hamburg, Germany
*Corresponding author e-mail: ivan.calandra@uni-hamburg.de

The 3D dental microwear texture analysis is useful in reconstructing the diets of extinct primates. This method is based on the comparison of fossils with extant species with known diets. The diets of primates are very diversified and include fruits, seeds, grass, tree leaves, bark, roots, tubers, and animal resources. Fruits remain the main component in the diets of most primates. We tested whether the proportion of fruits consumed can be significantly correlated with microtexture. Two microwear texture methods, the scale-sensitive fractal analysis (SSFA) and the ISO/FDIS 25178 texture analysis (ISO), are applied on eight primate species (*Alouatta seniculus*, *Gorilla gorilla*, *Lophocebus albigena*, *Macaca fascicularis*, *Pan troglodytes*, *Papio cynocephalus*, *Pongo abelii*, *Theropithecus gelada*). These species largely differ in their mean annual fruit proportions (from 0 to 90%) in their diet, as well as in their consumption of other hard items (seeds, bark, and grass). The complexity and heterogeneity (SSFA) of textures correlate with the proportion of fruits consumed. The textural fill volume (SSFA) indicates the proportion of hard items processed. Last, the anisotropy (SSFA) relates to the consumption of grass. On the other hand, the ISO parameters (valley height, root mean square height, material volume, density of peaks, and closed hill and dale areas) describe the functional interaction between food items and enamel facets during mastication: attrition as induced by tough and soft foods *vs.* abrasion as induced by local enamel fracturing caused by hard items.

Poster presented at the 15th International Symposium on Dental Morphology in Newcastle (UK) in 2011.

National Oceanography Centre, Southampton
UNIVERSITY OF SOUTHAMPTON AND
NATURAL ENVIRONMENT RESEARCH COUNCIL

National Oceanography Centre, Southampton

University of Southampton, Waterfront Campus,
European Way, Southampton SO14 3ZH, UK
t +44 (0)23 8059 6364 **f** +44 (0)23 8059 6247
e mva@noc.soton.ac.uk www.noc.soton.ac.uk

switchboard +44 (0)23 8059 6666

9 August 2011

To whom it may concern,

As an English native speaker, I have read the thesis of Mr. Ivan Calandra on the 'Tribology of dental enamel facets of Ungulates and Primates', and I confirm that the English employed in the thesis is correct and clear in both grammar and content.

Yours faithfully

Martin V. Angel MA PhD

Declaration on oath

I, Ivan Calandra, hereby declare on oath, that I have written the present dissertation by my own and have not used other than the acknowledged resources and aids.

Hamburg, 11.08.2011 signature